Identification of Prognostic Markers and Novel Therapeutic Targets of Resistance in Acute Lymphoblastic Leukemia

Dissertation
zur
Erlangung der naturwissenschaftlichen Doktorwürde
(Dr. sc. nat.)

vorgelegt der
Mathematisch-naturwissenschaftlichen Fakultät
der
Universität Zürich
von

Anna Rinaldi

aus
Italien

Promotionskomitee
PD Dr. Bourquin Jean-Pierre (Vorsitz und Leitung der Dissertation)
Prof Dr. Basler Konrad
Dr. Beat Bornhauser
Prof. Dr. Mauro Delorenzi
Prof. Dr. Ian Frew
PD Dr. Joëlle Tchinda

Zürich, 2015

STATEMENT OF AUTHORSHIP

I declare that I have used no other sources and aids other than those indicated. All passages quoted from publications or paraphrased from these sources are indicated as such, i.e. cited and/or attributed. This thesis was not submitted in any form for another degree or diploma at any university or other institution of tertiary education.

Zurich, May 2015

Anna Rinaldi

Summary

Significant improvement in the treatment of pediatric ALL has been achieved by multi-drug chemotherapy and risk-adapted treatment that accomplished an overall survival rate over 80%, but children who relapse with ALL still account for the majority of cancer-related deaths. Furthermore, the development of targeted approaches is urgently needed, as currently used multi-agent chemotherapy is associated with relevant short and long-term toxicity. Therefore, we used a combined genetic and functional approach to seek vulnerable targets and novel potent agents using a comprehensive xenograft model of drug resistant ALL subtypes, including a paradigm of resistant disease, *TCF3-HLF*-positive ALL.

As central coordinator of a large international consortium, I established xenografts of 14 cases of the rare, but always fatal, *TCF3-HLF*-positive ALL. We obtained whole-genome, -exome and -transcriptome sequencing analysis of leukemia patient samples and corresponding xenografts. Integrating clinical and genomic information from patients with the data generated using the leukemia xenograft model, we identified specific pattern of mutation, gene expression, and drug response profiles of resistant *TCF3-HLF*-positive ALL in comparison to treatment-responsive *TCF3-PBX1*-positive ALL. We show that the leukemia xenografts closely resemble the human disease and recapitulated the multiclonal hierarchies that are observed in patients. The *TCF3-HLF* translocation is associated with recurrent intragenic deletions of the lymphoid transcription factor gene *PAX5* or somatic mutations in the non-translocated allele of *TCF3* (acting upstream of *PAX5*), indicating that this initiating event must occur in a stage of lymphoid development characterized by reduced levels of PAX5. The transcriptional signature presents with a prevalence of stem cell, mesenchymal and myeloid features, consistent with reprogramming towards a hybrid, more drug-resistant hematopoietic state by *TCF3-HLF* ALL.

We developed a unique drug-profiling platform based on automated image analysis of patient samples. We selected therapeutic agents that are in clinical use or in clinical development to constitute a customized library of 98 compounds and investigated the potential of this approach on a set of 61 ALL patients. Distinct drug activity profiles were detected for defined genetic subtypes, including *TCF3-HLF*-translocated and *MLL*-rearranged leukemia. This approach also identified new subgroups based on particular sensitivity to specific classes of new agents. *TCF3-HLF* cases were extremely sensitive to the BCL-2 inhibitor venetoclax (ABT-199), revealing dependence on BCL-2 for survival. Furthermore, other subgroups of ALL were also very sensitive to this agent, including MLL-rearranged ALL and a subset of T-ALL cases, which represent subgroups with unmet medical needs. The drug-profiling data accurately predicts strong *in vivo* activity of venetoclax in leukemia xenografts, which identifies BCL-2 as a rationale for targeted therapeutic intervention and provides proof of concept for its use as an additional tool for precision medicine.

Using a proteomic approach in this xenograft model, we identified the glycophosphatidylinositol anchored surface protein Vanin-2 (VNN2, GPI-80), a marker of fetal hematopoietic stem cells, to be exclusively detectable at the cell surface of patients with more resistant disease and high risk of relapse. Based on our retrospective analysis in the context of a large multinational clinical trial, the detection of VNN2 by flow cytometry at diagnosis identifies a new subgroup of patients at risk for relapse. Remarkably, VNN2 was detected in all *TCF3-HLF*-positive ALL cases tested, providing a new strategy to improve the detection of this subgroup of patients, currently difficult to identify.

Interference with VNN2, using a specific monoclonal antibody, resulted in delayed homing of ALL to the bone marrow and spleen in the xenograft model, suggesting that VNN2 contributes directly to the leukemia pathogenesis.

In conclusion, with my PhD Thesis I contributed to the development of a translational research platform that integrates clinical and genomic information with functional drug activity data, with the aim to detect actionable features in leukemia, in particular with regard to *TCF3-HLF*-positive ALL, in a more personalized manner. Moreover, we discovered that VNN2/GPI80, a marker of fetal hematopoietic stem cells, can be used to identify patients with a more aggressive form of the disease (including patients with fatal *TCF3-HLF*-positive ALL) and these findings constitute the basis for further functional and clinical investigations.

Zusammenfassung

Durch die Entwicklung der Kombinationstherapie mit verschiedenen Chemotherapeutika und einer risiko-adaptierten Behandlung für Patienten mit pädiatrischer ALL konnte eine signifikante Verbesserung der Überlebensrate auf über 80% erreicht werden. Dennoch zählen refraktäre ALL immer noch zu den häufigsten krebs-assoziierten Todesfällen im Kindesalter. Des Weiteren ist die aktuelle Kombinationstherapie mit schwerwiegender Kurz- und Langzeittoxizität verbunden, so dass die Entwicklung von zielgerichteten Therapien von hoher Relevanz ist. Anhand der hoch resistenten *TCF3-HLF*-positiven ALL sollten in dieser Arbeit durch Kombination von genetischen und funktionalen Studien im Xenotransplantationsmodel neue wirkungsvolle und nutzbare Therapiemöglichkeiten identifiziert werden.

Als zentrale Koordinatorin eines grossen internationalen Konsortiums habe ich in dieser Arbeit Xenotransplantate von 14 Fällen der seltenen aber hoch riskanten *TCF3-HLF* ALL etabliert. Es wurden Genom-, Exom- und Transkriptomsequenzierungen der korrespondierenden Patientenproben und Xenotransplantate durchgeführt. Die Integration der klinischen und genomischen Informationen der Patientenproben und der Xenotransplantate sowie der Vergleich der resistenten *TCF3-HLF*-positive ALL mit der therapierbaren *TCF3-PBX1*-positiven ALL ergaben spezifische Muster für Mutationen, Genexpressionen und Wirkungsprofile für Medikamente. Wir konnten zeigen, dass leukämische Xenotransplantate eine hohe Übereinstimmung mit der initialen Krankheit zeigten und die multiklonalen Hierarchien, die in Patienten beobachtet wurden, rekapituliert wurden. Interessanterweise war die *TCF3-HLF* Translokation mit einer wiederkehrenden Deletion des lymphoiden Transkriptionsfaktors *PAX5* oder mit somatischen Mutationen in dem nicht-translozierten *TCF3*-Allel (agiert oberhalb von *PAX5*) assoziiert. Dies führte zu dem Modell, dass das Leukämie-initiierende Ereignis in einem spezifischen Kontext während der lymphoiden Differenzierung entstehen muss, welcher durch die reduzierte Dosis von PAX5 bevorzugt wird. Die transkriptionelle Signatur dieser Zellen zeigte eine Anreicherung für Stammzell-, mesenchymale und myeloide Faktoren, was mit der *TCF3-HLF* induzierten Reprogrammierung zu einem hybriden, therapie-resistenteren hämatopoietischen Status übereinstimmt.

In unserem Labor haben wir eine einzigartige Plattform zur Bestimmung von Wirkungsprofilen von Medikamenten entwickelt, die auf einer automatischen Bildanalyse des Patientenmaterials basiert. Für eine Gruppe von 61 ALL Patienten wurden 98 Medikamente, die bereits in der klinischen Entwicklung oder Gebrauch sind, auf deren therapeutisches Potenzial getestet. Für bestimmte genetische Subklassen, wie der *TCF3-HLF*-translozierten oder der MLL-rearrangierten ALL, konnten spezifische Wirkungsprofile von Medikamenten beschrieben werden. Des Weiteren identifizierte diese Studie auch neue Subgruppen, basierend auf ihrer spezifischen Sensitivität für bestimmte Medikamentenklassen. *TCF3-HLF* Patientenproben waren zum Beispiel besonders sensitiv auf den BCL-2 Inhibitor Venetoclax (ABT-199), was eine Abhängigkeit der ALL Zellen von BCL-2 annehmen lässt. Aber auch andere ALL-Subtypen, wie die MLL-rearrangierten ALL und ein Anteil der getesteten T-ALL zeigten eine hohe Sensitivität für diesen Inhibitor. Interessanterweise konnten die Daten der Wirkungsprofile für eine akkurate Vorhersage der Aktivität von Venetoclax in vivo genutzt werden. Mit dieser automatisierten Analyseplattform konnte BCL-2 als ein neues Ziel für die gerichtete therapeutische Intervention identifiziert werden und beweist die Nutzbarkeit unserer experimentellen Wirkungsprofile als ein weiteres Instrument für die personalisierte Medizin.

Des Weiteren wurde durch proteomische Analysen der Xenotransplantate das Glycophosphatidylinositol verankerte Oberflächenprotein Vanin-2 (VNN2, GPI-80), ein Marker für fötale hämatopoietische Stammzellen, ausschliesslich auf der Oberfläche von Patienten mit erhöhter Resistenz und hohem Risiko eines Rezidivs identifiziert. Eine retrospektive Analyse im Kontext einer grossen multinationalen klinischen Studie zeigte, dass die Präsenz von VNN2 zum Zeitpunkt der Diagnose eine neue Subgruppe von Patienten mit erhöhtem Rezidivrisiko klassifiziert. Bemerkenswert ist, dass VNN2 in allen *TCF3-HLF*-positiven ALL Patienten detektiert werden konnte und somit eine weitere Strategie zur Identifizierung von Subklassen darstellt, die im normalen Arbeitsablauf eventuell nicht erkannt werden würden. Die Blockierung von VNN2 mittels eines spezifischen monoklonalen Antikörpers ergab eine Verzögerung des "homings" der ALL im Knochenmark und der Milz im Xenotransplantat, was eine direkte Mitwirkung von VNN2 in die leukämische Pathogenese nahe legt.

Zusammengefasst ist meine Doktorarbeit ein wichtiger Beitrag zur Entwicklung einer translationalen Forschungsplattform, die klinische und genomische Informationen mit funktionalen Wirkungsprofilen von Medikamenten integriert, um personalisierte und nutzbare Eigenschaften in Leukämien, im Besonderen der fatalen *TCF3-HLF*-positiven ALL, zu identifizieren. Wir identifizierten den fötalen hämatopoetischen Stammzellmarker VNN2/GPI80 als Charakteristikum für refraktäre Leukämien und legen damit die Basis für weitere funktionale und klinische Untersuchungen zur Verbesserung der Chemotherapie von ALL.

Table of Contents

1 Introduction

1.1 Adult and Pediatric cancers: differences and similarities

Cancer is a term used to describe diseases in which atypical cells proliferate without control, invade surrounding normal tissues and eventually spread to other parts of the body through the blood and lymph systems. There are more than 100 different types of cancer and they are classified by the type of tissue in which the cancer originates and by the location in the body where the cancer first developed.

Cancers figure among the leading causes of morbidity and mortality worldwide, with approximately 14 million new cases and 8.2 million cancer related deaths per year (Ref. World Cancer Report 2014 related to 2012). The relative incidence of cancer types changes remarkably across different age groups (Figure 1) (1). Children (0-14 years) develop primarily hematological malignancies, neuroectodermal tumors and sarcomas. Carcinoma occurs mainly in adults. Distinct spectrum of cancers between adults and children is due to the different type of tissue that undergoes substantial expansion. For example, the B-cell repertoire develops mainly during the age 0-14 years and is associated with high proliferation of B-cell precursors. This event increases the possibility of the emergence and enrichment of genetic aberrations.

The development of cancer derives from the accumulation of genetic and epigenetic alterations in normal cells that provide a selective growth advantage. This process of mutations followed by clonal expansion leads to the formation of cancer. Notably, different tumor types display heterogeneity in the number of mutations, ranging from ~200 non-synonymous mutations per tumor to 2 (2) (Figure 2) Melanoma and lung tumors are among the tumors with the highest number of mutations due to the effect of mutagens (UV light and smoke) in the pathogenesis. While pediatric tumors and leukemia harbor only few point mutations (9.6 in average per tumor). The lower number of mutations in pediatric tumor can be explained by the fact that pediatric cancers occur in non–self renewing tissues or, in case of leukemia, from precursor cells that have not renewed themselves as often as in adults. It has been shown that, at least for some tumors, the number of mutations depends by the age and the cell division number (3). Additionally, the explosion in the amount of genomic data published in the last two decades shed light on the heterogeneity in the mutational landscape across different patients highlighting the need of patient specific therapies.

Although origin and genomic background of the cancers are heterogeneous, they share widely described common biological features, such as: a sustaining proliferative signaling, evading growth suppressors, resisting cell death, enabling replicative immortality, inducing angiogenesis, and activating invasion and metastasis (Figure 3) (4). These pathways are indeed targets of clinical or experimental anti-cancer drugs.

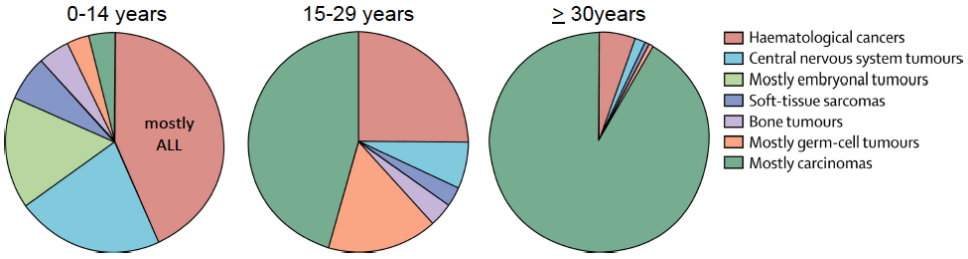

Figure 1. The relative incidence of cancer types changes across different age groups. Acute lymphoblastic leukemia is the most common disease in children. Relative proportions are for European populations covered by cancer registries. Data are derived from a total of 53'717 cases for age 0–14 years, 82'042 cases for age 15–29 years, and 5'950'220 cases for age ≥30 years. Adapted from (1).

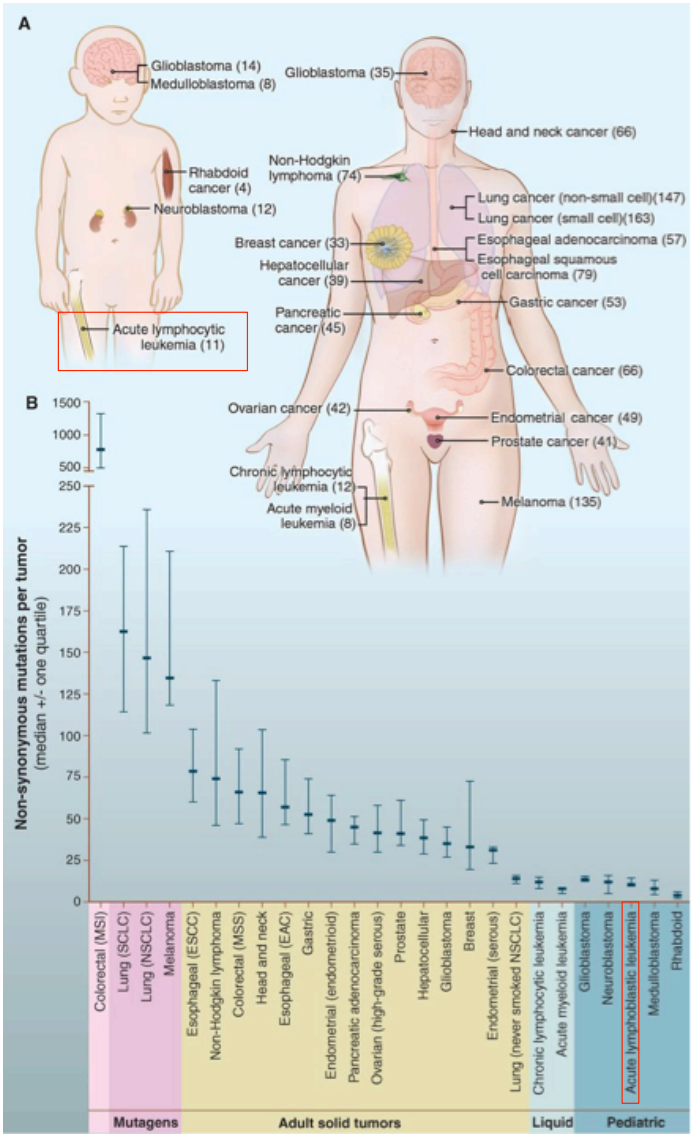

Figure 2. Different tumor types display heterogeneity in the number of mutations. (A) Tumors in children (left) and adults (right). Numbers in parentheses indicate the median number of non-synonymous mutations per tumor detected by genome-wide sequencing studies. (B) The median number of non-synonymous somatic mutations per human tumor. Error bars indicate the 25th and 75th quartiles. MSI, microsatellite instability; SCLC, small cell lung cancers; NSCLC, non–small cell lung cancers; ESCC, esophageal squamous cell carcinomas; MSS, microsatellite stable; EAC, esophageal adenocarcinomas. Adapted from (2).

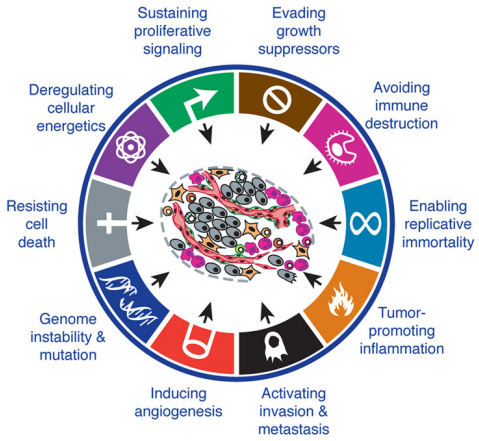

Figure 3. Cancers share widely described common biological features. The hallmarks of cancer and importance of tumor-associated microenvironment is summarized in the scheme. Adapted from (4).

1.2 Leukemia

Leukemia literally means "white blood" (*λευκός αίμα*, leukos aima) and is a cancer of the blood characterized by an abnormal increase of white blood cells.

Leukemias are usually divided into two major groups, acute and chronic leukemia. Acute leukemia is associated with a quick increase of immature white cells and may lead to death within a few weeks or months if not treated, while chronic leukemia progresses slowly, and is characterized by the abnormal proliferation of more mature white cells. Further classification depends on the lineage of the cell affected, distinguishing between myeloid and lymphoblastic leukemia: acute myeloid leukemia (AML), acute lymphoblastic leukemia (ALL), chronic myeloid leukemia (CML) and chronic lymphoblastic leukemia (CLL). While adults can get all types of leukemia, children typically show an acute form of the disease. The present doctoral thesis focuses on pediatric BCP-ALL (B-cell precursor acute lymphoblastic leukemia), which results from the clonal expansion of B-lymphoid cells arrested at an early stage of differentiation (Figure 4).

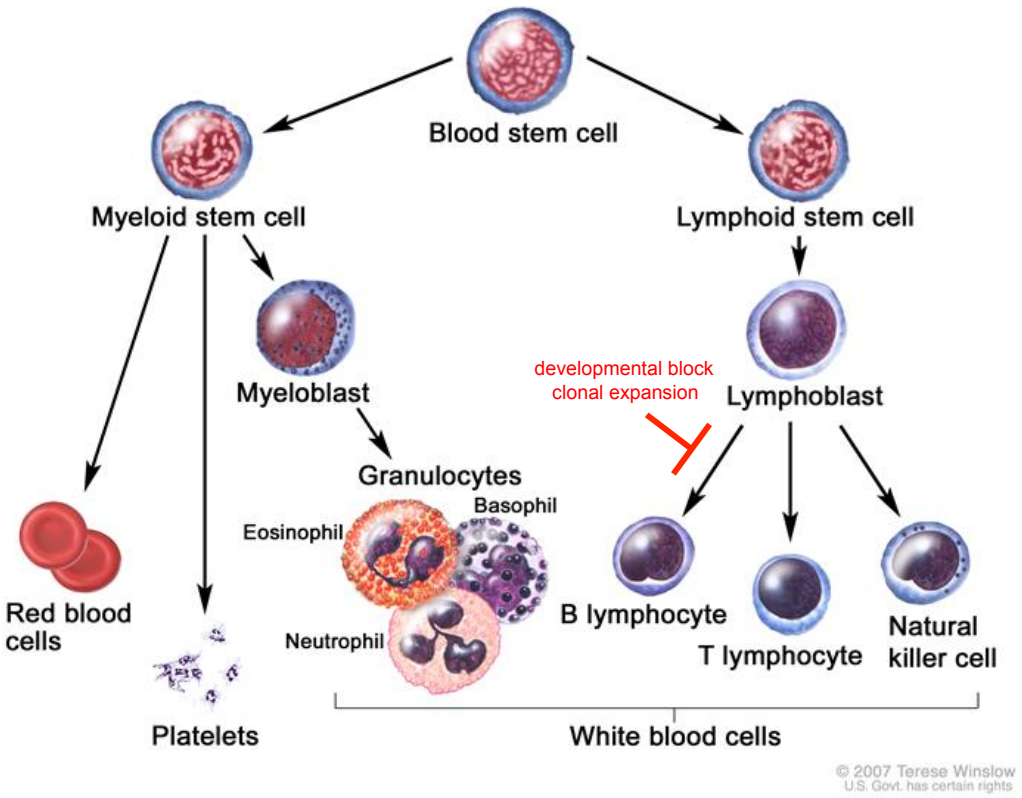

Figure 4. B-cell precursor ALL results from the developmental block and clonal expansion of committed B-cell precursor (red). Adapted from (5).

1.3 Childhood acute lymphoblastic leukemia (ALL)

1.3.1 Epidemiology

ALL is the most common cancer in children, representing about 30% of all childhood cancers and its diagnosis peak between the ages of 2 and 5 years. In Europe, ALL accounts for 80% of leukemia cases among children aged 0–14 years, with an annual incidence of 3-4 children per 100,000 individuals (6). In Switzerland, approximately 45 to 55 children per year are newly diagnosed with ALL (7). Around 80% of the cases belong to the B-cell precursor subtype, and the remaining 20% are T-ALL cases.

1.3.2 Etiology

Evidences indicated an association with disorders due to congenital genetic instability (i.e., Down syndrome, ataxia telangiectasia), prenatal exposure to X-rays, ionizing radiation and chemotherapeutic agents. Recent genome-wide studies reported associations between a higher risk for ALL and the presence of specific allelic variants (single nucleotide polymorphism in DNA sequence) of genes involved in the transcriptional regulation and differentiation of B-cell progenitors (*IKZF1, ARID5B, CEBPE* and *CDKN2A*) (8-10). Further studies have been conducted to investigate the role of infection, exposure to electromagnetic field and fetal growth, however very few of these findings are based on reproducible data or have a sufficient statistical power (11).

1.3.3 Symptoms

The common symptoms include fever, fatigue, bone or joint pain, bleeding and recurrent infections. These symptoms correlate with the uncontrolled growth of the malignant cell population invading the bone marrow, lymphoid organs, and extra-medullary (outside of the bone marrow) sites. Deregulated hematopoiesis leads to insufficient numbers of red, white mature blood cells and platelets and, indeed, common clinical features are anemia, neutropenia, thrombocytopenia, lymphadenopathy, splenomegaly and hepatosplenomegaly.

1.3.4 Diagnosis

Accurate diagnosis and classification are important for the successful treatment and biologic study of childhood acute leukemia. Disease subtypes, that are clinically and biologically relevant, are mainly classified based on patient clinical response, immunophenotype and genetic abnormalities of the disease. Bone marrow aspirates of the patient undergo multiple analyses:

a) Morphology

The morphologic diagnosis of leukemia requires examination of the bone marrow and is based on the microscopic features of the leukemia cells, analyzed by Wright-Giemsa-stained smears. ALL are classified according to the French-American-British (FAB) system. Analysis of the morphology still represents the fastest method to clinically diagnosis leukemia, and an experienced analyst can immediately distinguish between ALL or AML. However, the recent WHO International panel on ALL recommends the abandonment of the FAB classification, since it lacks independent clinical or prognostic significance, and suggests instead the use of the immunophenotypic classification described in the next section.

b) Immunophenotype

The diagnosis and treatment of ALL are depended on the tumor cells lineage and stage of maturation. Immunophenotypic analysis is, therefore, an essential part of the diagnostic phase, as it establishes the leukemic cell lineage and determines the stage of differentiation.

Immunophenotyping divides ALL into two broad, but clinically and biologically meaningful, categories: B-cell ALL (B-ALL) and T-cell ALL (T-ALL). A panel of antibodies is used to define the diagnosis of ALL by flow cytometry. This process includes markers that are highly lineage specific (for example, CD19 marks the B-lineage and CD7 the T-lineage). Additional markers are used for subtype classification (Table 1).

Type	Lineage specific	Subtype classification	
B ALL	CD19, CD22, CD79a, CD10	pro-B-ALL	no expression of others differentiation B-cell antigens
		common all	CD10
		pre-B-ALL	cytoplasmic IgM
		mature B ALL	cytoplasmic or surface kappa or lambda
T ALL	CD7, CD3	ETP	CD5, CD34, CD117, CD11b, CD13, CD65, HLA-DR
		pro-T	CD7
		pre-T	CD2, CD5, CD8
		cortical T	CD1a
		mature T	CD3, TCR

Table 1. Markers used for lineage assignment and subtype classification at diagnosis. Lineage markers according to WHO 2008 criteria (12). Subtype classification markers according to AIEOP-BFM ALL Immunophenotyping Consensus Guidelines (13), which is based on the European Group for the Immunological Characterization of Leukemia (EGIL) guidelines (14) .

c) Genetic features

ALL displays significant heterogeneity at genetic level. The genetic characteristics define disease subsets with distinct biologic behavior and prognostic implications. They are used in the risk stratification in most modern treatment protocols. Genetic abnormalities, such as chromosomal translocations, changes in ploidy, amplification and deletions in recurrent affected genes, are analyzed by chromosomal analysis, RT-PCR, fluorescence *in situ* hybridization and MLPA (Multiplex Ligation-dependent Probe Amplification), a multiplex PCR method that can detect abnormal copy numbers of genomic DNA.

1.4 Prognostic factors in acute lymphoblastic leukemia

The prognosis of childhood ALL has improved dramatically over the last five decades, as a result of therapy adaptation based on the risk for relapse and continual reconfiguration of existing chemotherapeutic drugs. Treatment protocols stratify patients based on multiple factors such as genetics, immunophenotype, patient age, white blood count and treatment response (Table 2).

	FAVORABLE OUTCOME	UNFAVORABLE OUTCOME
Clinical factors	Age: 1-9 years old Leukocyte count < 50,000 cells/uL B-ALL	Age: < 1 or > 10 years old Leukocyte count > 50,000 cells/uL T-ALL
Cytogenetic abnormalities	Hyperdiploidy *ETV6-RUNX1* t(12;21) *TCF3-PBX1* t(1;19)	Hypodiploidy *BCR-ABL1* t(9;22) *TCF3-HLF* t(17;19) *MLL* gene rearrangement *iAMP*21
Minimal residual disease	Negative MRD at day 33 with sensitivity of at least 10^{-4}	High risk: MRD level > 10^{-3} at day 78 Very high risk: positive MRD assessment at week 22

Table 2. Factors used for risk stratification in childhood ALL. Adapted from (15)

1.4.1 Cytogenetic abnormalities

Currently, 75% of childhood B-Cell Precursor (BCP) ALL patients are classified according to defined cytogenetic subgroups associated with clinical outcome (Figure 5 and Table 3 for a complete list, updated in January 2015).

A

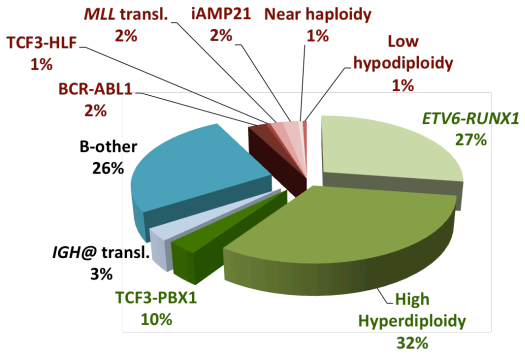

B

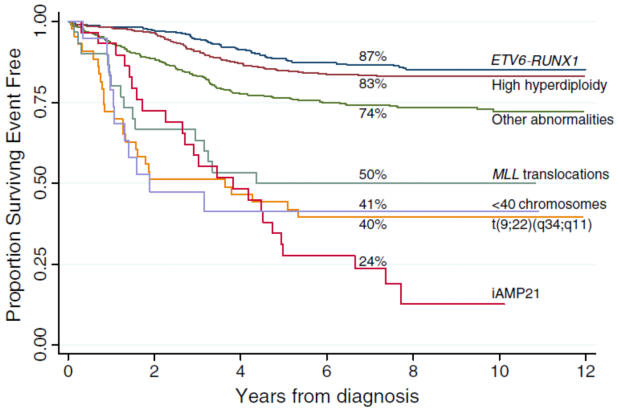

Figure 5. Cytogenetic alterations have strong implications on survival. A) B-cell precursor (BCP) ALL cytogenetic subtypes. Frequency of each subtype among BCP-ALL cases is shown. In red are the subtypes associated with poor prognosis and in green those with favourable outcome. Adapted from (16). B) Event free survival probability at 12 years of some cytogenetic subtypes shown in A. Adapted from (17).

Subtype	Frequency among childhood ALL (%)	Prognosis
Hyperdiploidy (more than 50 chromosomes)	20–30	Good
t(12;21)(p13;q22) translocation encoding *ETV6–RUNX1* fusion	15–25	Good
t(1;19)(q23;p13) translocation encoding *TCF3–PBX1* fusion	2–6	Good
t(8;14)(q24;q32), t(2;8)(q12;q24), t(2;8)(q12;q24) encoding; *MYC* rearrangement	2	Good
ERG-deregulated ALL	7	Good
Hypodiploidy (less than 44 chromosomes)	2–3	Poor
iAMP21	2	Poor
t(17;19)(q22;p13) translocation encoding *TCF3-HLF* fusion	1	Poor
t(9;22)(q34;q11.2) translocation encoding *BCR–ABL1* fusion	2–4	Poor*
Philadelphia-like ALL	10–15	Poor
t(4;11)(q21;q23) translocation encoding *MLL–AF4* fusion	1–2	Poor
CRLF2 rearrangement (*IGH–CRLF2*; *PAR1* deletion and *P2RY8–CRLF2*)	5–7	Poor

Table 3. Cytogenetic subtypes of B-cell precursor ALL that are associated with clinical outcome. *Historically poor outcome, prognosis improved with addition of imatinib and/or dasatinib to intensive chemotherapy. Adapted from (18) .

1.4.2 Clinical response (Minimal residual disease assessment)

Evaluation of treatment response is the most powerful predictor for the risk of disease recurrence. Precise time points over the treatment and residual leukemia thresholds have been established for the monitoring of the minimal residual disease (MRD). The predictive value of this strategy has been confirmed independently by several studies (Figure 6) (19-21). MRD can be assessed by quantitative RT-PCR and flow cytometry. RT-PCR detects leukemia specific immunoglobulin (Ig) and T-cell receptor (TCR) gene rearrangement or fusion transcripts. Immunophenotyping by flow cytometry discriminates lymphoblasts, since they typically show an aberrant pattern of expression of immunologic markers compared to healthy lymphocytes.

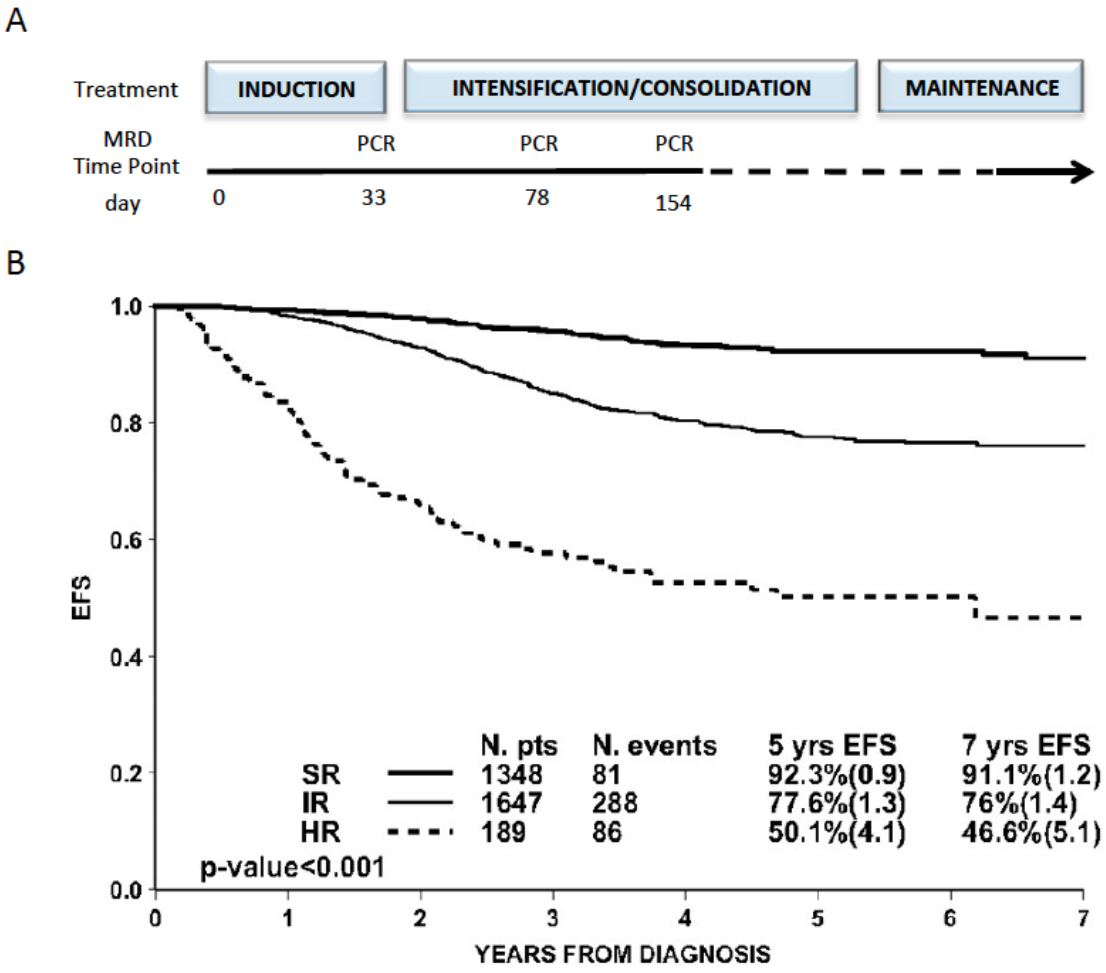

Figure 6. Minimal residual disease assessment by PCR is the most powerful predictor for the risk of disease recurrence. A) Scheme of the time points over the patient treatment phases, adapted from AIEOP-BFM ALL 2009. Patients are considered MRD standard risk (SR) if MRD is already negative at day 33 (with a sensitivity of at least 10^{-4}); MRD high risk (HR) if 10^{-3} or more at day 78; others are classified as intermediate risk (IR). Patients that are still positive at day 154 are classified as Very High Risk (VHR). B) Event-free survival according to PCR-MRD classification. Large prospective study of 3'184 BCP-ALL patients. 42% were MRD-SR, 52% MRD-IR, and 6% MRD-HR; they had a significantly different outcome with 7-year EFS estimates of 91.1%, 76%, and 46.6%, respectively.(22)

1.5 Clinical treatment of ALL pediatric patients

1.5.1 Phases of the treatment

Swiss patients with ALL are treated uniformly according to the international AIEOP-BFM-ALL-2009 treatment protocol (NCT01117441). The treatment includes three phases (Figure 7 and Table 4): induction of remission, intensification/consolidation and maintenance. Importantly, differences in the treatment regimens are applied according to risk group, aiming to obtain an effective treatment with low toxicity.

1) The induction of remission phase aims to eradicate the initial leukemia burden. Treatment regimen consists of a 3-drugs (vincristine, steroids and asparaginase) or of a more intense 4-drug mix (i.e., adding anthracycline). Patients with *BCR-ABL1* positive disease benefit from the early treatment with tyrosine kinase inhibitors.

2) The intensification/consolidation treatment phase has the goal to eliminate drug resistant residual leukemic cells and therefore reduce the risk of relapse. Administered drugs during this phase can vary based on the risk stratification.

3) The purpose of the maintenance phase is to preserve remission and contrast relapse.

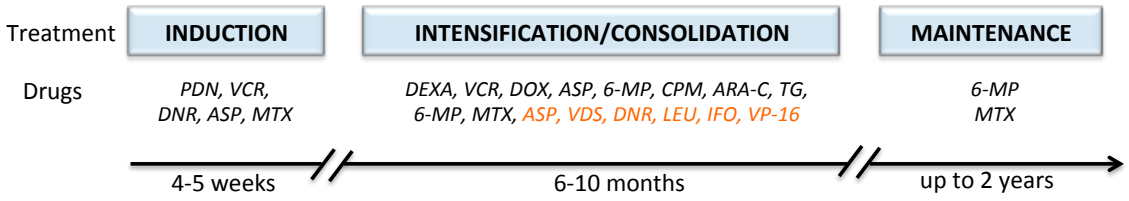

Figure 7. Scheme of the phases included in the treatment protocol for ALL. Combinations of different drugs are administered over the different treatment phases. Additional drugs for high risk cases are indicated in orange. Scheme adapted from AIEOP-BFM ALL 2009. Abbreviations: Prednisolone (PDN), Vincristine (VCR), Daunorubicin (DNR), Asparginase (ASP), Methotrexate (MTX), Cyclophosphamide (CPM), Cytarabine (ARA-C), Mercaptopurine (6-MP), Dexamethasone (DEXA), Vindesine (VDS), Ifosfamide (IFO), Etoposide (VP-16), Thioguanine (TG), Leucovorin (LEU).

1.5.2 Stem cell transplantation and intrathecal chemotherapy

Allogeneic hematopoietic stem cell transplantation counts as the most intensive treatment and is considered an option for resistant cases. Intrathecal chemotherapy with methotrexate, hydrocortisone and cytarabine is administered to ALL cases with an increased risk of relapse in the central nervous system, such as cases with: high risk genetic features, T-cell immunophenotype, large leukemia-cell burden, or the presence of leukemia cells in the cerebrospinal fluid.

CLASS	SUBCLASS	Mechanism	Drug name
Antimitotic		Bind tubulin and block elongation microtubules	Vincristine
		Stabilize microtubule and block disassemblying	Docetaxel, Paclitaxel
Antimetabolite	Analogue nucleoside	Incorporated in DNA	Thioguanine, Gemcitabine, Cytarabine, Clofarabine
	Analogue of hypoxanthine	Inhibit synthesis of AMP, GMP and first step of purine synthesis	Mercaptopurine
	Analogue of folic acid	Inhibit synthesis of GMP, AMP, dAMP, dGMP	Methotrexate
Antracycline		Inhibit topo II	Etoposide
		Intercalate DNA and stabilize cleavage complex	Daunorubicin, Doxorubicine Idarubicine, Mitoxantrone
		Inhibit topo I	Topotecan
DNA cross-linking	Alchilant	Attach alkyl group to the guanine base of DNA	Cyclophosphamide
Glucocorticoids		Ligand of GR inducing antinflammatory immunosuppressive effect	Prednisolone , Dexamethasone
Asparginase		Hydrolyzes the amino acid L- asparagine to L-aspartic acid and ammonia	Aspargine

Table 4. Classification of the most common drugs used for ALL based on the mechanism of action.

1.6 Key mechanisms driving leukemogenesis during B-cell development

B-cell development is a multistep process, in which hematopoietic stem cells (HSCs) differentiate sequentially into common lymphoid precursors (CLP), B-cell precursors and finally become mature B-cells expressing the B-cell receptor (Figure 8). Normal differentiation requires the coordination of the intrinsic cell differentiation program, appropriate recombination of the immunoglobulin forming the B-cell receptor and interactions with microenvironment.

Here I describe two mechanisms contributing to leukemogenesis during B-cell development:

1) Illegitimate RAG recombination activity
2) Mutations in transcription factors involved in B-cell development.

These mechanisms are important for understanding the findings present in Manuscript 1.

1.6.1 Illegitimate RAG recombination activity contribute to genome instability

In pro-B cell and pre-B cell precursors the genetic elements that encode the antigen specific B-cell receptors (BCR or immunoglobulin) are assembled by *V(D)J* rearrangement (Figure 9). Their rearrangement is primarily mediated by the RAG endonucleases, RAG1 and RAG2. RAG enzymes recognize recombination signal sequence (RSS) motifs consisting of a highly conserved heptamer (CACAGTG) and a less conserved nonamer (ACAAAAACC) sequence separated by a 12-bp or 23-bp sequence-independent space. RAG endonucleases bind DNA at RSS motifs and cleave DNA. Processing of these ends often involves the addition of Non-Template Sequence (NTS) at the breakpoint by Terminal Deoxynucleotidyl Transferase (TdT). It has been reports that in some cases RAG and TdT recombination can induce illegitimate recombination at genetic sites outside of the *V(D)J* regions. (23). Heptamers or nonamers outside the context of a conserved RSS and deaminated methyl CpGs elements have also been associated with mechanisms of RAG activity contributing to genome instability and the development of lymphoid malignancies.

1.6.2 Mutations in transcription factors involved in B-cell development

B-cell differentiation relies on the activation of multiple transcription factors (*RUNX1, ERG, IKAROS, TCF3, EBF1* and *PAX5*) at specific times during development (Figure 8 and 9) (24). Genomic studies have shown that mutations in these transcriptional regulators are highly enriched in ALL suggesting their important role in leukemogenesis. More information on *TCF3* and *PAX5* transcription factors are reported below because they are relevant for Manuscript 1.

a) *TCF3*

TCF3 (transcription factor 3) or also called E2A (immunoglobulin enhancer-binding factors E12/E47), is a transcription factor essential for B-cell development (25). TCF3 proteins (isoforms E12 and E47) derive from alternative splicing and contain the helix-loop-helix (HLH) DNA binding domain. E proteins activate transcription by binding to regulatory E-box sequences on target genes as homodimers or heterodimers. The E12 and E47 differ by 20% in their amino acid sequence of the HLH domain, however differences in their function have not been shown.

E2A is upregulated at the common lymphoid progenitor (CLP) stage of development and remains high in pro-B, pre-B and immature B cells in the bone marrow (26) (Figure 13). TCF3 drives the expression of a number of B-cell specific genes essential for B-cell development including *Pax5, Foxo1, Ebf1, Rag1, Rag2, Lgll1, Vpreb1* and *Cd79a.* Moreover, E2A represses myeloid/erythroid-lineage-specifying genes, such as *Gata1, Csf1r and Epor*.

Lymphoid defects in *Tcfe2a*$^{-/-}$ mice are already apparent at the CLP stage of the development and a major development block occurs at the pre-B cell and pro-B cell stages (27-29). E2A-deficient lymphoid cell lines have the capacity for multi lineage differentiation (30, 31).

TCF3 is implicated in several different types of hematological malignancies. In pediatric B-cell precursor ALL, *TCF3* is rearranged with *PBX1* or *HLF* genes to form *TCF3-PBX1* and *TCF3-HL*F chimeric transcription factors, while recurrent mutations in *TCF3* are found in Burkitt's lymphoma (32).

b) *PAX5*

The *PAX5* gene belongs to the paired box (PAX) gene family of transcription factors. PAX5 is expressed in constant level from the pro-B cell stage onwards until it is down regulated in plasma cells (Figure 13) (33). PAX5 binds to thousands of promoter regions and induces activation of genes important for the B-cell development, like co-receptors *Cd21* and *Cd19, MB-1/Cd79a,* and repression of alternative gene expression program, i.e. PAX5-repressed genes are *Mcsfr, Notch1* and *Flt3* (34-36). In absence of *Pax5*, B-cell development is arrested at the pro-B cell stage of differentiation (37), and *Pax5*$^{-/-}$ pre-B cells have extraordinary developmental plasticity showing hematopoietic stem cell features such as multi-potency and self-renewing capacity (38).

PAX5 is the most frequently mutated gene, which is affected in over one-third of B-ALL cases by deletions, sequence mutations or translocations. Most of the *PAX5* aberrations are hemizygous and somatically acquired. These mutations lead to reduced expression level of PAX5 (haploinsufficiency), but still allow the expression of PAX5 target genes, like *CD19, RAG1* and *RAG2*. Recent studies in *Pax5*$^{-/+}$ mice have showed that haploinsuffiency of PAX5 favors the acquisition of secondary genetic changes and therefore the leukemogenesis. *PAX5* deletions occur in about 13% of BCP-ALL cases, however, the frequency increases when ALL subgroups are considered. For example, 27% of *TEL-AML1*-positive ALL (39), 28% of high risk for relapse ALL (40), 51% of *BCR–ABL1*-positive ALL (41) have *PAX5* deletions. It has been shown that *PAX5* alterations are not associated with poor outcome, but rather seems to be a secondary important event, since it is frequently associated with other lesions.

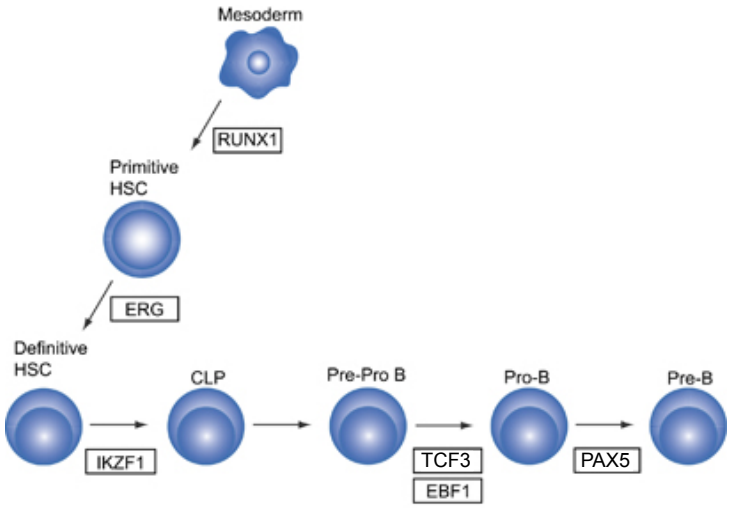

Figure 8. Overview of the normal function of the B-lineage transcription factors affected in B-cell precursor ALL. *RUNX1* is required for the emergence of primitive HSC, *ERG* for definitive HSC maintenance, *IKZF1* for the formation of Common Lymphoid Progenitors (CLPs), *TCF3* and *EBF1* for the generation of pro-B cells, *PAX5* to generate functional pre-B cells and maintain B-cell identity. (24)

.

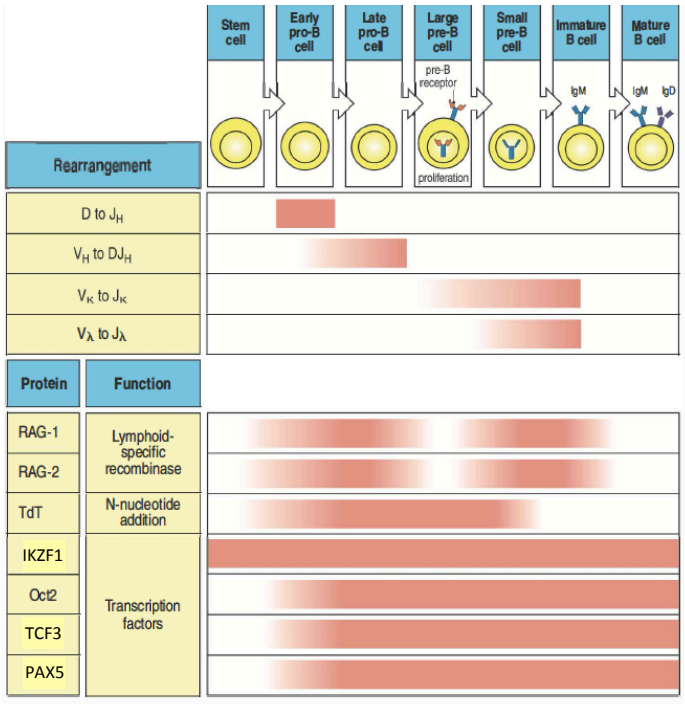

Figure 9. Expression of surface protein receptors and transcription factors in B-cell development. Adapted from (42).

1.7 Model of leukemogenesis

In most of the ALL cases chromosome translocations are often early or initiating events in leukemogenesis. A prenatal origin of the translocation in pediatric ALL has been demonstrated for *MLL-AF4* (43) and *TEL-AML1* (44)**.** Chromosomal rearrangements disrupt genes that regulate normal hematopoiesis or activate tyrosine kinases. Although these genetic changes are necessary to support the leukemic transformation, experimental models have showed that they are usually not sufficient to cause the disease, but additional structural alterations and/or sequence mutations are needed. Such cooperative lesions lead to the block of differentiation, aberrant proliferation and resistance to programmed cell death (Figure 10 and Table 4) (45).

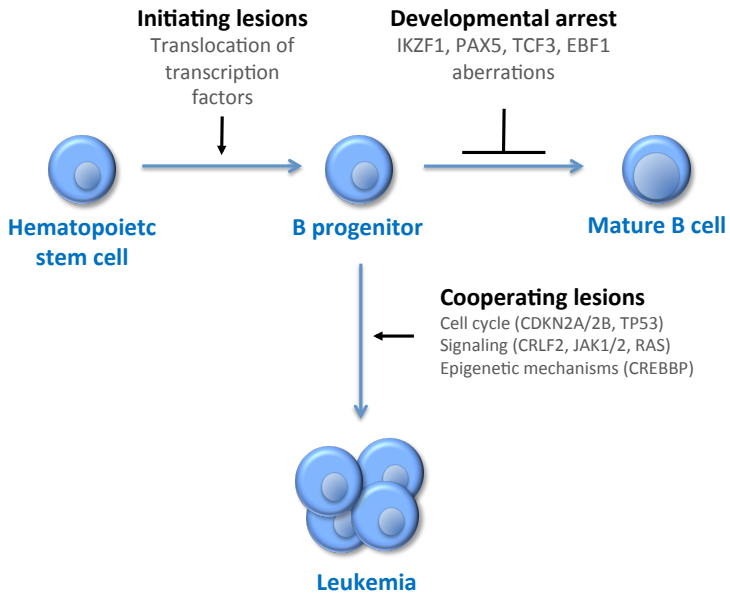

Figure 10. Molecular pathogenesis of ALL implicates the cooperation of initiating lesions and additional genetic alteration. Initiating lesions, usually translocations, are associated with additional aberrations affecting genes implicated in the lymphoid development (*IKZF1, RUNX1, TCF3, EBF1, PAX5, VPREB1* and *RAG1/RAG2*), control of survival and proliferation (*ABL1, NRAS/KRAS, JAK2, IL7R, CRLF2*), transcriptional regulators (*TBL1XR1, CREBBP, BTG1*) and tumor suppressor genes (*RB1, CDKN2A, CDKN2B and TP53*). Adapted from (45).

1.7.1 Recurrent genetic alterations

Increasing numbers of genome-wide studies (40, 46-51) have identified recurrent mutations in pathways that govern B-cell development, cell cycle, in signaling pathways, epigenetic regulators (Figure 11 and Table 5). A comparison of diagnostic and relapse ALL cases revealed clonal diversity comparable between the two disease states, although for half of the patients usually one minor clone from diagnosis survives, acquires additional mutations and becomes the relapse clone founder. Relapse-specific mutations have been found, such as *NT5C2* (52), *TP53* (53), *NRAS* (46, 54), *IKZF1* and *CREBBP* (55). Mutations in these genes were never present in the falling clones after treatment, except for RAS mutations (46).

Gene	Alteration type	Frequency (%)	Affected pathway	Clinical relevance
PAX5	Focal deletions, translocations, sequence mutations	31.7% of B-ALL, 70% of *TCF3-HLF* -positive B-ALL	B-lymphoid development	Important, but not essential for leukemogenesis; not associated with adverse outcomes
IKZF1	Focal deletions, sequence mutations	15%of B-ALL, 70–80% of *BCR–ABL1*-positive patients with ALL, 33% of patients with high-risk *BCR–ABL1*-negative B-ALL	Development of HSC to lymphoid precursor	Associated with poor outcome
JAK1/2	Pseudokinase, kinase domain mutations	18–35% DS-ALL, 10.7% high-risk *BCR–ABL1*-negative ALL	Constitutive JAK–STAT activation	Potential for targeting with kinase inhibitors
CRLF2	Rearrangement as *IGH–CRLF2* or *P2RY8–CRLF2* resulting in overexpression	5–16% B-ALL, >50% DS-ALL, 50% of Ph-like ALL	Constitutive STAT activation	Associated with poor outcome, potential for targeting with kinase inhibitors
Kinase activating alterations	Rearrangements of *ABL1, ABL2, CSF1R, EPOR, JAK2, PDGFRB*; sequence mutations of *IL7R* and *FLT3;* deletions of *SH2B3*	10% pediatric B-ALL	Activation of kinase signalling pathways	Associated with high-risk features and increased risk of relapse, potential for targeting with kinasese inhibtor
CREBBP	Focal deletion and sequence mutations	19% of relapsed ALL	Impaired histone acetylation and transcriptional regulation	Mutations selected at relapse, associated with glucocorticoid resistance
NT5C2	Sequence mutations	Up to 20% relapsed ALL	Purine metabolism	Mutations selected at relapse, confer resistance to nucleoside analogues
TP53	Sequence mutations	Hallmark of low hypodiploid ALL at diagnosis, otherwise uncommon in major clone at diagnosis	Tumor suppressor regulating cell cycle, apoptosis, senescence, DNA repair, changes in metabolism	Confer risk of developing hypodiploid ALL and relapse, associated with disease relapse

Table 5. Recurrent genetic alterations identified in pediatric B-cell precursor ALL. Adapted from (18).

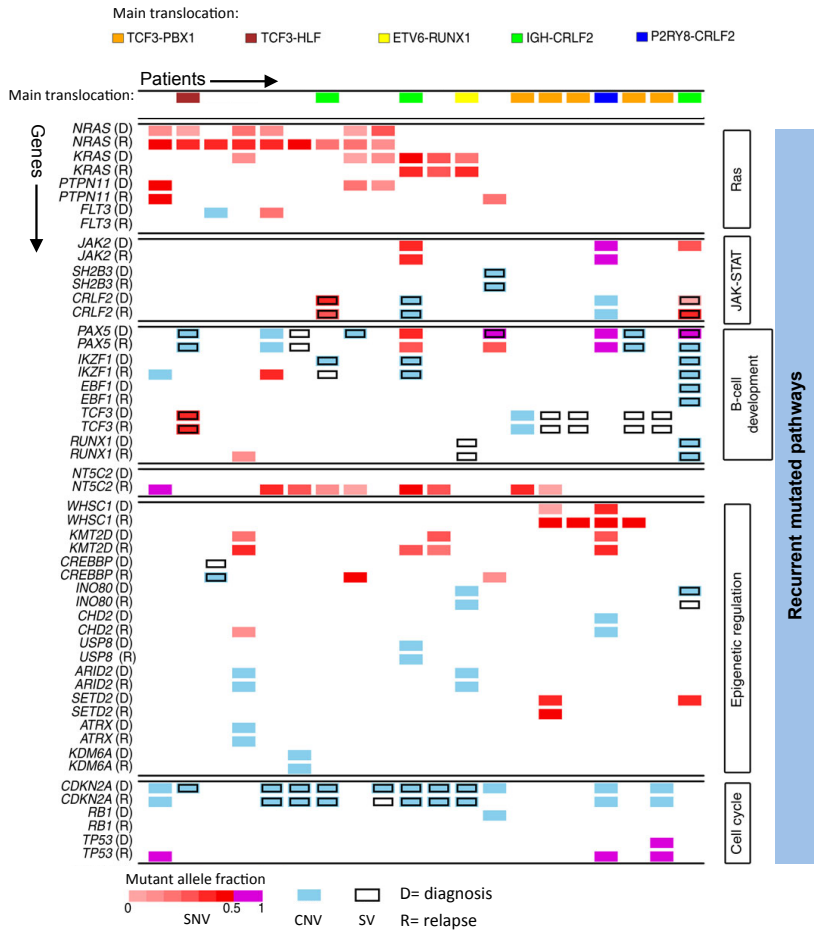

Figure 11. Recurrent mutated pathways in B-cell precursor ALL at diagnosis and relapse. Recurrent lesions are found in RAS pathway, JAK-STAT signaling, transcriptional regulation of lymphoid development, nucleoside metabolism, epigenetic modification and cell cycle regulation. Abbreviations: Single Nucleotide Variation (SNV), Copy-Number Variations (CNV), Structural Variations (SV). Adapted from (46).

1.7.2 Integration of the genomic and cytogenetic data to improve risk stratification criteria

Multiple genetic alterations are required in the pathogenesis of B-ALL, therefore development of new genetic biomarkers that consider constellations of genetic lesions, rather than single gene mutation or translocation, are needed (56). Specific patterns of lesions are associated with poor outcome, for example, *IKFZ1* deletions in *BCR-ABL1*-positive and *BCR-ABL1*-negative ALL (57). Recently Moorman et al. have defined new criteria of risk stratification combining cytogenetic data with the copy number variation profile of each patient. Based on this integrated approach clinical response could be predicted and a large subset of children suitable for treatment deintensification could be identified (58).

1.8 *TCF3-HLF* and *TCF3-PBX1* -positive ALL model

This thesis focuses on *TCF3-HLF* and *TCF3-PBX1*-positive ALL subtypes both of which are associated with the translocation of *TCF3*, but have opposite clinical outcomes (Figure 12). *TCF3-HLF*-positive ALL is rare (~1% of BCP-ALL cases) and currently not curable, while *TCF3-PBX1*-positive ALL is more frequent (10% of BCP-ALL) and associated with good outcomes (the median five-year event-free survival rate rich 78-85%).

Figure 12. Transactivation domain of *TCF3* is rearranged in *TCF3-HLF* and *TCF3-PBX1*-positive ALL subtypes resulting in disease with opposite outcomes. Both translocations involved the same N-terminal portion containing the transactivation domains of *TCF3*. Abbreviations: *TCF3*, transcription factor 3; *PBX1*, pre-B-cell leukemia transcription factor 1; HLH, hepatic leukemia factor; AD, activation domain; bHLH, basic helix-loop-helix; PAR, prolin/acidic amino acid rich domain; bZIP, basic leucin zipper; HD, homeodomain domain. Adapted from (59).

1.8.1 *TCF3-HLF*-positive ALL

The TCF3-HLF fusion protein is resulted from t(17;19)(q22;p13) translocation in which the N-terminal transactivation domains of *TCF3* are joined to the basic leucine zipper dimerization domain of *HLF. TCF3* is involved in the B-cell development and *HLF* is a member of the proline and acidic amino acid-rich basic leucine zipper (PAR bZip) transcription factor family. *HLF* is expressed in the liver, but not in the hematopoietic system.

Two types of genomic rearrangements underlie the fusion of *TCF3* with *HLF*. In type I rearrangement, a cryptic exon occurs between *TCF3* exon 16 and *HLF* exon 4. This cryptic exon insertion includes intronic portions of both *TCF3* and *HLF* genes. Type II rearrangement results from the fusion of *TCF3* exon 15 spliced to *HLF* exon 4. Non-template nucleotides are included at the break point in both types to maintain the proper *HLF* reading frame (60). No difference in the DNA-binding, but a slight difference in transcriptional transactivation activity were found in a comparison of type I and type II TCF3-HLF fusion proteins (61). However, no clear correlation of either type with outcome was detected.

An early study has shown the importance of TCF3-HLF protein for the survival of human leukemia cells. Overexpression of a dominant negative form of *TCF3-HLF*, which lacks the transactivation domain of *TCF3* and has a defective *HLF* basic domain, leads to apoptosis of leukemia cells (62). However, attempts to generate a transgenic mouse model of this disease failed. Overexpression of human *TCF3-HLF* under the control of the Eμ enhancer with the SV40 promoter did not recapitulate the abnormal proliferation of precursor B-cells (63). In this model, a *TCF3-HLF* fusion protein could be expressed by mature B-cells indicating that B-cells were not blocked in the development. Only half of the mice developed leukemia and in 90% of the cases was T-ALL. Another model used the Ig enhancer with its corresponding Ig promoter to express *TCF3-HLF* (64), but also in this model the human disease has not been recapitulated. These data suggest that additional mutations or a specific cell of origin may be required.

1.8.2 *TCF3-PBX1*-positive ALL

The TCF3-PBX1 fusion protein derives from the t(1;19)(q23;p13) translocation. The N-terminal portion of *TCF3* (19p13, exons 1-16) including the transactivation domains is joined with the C-terminal Hox homeodomain of *PBX1* (1q23, exons 4-9) (65). *PBX1* belongs to homeobox gene family, which are classical master regulators of developmental programs. *PBX1* is normally not express in B or T lymphocytes.

Targets of TCF3-PBX1 have been recently identified by chromatin immunoprecipitation (ChIP) in a human *TCF3-PBX1*-positive ALL cell line (697) and a primary *TCF3-PBX1*-positive ALL sample. ChIPseq data revealed that TCF3-PBX1 binds to promoter regions of genes that encode key components of the pre-BCR, including *IGLL1, VPREB1* and pre-BCR downstream signaling molecules (*BLK, LCK, SYK, ZAP70, PIK3CD*). TCF3-PBX1 induces the overexpression of BCL6 through pre-B signaling. The *BCL6* proto-oncogene represents an essential prosurvival factor at the pre-BCR checkpoint during early B-cell development. BCL6 reinforces the pre-BCR signaling activation by the transcriptional activation of multiple pre-BCR related proteins (IGLL1, VPREB1, BLK, SYK, PIK3D) and by the transcriptional repression of the inhibitory phosphatase PTPRO (66).

In *in vitro* experiments TCF3-PBX1 fusion protein seems capable to transform both lymphoid and fibroblast cell lines (67). However attempts to assess the oncogenic potential of E2A-Pbx1 translocation in primary murine B-lineage cells have not yielded successful mouse models (68), likely secondary genetic events are required for leukemic transformation.

1.9 Utility of Patient Derived Xenograft (PDX) mouse models in B-cell precursor ALL

In research the use of model systems is indispensable for studying biological phenomena underlying malignant cell transformation and cancer progression. Despite cell lines have been preferred as model system since they are inexpensive and easy to handle, their use implicates two major limitations: cell lines cannot be established from all patients and are not representative of the clonal heterogeneity of the tumor. In the field of ALL genetic engineered mouse models mimicking known genetic aberration are not always able to recapitulate the human disease, like *TCF3-HLF* (63, 64), *MLL-AF4* (69), *TEL-AML1* (70), *BCR-ABL1* (71)–positive ALL. Moreover, mouse model cannot be generated for ALL subtypes with unknown aberrations. Especially in the context of scientific research focus on the development of personalized medicine, alternative systems that allow to model patient specific features are needed.

In the last decade, PDXs have been established for several subtypes of leukemia with known (72-74) and unknown genetic (51, 75) aberrations. Primary patient material is transplanted by intravenous or intraosseal into immunodeficient mouse strains. Animals develop leukemia, which exhibits biological features and dissemination pattern similar to the one observed in humans. Leukemia cells circulate in the blood flow and accumulate mainly in the bone marrow and spleen. More than hundreds millions of cells can be usually harvested from the spleen of the mice even after transplanting only 1 million of patients cells. It has been shown that the leukemia samples after amplification in NSG mice (NOD.Cg-Prkdc^{scid}Il2rg^{tm1Wjl}/SzJ) generally reproduced the immunophenotype and drug sensitivity profile -although few clinical drugs were tested- of original human tumor (75, 76). However the influence of mouse microenvironment on the disease evolution in this system is still matter of investigation and it depends not only on the recipient (more or less permissive mouse strain) but also on the intrinsic properties of transplanted cells. It was shown that clonal composition of leukemia samples was to some extend altered after xenotransplantation (72, 73, 75, 77). This concerned rather quantitative than qualitative relationships between individual sub-clones and in majority of the cases clones present after xenotransplantation could be backtracked to diagnostic sample. Due to the possible variability associated with PDXs, their genetic characterization is required. Overall PDX models are very useful for representing the patient leukemias with known and unknown aberrations and the tumor multi-clonal composition. They also constitute a theoretically unlimited source of primary BCP-ALL cells for experimental use.

1.10 Integration of functional and genomics approaches to develop personalized cancer therapies

Integration of functional and genomic screening strategies aims to identify genetic biomarkers predictive of patient response to specific drugs and to develop effective and less toxic targeted therapies. Progresses in the next generation sequencing technics allowed to discover underlying biological pathways that drive leukemogenesis. Leukemia specific targets have been identified, but therapeutic options targeting these lesions are still rare. The only successful example in the field of leukemia is the clinical use of tyrosine kinases inhibitors (TKIs), which selectively target the protein product of the *BCR-ABL1* translocation. The development of tyrosine kinase inhibitors (TKIs), such as imatinib, consistently improved the outcome of chronic myelogenous leukemia (CML) (78) and pediatric *BCR-ABL1*-positive ALL (79). Therefore, development of new targeted therapies to extend to other subtypes of ALL, it remains the next challenge.

1.10.1 Next-generation sequencing methods

Next generation sequencing (NGS) methods enable the sequencing of millions of fragments of DNA from a single sample at the same time. This unprecedented throughput, scalability and speed, have led to previously unimaginable scientific achievements and novel biological applications. Different NGS techniques have diverse capability and sensitivity in detecting mutations and structural variations:

-Targeted sequencing provides sensitive and deep coverage of targeted sites, but only a set of genes or hotspot of mutations are studied.

-Exome sequencing detects mutations present at subclonal level in all protein-coding region of the genome.

-Transcriptome sequencing is the most informative approach, which allows the identification of chromosomal rearrangements, mutations, expression of the mutations, gene-expression profiling, new transcripts and gene isoforms.

-WGS entails the sequencing of the whole genome of a sample, but with less sensitivity respect exome sequencing due to the large size of the human genome and variation in the sequencing coverage along the genome (18).

1.10.2 *In vitro* drug screening using primary patient cells

Preclinical *in vitro* drug screenings are essential to validate genomic biomarkers, explore the molecular basis of drug activity and identify novel effective compounds.

In the last few years *in vitro* drug screening platforms using patient cells have been developed. Tyner et al. (80) assessed the sensitivity to 66 small molecule kinase inhibitors of 151 leukemia patient samples. Promising data have showed that *in vitro* drug sensitivity could predict clinical drug response, as well as pathway dependence. For example, based on *in vitro* drug profile data, kinases targeting ABL1 and related pathways were predicted as the best targets for targeted therapy in a *BCR-ABL1*-positive ALL case. Pemovska et al. (81) have performed drug screening of primary AML patient cells. In the library were included 187 drugs targeting pathways affected in cancer like, cell cycle, apoptosis, signaling and epigenetic regulators. The compounds included were already used in the clinic or in late phase of the clinical trials. Although each individual sample showed a drug selective-response profile, similar drug sensitivity patterns were observed across the samples. Also in this study correlation between *in vitro* drug response and clinical response was shown for few samples and they could identify associations between gene mutated and response to drug targeting

the affected gene (i.e., samples with *FLT3* mutation were sensitive to TKIs as expected). However, beyond few examples of drug sensitivity and gene mutation associations, the majority of drug sensitivity or resistant profile could not be directly attributed to obvious genetic alterations.

1.10.3 *In vitro* high-throughput drug screening in co-culture with bone marrow stromal cells

Hartwell et al. (82) have recently performed a high-throughput drug screening system that includes the supportive interactions of the leukemia stem cells with the microenvironment. Leukemia stem cells were generated by retroviral transduction of *MLL-AF9* (frequent translocation in AML) in murine granulocyte-monocyte progenitors and the transduced cells were amplified in BALB6 mice. These leukemia stem cells were co-culture with a murine stromal cell line (OP9) and sensitivity to 14'718 compounds was tested. Co-culture system enabled to assess drug response in a more physiological context, indeed the bone marrow niche supports survival and have a chemoprotective effect in AML (83). Similar findings have been shown for ALL. Indeed, direct contact or secreted cytokine and growth factor provided by the cells of the tumor niche support the survival (84-86) and protect also primary ALL cells from chemotherapy (87, 88). Therefore in this thesis (Manuscript 1 and 2) ALL drug response profiles were performed in co-culture on human bone marrow derived human mesenchymal stromal cells (MSC).

1.10.4 Multi-parametric approach to analyze *in vitro* drug response

When assessing the sensitivity of *in vitro* cultures to drugs, dose response curves are used to evaluate the efficacy and the potency of the drug. Commonly, only the IC_{50} value is calculated to represent the drug response, but additional parameters can be used to describe dose repose curves (Figure 13), such us EC_{50}, AUC, EC_{90}, E_{max}. A recent study (89) has suggested that the most informative parameter varied with drug and dose range. And more attention should be given to E_{max} (concentration with maximal response effect), because high level of E_{max} could reflect that the drug is not effective or the tumor tested contains resistant subclones. Therefore, a more accurate evaluation of dose response curves can lead to a better understanding of experimental drugs' potency and efficacy, which in turn can lead to more precise assessment of anticancer agents *in vitro*.

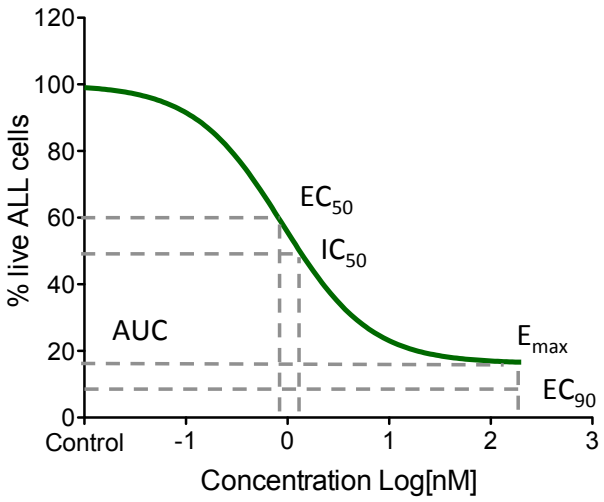

Figure 13. Graph showing a representative drug response curve described by multi-parameters. EC_{50}, drug dose that induces a response halfway between the baseline and maximum effect. IC_{50}, drug dose that induces inhibition in 50% of the cells. AUC, Area under the curve, EC_{90}, concentration of a drug, which induces 90% of the response between the baseline and maximum effect, E_{max}, concentration that induces maximal response.

1.11 BCL-2

1.11.1 Apoptosis

In physiological conditions apoptosis is a regulated process important for the removal of aged and damaged cells. In cancer cells block of the apoptosis determine their abnormal proliferation.
Apoptosis occurs through two pathways: i) The intrinsic pathway is caused by chemotherapeutic agents, irradiation or growth factor withdrawal. BCL-2 family proteins and other modulators of apoptosis are activated and lead to mitochondrial outer membrane permeabilization (MOMP). MOMP causes the release of cytochrome *c* and multiple pro-apoptotic molecules leading to the activation of caspases. ii) The extrinsic pathway is activated by death ligands (FASL or TRAIL) or tumor necrosis factor-α (TNFα). These ligands engage their cognate receptors to trigger the formation of death-inducing signaling complex (DISC). DISC recruitment leads to the activation of caspases. The caspase cascade is responsible for the structural and biochemical cellular changes associated with apoptosis.

1.11.2 Importance of BCL2 in ALL

BCL2 (B cell lymphoma 2) is the first identified apoptotic regulator, originally cloned in 1984 from the breakpoint of a t(14;18) translocation present in human B-cell follicular lymphoma (90). Following studies have identified other proteins with sequence similarities to BCL2. They were classified based on their pro-apoptotic or pro-survival role. Anti-apoptotic proteins (BCL-2, BCL-XL, BCL-w, MCL-1, and BFL-1) share 4 BCL2 homology (BH) domains. Pro-apoptotic proteins are: BAX, BAK and BOK, contain 3 BH domains, and BIM, BID, BAD, NOXA and PUMA with only 1 BH domain, in particular the BH3, are called BH3-only proteins. BH3-only proteins can directly activate BAK and BAX or displace their interacting anti-apopototic proteins. Oligomerizazion of BAX and BAK leads to the formation of pores in the mitochondrial membrane, which results in MOMP (91).
High BCL-2 levels have been detected in many human lymphoid malignancies: follicular lymphomas, due to the (14;18) translocation involving the BCL2 gene (90); diffuse large B-cell lymphomas, because of the (14;18) translocation and also the BCL2 gene amplification (92); chronic lymphocytic leukemias, as a result of epigenetics mechanisms (93) or post-transcriptional regulation (94). The importance of BCL-2 is also emerging in pediatric ALL. High level of BCL-2 became recently a hallmark of immature subtypes of T-ALL (95). Further studies in B-ALL have showed high levels of BCL-2 (96) and its importance in the control of glucocorticoid-induced apoptosis (97).

1.11.3 Venetoclax (ABT-199) BCL-2 specific inhibitor

Venetoclax (ABT-199) is a BH3-mimetic agent that binds the hydrophobic BH3-binding groove of BCL-2 and prevents the binding of pro-apoptotic family members. Venetoclax is the first BH3-mimetic small molecule inhibitor specific for BCL-2 (98). In contrast to the broader BH3 mimetic Navitoclax, which binds BCL-2 and BCL-XL and exhibits on target thrombocytopenia, venetoclax spares human platelets. Currently, venetoclax is in advanced phases of clinical trials for CLL, NHL, CML, AML, lymphomas (99).
Based on previous studies, sensitivity to venetoclax could not always be associated with high levels of BCL-2. It has been shown that high BCL-2 expression correlates with sensitivity to venetoclax in NHL cell lines and T cell lines (95, 98), but in a later study the ratio BCL-2:BCL-XL was suggested predictive of the response to venetoclax in T ALL (100). Mechanisms of resistance to venetoclax are not yet well described. In one study, it has been shown that the overexpression of MCL-1 compensates and maintains cell survival when BCL-2 is inhibited by venetoclax in primary ALL samples (96)

1.12 Cell Surface proteins as biomarkers in ALL

Biomarkers are important for disease detection, diagnosis and could be used for prognostic and therapeutic purposes. Novel biomarkers are needed in the field of ALL for the early detection of patients that are not sensitive to current treatments. As described in Manuscript 3, we have identified VNN2 (GPI-80) as a promising biomarker of resistant ALL cases.

1.12.1 VNN2 (GPI-80)

GPI-80, gycosylphospatidyl inositol-80, or also called VNN2, is a member of the Vanin or pantetheinase gene family. Vanin genes share high degree of homology and comprise VNN1, VNN2, and VNN3 in humans, while in mouse only Vanin-1 and Vanin-3 have been identified. For all Vanin proteins pantetheinease activity (hydrolysis of pantetheine into pantothenic acid (Vitamin B5) and cysteamine) was detected *in vitro*.

VNN1/Vanin-1 is a GPI-linked membrane-associated ectoenzyme responsible of the pantetheinease activity in mice. The mouse Vanin-1 functions are the best documented, since Vanin-1-deficient mice have been characterized in physiological and pathophysiological conditions. In physiological conditions, it has been showed that vanin-1 is expressed by perivascular thymus stromal cells and contributes to the homing of hematopoietic precursor cells to the thymus in mouse (101). Studies on several mouse models of chronic inflammatory diseases have suggested that VNN1 promotes inflammation during an infection (102-104).

Two independent groups have identified VNN2. Galland et al. in the '98 (105) discovered two human cDNAs homologous to mouse vanin-1 gene, therefore called VNN1 and VNN2. And one year later, Suzuki et al. (106) identified a protein recognized by the monoclonal antibody, 3H9 clone, which modulated adhesion and transmigration of activated human neutrophils. This protein was named GPI-80 (80-kDa protein with GPI-anchor). VNN2 is widely expressed by different tissues, such as blood, colon, spleen, placenta, kidney, liver and lung (107), and in neutrophils VNN2 expression increases during differentiation and maturation (108). In contrast to vanin-1/VNN1, VNN2 mouse models have not been established, but evidences in human neutrophils have suggested that VNN2 supports the adhesion and invasion processes (Figure 14). VNN2 is localized on plasma membrane and in secretory vesicles of neutrophils (109). Stimulation of the neutrophils with chemotactic peptides (110) and TNF-*a (111)* induces mobilization of the secretory vesicles determining an increased expression of VNN2 of the surface membrane and the release of VNN2 from the secretory vesicles as soluble form. Membrane VNN2 associates with the adhesion molecule Mac-1 (integrin complex that consists of ITGAM and ITGB2 dimer), and modulates Mac-1 functionality. When chemotaxis occurs VNN2 protein shifts from the plasma membrane to the podia of the neutrophils together with ITGB2, which is increased by VNN2.

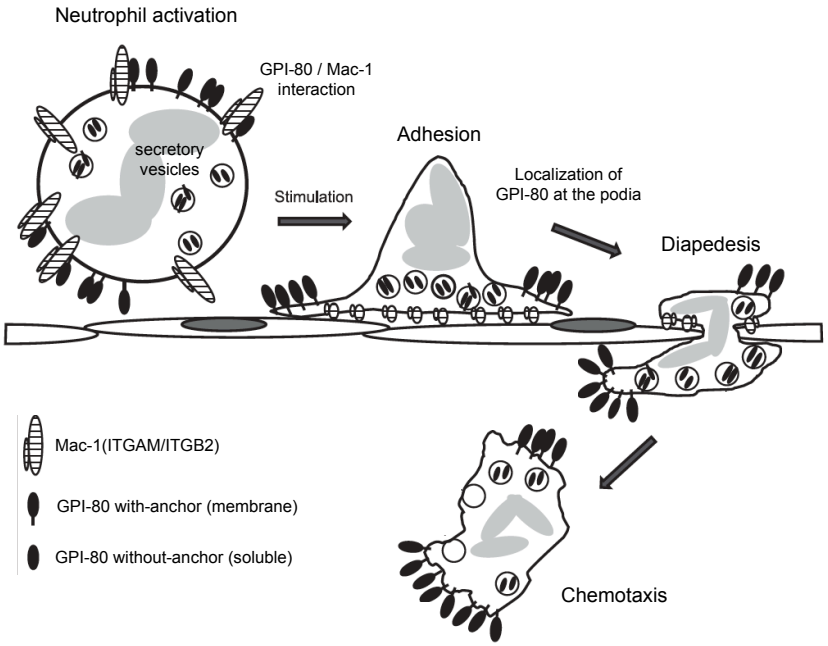

Figure 14. VNN2 (GPI-80) cooperates with Mac-1 complex during the extravasation of human neutrophils. GPI-80 is present on the cellular membrane associated with Mac-1 complex, and as soluble form (GPI-80 without GPI-anchor) is stored in secretory vesicles. Once activated by stimulators, neutrophils adhere to endothelial cells via Mac-1 and migrate into the interstitial space. During adhesion to endothelial cells, some of the GPI-80 molecules move to the pseudopodia of the neutrophils. Functions of the intracellular stores and of the soluble form of GPI-80 are not clear. Black ellipses show GPI-80, and striped ellipses show dimers of Mac-1 (ITGAM/ITGB2 dimer). Adapted from (112).

A recent study has demonstrated that VNN2 is functionally required for the self-renewal of fetal liver HSC. (113) Knockdown of VNN2 or ITGAM was sufficient to block hematopoietic stem progenitors cells (HSPC) expansion in culture and mouse. Since VNN2 does not have an intracellular domain to convey a signal from the niche, the cooperation with Mac-1 integrin complex may be essential for self-renewal.

Evidences in pathological conditions have also suggested VNN2 as indicator of acute inflammatory phase with neutrophil activation in arthritis and myocardial infarction. Indeed, soluble VNN2 molecules have been detected in synovial fluids of rheumatoid arthritis patients (110), and in serum of the patients with isolated atherosclerotic coronary artery disease (114). Furthermore, in one study high levels of membrane and soluble VNN2 proteins have been associated with late stage of human thymoma (115).

2 Subject of investigation and my contributions

Genomic profiling has revolutionized our understanding of the genetic basis of ALL by identifying recurrent genomic lesions important for leukemogenesis. However the translation of this knowledge for the development of targeted therapeutic options and for the improvement of risk stratification a diagnosis remains very limited.

To complement the genomic knowledge the major aims of my PhD thesis were to

1) Develop an integrated platform for functional and genomic evaluation of patients with drug resistant acute lymphoblastic leukemia (ALL)
2) Establish a xenograft model of the disease progression for clinical relevant subtypes of ALL, including *TCF3-HLF* and *TCF3-PBX1* -positive ALL
3) Generate the drug response profile *TCF3-HLF* and *TCF3-PBX1* -positive ALL in our platform and evaluate promising compounds in our preclinical *in vivo* mouse model
4) Investigate the clinical relevance of VNN2 protein as independent marker of poor outcome and the role of VNN2 in the biology of leukemia

I significantly contributed in:

- Manuscript 1: Genomics and drug profiling of fatal *TCF3-HLF*-positive acute lymphoblastic leukemia identifies recurrent mutation patterns and novel therapeutic options (equal first author)
  Major contributions to Figures 3, 5, 6; Supplementary Figure 2, 6, 7, 9, 10, 11, 12, 13; Supplementary Tables 20, 23, 24, 25.

- Manuscript 2: Drug response profiling to identify selective pharmacological activity in drug resistant ALL (equal first author)
  Major contributions to Figure 1, 3, 7; Table 2.

- Manuscript 3: Vanin-2 (GPI-80) identifies aggressive subtypes of childhood acute lymphoblastic leukemia (advanced draft)
  Own experiments represented in Figure 1, 5; Supplementary Figure 2, 3, 4, 5, 6, 7, 10, 12, 13, 14; Table 1; Supplementary Table 2, 7.

- Proposal for prospective evaluation of VNN2 as prognostic marker by FACS for BCP-ALL

3 Results

Manuscript 1

Genomics and drug profiling of fatal *TCF3-HLF*-positive acute lymphoblastic leukemia identifies recurrent mutation patterns and novel therapeutic options

Ute Fischer[§], Michael Forster[§], Anna Rinaldi[§], Thomas Risch[§], Stéphanie Sungalee[§], Hans-Jörg Warnatz[§], Beat Bornhauser, Michael Gombert, Christina Kratsch, Adrian Stütz, Marc Sultan, Joelle Tchinda, Catherine Worth, Vyacheslav Amstislavskiy, Nandini Badarinarayan, André Baruchel, Thies Bartram, Giuseppe Basso, Cengiz Canpolat, Gunnar Cario, Hélène Cavé, Dardane Dakaj, Mauro Delorenzi, Maria Pamela Dobay, Cornelia Eckert, Eva Ellinghaus, Sabrina Eugster, Viktoras Frismantas, Sebastian Ginzel, Oskar Haas, Olaf Heidenreich, Georg Hemmrich-Stanisak, Kebria Hezaveh, Jessica Höll, Sabine Hornhardt, Peter Husemann, Priyadarshini Kachroo, Christian Kratz, Geertruy te Kronnie, Blerim Marovca, Felix Niggli, Alice C. McHardy, Anthony Moorman, Renate Panzer-Grümayer, Britt Petersen, Benjamin Raeder, Meryem Ralser, Philip Rosenstiel, Daniel Schäfer, Martin Schrappe, Stefan Schreiber, Moritz Schütte, Björn Stade, Ralf Thiele, Nicolas von der Weid, Ajay Vora, Marketa Zaliova, Langhui Zhang, Thomas Zichner, Martin Zimmermann, Hans Lehrach, Arndt Borkhardt[§], Jean-Pierre Bourquin[1§], Andre Franke[§], Jan Korbel[§], Martin Stanulla[1§], Marie-Laure Yaspo[§]

[§] equal contributions to this work – listing in alphabetical order

[1] corresponding authors

Abstract

TCF3-HLF fusion gene-positive acute lymphoblastic leukemia (ALL) is currently not curable. We used an integrated approach to reveal distinct mutation, gene expression, and drug response profiles in *TCF3-HLF*-positive ALL and treatment-responsive *TCF3-PBX1*-positive ALL. In *TCF3-HLF*-positive ALL, recurrent intragenic deletions of the lymphoid transcription factor gene *PAX5* or somatic mutations in the non-translocated allele of *TCF3* (acting upstream of *PAX5)* were common and frequently observed in conjunction with RAS pathway aberrations. Despite a probable lymphoid-committed cell of origin, the *TCF3-HLF*-positive ALL transcriptome was enriched for stem cell and myeloid features, consistent with reprogramming towards a hybrid, more drug-resistant hematopoietic state. These genomic profiles were maintained in matched patient-derived xenografts. *TCF3-HLF*-positive ALL revealed a distinct drug-response profile with resistance to some agents commonly used for its treatment, but sensitivity towards glucocorticoids and agents in clinical development. Striking on-target sensitivity was achieved with the BCL2-specific inhibitor venetoclax (ABT-199) indicating relevant BCL2-dependency. Our integrated approach thus has revealed new options for the treatment of this fatal disease.

For detailed information see attached manuscript 1

Manuscript 2

Drug response profiling to identify selective pharmacological activity in drug resistant ALL

Viktoras Frismantas[§], Maria Pamela Dobay[§], Anna Rinaldi[§], Joachim Kunz, Blerim Marovca, Peter Horvath, Salome Higi, Sabrina Eugster, Pamela Voegeli, Mauro Delorenzi, Gunnar Cario, Martin Schrappe, Martin Stanulla, Andreas E. Kulozik, Martina U. Muckenthaler, Arend Von Stackelberg, Cornelia Eckert, Thomas Radimerski, Beat C. Bornhauser[§] and Jean-Pierre Bourquin[1§]

[§] equal contributions to this work – listing in alphabetical order

[1] corresponding authors

Abstract

Novel strategies are needed to identify vulnerable targets in individual patients with chemotherapy resistant acute lymphoblastic leukemia (ALL). Here we describe a high-throughput drug response profiling platform based on automated image analysis of primary ALL cells co-cultured with mesenchymal stroma cells (MSC) and provide a bioinformatics toolkit for flexible data processing and analysis. Screening a 60-compound library of clinically relevant new agents for activity in 61 primary ALL samples enriched for resistant cases, we identified consistent drug sensitivity and resistance patterns in genetically defined subgroups such as *MLL-AF4* positive ALL or refractory relapsed ALL. Striking activity was detected for the BCL2-specific BH3-mimetic venetoclax (ABT-199) in a relevant proportion of BCP-ALL, in *MLL-AF4* positive ALL and in a smaller subset of T-ALL, providing a direct approach to identify BCL2 dependent ALL subsets. Higher sensitivity to venetoclax on this platform predicted antileukemic activity in xenografts in vivo. Matrix combination testing identified recurrent synergistic activity of venetoclax with the BRD4 inhibitor JQ1 providing a new rationale for experimental therapy. Integration of drug activity profiling with other diagnostic testing should be evaluated in the clinical context to improve the selection of patients at urgent medical need in future clinical trials.

For detailed information see attached manuscript 2

Manuscript 3

Vanin-2 (GPI-80) identifies aggressive subtypes of childhood acute lymphoblastic leukemia

Anna Rinaldi, Nastassja Scheidegger, Gunnar Cario, Andreas Hofmann, Paulina Mirkowska, Elena Vendramini, Martina Temperli, Marco Giordan, Guimaraes Andreia, Cornelia Eckert, Mecklenbräuker Astrid, Andishe Attabashi, Renate Panzer-Grümayer, Maria Pamela Dobay, Truus teKronnie, Giuseppe Basso, Martin Stanulla, Martin Zimmermann Bernd Wollscheid, Beat Bornhauser and Jean-Pierre Bourquin

Abstract

The glycophosphatidylinositol anchored surface protein Vanin-2 (VNN2, GPI-80), which has been implicated in leukocyte adherence and migration, identifies human fetal liver hematopoietic stem/ progenitor cells (HSPCs) with self-renewal ability and is required for their hematopoietic function. Comparing the cell surface glycoproteome of 19 acute lymphoblastic leukemia (ALL) samples, we identified VNN2 as a unique feature in patients with a very high risk of relapse by minimal residual disease. In a retrospective analysis of 663 patients on the ALL-BFM-2000 treatment protocol high VNN2 transcript levels were associated with decreased event free survival. We show in a subset of this cohort that VNN2 detection by flow cytometry may serve as a prognostic marker instead. Furthermore all of 12 *TCF3-HLF*-positive ALL, which defines a currently incurable ALL subtype, were strongly surface VNN2, providing a simple procedure to preselect samples for specific diagnostic testing. VNN2 expression was not associated with other cytogenetic and copy number abnormality. Antibody interference with VNN2 resulted in delayed homing of ALL to the bone marrow of immunodeficient mice, suggesting a potential role of VNN2 in leukemia trafficking. Thus surface VNN2 expression identifies *TCF3-HLF3*-positive ALL as well as subset of ALL with unfavorable biology that cannot be defined by other diagnostic features and warrants prospective clinical investigation.

For detailed information see attached manuscript 3

VNN2 Prospective analysis proposal

Proposal for prospective evaluation of VNN2 as prognostic marker for BCP-ALL

Major relevant findings and standard operating procedure (SOP) for the staining and analysis of VNN2 at diagnosis are described in this proposal. Currently the children's hospital of Zürich (Switzerland), Padova (Italy), Monza (Italy), Berlin (Germany), Wien (Austria) are performing the prospective analysis based on this SOP.

For detailed information see attached document

4 Discussion

4.1 Rationale

Although cure rates for childhood acute lymphoblastic leukemia (ALL) are approaching 85%, the development of new-targeted treatments is essential for relapsed cases and for reducing toxicity of the standard chemotherapy regimens currently employed. Integration of advanced biomedical technologies, such as next generation genome sequencing and high-throughput drug screening, aim to identify both genetic biomarkers that can predict treatment response as well as targets for the development of individualized treatment. This dissertation describes an unprecedented combined genetic and functional study focus on clinically relevant subtypes of ALL.

4.1.1 Genomic characterization is not sufficient for the development of targeted therapies

Different subtypes of ALL can be defined based on recurring chromosomal abnormalities, such as aneuploidy (hyperdiploid and hypodiploid) and chromosomal rearrangements (*TEL-AML1, TCF3-PBX1, TCF3-HLF, BCR-ABL1, MLL-AF4, CRLF2*-rearrangement). Importantly, an increasing number of these subgroups are currently being investigated using next generation sequencing techniques. These revealed that constellations of characteristic genetic alterations, which perturb essential cellular pathways, are found in addition to the defining chromosomal alterations. For example, constellations including alterations in receptor tyrosine kinases, RAS pathway mutations or germline *TP53* mutations were discovered in distinct cytogenetic subgroups with hypodiploid ALL (48). Most recently, it has been described that the *BCR-ABL1*-like ALL subtype (50), which is characterized by gene expression signatures that resemble *BCR-ABL1*-positive ALL, has different kinases involved in the rearrangements such us *ABL1, ABL2, CRLF2, JAK2, PDGFRB*. 60% of the *BCR-ABL1*-like patients do not respond to standard treatments (116), but preliminary data from in vitro experiments and clinical trials (117, 118) recently suggested that this subtype might be sensitive to tyrosine kinases inhibitors (TKI). Therefore, introduction of TKI for the treatment of BCR-ABL1-like positive ALL seems to be a promising therapeutic option. However, it is not obvious whether the TK rearrangements are the main cause of the treatment resistance. Indeed, further lesions were detected in *IKZF1, PAX5* and genes of Ras pathway. Likely specific constellations of genomic lesions result in a resistant disease phenotype. The challenge will be to design clinical trials for *BCR-ABL1*-like ALL cases to address two different questions: i) does the implementation of TKI in the current treatment benefit resistant patients and ii) can TKI be used to deescalate treatment intensity for patients with good risk profiles. Here, a combination of novel genomic technologies and current functional stratification schemes based on response to chemotherapy in patients will be required for stratification of future treatments. Thus, also in this prototypic situation for a targeted intervention in ALL, integrated genomic and functional approaches will be needed. These considerations indicate that due to the genetic heterogeneity and the complexity of the cellular network intrinsic in ALL biology, genomic characterization alone is not sufficient for the clinical development of targeted therapies.

4.1.2 Integration of genomic profiling and functional investigations based on the leukemia xenograft system

Aiming to complement the knowledge derived from genomic studies, we have used an integrated approach that combines genomic characterization and functional validation of resistant subtypes of ALL (Figure 15). The integrated study showed in this thesis (Manuscript 1 and 2) is comprised of:

1) Generation of Patient Derived Xenografts (PDXs) of clinically relevant subtypes of ALL to model the disease.

2) Integration of the genomic analysis of patient and matched PDX samples obtained at diagnosis and after treatment to define the molecular features of resistant disease.

3) High throughput *in vitro* drug screening of primary ALL in co-culture with human bone marrow stromal cells for the identification of active compounds and informative drug response profiles.

4) Preclinical *in vivo* validation of promising compounds as single agents and in combination with drugs currently used in treatment protocols.

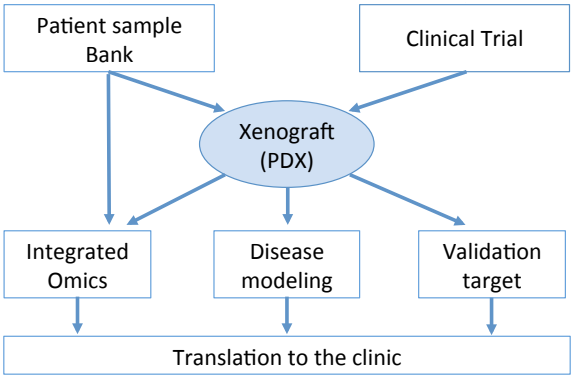

Figure 15. Scheme of the integrated strategy described in this thesis. Patient samples bank, clinical trial, xenograft: primary patient samples classified based on clinical criteria (genetic features and treatment response) were transplanted in immunodeficient mice (NSG) to generate PDXs from diagnostic and relapse samples. Genomic and transcriptomic analysis of primary patient samples and matched PDXs provides opportunities to characterize the genetic background of relevant subsets of ALL and evaluate the conservation of the genomic and transcriptomic features in the matched PDX. Disease modeling: PDXs were used to amplify the patient material and model the individual genomic features at diagnosis and after treatment. Validation target: PDXs were used for in vivo and in vitro experiments allowing the validation of targets and identification of promising compounds. Translation to the clinic: data derived from the functional genomic characterization will help guide the development of new biomarkers and targeted therapies.

4.2 Patient derived xenograft (PDX)

4.2.1 PDXs used to model relevant subtypes of ALL

As part of the European AEIOP-BFM-ALL and IntReALL study groups we had access to large banks of primary diagnostic and relapse samples with clearly defined clinical backgrounds. Importantly, we included samples associated with good and poor outcomes based on genetic features and response to treatment, which are two important risk factors used in the clinic (Figure 16). From 2010 until now, our laboratory established PDXs for more than 200 cases. Among the resistant subtypes of ALL we included samples associated with defined genetic subgroups – like *TCF3-HLF, BCR-ABL1, MLL-AF4, BCR-ABL1*-like – as well as cases with unknown genetic features that are refractory to induction treatment or have high risk of relapse. When possible, paired diagnosis and relapse samples were included. Furthermore, we included ALL subtypes associated with good prognosis, such as *TCF3-PBX1, TEL-AML1*, hyperdiploid – each associated with a specific cytogenetic subgroup – and other cases that respond well to treatment for which cytogenetic features are unknown. To investigate the potential relevance of our integrated model shown in Figure 15, we decided to focus on subtypes with defined cytogenetic features in this thesis (Manuscript 1). In particular, we compared *TCF3-HLF* and *TCF3-PBX1*-positive ALL because although they both rearranged the same portion of the transcription factor *TCF3* in the chimeric fusion protein, they have completely opposite clinical outcomes. *TCF3-HLF*-positive ALL is a fatal subtype, while *TCF3-PBX1*-positive ALL is associated with a good outcome.

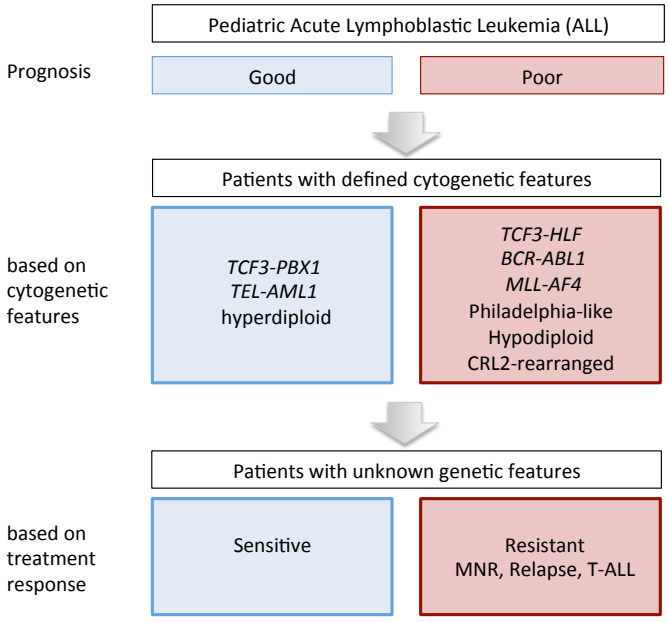

Figure 16. Clinically relevant ALL subtypes included in the PDX cohort. Genetic lesions and response to treatment are important criteria for risk stratification. 75% of the samples can be classified based on cytogenetic features that are associated with good or poor prognosis. 25% of the remaining patients are classified mainly based response to treatment. MNR: Morphological not responder (refractory cases to induction treatment).

4.2.2 Resemblance of the clonal composition of Patient Derived Xenograft (PDX) to the original sample

Several studies have investigated the effect of passaging primary patient cells in the xenogenic environment (51, 72-75, 77) of immunodeficient mice on the clonal composition of the samples. A study (73) focused on *BCR-ABL1*-positive ALL has shown that the clonal evolution process in the PDX model can occur according different behaviors even within samples belonging to the same cytogenetic subgroup. In half of the cases, the major clones at diagnosis were conserved in the PDXs (defined as concordant PDXs), while in the other half of patients, minor subclones of the diagnostic samples were amplified in the xenograft (defined as discordant PDXs). The different PDX behavior was clearly associated with the additional cooperative lesions of the diagnostic samples. Those with *CDKN2A/2B* and *PAX5* deletions (recurrent affected genes ALL) displayed a concordant behavior. This group was also associated with a poor clinical outcome and a rapid kinetics of engraftment. This study suggests that genetically distinct subclones have different repopulation capacity in the mouse, which might have clinical relevance.

Our laboratory (75) has established PDX models of samples not associated with specific cytogenetic subgroups, but clinically classified based on treatment response. Compared with the previous study, clonal evolution was investigated by cytogenetic, FISH and Ig/TCR rearrangements, in addition to CNA analysis. Overall, the xenograft samples were highly correlated with the original diagnostic samples, including conservation of the clonal complexity as well. The clonal composition of PDXs derived from chemo-resistant patients remained stable on serial passages in mice and was associated with shorter kinetics of engraftment. In contrast, PDXs of sensitive cases had longer engraftment kinetics, which became comparable to the engraftment kinetics of resistant cases only at the secondary passages and interestingly, few new clones were detected in the secondary transplantations. This evidence suggests that sensitive cases may undergo a stronger selective pressure, while the genetic features of resistant cases favor the tumor propagation in the unfriendly microenvironment of the mice or enables the leukemia to propagate in a less microenvironment-dependent manner.

Furthermore a study (51) in T-ALL has characterized paired diagnosis and relapse patient samples, and PDXs derived from the transplantation of the diagnostic samples. Multiple techniques were used, like genome-wide DNA array, cytogenetic, FISH, quantitative genomic PCR for specific backtracking abnormalities and microarray analysis. Notably, the PDXs resembled relapse samples more closely than diagnostic samples, suggesting that PDXs can model the process of relapse in patients. PDXs often contained additional genetic lesions in oncogene and tumor suppressor genes like, *PTEN, MYC, CDKN2A* and *NOTCH1* that are also found in relapsed cases.

This data suggests that it is important to understand the extent to which the clonal architecture is affected in PDXs and to assess stability upon multiple passages in mice in order to validate the basis of this experimental model. Here we provide one of the first in-depth analyses performed by using next generation sequencing approaches of a PDX model focusing on *TCF3*-translocated ALL.

4.2.3 Genomic characterization of *TCF3*-translocated ALL PDX models

Genomic analysis of our PDX models of *TCF3-HLF* and *TCF3-PBX1* -positive ALL showed a high degree of resemblance between patient samples and matched PDXs. Both translocations remained conserved in all PDXs. Moreover, we could identify lesions affecting genes recurrently mutated in ALL that remained generally stable in the PDXs. Compared to *TCF3-PBX1*-positive ALL in which only 1 to 4 mutations were detected per patient, in the resistant *TCF3-HLF* -positive ALL we identified a higher number of lesions and recurrent alterations of *PAX5* and *TCF3* genes. This evidence suggests that the translocation is the initiating event for both ALL subtypes, while the additional lesions cooperate in the leukemogenesis process and possibly in the disease progression.

Recently, the clinical relevance of combined specific patterns of cooperative lesions with cytogenetic features (73) has been demonstrated. Indeed, a higher complexity in the mutational pattern is associated with poor risk in ALL, as also shown by our data.

Interestingly, the SNVs identified in the chemo-sensitive *TCF3-PBX1*-positive ALL subtype tend to be more stable in the PDX models than those in *TCF3-HLF*-positive ALL. This, in a sense, may contradict the idea of a need for additional selection to establish sensitive cases in xenografts. Differences between ALL subtypes may exist, and additional epigenetic adaptation may occur which has not been investigated in this thesis. Moreover we uncovered clonal volatility of certain SNVs. A few mutations that were present in a fraction of cells of the tumor at diagnosis were not detected in PDXs, including *GNB1* and *DDX3X*, suggesting that these are either non-essential mutations or may cause drug sensitivity. In our model, Ras mutations were generally subclonal, almost exclusively present in the *TCF3-HLF*-positive samples and with variable persistence over disease progression. In one patient we could detect SNVs in *NRAS, KRAS*, and *FLT3* at diagnosis, but only the clones with *KRAS* and *FLT3* mutations were maintained. In another case we could identify a switch of the mutation from NRAS at diagnosis to *KRAS* in the PDXs. This data fits to observations in the clinic, in which RAS mutations are associated with more resistant ALL and paired sample analysis identified gains, losses and switches of RAS mutations (46, 54). In our model, mutations in RAS patway likely contribute to the more aggressive phenotype of *TCF3-HLF*-positive ALL and to the leukemia progression, but are not critical for the leukemia initiation and survival.

Analysis of the transcriptome revealed that the signatures between patients and PDXs were strongly conserved. Therefore, the translocation has a strong impact in defining the cellular reprogramming. The high degree of resemblance between patient and PDXs of *TCF3*-translocated ALL allows us to use this model in further experiments in order to study its biology. For example, in our laboratory *TCF3-HLF* PDXs are used to decipher the transcriptional target of the translocation.

4.2.4 Identification of leukemia-associated markers using the PDX model

To identify new markers that are associated with resistant disease we took advantage of the xenograft system to perform a comprehensive proteomic analysis of the cell surface of ALL (76). Our group has shown that the immunophenotype of xenografts resembles closely the immunophenotype of corresponding patients at diagnosis. Here I have used this dataset to identify markers that are preferentially detected on the surface of highly resistant disease in ALL (Manuscript 3). We focus on the GPI-80/VNN2 protein because it is exclusively expressed by resistant cases, including *TCF3-HLF*-positive ALL. Remarkably, it has been shown that VNN2 is essential for the self-renewal and survival

of fetal liver hematopoietic stem cells (113), and contributes to the migration and adhesion of neutrophils (106). This evidence suggests a potential role of VNN2 in sustaining the cellular proliferation of the leukemia and leading to a more clinically aggressive phenotype. Indeed, relapse in extra-medullary organs and expression of myeloid marker is clinically associated with poor prognosis. Importantly, we could validate that the expression of VNN2 in PDXs remains stable over passages. Small fluctuation of the positivity could be found in a few samples, in which VNN2 was not expressed by all the cells of the tumor. This could be due to an out growth of VNN2 negative clones.

4.3 Contribution of the genomic study of *TCF3-HLF*-positive ALL to our understanding of leukemogenesis

Our study identified a novel so far unrecognized genomic pattern in *TCF3-HLF*-positive ALL. We detected a recurrent heterozygous deletion of *PAX5* (60% of the cases) and SNV in the transcription factor *TCF3* (30% of the cases), which acts upstream of *PAX5*, and likely results in alterations of the *PAX5* function. In addition, mutations in an early form of the B-cell receptor *VPREB1* were found in one case without lesions in *PAX5* and *TCF3* (Fig 17). Additional evidence that sustained the importance of this *PAX5* alteration in the *TCF3-HLF*-positive ALL is the detection of a reduction of *PAX5* transcript levels in all cases. We did not identify recurrent mutations in B-cell development factors that act at different stages in lymphoid cell development, such as *IKFZ1*, which was found to be associated with *BCR-ABL1*-positive ALL, *BCR-ABL1*-like ALL and with poor prognosis when combined with other lesions (57, 119). Thus, a distinct pattern of cooperative lesions appears to be required for *TCF3-HLF*-positive ALL. This has important implications for disease modeling. So far, all attempts to engineer the translocation in mice have not recapitulated the human disease (63, 64). Our data suggest that the translocation should be modeled in the context of PAX5 haploinsufficiency.

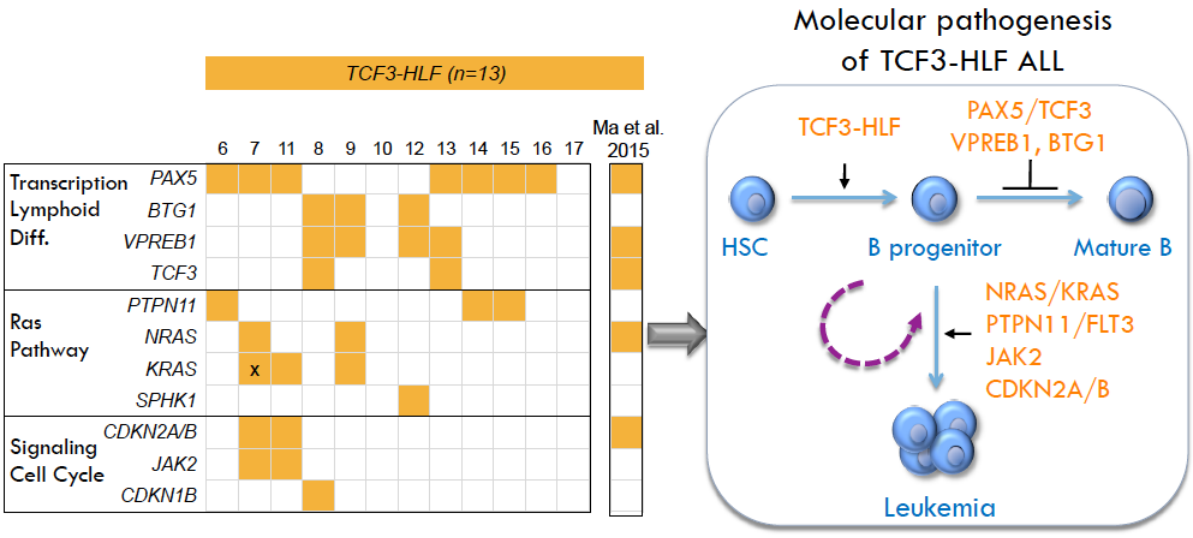

Figure 17. Model of the molecular pathogenesis of TCF3-HLF positive ALL based on our findings. Recurrent lesions in genes involved in the lymphoid development, RAS pathway and cell cycle have been found in treatment resistant *TCF3-HLF* -positive ALL. (N=12 samples were included in our study, n=1 from a recent publication showing concordant results (46)).

4.4 Development of a large scale drug-screening platform for primary ALL samples

4.4.1 Co-culture of primary leukemia cells on mesenchymal stromal cells

Cell lines are a valuable model system to study biological mechanisms and guide the early phase of drug development. In 2012 Barretina (120) and Garnett (121) described two large-scale independent studies on human cancer cell lines. Many cell lines were profiled at the genomic and transcriptomic levels, and tested for sensitivity to approved and potential new drugs. They illustrated some expected associations between drug response sensitivity and genotype, but the utility of this system for the discovery of relevant functional networks in leukemia remains to be assessed. Indeed, such cells lines represent exceptional cases in which selection of additional features results in independence from the microenvironment.

Other groups recently performed *in vitro* drug screenings by using patient samples. Promising data were generated by Tyner et al. (80) and Pemovska et al. (81), who performed functional drug sensitivity assays of ALL in a monoculture system. However, this type of culture setting does not provide the protective effect of the microenvironment (bone marrow niche) and does not allow for the survival of a considerable fraction of ALL samples, as we show in Manuscript 2.

Hartwell et al. (82) established a screening platform based on co-culture of primary patient (AML) cells, with murine bone marrow stromal cells, attempting to overcome the limitations due to the monoculture settings. We independently established a comparable platform to perform *in vitro* drug screenings of human ALL samples in a more physiologic context (Manuscript 1 and 2 and Figure 18), by using primary patient (ALL) cells in co-culture with human bone marrow cells.

This system offers several advantages:

- To couple *in vitro* drug screening with the PDX model for further functional investigation
- To integrate clinical and biological data from the corresponding patient material
- To screen a large number of defined cases
- To screen large compound libraries at good resolution by using several drug concentrations

4.4.2 Survival and proliferation

Survival and proliferation are two essential points that need to be considered during drug sensitivity assessments. Drug sensitivity profiles of cells that are undergoing apoptosis independent of the treatments are likely not representative of the leukemia sensitivity *in vivo*. Moreover, the effect of chemotherapeutic agents and compounds targeting proteins involved in the cell cycle, like polo kinase and aurora kinase, strongly depend on cell proliferation.

In our platform, analysis of the proportion of cells in S-phase at the time of the drug screening read-out revealed a high variability across the samples. Although all samples tested had a fraction of cells in S-phase, the proportion would vary from 10% up to 70%. This variation could generate a bias in the response analysis to compounds targeting cell the cycle. That is, the level of sensitivity could reflect the amount of cells in S-phase, rather than intrinsic mechanisms of resistance. Indeed, in the case of T ALL we could see a correlation between the sensitivity to drugs targeting the cell cycle and the fraction of cells in S-phase (Manuscript 2). A similar correlation was also described in Manuscript 1:

TCF3-HLF-positive cases had a lower fraction of cell in S-phase as compared with the *TCF3-PBX1*-positive ALL cases. And indeed, they were also more resistant to drugs targeting cell cycle (vincristine, paclitaxel, barasertinib). The fact that we detect subgroups with distinct cell cycle features and apoptosis rates on our platform warrants further investigation, as this information may be of clinical relevance. Our study of the paradigm subtype for highly resistant disease *TCF3-HLF* is a good example. Indeed, we consistently detected a higher fraction of quiescent cells in the resistant *TCF3-HLF*-positive ALL subtype. This may explain the lower susceptibility to clinical drugs like antimitotics and antimetabolites. But in contrast, evidence also suggests that a loss of cell cycle checkpoint controls can be associated with resistant disease, as for example mutations in *TP53* are more frequently observed at relapse (53) and rapid progression in mouse xenografts was shown to be associated with early relapse in ALL (73, 122). These facts will have to be taken into consideration when integrating data for precision medicine in ALL.

4.4.3 Correlation of *in vivo* and *in vitro* drug activity in our models

Obviously an *in vitro* platform will have major limitations compared with an individual patient's situation. Testing drugs in patients will reveal important features that are related to the patient's ability to absorb, distribute, metabolize, and eliminate the drug (pharmacokinetics), all of which are not reflected in the *in vitro* settings. The biochemical and physiological effects and the mechanism of drug action at organ and cellular levels (pharmacodynamics) are also different. Pharmacokinetic and pharmacodynamic aspects are very important for the identification of safe and effective therapeutic management of drugs in patients. Second, the 2D co-culture system with mesenchymal stromal cells cannot replace the 3-D bone marrow niche, such as the interaction with other cell types, the native tissue architecture, the influence of cytokines and other cell signaling molecules. For these reasons, our approach will most likely be useful to identify interacting activity patterns, which, in combination with other information, will lead to possible actionable features to be validated in the clinical setting. It is possible that characteristics detected by the platform will be of immediate use in the clinical setting: for example, predicting a completely resistant phenotype based on leukemia-intrinsic features or detecting specific sensitivity to a given drug based on subtype specific features.

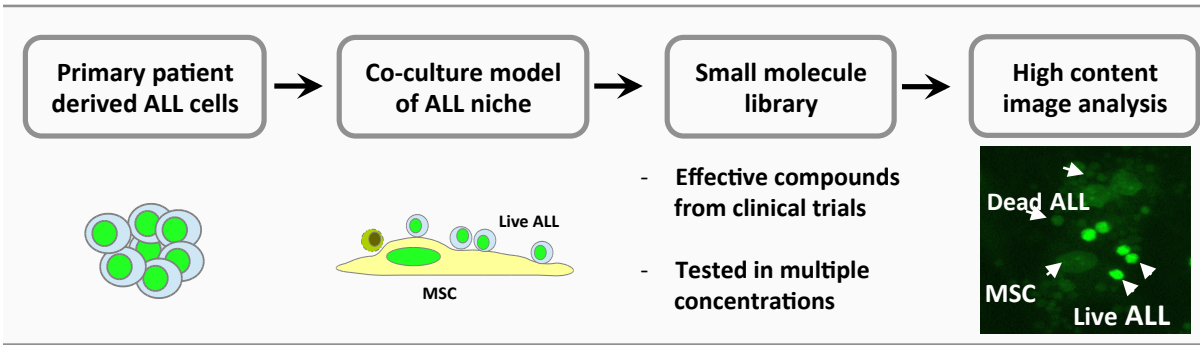

Figure 18. Drug screening platform of primary ALL used to generate drug response profiles.

4.5 Proof of concept data to support the use of *in vitro* drug profiling in translational research

Strong preliminary data on this platform show that the biological features of the leukemia are revealed by distinct profiles. Drug activity profiles vary from patient to patient, even in subtypes that are clearly characterized by a genetic feature such as *TCF3-HLF*-positive ALL, as shown here.

However, recurrent drug activity information can be retrieved for clinically defined subsets. For example, *TCF3-HLF*-positive cases resulted resistant to drugs targeting the cell cycle (i.e., vincristine, paclitaxel, BI-2536, barasertinib) and tirosine kinases (dasatinib, lestaurtinib), while a striking sensitivity was shown for the BCL-2 specific inhibitor venetoclax (ABT199).
Our platform provides relevant functional screening for detecting drug sensitivity. This was clearly demonstrated for venetoclax. For example, based on previous studies, sensitivity to venetoclax could not always be associated with high levels of BCL-2. It has been shown that high BCL-2 expression correlates with sensitivity to venetoclax in NHL cell lines and T cell lines (95, 98), but in a later study the ratio BCL-2:BCL-XL was suggested to be predictive of the response to venetoclax in T ALL (100).

Due to the multiclonal composition of ALL, multiple drug combinations are used in clinical treatment regiments (123). However, relapse still occurs. shRNA libraries have been used to investigate pathways critical to drug resistance, for example in *BCR-ABL1*-positive ALL resistant to the TKI imatinib (116). *In vitro* high-throughput screening assays (124) and *in vivo* preclinical models (125) using PDXs ALL have been also used to identify compounds able to sensitize ALL to the clinical drugs. Our system will contribute to investigate possible drug combinations, guided by the integration of genomics, *in vitro* drug profiling and *in vivo* validation in xenografts.

So far, based on data shown in Manuscript 1 and 2 for the novel compound venetoclax, and previous publications of our laboratory for the clinical drug (dexamethasone) (75, 126), *in vitro* activity correlated with drug activity in xenografts *in vivo*, suggesting that indeed this platform will extend our capability for productive research.
In vivo experiments combining dexamethasone and vincristine – both clinical drugs – with ABT199 revealed promising preliminary data (not shown here). Indeed, based on transgenic mice overexpressing murine Bcl-2, or mice expressing a conditional human *BCL2* gene, it has been suggested that BCL-2 facilitates tumor cell maintenance and survival, but is not sufficient for the development leukemia (127, 128). Therefore, BCL-2 overexpression is not considered the driver of the leukemia and it seems improbable that even sustained inhibition of BCL-2 can be curative.

Importantly, we could test *TCF3-HLF*-positive patient samples on our drug screening platform (Manuscript 2) and compare to the samples included in our biobank including *TCF3-HLF* and *TCF3-PBX1*-positive ALL, and other subtypes showed here in Figure 19. Notably, drug profiles of these 2 cases were comparable to the other *TCF3-HLF*-positive cases previously tested. One of them (depicted with red dot) was resistant to induction treatment with cytarabine, dexamethasone, vincristine, methotrexate and these clinical data were also confirmed by our *in vitro* drug response profile. Remarkably, our screening identified sensitivity for other clinical drugs, like doxorubicine, mitoxantrone, bortezomib and novel agents in advanced phases of clinical trials like venetoclax.

These data underscore the relevance of our drug-screening platform to evaluate the response of patient samples to clinical or promising novel drugs.

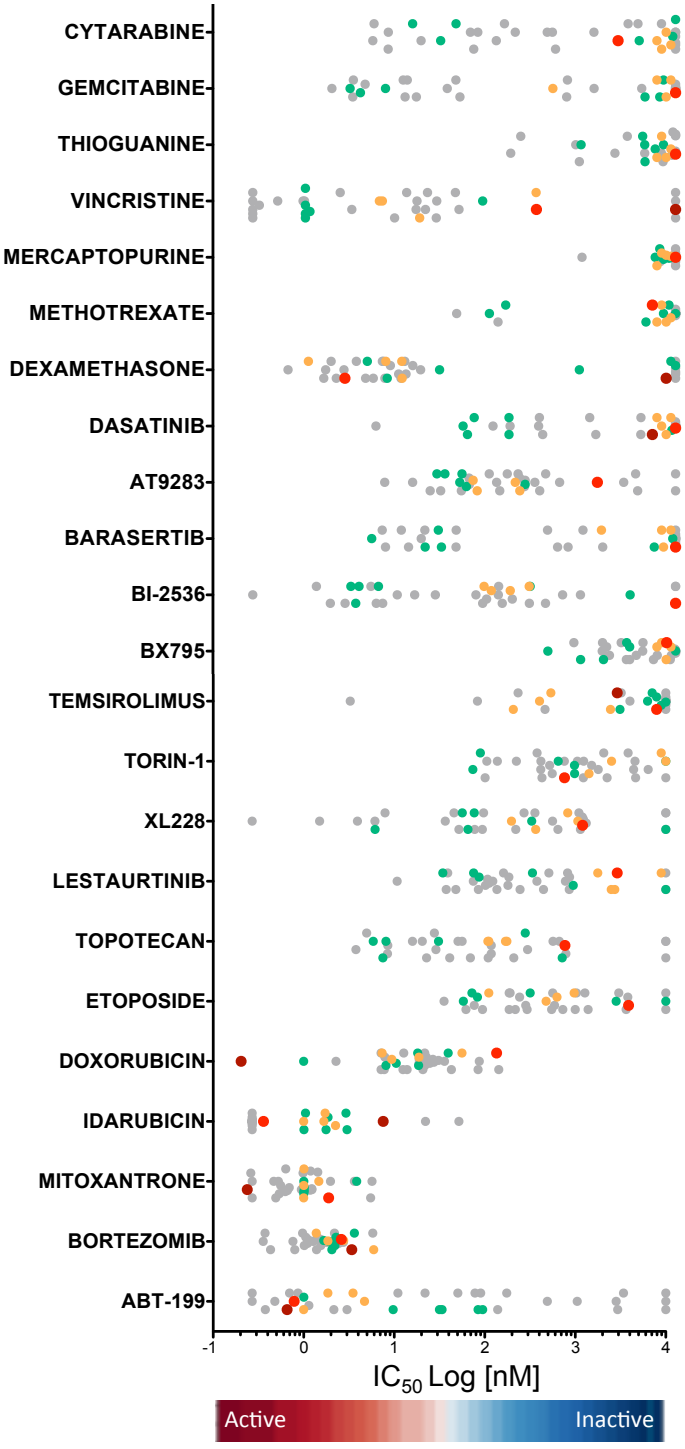

Figure 19. Drug profiling data of refractory *TCF3-HLF*-positive patients compared to our experience for the same therapeutic agents on the platform. *TCF3-HLF*-positive ALL patients are in red and dark red. For comparison, the corresponding drug activity is indicated for the PDXs of *TCF3-HLF* (n=5, orange), *TCF3-PBX1* (n=5 green) positive ALL and 25 additional ALL samples (grey) tested on the same platform, including standard risk (SR, n=5, square), medium risk (MR, n=4, circles), and high risk (HR, n=16, triangles) cases.

4.6 Impact of our models on translational research

Taken together we envision, in the near future, that our models will have a significant impact on the field from different aspects:

1. The molecular portrait of *TCF3-HLF*-positive ALL that we describe here provides relevant information for future research efforts such as mouse model generation, functional analysis of the mutated genes and activated pathways that might be targets for new therapy.
2. The collection of PDX drug-screening profiles shown in this thesis could be used to predict the clinical response of those that have similar genetic features, and identify alternative therapeutic options. Genomic characterization of the patients and the repository profile data would help to identify patients eligible for specific treatment protocols already at diagnosis, thereby avoiding inactive treatments or cytotoxic effects.
3. Evaluation of the drug-profiling platform as a tool to detect drugable targets in ALL patients who do not respond to induction treatment. Our laboratory already initiated a multicenter project to profile such cases systematically at the genomic and functional level.
4. Use of systematic drug-profiling at relapse in treatment resistant cases to evaluate its predictive potential and establish novel therapeutic options.
5. Acceleration of the discovery of unexpected drug resistance and sensitivity phenotypes. Our data already suggest several candidate drugs (BH3-mimetics, SMAC-mimetics, TKI, BRD4 and HDACs) with interesting activity profiles in ALL subsets for which no drugable targets can be identified so far, like *TCF3-HLF* positive ALL, MLL rearranged ALL, T-ALL.

Clinical importance of VNN2

1. Biomarker to screen for *TCF3-HLF*-positive ALL by flow cytometry and select the samples that need to be validated by FISH at diagnosis. Moreover VNN2 can be used for analysis of residual leukemia cells during patient treatment.
2. VNN2 expression appears to be associated with a higher risk of relapse. Implementation of VNN2 at diagnosis would be useful in detecting relapse cases that are not identified by current tools.
3. Based on the work shown in this thesis (Manuscript 3) a prospective analysis of VNN2 expression in diagnostic samples has already started (Prospective analysis proposal) in different European centers (Switzerland, Italy, Austria) to validate the clinical relevance and the future implementation of VNN2 as an additional diagnostic biomarker predictive of poor outcomes. First preliminary data confirm the existence of a small subset of VNN2 positive ALL in the range of 10% percent.
4. Genomic characterization of VNN2 positive samples is ongoing and we aim to integrate these data with the PDX model to investigate the biological basis underlying cellular programs associated with VNN2 in leukemia.

5 References

1. Pritchard-Jones K, Sullivan R. Children with cancer: driving the global agenda. The Lancet Oncology. 2013;14(3):189-91.
2. Bert Vogelstein NP, Victor E. Velculescu, Shibin Zhou,, Luis A. Diaz Jr. KWK. Cancer Genome Landscapes. science. 2013;339.
3. Vogelstein CTaB. Variation in cancer risk amongtissues can be explained by thenumber of stem cell divisions. 2015 Contract No.: 6217.
4. Hanahan D, Weinberg RA. Hallmarks of cancer: the next generation. Cell. 2011;144(5):646-74.
5. http://www.cancer.gov.
6. http://www.euro.who.int. 2009.
7. Niggli FK BN. Akute Leukämien im Kindesalter. In: Schweizer Zeitschrift für Onkologie. 2013.
8. Papaemmanuil E, Hosking FJ, Vijayakrishnan J, Price A, Olver B, Sheridan E, et al. Loci on 7p12.2, 10q21.2 and 14q11.2 are associated with risk of childhood acute lymphoblastic leukemia. Nature genetics. 2009;41(9):1006-10.
9. Trevino LR, Yang W, French D, Hunger SP, Carroll WL, Devidas M, et al. Germline genomic variants associated with childhood acute lymphoblastic leukemia. Nature genetics. 2009;41(9):1001-5.
10. Sherborne AL, Hosking FJ, Prasad RB, Kumar R, Koehler R, Vijayakrishnan J, et al. Variation in CDKN2A at 9p21.3 influences childhood acute lymphoblastic leukemia risk. Nature genetics. 2010;42(6):492-4.
11. The Childhood Leukemia International Consortium Catherine Metayer.
12. Vardiman JW, Thiele J, Arber DA, Brunning RD, Borowitz MJ, Porwit A, et al. The 2008 revision of the World Health Organization (WHO) classification of myeloid neoplasms and acute leukemia: rationale and important changes. Blood. 2009;114(5):937-51.
13. AIEOP-BFM ALL Immunophenotyping Consensus Guidelines 2013.
14. Bene MC, Castoldi G, Knapp W, Ludwig WD, Matutes E, Orfao A, et al. Proposals for the immunological classification of acute leukemias. European Group for the Immunological Characterization of Leukemias (EGIL). Leukemia. 1995;9(10):1783-6.
15. Euster S. Master Thesis. 1014.
16. Harrison M. Leukaemia Research Cytogenetics Group 2014.
17. Pui CH, Carroll WL, Meshinchi S, Arceci RJ. Biology, risk stratification, and therapy of pediatric acute leukemias: an update. Journal of clinical oncology : official journal of the American Society of Clinical Oncology. 2011;29(5):551-65.
18. Roberts KG, Mullighan CG. Genomics in acute lymphoblastic leukaemia: insights and treatment implications. Nature reviews Clinical oncology. 2015.
19. Attarbaschi A, Mann G, Panzer-Grumayer R, Rottgers S, Steiner M, Konig M, et al. Minimal residual disease values discriminate between low and high relapse risk in children with B-cell precursor acute lymphoblastic leukemia and an intrachromosomal amplification of chromosome 21: the Austrian and German acute lymphoblastic leukemia Berlin-Frankfurt-Munster (ALL-BFM) trials. Journal of clinical oncology : official journal of the American Society of Clinical Oncology. 2008;26(18):3046-50.
20. Flohr T, Schrauder A, Cazzaniga G, Panzer-Grumayer R, van der Velden V, Fischer S, et al. Minimal residual disease-directed risk stratification using real-time quantitative PCR analysis of immunoglobulin and T-cell receptor gene rearrangements in the international multicenter trial AIEOP-BFM ALL 2000 for childhood acute lymphoblastic leukemia. Leukemia. 2008;22(4):771-82.
21. Schrappe M. Minimal residual disease: optimal methods, timing, and clinical relevance for an individual patient. Hematology / the Education Program of the American Society of Hematology American Society of Hematology Education Program. 2012;2012:137-42.
22. Conter V, Bartram CR, Valsecchi MG, Schrauder A, Panzer-Grumayer R, Moricke A, et al. Molecular response to treatment redefines all prognostic factors in children and adolescents with B-cell precursor acute lymphoblastic leukemia: results in 3184 patients of the AIEOP-BFM ALL 2000 study. Blood. 2010;115(16):3206-14.
23. Papaemmanuil E, Rapado I, Li Y, Potter NE, Wedge DC, Tubio J, et al. RAG-mediated recombination is the predominant driver of oncogenic rearrangement in ETV6-RUNX1 acute lymphoblastic leukemia. Nature genetics. 2014;46(2):116-25.
24. Tijchon E, Havinga J, van Leeuwen FN, Scheijen B. B-lineage transcription factors and cooperating gene lesions required for leukemia development. Leukemia. 2013;27(3):541-52.
25. Bain G, Maandag EC, Izon DJ, Amsen D, Kruisbeek AM, Weintraub BC, et al. E2A proteins are required for proper B cell development and initiation of immunoglobulin gene rearrangements. Cell. 1994;79(5):885-92.
26. Kwon K, Hutter C, Sun Q, Bilic I, Cobaleda C, Malin S, et al. Instructive role of the transcription factor E2A in early B lymphopoiesis and germinal center B cell development. Immunity. 2008;28(6):751-62.
27. Dias S, Silva H, Jr., Cumano A, Vieira P. Interleukin-7 is necessary to maintain the B cell potential in common lymphoid progenitors. The Journal of experimental medicine. 2005;201(6):971-9.

28. Dias S, Mansson R, Gurbuxani S, Sigvardsson M, Kee BL. E2A proteins promote development of lymphoid-primed multipotent progenitors. Immunity. 2008;29(2):217-27.
29. Borghesi L, Aites J, Nelson S, Lefterov P, James P, Gerstein R. E47 is required for V(D)J recombinase activity in common lymphoid progenitors. The Journal of experimental medicine. 2005;202(12):1669-77.
30. Ikawa T, Kawamoto H, Wright LY, Murre C. Long-term cultured E2A-deficient hematopoietic progenitor cells are pluripotent. Immunity. 2004;20(3):349-60.
31. Nechanitzky R, Akbas D, Scherer S, Gyory I, Hoyler T, Ramamoorthy S, et al. Transcription factor EBF1 is essential for the maintenance of B cell identity and prevention of alternative fates in committed cells. Nature immunology. 2013;14(8):867-75.
32. Schmitz R, Young RM, Ceribelli M, Jhavar S, Xiao W, Zhang M, et al. Burkitt lymphoma pathogenesis and therapeutic targets from structural and functional genomics. Nature. 2012;490(7418):116-20.
33. Fuxa M, Busslinger M. Reporter gene insertions reveal a strictly B lymphoid-specific expression pattern of Pax5 in support of its B cell identity function. Journal of immunology. 2007;178(12):8222-8.
34. Delogu A, Schebesta A, Sun Q, Aschenbrenner K, Perlot T, Busslinger M. Gene repression by Pax5 in B cells is essential for blood cell homeostasis and is reversed in plasma cells. Immunity. 2006;24(3):269-81.
35. Pridans C, Holmes ML, Polli M, Wettenhall JM, Dakic A, Corcoran LM, et al. Identification of Pax5 target genes in early B cell differentiation. Journal of immunology. 2008;180(3):1719-28.
36. Schebesta A, McManus S, Salvagiotto G, Delogu A, Busslinger GA, Busslinger M. Transcription factor Pax5 activates the chromatin of key genes involved in B cell signaling, adhesion, migration, and immune function. Immunity. 2007;27(1):49-63.
37. Nutt SL, Thevenin C, Busslinger M. Essential functions of Pax-5 (BSAP) in pro-B cell development. Immunobiology. 1997;198(1-3):227-35.
38. Rolink AG, Nutt SL, Melchers F, Busslinger M. Long-term in vivo reconstitution of T-cell development by Pax5-deficient B-cell progenitors. Nature. 1999;401(6753):603-6.
39. van der Weyden L, Giotopoulos G, Rust AG, Matheson LS, van Delft FW, Kong J, et al. Modeling the evolution of ETV6-RUNX1-induced B-cell precursor acute lymphoblastic leukemia in mice. Blood. 2011;118(4):1041-51.
40. Zhang J, Mullighan CG, Harvey RC, Wu G, Chen X, Edmonson M, et al. Key pathways are frequently mutated in high-risk childhood acute lymphoblastic leukemia: a report from the Children's Oncology Group. Blood. 2011;118(11):3080-7.
41. Iacobucci I, Lonetti A, Paoloni F, Papayannidis C, Ferrari A, Storlazzi CT, et al. The PAX5 gene is frequently rearranged in BCR-ABL1-positive acute lymphoblastic leukemia but is not associated with outcome. A report on behalf of the GIMEMA Acute Leukemia Working Party. Haematologica. 2010;95(10):1683-90.
42. Janeway. Immunobiology,. 8th ed.
43. Gale KB, Ford AM, Repp R, Borkhardt A, Keller C, Eden OB, et al. Backtracking leukemia to birth: identification of clonotypic gene fusion sequences in neonatal blood spots. Proceedings of the National Academy of Sciences of the United States of America. 1997;94(25):13950-4.
44. Wiemels JL, Cazzaniga G, Daniotti M, Eden OB, Addison GM, Masera G, et al. Prenatal origin of acute lymphoblastic leukaemia in children. Lancet. 1999;354(9189):1499-503.
45. Inaba H, Greaves M, Mullighan CG. Acute lymphoblastic leukaemia. Lancet. 2013;381(9881):1943-55.
46. Ma X, Edmonson M, Yergeau D, Muzny DM, Hampton OA, Rusch M, et al. Rise and fall of subclones from diagnosis to relapse in pediatric B-acute lymphoblastic leukaemia. Nature communications. 2015;6:6604.
47. Andersson AK, Ma J, Wang J, Chen X, Gedman AL, Dang J, et al. The landscape of somatic mutations in infant MLL-rearranged acute lymphoblastic leukemias. Nature genetics. 2015;47(4):330-7.
48. Holmfeldt L, Wei L, Diaz-Flores E, Walsh M, Zhang J, Ding L, et al. The genomic landscape of hypodiploid acute lymphoblastic leukemia. Nature genetics. 2013;45(3):242-52.
49. Mullighan CG, Miller CB, Radtke I, Phillips LA, Dalton J, Ma J, et al. BCR-ABL1 lymphoblastic leukaemia is characterized by the deletion of Ikaros. Nature. 2008;453(7191):110-4.
50. Roberts KG, Li Y, Payne-Turner D, Harvey RC, Yang YL, Pei D, et al. Targetable kinase-activating lesions in Ph-like acute lymphoblastic leukemia. The New England journal of medicine. 2014;371(11):1005-15.
51. Clappier E, Gerby B, Sigaux F, Delord M, Touzri F, Hernandez L, et al. Clonal selection in xenografted human T cell acute lymphoblastic leukemia recapitulates gain of malignancy at relapse. The Journal of experimental medicine. 2011;208(4):653-61.
52. Meyer JA, Wang J, Hogan LE, Yang JJ, Dandekar S, Patel JP, et al. Relapse-specific mutations in NT5C2 in childhood acute lymphoblastic leukemia. Nature genetics. 2013;45(3):290-4.
53. Hof J, Krentz S, van Schewick C, Korner G, Shalapour S, Rhein P, et al. Mutations and deletions of the TP53 gene predict nonresponse to treatment and poor outcome in first relapse of childhood acute lymphoblastic leukemia. Journal of clinical oncology : official journal of the American Society of Clinical Oncology. 2011;29(23):3185-93.
54. Irving J, Matheson E, Minto L, Blair H, Case M, Halsey C, et al. Ras pathway mutations are prevalent in relapsed childhood acute lymphoblastic leukemia and confer sensitivity to MEK inhibition. Blood. 2014;124(23):3420-30.
55. Mar BG, Bullinger LB, McLean KM, Grauman PV, Harris MH, Stevenson K, et al. Mutations in epigenetic regulators including SETD2 are gained during relapse in paediatric acute lymphoblastic leukaemia. Nature communications. 2014;5:3469.
56. Bourquin JP. The clinical path to integrated genomics in ALL. Blood. 2014;124(9):1380-1.

57. Mullighan CG, Su X, Zhang J, Radtke I, Phillips LA, Miller CB, et al. Deletion of IKZF1 and prognosis in acute lymphoblastic leukemia. The New England journal of medicine. 2009;360(5):470-80.
58. Moorman AV, Enshaei A, Schwab C, Wade R, Chilton L, Elliott A, et al. A novel integrated cytogenetic and genomic classification refines risk stratification in pediatric acute lymphoblastic leukemia. Blood. 2014;124(9):1434-44.
59. C W. olekulare Onkologie : Entstehung, Progression, klinische Aspekte - NLM Catalog - NCBI. 3., komplett aktualisierte und erw. Aufl. ed. Germany: Stuttgart ; New York : Thieme, c2010.;. 2014.
60. Hunger SP, Devaraj PE, Foroni L, Secker-Walker LM, Cleary ML. Two types of genomic rearrangements create alternative E2A-HLF fusion proteins in t(17;19)-ALL. Blood. 1994;83(10):2970-7.
61. Hunger SP, Brown R, Cleary ML. DNA-binding and transcriptional regulatory properties of hepatic leukemia factor (HLF) and the t(17;19) acute lymphoblastic leukemia chimera E2A-HLF. Molecular and cellular biology. 1994;14(9):5986-96.
62. Inaba T, Inukai T, Yoshihara T, Seyschab H, Ashmun RA, Canman CE, et al. Reversal of apoptosis by the leukaemia-associated E2A-HLF chimaeric transcription factor. Nature. 1996;382(6591):541-4.
63. Smith KS, Rhee JW, Naumovski L, Cleary ML. Disrupted differentiation and oncogenic transformation of lymphoid progenitors in E2A-HLF transgenic mice. Molecular and cellular biology. 1999;19(6):4443-51.
64. Honda H, Inaba T, Suzuki T, Oda H, Ebihara Y, Tsuiji K, et al. Expression of E2A-HLF chimeric protein induced T-cell apoptosis, B-cell maturation arrest, and development of acute lymphoblastic leukemia. Blood. 1999;93(9):2780-90.
65. Nourse J, Mellentin JD, Galili N, Wilkinson J, Stanbridge E, Smith SD, et al. Chromosomal translocation t(1;19) results in synthesis of a homeobox fusion mRNA that codes for a potential chimeric transcription factor. Cell. 1990;60(4):535-45.
66. Geng H, Hurtz C, Lenz KB, Chen Z, Baumjohann D, Thompson S, et al. Self-Enforcing Feedback Activation between BCL6 and Pre-B Cell Receptor Signaling Defines a Distinct Subtype of Acute Lymphoblastic Leukemia. Cancer cell. 2015;27(3):409-25.
67. Monica K, LeBrun DP, Dedera DA, Brown R, Cleary ML. Transformation properties of the E2a-Pbx1 chimeric oncoprotein: fusion with E2a is essential, but the Pbx1 homeodomain is dispensable. Molecular and cellular biology. 1994;14(12):8304-14.
68. Kamps MP, Look AT, Baltimore D. The human t(1;19) translocation in pre-B ALL produces multiple nuclear E2A-Pbx1 fusion proteins with differing transforming potentials. Genes & development. 1991;5(3):358-68.
69. Chen W, Li Q, Hudson WA, Kumar A, Kirchhof N, Kersey JH. A murine Mll-AF4 knock-in model results in lymphoid and myeloid deregulation and hematologic malignancy. Blood. 2006;108(2):669-77.
70. Tsuzuki S, Seto M, Greaves M, Enver T. Modeling first-hit functions of the t(12;21) TEL-AML1 translocation in mice. Proceedings of the National Academy of Sciences of the United States of America. 2004;101(22):8443-8.
71. Daley GQ, Van Etten RA, Baltimore D. Induction of chronic myelogenous leukemia in mice by the P210bcr/abl gene of the Philadelphia chromosome. Science. 1990;247(4944):824-30.
72. Bardini M, Woll PS, Corral L, Luc S, Wittmann L, Ma Z, et al. Clonal variegation and dynamic competition of leukemia-initiating cells in infant acute lymphoblastic leukemia with MLL rearrangement. Leukemia. 2015;29(1):38-50.
73. Notta F, Mullighan CG, Wang JC, Poeppl A, Doulatov S, Phillips LA, et al. Evolution of human BCR-ABL1 lymphoblastic leukaemia-initiating cells. Nature. 2011;469(7330):362-7.
74. Anderson K, Lutz C, van Delft FW, Bateman CM, Guo Y, Colman SM, et al. Genetic variegation of clonal architecture and propagating cells in leukaemia. Nature. 2011;469(7330):356-61.
75. Schmitz M, Breithaupt P, Scheidegger N, Cario G, Bonapace L, Meissner B, et al. Xenografts of highly resistant leukemia recapitulate the clonal composition of the leukemogenic compartment. Blood. 2011;118(7):1854-64.
76. Mirkowska P, Hofmann A, Sedek L, Slamova L, Mejstrikova E, Szczepanski T, et al. Leukemia surfaceome analysis reveals new disease-associated features. Blood. 2013;121(25):e149-59.
77. van Delft FW, Horsley S, Colman S, Anderson K, Bateman C, Kempski H, et al. Clonal origins of relapse in ETV6-RUNX1 acute lymphoblastic leukemia. Blood. 2011;117(23):6247-54.
78. Druker BJ, Guilhot F, O'Brien SG, Gathmann I, Kantarjian H, Gattermann N, et al. Five-year follow-up of patients receiving imatinib for chronic myeloid leukemia. The New England journal of medicine. 2006;355(23):2408-17.
79. Schultz KR, Bowman WP, Aledo A, Slayton WB, Sather H, Devidas M, et al. Improved early event-free survival with imatinib in Philadelphia chromosome-positive acute lymphoblastic leukemia: a children's oncology group study. Journal of clinical oncology : official journal of the American Society of Clinical Oncology. 2009;27(31):5175-81.
80. Tyner JW, Yang WF, Bankhead A, 3rd, Fan G, Fletcher LB, Bryant J, et al. Kinase pathway dependence in primary human leukemias determined by rapid inhibitor screening. Cancer research. 2013;73(1):285-96.
81. Pemovska T, Kontro M, Yadav B, Edgren H, Eldfors S, Szwajda A, et al. Individualized systems medicine strategy to tailor treatments for patients with chemorefractory acute myeloid leukemia. Cancer discovery. 2013;3(12):1416-29.
82. Hartwell KA, Miller PG, Mukherjee S, Kahn AR, Stewart AL, Logan DJ, et al. Niche-based screening identifies small-molecule inhibitors of leukemia stem cells. Nature chemical biology. 2013;9(12):840-8.
83. Konopleva M, Tabe Y, Zeng Z, Andreeff M. Therapeutic targeting of microenvironmental interactions in leukemia: mechanisms and approaches. Drug resistance updates : reviews and commentaries in antimicrobial and anticancer chemotherapy. 2009;12(4-5):103-13.
84. Bradstock K, Bianchi A, Makrynikola V, Filshie R, Gottlieb D. Long-term survival and proliferation of precursor-B acute lymphoblastic leukemia cells on human bone marrow stroma. Leukemia. 1996;10(5):813-20.

85. Umiel T, Friedman S, Zaizov R, Cohen IJ, Gozes Y, Epstein N, et al. Long-term culture of infant leukemia cells: dependence upon stromal cells from the bone marrow and bilineage differentiation. Leukemia research. 1986;10(8):1007-13.
86. Manabe A, Coustan-Smith E, Behm FG, Raimondi SC, Campana D. Bone marrow-derived stromal cells prevent apoptotic cell death in B-lineage acute lymphoblastic leukemia. Blood. 1992;79(9):2370-7.
87. Williams RT, den Besten W, Sherr CJ. Cytokine-dependent imatinib resistance in mouse BCR-ABL+, Arf-null lymphoblastic leukemia. Genes & development. 2007;21(18):2283-7.
88. Iwamoto S, Mihara K, Downing JR, Pui CH, Campana D. Mesenchymal cells regulate the response of acute lymphoblastic leukemia cells to asparaginase. The Journal of clinical investigation. 2007;117(4):1049-57.
89. Fallahi-Sichani M, Honarnejad S, Heiser LM, Gray JW, Sorger PK. Metrics other than potency reveal systematic variation in responses to cancer drugs. Nature chemical biology. 2013;9(11):708-14.
90. Tsujimoto Y, Finger LR, Yunis J, Nowell PC, Croce CM. Cloning of the chromosome breakpoint of neoplastic B cells with the t(14;18) chromosome translocation. Science. 1984;226(4678):1097-9.
91. Davids MS, Letai A. Targeting the B-cell lymphoma/leukemia 2 family in cancer. Journal of clinical oncology : official journal of the American Society of Clinical Oncology. 2012;30(25):3127-35.
92. Monni O, Joensuu H, Franssila K, Klefstrom J, Alitalo K, Knuutila S. BCL2 overexpression associated with chromosomal amplification in diffuse large B-cell lymphoma. Blood. 1997;90(3):1168-74.
93. Hanada M, Delia D, Aiello A, Stadtmauer E, Reed JC. bcl-2 gene hypomethylation and high-level expression in B-cell chronic lymphocytic leukemia. Blood. 1993;82(6):1820-8.
94. Cimmino A, Calin GA, Fabbri M, Iorio MV, Ferracin M, Shimizu M, et al. miR-15 and miR-16 induce apoptosis by targeting BCL2. Proceedings of the National Academy of Sciences of the United States of America. 2005;102(39):13944-9.
95. Peirs S, Matthijssens F, Goossens S, Van de Walle I, Ruggero K, de Bock CE, et al. ABT-199 mediated inhibition of BCL-2 as a novel therapeutic strategy in T-cell acute lymphoblastic leukemia. Blood. 2014;124(25):3738-47.
96. Alford SE, Kothari A, Loeff FC, Eichhorn JM, Sakurikar N, Goselink HM, et al. BH3 Inhibitor Sensitivity and Bcl-2 Dependence in Primary Acute Lymphoblastic Leukemia Cells. Cancer research. 2015;75(7):1366-75.
97. Jing D, Bhadri VA, Beck D, Thoms JA, Yakob NA, Wong JW, et al. Opposing regulation of BIM and BCL2 controls glucocorticoid-induced apoptosis of pediatric acute lymphoblastic leukemia cells. Blood. 2015;125(2):273-83.
98. Souers AJ, Leverson JD, Boghaert ER, Ackler SL, Catron ND, Chen J, et al. ABT-199, a potent and selective BCL-2 inhibitor, achieves antitumor activity while sparing platelets. Nature medicine. 2013;19(2):202-8.
99. https://clinicaltrials.gov.
100. Chonghaile TN, Roderick JE, Glenfield C, Ryan J, Sallan SE, Silverman LB, et al. Maturation stage of T-cell acute lymphoblastic leukemia determines BCL-2 versus BCL-XL dependence and sensitivity to ABT-199. Cancer discovery. 2014;4(9):1074-87.
101. Aurrand-Lions M, Galland F, Bazin H, Zakharyev VM, Imhof BA, Naquet P. Vanin-1, a novel GPI-linked perivascular molecule involved in thymus homing. Immunity. 1996;5(5):391-405.
102. Berruyer C, Martin FM, Castellano R, Macone A, Malergue F, Garrido-Urbani S, et al. Vanin-1-/- mice exhibit a glutathione-mediated tissue resistance to oxidative stress. Molecular and cellular biology. 2004;24(16):7214-24.
103. Berruyer C, Pouyet L, Millet V, Martin FM, LeGoffic A, Canonici A, et al. Vanin-1 licenses inflammatory mediator production by gut epithelial cells and controls colitis by antagonizing peroxisome proliferator-activated receptor gamma activity. The Journal of experimental medicine. 2006;203(13):2817-27.
104. Martin F, Penet MF, Malergue F, Lepidi H, Dessein A, Galland F, et al. Vanin-1(-/-) mice show decreased NSAID- and Schistosoma-induced intestinal inflammation associated with higher glutathione stores. The Journal of clinical investigation. 2004;113(4):591-7.
105. Galland F, Malergue F, Bazin H, Mattei MG, Aurrand-Lions M, Theillet C, et al. Two human genes related to murine vanin-1 are located on the long arm of human chromosome 6. Genomics. 1998;53(2):203-13.
106. Suzuki K, Watanabe T, Sakurai S, Ohtake K, Kinoshita T, Araki A, et al. A novel glycosylphosphatidyl inositol-anchored protein on human leukocytes: a possible role for regulation of neutrophil adherence and migration. Journal of immunology. 1999;162(7):4277-84.
107. Jansen PA, Kamsteeg M, Rodijk-Olthuis D, van Vlijmen-Willems IM, de Jongh GJ, Bergers M, et al. Expression of the vanin gene family in normal and inflamed human skin: induction by proinflammatory cytokines. The Journal of investigative dermatology. 2009;129(9):2167-74.
108. Takeda Y, Fu J, Suzuki K, Sendo D, Nitto T, Sendo F, et al. Expression of GPI-80, a beta2-integrin-associated glycosylphosphatidylinositol-anchored protein, requires neutrophil differentiation with dimethyl sulfoxide in HL-60 cells. Experimental cell research. 2003;286(2):199-208.
109. Dahlgren C, Karlsson A, Sendo F. Neutrophil secretory vesicles are the intracellular reservoir for GPI-80, a protein with adhesion-regulating potential. Journal of leukocyte biology. 2001;69(1):57-62.
110. Huang J, Takeda Y, Watanabe T, Sendo F. A sandwich ELISA for detection of soluble GPI-80, a glycosylphosphatidyl-inositol (GPI)-anchored protein on human leukocytes involved in regulation of neutrophil adherence and migration--its release from activated neutrophils and presence in synovial fluid of rheumatoid arthritis patients. Microbiology and immunology. 2001;45(6):467-71.
111. Nitto T, Araki Y, Takeda Y, Sendo F. Pharmacological analysis for mechanisms of GPI-80 release from tumour necrosis factor-alpha-stimulated human neutrophils. British journal of pharmacology. 2002;137(3):353-60.

112. Nitto T, Onodera K. Linkage between coenzyme a metabolism and inflammation: roles of pantetheinase. Journal of pharmacological sciences. 2013;123(1):1-8.
113. Prashad SL, Calvanese V, Yao CY, Kaiser J, Wang Y, Sasidharan R, et al. GPI-80 defines self-renewal ability in hematopoietic stem cells during human development. Cell stem cell. 2015;16(1):80-7.
114. Inoue T, Kato T, Hikichi Y, Hashimoto S, Hirase T, Morooka T, et al. Stent-induced neutrophil activation is associated with an oxidative burst in the inflammatory process, leading to neointimal thickening. Thrombosis and haemostasis. 2006;95(1):43-8.
115. Sasaki H, Ide N, Sendo F, Takeda Y, Adachi M, Fukai I, et al. Glycosylphosphatidyl inositol-anchored protein (GPI-80) gene expression is correlated with human thymoma stage. Cancer science. 2003;94(9):809-13.
116. Khorashad JS, Eiring AM, Mason CC, Gantz KC, Bowler AD, Redwine HM, et al. shRNA library screening identifies nucleocytoplasmic transport as a mediator of BCR-ABL1 kinase-independent resistance. Blood. 2015;125(11):1772-81.
117. Weston BW, Hayden MA, Roberts KG, Bowyer S, Hsu J, Fedoriw G, et al. Tyrosine kinase inhibitor therapy induces remission in a patient with refractory EBF1-PDGFRB-positive acute lymphoblastic leukemia. Journal of clinical oncology : official journal of the American Society of Clinical Oncology. 2013;31(25):e413-6.
118. Lengline E, Beldjord K, Dombret H, Soulier J, Boissel N, Clappier E. Successful tyrosine kinase inhibitor therapy in a refractory B-cell precursor acute lymphoblastic leukemia with EBF1-PDGFRB fusion. Haematologica. 2013;98(11):e146-8.
119. Stanulla M. IKZF1 correlates with poor prognosis. ASH Abstract. 2014.
120. Barretina J, Caponigro G, Stransky N, Venkatesan K, Margolin AA, Kim S, et al. The Cancer Cell Line Encyclopedia enables predictive modelling of anticancer drug sensitivity. Nature. 2012;483(7391):603-7.
121. Garnett MJ, Edelman EJ, Heidorn SJ, Greenman CD, Dastur A, Lau KW, et al. Systematic identification of genomic markers of drug sensitivity in cancer cells. Nature. 2012;483(7391):570-5.
122. Meyer LH, Eckhoff SM, Queudeville M, Kraus JM, Giordan M, Stursberg J, et al. Early relapse in ALL is identified by time to leukemia in NOD/SCID mice and is characterized by a gene signature involving survival pathways. Cancer cell. 2011;19(2):206-17.
123. 2009 A-BA. INTERNATIONAL COLLABORATIVE TREATMENT PROTOCOL FOR CHILDREN AND
ADOLESCENTS WITH ACUTE LYMPHOBLASTIC LEUKEMIA. 2011.
124. Toscan CE, Failes T, Arndt GM, Lock RB. High-throughput screening of human leukemia xenografts to identify dexamethasone sensitizers. Journal of biomolecular screening. 2014;19(10):1391-401.
125. Samuels AL, Beesley AH, Yadav BD, Papa RA, Sutton R, Anderson D, et al. A pre-clinical model of resistance to induction therapy in pediatric acute lymphoblastic leukemia. Blood cancer journal. 2014;4:e232.
126. Bonapace L, Bornhauser BC, Schmitz M, Cario G, Ziegler U, Niggli FK, et al. Induction of autophagy-dependent necroptosis is required for childhood acute lymphoblastic leukemia cells to overcome glucocorticoid resistance. The Journal of clinical investigation. 2010;120(4):1310-23.
127. Vaux DL, Cory S, Adams JM. Bcl-2 gene promotes haemopoietic cell survival and cooperates with c-myc to immortalize pre-B cells. Nature. 1988;335(6189):440-2.
128. Letai A, Sorcinelli MD, Beard C, Korsmeyer SJ. Antiapoptotic BCL-2 is required for maintenance of a model leukemia. Cancer cell. 2004;6(3):241-9.

Acknowledgements

This thesis represents a fantastic rewarding experience of 4 years of PhD.

Intellectual curiosity, passion, keen desire of developing projects and hard work were the pillars for such great work; however, the successful completion of this thesis could not be possible without the support of several people. This is why I want to express my most sincere gratitude to all of them.

First of all I wish to thank my advisor PD Dr. Jean-Pierre Bourquin. It is hard to explain how much I appreciate his contribution of time, support, help and funding in making my PhD experience so productive and stimulating. It has been a true honor to be one of his PhD students. His great knowledge of the field, his unparalleled research expertise, his great intuitions have been like milestones in my way and have driven my learning and development. His great energy, dedication and enthusiasm have always been very contagious and significant in increasing my passion.

I am also very grateful to my co-advisor Dr. Beat Bornhauser for his scientific advices and insightful discussions during the planning of experiments. His contribution was essential for the success of the projects presented in this thesis.

I would like to thank the members of my thesis committee, Prof. Dr. Basler, Dr. Frew, Dr. Mauro De Lorenzi and Dr. Tchinda for their availability and interesting discussions during the committee meeting. I wish to particularly thank Dr. Tchinda that has been directly involved in the project, offering her great experience on the diagnostic field.

My next special thanks goes to the passionate and committed bioinformatician Dr. Pam Dobay. It was such a stimulating and interesting experience to collaborate with her.

Of course, I thank all the collaborators of the European research centers that have been involved in the research projects. I thank also all the members of the diagnostic and hematology Lab of the Kinderspital that were very helpful for the project and for the translation of our research results into the clinic.

And now the biggest *thanks* to all the members of the leukemia group. The familiar environment and the pleasant relationships have allowed me to go to work happy every day. I would not exchange the "leukemia lab" with any other lab. I mean for the people, not for the leased PCs and the vintage location!!!!

I want to thank my fellow in the drug-screening adventure, Viktoras. He has been a big support by helping and understanding me in all situations, while representing an example of sincere respect for people and ideas.

I want to thank my office mate Blerim to be always ready for a smile and a hug, and for the perfect teamwork.

Thanks to my great Master student Sabrina for the pleasant experiences spent in and outside the lab; more thanks for the private cross-country ski lesson, the hospitality in Stockholm and for sharing her expertise in Excel with me!

I want to thank Lena not only for her effort to be a tidy colleague in this jungle of pipets, empty tip-boxes and full waste :D, but especially to be a friend able to understand and support me.
Thanks Nastassja for being always there to help me; Julia, always ready to give me unconditional help, especially during my hard times with the Western Blot! Salome, my historical fellow of "Italian–German tandem"; Andreia, for her contagious cheerfulness; Orrin, *thaaaaank you!* for being always available and fun; Scott, for his scientific and not scientific suggestions; Yun, for his impressive example of dedication to research; Daniela, very helpful during the FACS- and sorting-experiments; Antonia, always very nice to me. Guys, you have all been more than colleagues!
I want to thank also former students of Leukemia lab Laura, Jeannette, Paulina, Maike, Michael and Raphael.
Thanks Klaudjia, Laura, Lucie, Min, Chiara and Irina for sharing my *ups and downs,* outside and inside work, for the nice time spent together and for becoming my friends for a lifetime.
I thank also all the colleagues and PI of AFS, in particular Marco and Michele always ready to help me, and Alex, Sam, Verena, Maria, Florian, Giulio, Vale, Elisa, Gabriele, Dimitra for the nice time.

Finally, my best friend Sara that, although we have been far apart in these four years, nothing changed in our friendship. I am very much indebted to my boyfriend who supported me along these years, even if he always preferred having me close in Italy. I owe a lot to my parents, who unconditionally helped me at every stage of my personal and academic life.

Curriculum vitae

Anna Rinaldi

Born 10.06.1984 in Milan
Italian Citizen

Private address
Culmannstrasse 20
8006 Zürich
M +41 76 768 98 40
rinaldi.anna.ra@gmail.com

EDUCATION

Master of Industrial Biotechnology University of Milano - Bicocca	110/110 *cum laude*	12/2006 - 07/2009
Bachelor of Biotechnology University of Milano - Bicocca	101/110	10/2003 - 12/2006
Liceum focus on science Liceo Scientifico Tecnologico - "E.FERMI" Di Desio	95/100	09/1998 - 07/2003

WORK EXPERIENCE

PhD Student Cancer Network Program of Zürich 01/2011 - 07/2015
Oncology drug discovery and biomarker development for pediatric leukemia
http://www.cnz.uzh.ch/phdprogram/ParticipantsRZ/Rinaldi.html
University Children's Hospital Zürich http://www.eicr.uzh.ch/research_en.html

Research Associate 09/2009 - 01/2011
DIBIT, San Raffaele Scientific Institute, Milan, Italy
Study of human self-reactive CD1-restricted T cells

Master thesis 01/2008 - 07/2009
DIBIT, San Raffaele Scientific Institute, Milan, Italy
Experimental thesis on development and anti-tumour function of iNKT lymphocytes after hematopoietic stem cell transplant in leukemic patients

PUBLICATIONS

Ute Fischer[§], Michael Forster[§], Anna Rinaldi[§], Thomas Risch[§], Stéphanie Sungalee[§], Hans-Jörg Warnatz[§] et al. Genomics and drug profiling of fatal *TCF3-HLF*-positive pediatric acute lymphoblastic leukemia identifies recurrent mutation patterns and novel therapeutic options [§] equal contributions, in alphabetical order (Nature Genetics, 2015).

Viktoras Frismantas[§], Maria Pamela Dobay[§], Anna Rinaldi[§], et al. Drug response profiling to identify selective pharmacological activity in drug resistant ALL (Submitted to Blood).

Anna Rinaldi, Nastassja Scheidegger, Paulina Mirkowska, et al. Vanin-2 (GPI-80) identifies aggressive subtypes of childhood acute lymphoblastic leukemia (Advanced draft).

Claudia de Lalla, Anna Rinaldi, et al. Invariant NKT Cell Reconstitution in pediatric Leukemia patients given HLA-haploidentical stem cell transplantation defines distinct CD4+ and CD4 subset dynamics and correlates with remission state. J Immunol, 2011.

Claudia de Lalla[§], Marco Lepore[§], Francesco M. Piccolo, Anna Rinaldi, et al. [§]the authors equally contributed to the work. High-frequency and adaptive-like dynamics of human CD1 self-reactive T cells. Eur. J. Immunol, 2011.

Manuscripts

Manuscript 1

Genomics and drug profiling of fatal *TCF3-HLF*-positive acute lymphoblastic leukemia identifies recurrent mutation patterns and novel therapeutic options

Manuscript 2

Drug response profiling to identify selective pharmacological activity in drug resistant ALL

Manuscript 3

Vanin-2 (GPI-80) identifies aggressive subtypes of childhood acute lymphoblastic leukemia

Proposal

Proposal for prospective evaluation of VNN2 as prognostic marker for BCP-ALL

nature genetics

Genomics and drug profiling of fatal *TCF3-HLF*–positive acute lymphoblastic leukemia identifies recurrent mutation patterns and therapeutic options

***TCF3-HLF*–positive acute lymphoblastic leukemia (ALL) is currently incurable. Using an integrated approach, we uncovered distinct mutation, gene expression and drug response profiles in *TCF3-HLF*–positive and treatment-responsive *TCF3-PBX1*–positive ALL. We identified recurrent intragenic deletions of *PAX5* or *VPREB1* in constellation with the fusion of *TCF3* and *HLF*. Moreover somatic mutations in the non-translocated allele of *TCF3* and a reduction of *PAX5* gene dosage in *TCF3-HLF* ALL suggest cooperation within a restricted genetic context. The enrichment for stem cell and myeloid features in the *TCF3-HLF* signature may reflect reprogramming by *TCF3-HLF* of a lymphoid-committed cell of origin toward a hybrid, drug-resistant hematopoietic state. Drug response profiling of matched patient-derived xenografts revealed a distinct profile for *TCF3-HLF* ALL with resistance to conventional chemotherapeutics but sensitivity to glucocorticoids, anthracyclines and agents in clinical development. Striking on-target sensitivity was achieved with the BCL2-specific inhibitor venetoclax (ABT-199). This integrated approach thus provides alternative treatment options for this deadly disease.**

One of the hallmarks of pediatric ALL is the presence of subtype-defining chromosomal translocations that cause gene fusions involving master regulators of hematopoietic development. These initiating lesions often cooperate with specific somatic aberrations, including monoallelic deletions of B cell developmental genes, such as *PAX5, IKZF1* and *EBF1* (ref. 1). Other cooperative liaisons are represented by trisomy 21q22 with *CRLF2* activation[2–4] or near-haploid ALL with activation of receptor tyrosine kinase or RAS signaling[5]. RAS pathway mutations appear in high-risk ALL but are often lost with disease progression, which suggests involvement of additional tumorigenic factors[6,7]. The patterns of recurrent genomic alterations need to be better understood, because apart from tyrosine kinase inhibitor–supplemented treatment of *BCR-ABL1*–positive ALL, the only proven successful first-line treatment strategies for high-risk ALL are chemotherapy intensification and early allogeneic hematopoietic stem cell transplantation[8].

The translocation t(1;19)[9] that results in a fusion of the transcriptional activation domain of the B cell developmental transcription factor TCF3 to the DNA-binding domain of PBX1 occurs in about 5–10% of precursor B cell (pre-B cell) ALL patients and is associated with a median five-year event-free survival probability of 78–85%[10]. In contrast, the translocation t(17;19)(q22;p13), resulting in the fusion gene *TCF3-HLF*, defines a rare subtype of ALL (<1% of pediatric ALL) that is typically associated with relapse and death within two years from diagnosis[11,12]. Both translocations disrupt one allele of *TCF3,* which drives the B cell differentiation program upstream of the transcription factor *PAX5* (ref. 13). As an initiating event, expression of *TCF3-HLF* leads to transcriptional reprogramming in pre-leukemic cells. Possible direct targets of TCF3-HLF include the transcription factor gene *LMO2*, which is implicated in initiation of T cell ALL[14,15], and the transcriptional repressor *SNAI1* (*SLUG*), which regulates embryonic development and apoptosis[16,17]. Further targets have been proposed, including *BCL2* (ref. 14). The *TCF3-HLF* fusion likely requires additional events to cause leukemia, because *TCF3-HLF* transgenic and knock-in mice did not recapitulate the human phenotype[18,19].

Here we report that the genomic and transcriptomic landscape of *TCF3-HLF*–positive ALL differs markedly from *TCF3-PBX1*–positive ALL. The *TCF3-HLF* fusion likely occurs in B lymphoid progenitors in the context of *PAX5* haploinsufficiency and is associated with transcriptional reprogramming toward an immature, hybrid hematopoietic state. Drug response profiling in patient-derived xenografts, which maintained the genomic and global transcriptome landscapes of the corresponding primary leukemic samples, identified resistance patterns to drugs commonly used for the treatment of *TCF3-HLF*–positive patients. A general trait of *TCF3-HLF*–positive ALL in our study is extreme sensitivity toward the BCL2-specific inhibitor ABT-199 (venetoclax), indicating new therapeutic options for this fatal ALL subtype.

RESULTS

The *TCF3-HLF* ALL patient cohort

We applied high-throughput sequencing analysis integrating short and large insert size paired-end whole-genome, whole-exome and transcriptome sequencing to a discovery cohort consisting of five diagnostic pre-treatment samples of *TCF3-PBX1*–positive ALL (samples 1a–5a) and *TCF3-HLF*–positive ALL (samples 6a–9a and 11a). As nontumor controls we used matched bone marrow samples collected after induction treatment for minimal residual disease (MRD) evaluation (maximum leukemic cell load $\leq 10^{-3}$; samples

A full list of authors and affiliations appears at the end of the paper.

Received 2 December 2014; accepted 29 June 2015; published online 27 July 2015; doi:10.1038/ng.3362

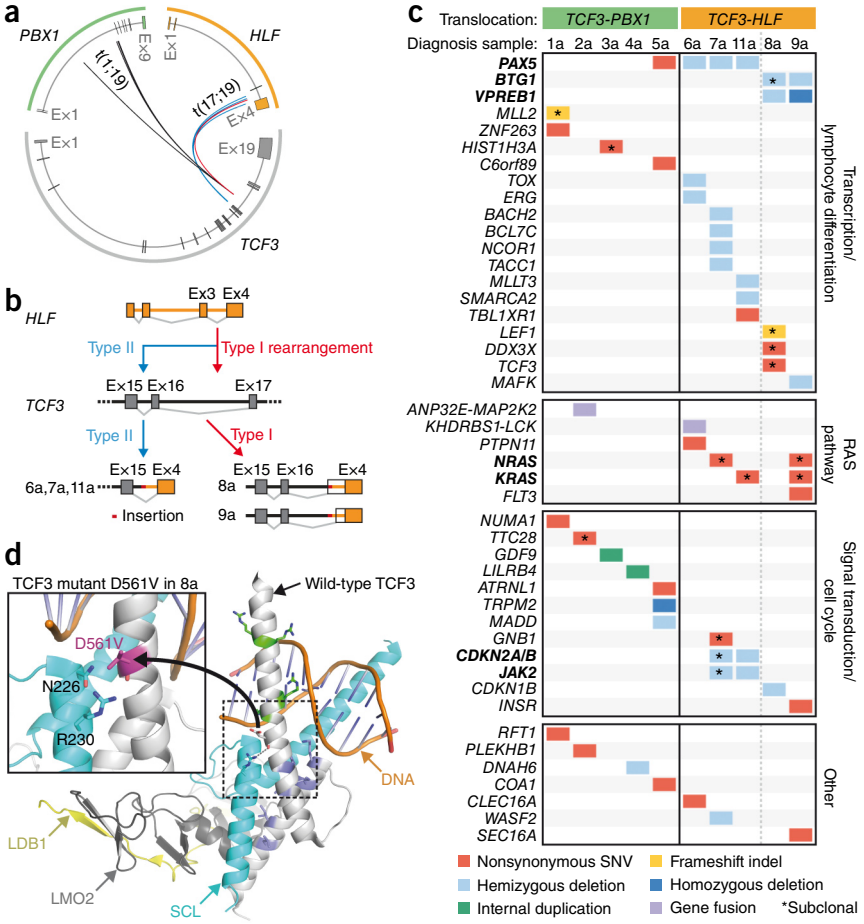

Figure 1 Genetic lesions identified in pediatric *TCF3-HLF*– and *TCF3-PBX1*–positive ALL. (**a**) Breakpoints in *TCF3*, *PBX1* and *HLF* cluster in genomic hotspot regions. Boxes correspond to exonic regions; arcs represent fusions in patient samples. (**b**) *TCF3* breakpoints cluster in two *TCF3* intronic regions: between exons 16 and 17 (type I) and between exons 15 and 16 (type II). On the transcript level, type I translocations join *TCF3* exon 16 to *HLF* exon 4, including inserted nontemplate and intronic sequences and new splice acceptor sites (patients 8 and 9). Type II translocations occur downstream of exon 15 and exclude *TCF3* exon 16 from the fusion transcript (patients 6, 7 and 11). (**c**) Schematic of somatic structural and nucleotide variations in samples. *TCF3-HLF*–positive ALL is characterized by mutually exclusive *PAX5, BTG1* and *VPREB1* deletions and nonsynonymous nucleotide variations in *TCF3* (p.Asp561Val, 'D561V' in patient 8). Indel, insertion-deletion. Recurrently affected genes are indicated by bold symbols. (**d**) Models of wild-type and mutant TCF3 based on the crystal structure of TCF3 in complex with the transcription factors SCL, LMO2 and LDB1 bound to DNA[58]. Upon LMO2 binding, bonds are formed between TCF3 and SCL, including a hydrogen bond (dashed line) between D561 and R230, reducing the DNA binding capacity of the complex. Inset, D561V introduces a hydrophobic valine residue close to polar residues that may interfere with hydrogen bonding, thus altering the DNA-binding properties of the complex.

1b–9b and 11b; **Supplementary Table 1**).

For validation, we used additional DNA samples from seven *TCF3-HLF*–positive cases (diagnostic samples 10a, 12a, 13a, 14a, 15a, 16a, 17a, remission samples 10b, 12b, 13b) and 24 *TCF3-PBX1*–positive cases (**Supplementary Tables 2** and **3**). In most cases *TCF3-HLF*–positive ALL responded to induction chemotherapy but remained MRD-positive. Nine children included in this study died owing to disease progression and treatment-related toxicities within 2 years on average, and only one patient is in remission after a short follow-up time, reflecting the dismal prognosis of *TCF3-HLF*–positive ALL.

TCF3 breakpoints suggest a committed lymphoid cell of origin

Consistent with previous reports[20,21], all *TCF3* translocation breakpoints were restricted to three hotspot regions (**Fig. 1a**,**b** and **Supplementary Fig. 1**). Those were associated with small non-template nucleotide insertions indicative of terminal deoxynucleotide transferase (TdT) activity characteristic of an early B cell stage (**Supplementary Table 4**). In *TCF3*, the breakpoints clustered in close proximity to CpG elements in the absence of classical RAG consensus sequence sites (**Supplementary Fig. 1**), which is a characteristic feature of translocations that occur in lymphoid progenitors at the pro-/pre-B stage. This may represent illegitimate RAG-mediated recombination at cryptic sites, possibly in the context of deaminated CpG nucleotides as proposed for *TCF3-PBX1* translocations[22]. Consistent with the idea that *TCF3-HLF* fusion may occur at a lymphoid-committed rather than a pluripotent progenitor stage, we detected this translocation only in sorted pre-B cell populations containing leukemic cells but neither in stem cells nor in myeloid progenitor cells (**Supplementary Fig. 2**).

TCF3-HLF ALL and impaired pro– to pre–B cell transition

Pre–B cell ALL is frequently associated with somatic copy number alterations affecting B cell developmental genes. *PAX5* deletions are generally observed in 13% of ALL cases and in up to 28% of high-risk ALL[23]. We observed enrichment for monoallelic *PAX5* deletions in *TCF3-HLF*–positive ALL, identifying such events in 67% of the cases (**Fig. 1c** and **Supplementary Table 2**). Illegitimate RAG-mediated recombination appears to be implicated in the generation of such events in *TCF3-HLF*–positive ALL, given the close proximity to RSS motifs (**Supplementary Table 5**). In most samples without *PAX5* deletion, we identified hemi- and homozygous deletions of *VPREB1,* which encodes a component of the surrogate light chain of the pre–B cell receptor (**Fig. 1c** and **Supplementary Table 6**), independent of the lambda light chain locus. *VPREB1* deletions in pediatric ALL result in failure to form a viable surrogate light chain in the pre-B cell receptor, an event associated with lower overall survival[24]. In addition, we detected *BTG1* gene deletions in three of eight *TCF3-HLF*–positive cases without *PAX5* deletions (**Supplementary Fig. 3a**,**b**). *BTG1* deletions occur frequently in ALL positive for *ETV6-RUNX1* (19%) or *BCR-ABL1* (26%) and may confer a proliferative advantage[25]. In contrast, we detected no deletion, but only a single *PAX5* nonsense mutation in 29 *TCF3-PBX1*–positive cases (**Fig. 1** and **Supplementary Table 3**). Our results indicate that cooperative genetic events affecting genes regulating the pro- to pre-B cell transition, in particular *PAX5, BTG1* and *VPREB1,* but not *IKZF1,* are selected in *TCF3-HLF*–translocated cells. Other deleted genes associated with pre-B cell ALL[26] were *JAK2* and *CDKN2A/B* (patient 7a and 11a) and transcriptional regulators such as *ERG, NCOR1, TOX, BACH2, BCL7C, MLLT3, SMARCA2* and *MAFK* (**Fig. 1c**).

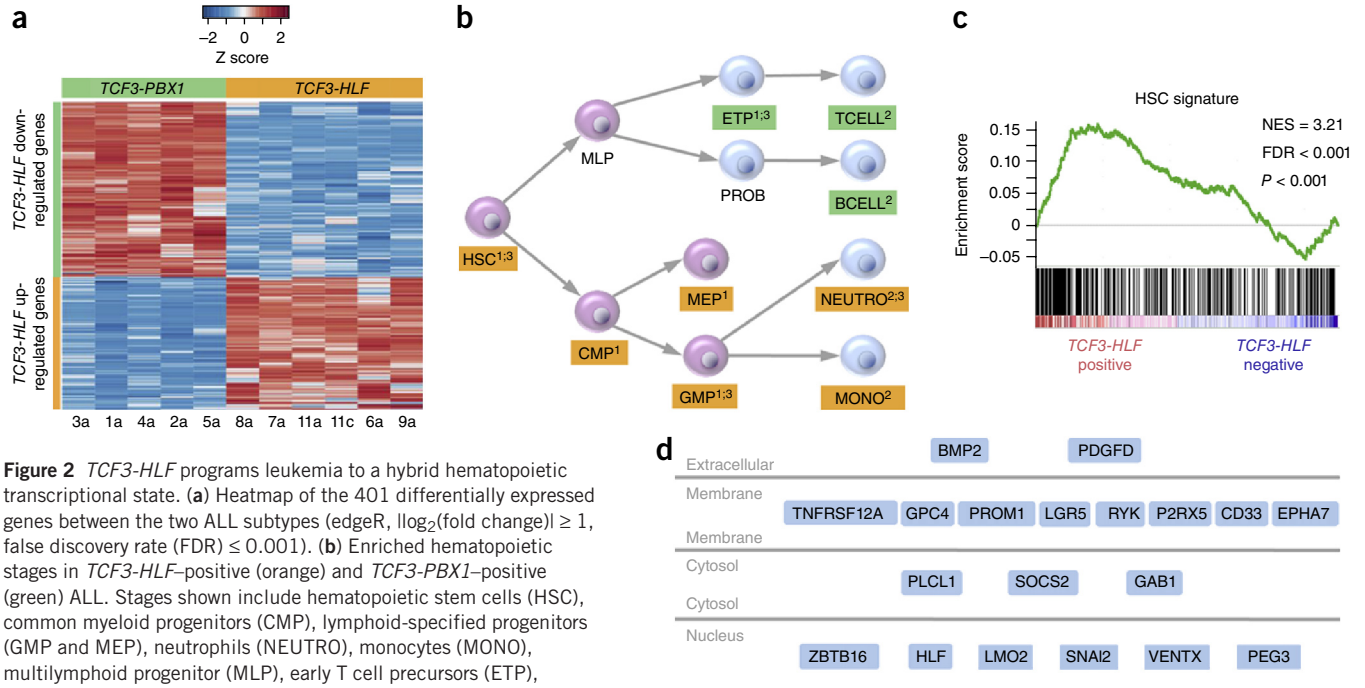

Figure 2 *TCF3-HLF* programs leukemia to a hybrid hematopoietic transcriptional state. (**a**) Heatmap of the 401 differentially expressed genes between the two ALL subtypes (edgeR, $|\log_2(\text{fold change})| \geq 1$, false discovery rate (FDR) ≤ 0.001). (**b**) Enriched hematopoietic stages in *TCF3-HLF*–positive (orange) and *TCF3-PBX1*–positive (green) ALL. Stages shown include hematopoietic stem cells (HSC), common myeloid progenitors (CMP), lymphoid-specified progenitors (GMP and MEP), neutrophils (NEUTRO), monocytes (MONO), multilymphoid progenitor (MLP), early T cell precursors (ETP), pro-B cells (PROB), T cells (TCELL) and B cells (BCELL). Gene set enrichment analysis was carried out using a Genomatix genome analyzer and gene set enrichment analysis (GSEA)[77] (GSEA: FDR ≤ 0.02; Genomatix genome analyzer: adjusted $P \leq 0.02$). The source of the significantly enriched gene sets is noted by the superscript: 1, curated gene sets of hematopoietic precursors[31]; 2, human immunologic gene signatures (MSigDB v4.0)[32]; 3, text mining–based tissue-specific gene sets[78]. (**c**) Enrichment plot for the HSC signature[31]. FDR, false discovery rate. NES, normalized enrichment score. (**d**) Components of the *TCF3-HLF*–positive ALL signature reveal functional annotation related to stem cells and their cellular location (Genomatix genome analyzer: $P = 4.65 \times 10^{-4}$, adjusted $P < 0.001$).

Recurrent RAS pathway mutations in *TCF3-HLF* ALL

We identified only a few additional somatic alterations affecting protein-coding sequences in both *TCF3-PBX1*- and *TCF3-HLF*–positive ALL (**Fig. 1c**, and **Supplementary Tables 6** and **7**), involving among others, genes associated with pre-B cell ALL[26] (*TCF3*, *PAX5* and *LEF1*) and transcriptional and chromatin regulation (*ZNF263*, *MLL2*, *HIST1H3A* and *C6orf89*). We observed a prominent association of *TCF3-HLF*–positive ALL with activating mutations in RAS signaling pathway genes (*NRAS*, *KRAS* and *PTPN11*), detectable in four of five discovery cases (**Fig. 1c**) and in three of five additional *TCF3-HLF*–positive validation samples (*PTPN11* and *SPHK1)* (**Supplementary Table 2**). We identified no RAS pathway mutations in the *TCF3-PBX1*–positive discovery cohort and only one oncogenic *NRAS* mutation in the 24 *TCF3-PBX1*–positive validation cases (**Supplementary Table 3**). *NRAS* and *KRAS* mutations were generally detected in subclones (**Supplementary Table 7**). We discovered a new fusion gene, *KHDRBS1-LCK*, due to an interstitial chromosomal deletion in one *TCF3-HLF*–positive sample (6a), triggering the overexpression of the *LCK* tyrosine kinase (**Supplementary Fig. 4**). This was also present in three of 74 randomly selected ALL samples, demonstrating that *KHDRBS1-LCK* fusion is recurrent in ALL (**Supplementary Fig. 5**). LCK is a drug target in RAS-dependent cancer cells that have higher *LCK* expression[27], suggesting a possible interplay with RAS-related signaling networks in *TCF3-HLF*–positive ALL. Oncogenic activation of LCK associated with t(1;7)(p34;q34) translocation had been reported in the T cell leukemia cell line HSB2 (ref. 28). Our data indicate a frequent association of proliferation-driving mutations in *TCF3-HLF*–positive ALL in the context of stalled B cell differentiation.

Mutations affecting the second *TCF3* allele in *TCF3-HLF* ALL

We identified a mutation in the basic helix-loop-helix region of *TCF3* (p.Asp561Val, D561V, **Fig. 1c**,**d**) affecting the non-translocated chromosome in one *TCF3-HLF*–positive case (8a). Mutations at this position have been reported in sporadic Burkitt lymphoma[29] and may reduce binding to its negative regulator ID3 (ref. 29). Based on available crystal structure data, p.Asp561Glu may affect the interaction of TCF3 with the transcription factor SCL (also known as TAL1; **Fig. 1d**), possibly altering TCF3 protein complexes. We detected a second *TCF3* mutation (p.Ser467Gly) in another *TCF3-HLF*–positive case (13a, **Supplementary Table 2**). The functional consequences of this mutation are currently unclear. We could not detect any somatic mutations in *TCF3* by targeted sequencing of 1,033 unselected ALL patients from the European multicenter trial AIEOP-BFM ALL 2000, suggesting a specific association with *TCF3-HLF*–positive ALL (**Supplementary Table 8**). Thus, deregulation of normal TCF3 function may also contribute to *TCF3-HLF*–positive ALL. Corroborating our findings, a recent study included a single *TCF3-HLF* case, as part of a cohort comparing diagnostic and relapse ALL samples, which showed a *PAX5* deletion and two mutations in *TCF3* (p.His460Tyr and p.Gly470fs), all of which were conserved at relapse[30]. The relapse sample featured a *VPREB1* deletion as well as a shift in subclonal mutations in *NRAS* (p.Gly12Asp and p.Gly12Val), reinforcing the idea of cooperative effects between *TCF3-HLF*, and alteration of *PAX5* and *VPREB1* gene dosage. Taken together, seven of 11 *TCF3-HLF* cases were hemizygous for *PAX5*, whereas five samples featured *VPREB1* deletions (**Supplementary Fig. 6**).

Reprogramming toward a more immature state in *TCF3-HLF* ALL

Consistent with the occurrence of *TCF3-HLF* and *TCF3-PBX1* translocations in lymphoid precursors, both leukemia subtypes had in common a gene expression signature of B lymphoid cells (including *PAX5, BLK, CD19, CD22, CD79B, TCF3, EBF1, VPREB1, RAG1, ROR1, BLNK* and *DNTT*; **Supplementary Tables 9** and **10**), but differential expression of 401 genes (false discovery rate ≤ 0.001) strongly distinguished

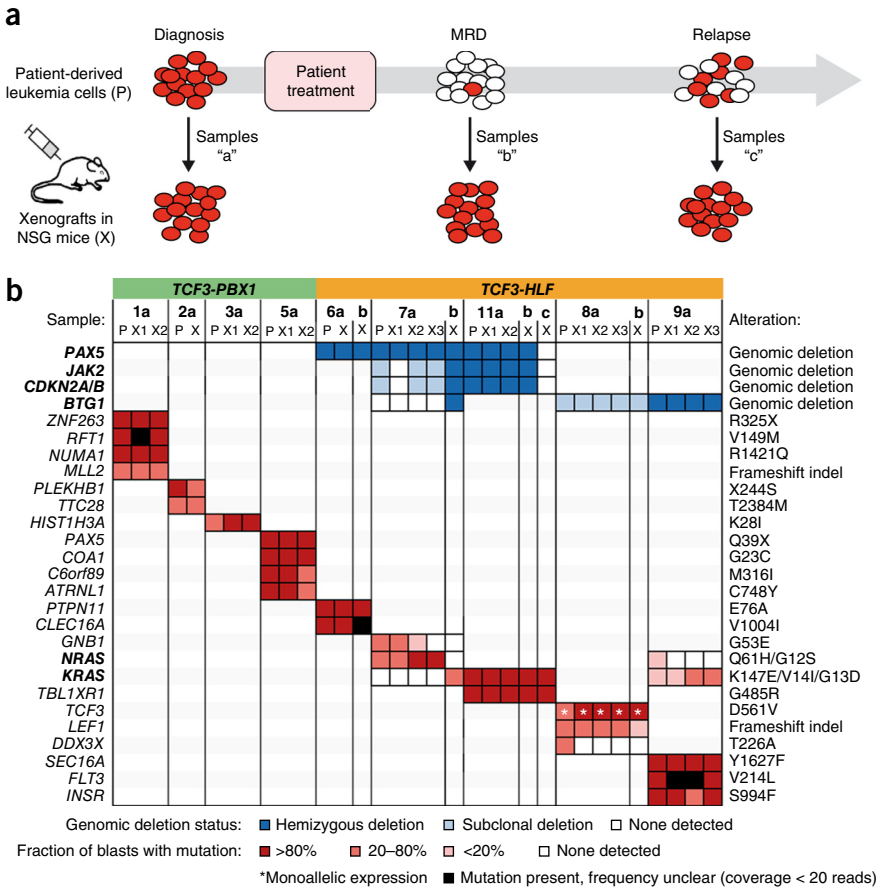

Figure 3 The genomic landscape of *TCF3-HLF*– and *TCF3-PBX1*–positive ALL is preserved in patient-derived leukemia xenografts. (**a**) Xenografts were established from cryopreserved patient samples at diagnosis (samples "a"), at follow-up with minimal residual disease (MRD, <1 leukemic cell in 10,000 cells, samples "b") or from disease progression (samples "c") and subjected to whole exome and transcriptome sequencing as well as multiplex ligation-dependent probe amplification (MLPA). All available MRD samples from *TCF3-HLF*–positive cases were successfully engrafted. (**b**) Comparison of all transcriptionally expressed nucleotide variations and of selected recurrent deletions frequently found in pediatric ALL in corresponding patient (P) and xenograft (X) samples. Deletions and nucleotide variations are colored according to their frequency in the analyzed leukemic cell population. Deletion frequencies were calculated by integrating whole genome and whole exome sequencing data with MLPA data. Nucleotide variation frequencies were calculated by integrating whole genome, whole exome and transcriptome sequencing data. Recurrently affected genes are indicated by bold symbols.

the two *TCF3*-translocated subtypes (**Fig. 2a**, and **Supplementary Tables 11** and **12**). *In silico* prediction of transcription factor binding sites in the corresponding promoter regions revealed enrichment for PBX (*Z* score = 3.72) and HLF (*Z* score = 2.99) binding motifs associated with *TCF3-PBX1* and *TCF3-HLF* gene signatures, respectively (**Supplementary Tables 13** and **14**). Further, *PBX1* and *HLF* were the only transcription factors among those with enriched binding motifs that were significantly differentially expressed between the two ALL subtypes, and between leukemia and remission samples. The chimeric *HLF* transcript was strongly induced in *TCF3-HLF*, but we detected no wild-type *HLF* expression. We predicted 39 potential HLF targets, including the known target *SNAI2* (*SLUG*)[16], *GPC4* and *BMP3* involved in stem cell proliferation, which showed induced expression in *TCF3-HLF* samples (**Supplementary Table 15**). Other potential TCF3-HLF targets that regulate developmental programs and cell survival, such as *LMO2* (ref. 14) and *BCL2* (ref. 14), were not predicted. However, their expression was increased in *TCF3-HLF*–positive ALL.

Gene set enrichment analysis using gene sets from sorted human hematopoietic stem cells and early progenitor populations[31] as well as curated oncogenic (C6) and human immunologic (C7) signatures from MsigDB[32] revealed an enrichment for stem cell and myeloid signatures in *TCF3-HLF*–positive ALL. In contrast, lymphoid features were more prominent in *TCF3-PBX1*–positive ALL (**Fig. 2b** and **Supplementary Table 16**). The hematopoietic stem cell signature[31] ranked among the top gene sets enriched in *TCF3-HLF*–positive ALL (**Fig. 2c** and **Supplementary Table 17**). We obtained similar results using an independent method based on text mining annotations (**Fig. 2d**, and **Supplementary Tables 18** and **19**). We also consistently detected high expression of the stem cell marker *LGR5* (ref. 33) in *TCF3-HLF*–positive ALL, suggesting a reactivation of immature features shared with other stem cell populations. Consistent with previous reports, the myeloid marker CD33 was expressed in *TCF3-HLF*–positive blasts, which provides a target for antibody-directed therapy[12,34]. Other differentially expressed genes, such as *BMP2* (ref. 35), could present additional therapeutic targets.

Our results are consistent with a model in which *TCF3-HLF* arises in lymphoid cells and promotes transcriptional reprogramming toward a hybrid hematopoietic state. We also detected features of mesenchyme-derived tissues in *TCF3-HLF*–positive ALL, which may indicate a profound cellular reprogramming toward a drug-resistant state.

Mutation profiles of *TCF3-HLF* ALL are conserved in xenografts

We generated leukemia xenografts in nonobese diabetic severe combined immunodeficiency (NOD/SCID)/IL2rγ^{null} (NSG) mice for all cases included in this study (**Supplementary Table 20**)[36,37]. We also established for the first time to our knowledge leukemia xenografts from follow-up samples with MRD, some with less than 0.1% ALL cells after induction chemotherapy (**Fig. 3a**, and **Supplementary Tables 1** and **20**). Leukemia and MRD engraftment was rapid with conserved and predictable kinetics for xenografts derived from the same patient (**Supplementary Fig. 7**), suggesting that no major adaptation to the mouse microenvironment was needed for proliferation. Most SNVs and intra-chromosomal deletions that had been present at diagnosis were conserved in the corresponding xenografts (**Fig. 3b** and **Supplementary Table 7**). Only deletions detected in the relapse sample 11c were not conserved in the corresponding xenografts, and a deletion in *BTG1* emerged in one MRD-derived sample (7b, **Supplementary Fig. 3c**,**d**). A few mutations were lost in MRD or relapse xenograft samples, including *GNB1* and *DDX3X*, indicating that these are probably dispensable or may cause drug sensitivity. Mutations in the RAS pathway were largely maintained in xenografts. However, the *NRAS* mutation p.Gln61His identified in the primary

MRD sample 7b was not detected in the corresponding xenograft. Instead, we identified a heterozygous damaging mutation in *KRAS* (p.Lys147Glu) associated with Noonan syndrome[38]. In patient 9a, we identified two subclones displaying either a *KRAS* (p.Gly13Asp) or an *NRAS* (p.Gly12Ser) mutation. The corresponding xenograft retained only the *KRAS* mutated subclone. Thus, maintenance and acquisition of RAS pathway mutations in xenografts support the notion that they occur later during selection at a multiclonal level and confer a selective advantage in *TCF3-HLF*–positive ALL. No other SNVs emerged *de novo* in the xenografts. In summary, the molecular characteristics of both leukemia subtypes were largely conserved in the xenografts, confirming the validity of this model.

TCF3-HLF–associated gene expression is maintained in xenografts

Hierarchical clustering based on the gene signature specifying the two leukemia subtypes showed that the expression profile and the subtype specificity of the primary leukemia were maintained in the xenografts (**Fig. 4**). The genes most significantly upregulated in matched patient and xenograft samples from *TCF3-HLF*–positive leukemia specified stem cell features (**Supplementary Tables 21** and **22**). Similar to the case in patient samples, we detected features of mesenchyme-derived tissues in xenografts derived from *TCF3-HLF*–positive ALL. *TCF3-HLF*–positive leukemias and xenografts displayed systematic downregulation of *PAX5* expression to halved levels. Though monoallelic deletions of *PAX5* were a prominent feature of *TCF3-HLF*–positive ALL, we also saw reduced expression in diploid cases, hinting at alternative molecular mechanisms. The recapitulation of this pattern in the xenograft samples enforces the notion that *TCF3-HLF*–positive leukemia emerges in a specific cellular context with reduced *PAX5* expression (**Supplementary Fig. 8**). The essential molecular features of *TCF3-HLF*–positive samples were maintained in xenografts, providing a useful model of this disease.

Drug activity profiling of *TCF3-HLF* and *TCF3-PBX1* ALL

To determine drug sensitivity and resistance profiles, we established ALL cocultures on human mesenchymal stromal cells under serum-free conditions[39]. Both subtypes depend on stroma for survival (**Supplementary Fig. 9**). *TCF3-PBX1*–positive ALL had a higher proportion of cells in S phase than *TCF3-HLF*–positive ALL on such cultures, reflecting consistent biological differences. By screening 98 bioactive agents, including many agents in clinical development (**Supplementary Table 23**), on an automated microscopy–based platform, we unambiguously discriminated the two translocations based on their drug sensitivity profiles, using either single (log half maximal inhibitory concentration (IC_{50}), **Fig. 5a** and **Supplementary Fig. 10**) or multiple response parameters ($logIC_{50}$, log 90% effective concentration (EC_{90}), $logEC_{50}$ and area under the curve (AUC), **Fig. 5b** and **Supplementary Table 24**). To capture informative differences, we compared the responses of xenografts derived from *TCF3-HLF*–positive ALL to xenografts derived from other high-risk pre-B and T ALL patients on the same platform (**Fig. 5c** and **Supplementary Table 25**). This provided information about the activity range of each drug on the respective ALL subtype. *TCF3-HLF*–positive cases were consistently more resistant to various drugs from the same class, including nucleotide analogs (for example, cytarabine), mitotic spindle inhibitors (for example, vincristine), polo-like and aurora kinase inhibitors. Given the importance of cytarabine and vincristine in standard ALL therapy, the implications of these observations need to be further explored. *TCF3-HLF*–positive ALL was very resistant to dasatinib in this assay, whereas *TCF3-PBX1*–positive ALL responded well. This partly challenges a recent report[40], which had proposed dasatinib as an alternative for the treatment of these leukemias based on strong *in vitro* activity in one *TCF3-HLF*– and ten *TCF3-PBX1*–positive primary ALL samples. However, *in vivo* studies will be required to verify these differences in drug response, as differences in cell-cycle activity may influence the pattern of response *in vitro*.

TCF3-HLF–positive ALL were sensitive to glucocorticoids (prednisone and dexamethasone) and to other drugs that could be relevant for the treatment of resistant ALL, including mTOR inhibitors, anthracyclines, bortezomib, the HSP90 inhibitor AUY922 and panobinostat. However, in spite of the good response of patients with *TCF3-HLF*–positive leukemia to prednisone therapy and the observed responsiveness of *TCF3-HLF*–positive ALL cells to glucocorticoids and anthracyclines that are commonly used in ALL treatment, patients who undergo this treatment relapse. Our transcriptome data suggested that resistance to apoptosis due to high expression of the anti-apoptotic oncoprotein BCL2 might promote cancer cell survival and constitute a druggable target (**Supplementary Fig. 11**). *BCL2* is a putative transcriptional target of TCF3-HLF[14]. Of note, PAX5, commonly deleted in our cohort, normally represses *BCL2* transcription[41].

TCF3-HLF ALL is extremely sensitive to the BCL2 antagonist venetoclax

To assess the role of *BCL2* overexpression in *TCF3-HLF*–positive ALL and to provide preclinical evidence for therapeutic activity,

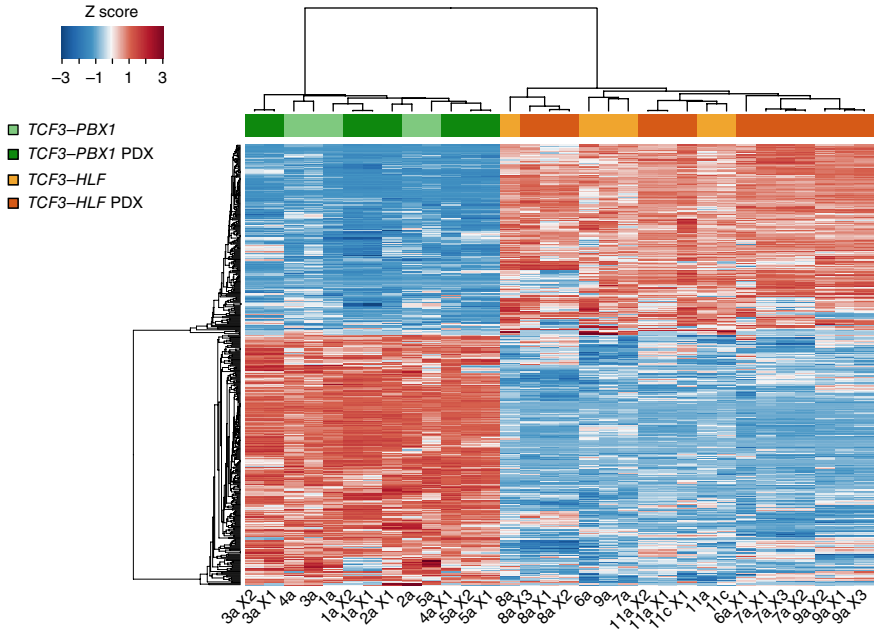

Figure 4 Major components of the gene expression signature of *TCF3-HLF*– and *TCF3-PBX1*–positive ALL are conserved in patient-derived xenografts. Hierarchical clustering of primary and patient derived xenograft (PDX) ALL samples based on the expression of the 401 genes of the signature defined with primary samples (**Fig. 2**) shows that xenografts clearly group with their corresponding primary samples.

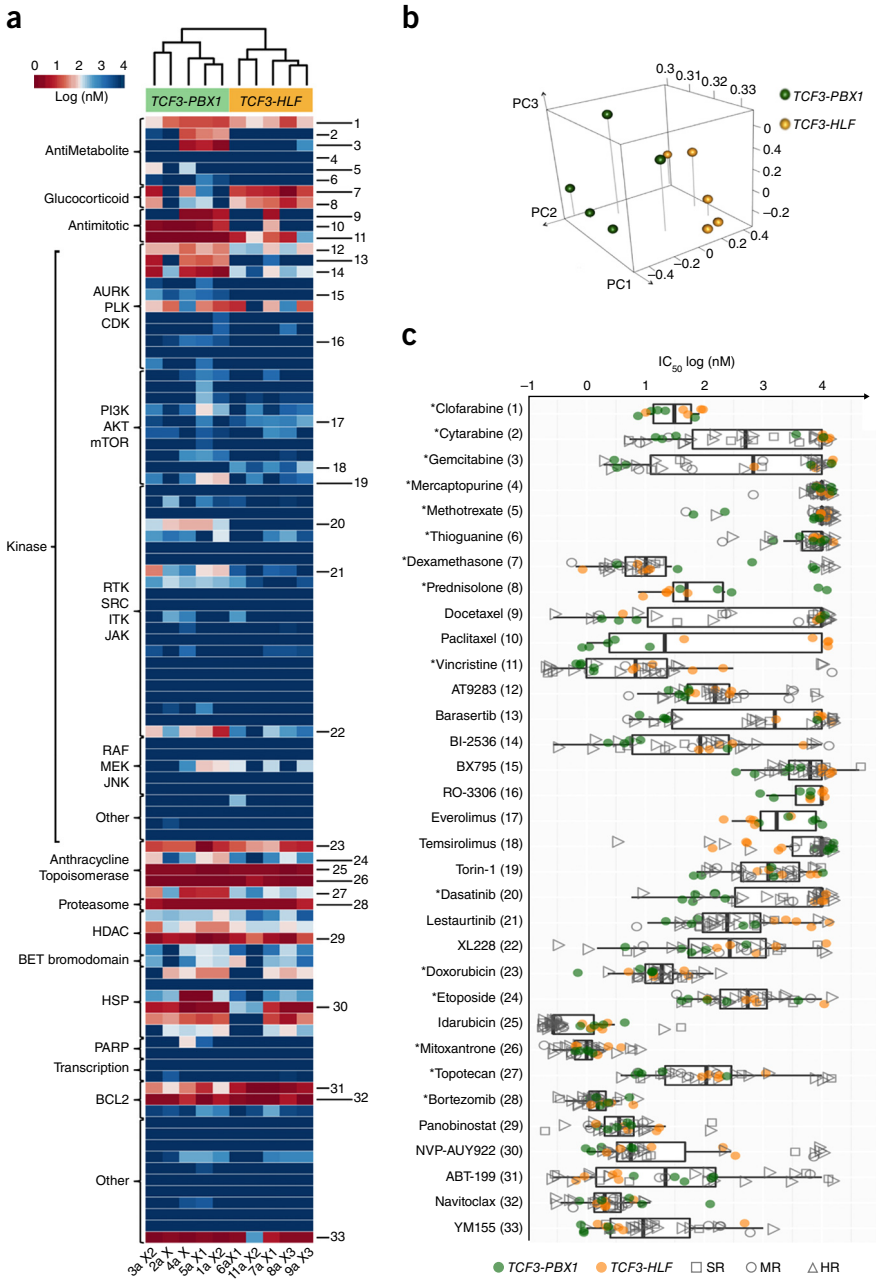

Figure 5 Drug activity profiling of *TCF3*-translocated leukemia reveals relevant differences in drug sensitivity. (**a**) Unsupervised clustering based on the drug activity profile of 98 compounds (log IC_{50}). Fitted values are provided in **Supplementary Table 24** (absolute IC_{50}). Numbers identify the compounds shown in **c**. (**b**) Principal component analysis of the response variables IC_{50}, EC_{50}, EC_{90} and AUC (**Supplementary Table 24**) show *TCF3-PBX1*–positive and *TCF3-HLF*–positive ALL in two distinct clusters. The separation of *TCF3-PBX1*–positive and *TCF3-HLF*–positive ALL is determined by responses to topoisomerases, BCL2 inhibitors, glucocorticoids and antimitotic agents, which correlate with the first three principal components. (**c**) Selection of drugs based on differences in sensitivity or resistance in *TCF3-PBX1*–positives and *TCF3-HLF*–positives. For comparison, the corresponding drug activity is indicated for 25 additional ALL samples tested on the same platform, including standard risk (SR, $n = 5$), medium risk (MR, $n = 4$) and high risk (HR, $n = 16$) cases (**Supplementary Table 25**). Boxplots extend from the first to the third quartiles (hinges) of the response range for each compound. Whiskers correspond to values from the hinge to the lowest or highest values within 1.5× of the distance between the first and third quartiles, respectively. Drugs with differential activity include docetaxel, paclitaxel, vincristine, AT9283, barasertib, BI2536, torin-1, dasatinib, lestaurtinib and XL228 ($P \leq 0.05$). Drugs which are active across the patients include doxorubicin, idarubicin, mitoxantrone, bortezomib, panobinostat, NVP-AUY922, ABT-199 (venetoclax) and navitoclax. Asterisks indicate drugs currently in clinical use.

we tested the BCL2-targeting drug venetoclax (ABT-199) in our xenograft model (**Fig. 5c**). This BH3-mimetic compound is a highly specific small molecule inhibitor that competes with pro-apoptotic BCL2 family proteins for binding to BCL2, and shifts the balance of pro-death and pro-survival signals inside the cell in favor of cell death[42]. Venetoclax is in clinical development (phase II and III trials) for chronic lymphocytic leukemia and lymphoma, and holds promise for ALL and acute myeloid leukemia.

TCF3-HLF–positive ALL samples were more sensitive to venetoclax than *TCF3-PBX1*–positive samples (**Fig. 6a**), which correlated with higher *BCL2* transcript and protein expression (**Fig. 6b**). A two-week treatment course of daily venetoclax administration delayed leukemia progression significantly in ALL xenografts from three different *TCF3-HLF*–positive cases (**Fig. 6c**,**d**). Treatment of mice in the control arm that reached maximal leukemia burden resulted in very rapid reduction of the leukemic load (**Fig. 6e**). Xenografts from MRD or relapse remained sensitive to venetoclax (**Supplementary Fig. 11**). Profiling of primary cells from two additional cases with refractory ALL confirmed exquisite sensitivity to venetoclax (**Supplementary Fig. 12**). Combined treatment of patient-derived xenografts from patients 6–11 with venetoclax and either vincristine or dexamethasone indicated a potentially synergistic effect in some of those patients (**Supplementary Fig. 13** and **Supplementary Table 26**). Our data identified BCL2 dependency in *TCF3-HLF* ALL as a druggable target, and illustrate how integration of drug response profiling and molecular genetic analyses can inform the development of innovative treatment strategies in patients with unmet therapeutic needs.

DISCUSSION

To our knowledge, a long-term cure has never been achieved for patients with *TCF3-HLF*–positive ALL. Our study revealed a recurrent pattern of *TCF3-HLF* accompanied by abnormalities that affect transcriptional regulation of lymphoid development. We found frequent deletions of *PAX5* and *VPREB1* in association with *TCF3-HLF*, but did not detect deletions of Ikaros family members, which are commonly affected in ALL[1,23]. We also uncovered recurrent mutations of the transcription factor TCF3, which acts upstream of PAX5 in

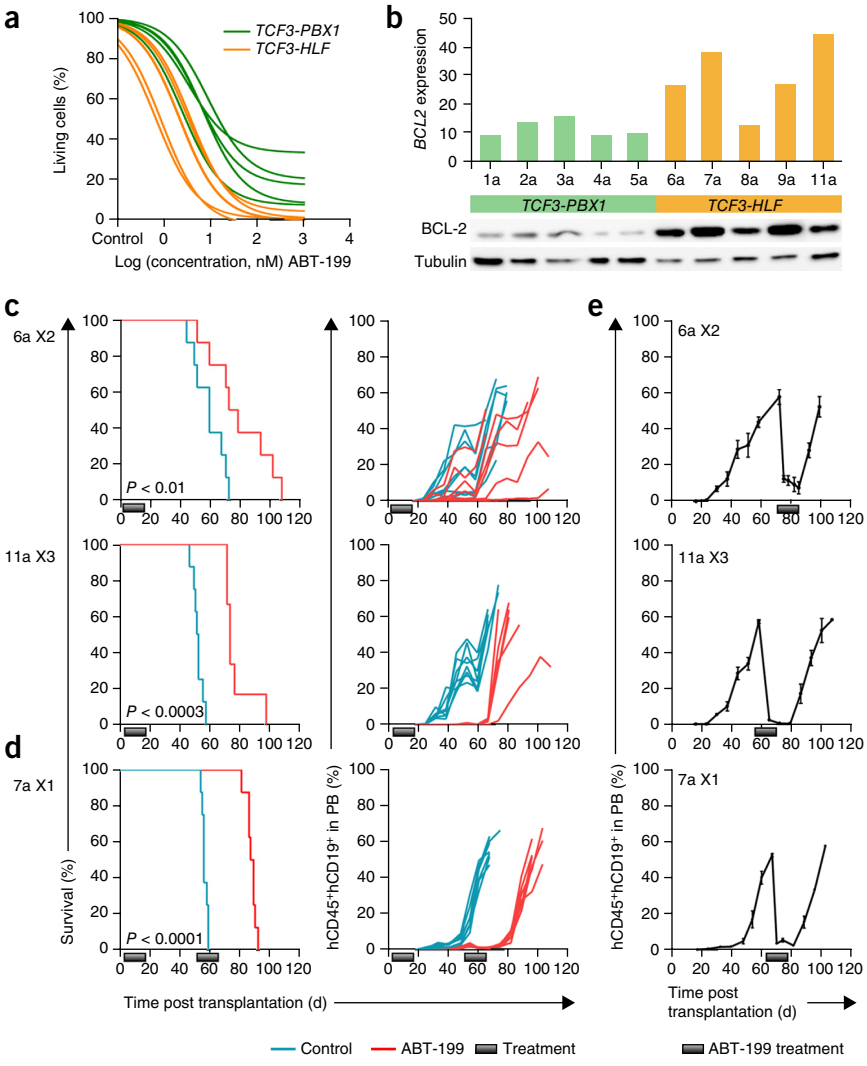

Figure 6 The BCL2 antagonist ABT-199 (venetoclax) shows promising anti-leukemic activity in *TCF3-HLF*–positive xenografts. (**a**) *In vitro* dose response curves normalized against DMSO-treated controls. (**b**) Merged absolute reads per kilobase of exon model per million mapped reads (RPKM) values of xenografts derived from the same primary leukemia sample (top) and immunoblot for BCL2 (bottom) in patient-derived xenografts as indicated. Tubulin was used as a loading control. (**c**,**d**) *In vivo* response to ABT-199 on *TCF3-HLF*–positive xenografts. Treatment (gray bars) with 100 mg kg^{-1} qd ABT-199 (red) or with vehicle control (turquoise) were administered orally for 14 d (6–8 mice per treatment arm). Two treatment courses were administrated to xenograft 7a. For survival analysis an event was defined when at least 25% of leukemic cells were detected by FACS ($mCD45^{-}hCD19^{+}hCD45^{+}$) in the peripheral blood. Differences in the survival of mice receiving ABT-199 or vehicle control were determined by the Mantel-Cox test and verified by the Gehan-Breslow-Wilcoxon test. (**e**) Mice from the control arm of **c**,**d** were treated with ABT-199 when more than 50% of ALL cells were detected in the blood. Mean and s.d. are shown ($n = 4$).

lymphoid development, potentially impairing structural interactions with other transcription cofactors[29]. *PAX5* expression was reduced by twofold in all *TCF3-HLF*–positive cases, underscoring the possibility of an interaction between TCF3-HLF, TCF3 and PAX5. *PAX5* is required for B lymphoid lineage commitment and maturation[43], and is frequently deleted in high-risk ALL with complex patterns of copy number abnormalities[23]. Similarly, deletions in *IKFZ1*, which is required for the development of B and T lymphoid lineages and has additional stem cell–like functions[44], are detected both in high-risk *BCR-ABL1*–positive and –negative ALL, and in the more favorable *ERG*-altered ALL subtype[45], but never in *TCF3-HLF*–positive ALL. We also detected focal deletions of *VPREB1* in *TCF3-HLF* ALL, which may lead to a developmental arrest associated with lack of pre–B cell receptor formation and the resulting loss of negative feedback on RAG-mediated recombination[46]. *VPREB1* deletions were present at a similar frequency compared to other high-risk ALLs, such as *BCR-ABL1*–like and *BCR-ABL1*–positive ALL (~30–40% of cases)[47] or hypodiploid ALL (~30%)[24], associated with poorer overall survival in high-risk pre–B cell ALL patients[24]. However, specific ALL subtypes associated with good prognosis (for example, *ETV6-RUNX1*–positive ALL) also present high frequencies of *VPREB1* deletions[24], suggesting an important impact of the genomic context[24]. Thus, distinct patterns of association emerge that are likely to reflect important underlying biological mechanisms. Based on our results, we propose that a reduction of *PAX5* gene dosage constitutes a favorable context for the oncogenic activity of *TCF3-HLF*.

As observed for hypodiploid ALL[5] and in subsets of *MLL*-rearranged ALL[48], we identified mutations in *NRAS*, *KRAS* and *PTPN11* in *TCF3-HLF*–positive ALL. In our xenograft models we detected variable persistence of *NRAS* and a switch to *KRAS* mutations, indicating that RAS mutations are multiclonal and might not be strictly required for disease progression in *TC3-HLF*–positive ALL. Indeed, mutations in the RAS pathway are enriched at relapse in ALL[7,30,48] but mostly in a subclonal pattern with losses or switches in *NRAS* and *KRAS* from diagnosis to relapse. These represent secondary events, possibly compensating functional effects of the initiating events. Mutations in the RAS pathway might not represent optimal therapeutic targets, given their volatility and the potential to select for slower-proliferating, more resistant subclones. The *TCF3-HLF* gene expression signature, enriched for components of stem cell and myelomonocytic stages, was very similar among leukemias and maintained in xenografts, specifying additional, novel markers associated with stem cell function, such as *LGR5*, which marks epithelial stem cells[49] and embryonic and fetal hematopoietic progenitor cells in mice[50]. Thus, in analogy to experimental induction of pluripotent stem cells[51,52], *TCF3-HLF* likely induces a whole set of factors that carry out reprogramming and leukemic transformation in the context of low *PAX5* expression. Deletion of *PAX5* in early B cell progenitors induced dedifferentiation to a state with myeloid and T cell potential[43,53]. Moreover, rescue with low-level expression of PAX5 in knockout mice generates a stalled biphenotypic B-lymphoid/myeloid state[54]. Together with an activating mutation in *STAT5*, *PAX5* haploinsufficiency initiates ALL in mice[41]. Based on these data, we propose that the initiating *TCF3-HLF* fusion results in severe transcriptional reprogramming with dedifferentiation. The favorable context for transformation is secured through

secondary cooperating lesions in early B cell differentiation genes including *TCF3* and *PAX5*.

A central question remains pertaining to the cell of origin in different ALL subtypes. Our study provides important clues that should be further addressed using disease models. The molecular analysis of the *TCF3-HLF* and *TCF3-PBX1* fusion gene breakpoints indicated that the *TCF3-HLF*, like the *TCF-PBX1* translocation, originates in cells already committed to lymphoid differentiation. Furthermore, we found the associated somatic structural variants to be RAG-mediated, which is comparable to patterns identified recently in *ETV6-RUNX1*–positive ALL, the most frequent pre-B cell ALL subtype, which is consistent with expression of RAG in *TCF3-HLF*–positive ALL[55]. We favor the hypothesis that the *TCF3-HLF* translocation occurs in a B cell progenitor and that the specific lineage context is constrained further in a restricted developmental stage by additional mutations. The detection of *TCF3-HLF* being restricted to leukemic cells supports this idea, although initiation in a more immature compartment cannot be formally excluded.

The molecular landscapes of *TCF3-HLF*–positive ALL were largely conserved in xenografts, providing a valuable, well characterized, model for preclinical testing. Drug activity profiling revealed that *TCF3-HLF*–positive cases were more resistant to several standard ALL drugs, such as nucleotide analogs (for example, cytarabin) and mitotic spindle inhibitors (for example, vincristine). We detected activity for other relevant drug classes, such as mTOR inhibitors, the proteasome inhibitor bortezomib, the HSP90 inhibitor AUY922 and the HDAC inhibitor panobinostat. The BCL2 inhibitor venetoclax (ABT-199)[42] was highly active in all *TCF3-HLF*–positive cases analyzed, which we confirmed using primary ALL cells from two additional cases with refractory disease. These results refine data obtained using the broader spectrum BH3 mimetic ABT-737 in *TCF3-HLF*–positive cell lines[14]. Given the activity of venetoclax also in other ALL subsets including immature T cell ALL (refs. 56,57 and our own unpublished data) and the lack of on-target thrombocytopenia caused by ABT-737, venetoclax should be explored for experimental therapy in refractory ALL in selected cases based on such functional data. Thus integrated genomic and functional analyses of *TCF3-HLF*–positive ALL provide insight into the molecular context and associated components and offer unprecedented possibilities to investigate new agents for the treatment of these children who currently lack effective therapeutic options.

URLs. Information on the two image processing programs used for *in vitro* drug screening and automated microscopy can be found at http://acc.ethz.ch/.

METHODS

Methods and any associated references are available in the online version of the paper.

Accession codes. Sequencing data are available from the public POPGEN repository (2015-UFO-NG-1; Christian Albrechts University, Kiel) upon written request accompanied by a positive internal review board vote for research addressing leukemia-related questions. Sequencing data transfer can proceed upon positive review and signing of a material transfer agreement.

ACKNOWLEDGMENTS

We thank all participants and personnel involved in the clinical trials in Austria, France, Germany, United Kingdom and Switzerland. We thank T. Radimerski and Novartis for providing essential compounds. We thank the Leukaemia & Lymphoma Research (LLR) Childhood Leukaemia Cell Bank in the UK for providing primary patient samples. This work was supported by the German Federal Office for Radiation Protection (grant St.Sch. 3611S70014), by the Swiss National Research Foundation SNF 310030-133108, the foundation 'Kinderkrebsforschung Schweiz', the 'Krebsliga Zurich', the Sassella Foundation, the Fondation Panacée, the clinical research focus program 'Human Hemato-Lymphatic Diseases' of the University of Zurich, the Deutsche Forschungsgemeinschaft (DFG), Clusters of Excellence 'Inflammation at Interfaces', the EU Seventh Framework Program (FP7/2007-2013, grant 262055, ESGI; FP7-HEALTH-F2-2011 grant 261474, ENCCA; ERA-Net Transcan, Validation of biomarkers for personalized cancer medicine, TRANSCALL; Health-F2-2010 grant 260791, EUROCANPLATFORM), the 'Katharina Hardt Stiftung', the 'Deutsche José Carreras Leukämie-Stiftung', the 'Madeleine Schickedanz-Kinderkrebs-Stiftung', the 'Deutsche Krebshilfe – Dr. Mildred Scheel Stiftung' (grants 108613, 102588 and 108588), the Foundation of Experimental Biomedicine in Zurich, the Max Planck Society, and the 'Verein für krebskranke Kinder Hannover e.V.'. We thank A. Dehos, B. Grosche, T. Jung, W. Weiss and G. Ziegelberger, German Federal Office for Radiation Protection, as well as B. Heinzow, State Office for Social Services of Schleswig-Holstein, and A. Böttger, German Federal Ministry for the Environment, Nature Conservation, Building and Nuclear Safety for their support and critical discussions. We are grateful for the excellent technical assistance offered by the sequencing team of the Department of Vertebrate Genomics of the Max Planck Institute for Molecular Genetics (Berlin) and by the team of the Genomics Core facility of the European Molecular Biology Laboratory. We thank K. Alemazkour for excellent technical assistance regarding whole exome sequencing at the Department of Pediatric Oncology, Hematology and Clinical Immunology (Düsseldorf, Germany). We thank N. Forgo, Institute for Legal Informatics, Leibniz University Hannover, and H.-D. Tröger, Hannover Medical School, for legal and ethical counselling.

AUTHOR CONTRIBUTIONS

A. Borkhardt, A.F., J.O.K., J.-P.B., M.-L.Y. and M. Stanulla jointly designed the project. A. Baruchel, A.V., A.V.M., C.C., C.P.K., F.N., G.B., G.C., G.t.K., H.C., M. Schrappe, M. Stanulla, N.v.d.W., O.A.H., C.E. and R.P.-G. provided samples or clinical data. A. Borkhardt, A.C.M., A.F., A.V., C.E., G.H.-S., H.L., J.-P.B., J.O.K., J.T., M.D., M.F., M.-L.Y., M.P.D., M. Schrappe, M. Stanulla, M. Zimmermann, O.A.H., P.R. and T.Z. contributed reagents, materials or analysis tools. A.M.S., B.B., B.M., C.E., C.L.W., H.-J.W., J.I.H., J.-P.B., M.F., M.G., S. Sungalee and U.F. designed experiments. A.M.S., A.R., B.B., B.R., B.S., B.S.P., C.E., C.K., C.L.W., D.D., D.S., H.-J.W., J.T., K.H., L.Z., M.G., M.R., M. Zaliova, M. Sultan, P.K., S.E., S. Sungalee, T.B., U.F. and V.F. performed experiments. A.R., B.S., B.S.P., C.E., C.K., C.L.W., D.S., E.E., J.I.H., H.-J.W., M.G., M.P.D., M.F., N.B., S.G., G.H.-S., P.H., P.K., M.-L.Y., M.R., M. Stanulla, M. Schütte, M. Zaliova, S. Sungalee, T.R., U.F. and V.A. analyzed data. A. Borkhardt, A.C.M., A.F., B.B., H.L., J.-P.B., J.O.K., M.D., M.F., M.-L.Y., M. Stanulla, O.H., R.T. and S. Schreiber, U.F. supervised research. A.R., C.L.W., D.S., H.-J.W., M.F., M.P.D., M. Stanulla, P.K., S. Sungalee, T.R. and U.F. prepared tables and figures. J.-P.B., M. Stanulla and M.-L.Y. wrote the manuscript. A. Borkhardt, A.F., A.R., A.V.M., H.-J.W., J.O.K., M.F., M.P.D., O.H., S.H., S. Sungalee, T.R. and U.F. contributed to the writing of the manuscript. All authors critically reviewed the manuscript for its content.

COMPETING FINANCIAL INTERESTS

The authors declare no competing financial interests.

Reprints and permissions information is available online at http://www.nature.com/reprints/index.html.

1. Mullighan, C.G. *et al.* Genome-wide analysis of genetic alterations in acute lymphoblastic leukaemia. *Nature* **446**, 758–764 (2007).
2. Russell, L.J. *et al.* Deregulated expression of cytokine receptor gene, CRLF2, is involved in lymphoid transformation in B-cell precursor acute lymphoblastic leukemia. *Blood* **114**, 2688–2698 (2009).
3. Mullighan, C.G. *et al.* Rearrangement of CRLF2 in B-progenitor- and Down syndrome-associated acute lymphoblastic leukemia. *Nat. Genet.* **41**, 1243–1246 (2009).
4. Hertzberg, L. *et al.* Down syndrome acute lymphoblastic leukemia, a highly heterogeneous disease in which aberrant expression of CRLF2 is associated with mutated JAK2: a report from the International BFM Study Group. *Blood* **115**, 1006–1017 (2010).
5. Holmfeldt, L. *et al.* The genomic landscape of hypodiploid acute lymphoblastic leukemia. *Nat. Genet.* **45**, 242–252 (2013).
6. Zhang, J. *et al.* Key pathways are frequently mutated in high-risk childhood acute lymphoblastic leukemia: a report from the Children's Oncology Group. *Blood* **118**, 3080–3087 (2011).
7. Irving, J. *et al.* Ras pathway mutations are highly prevalent in relapsed childhood acute lymphoblastic leukaemia, may act as relapse-drivers and confer sensitivity to MEK inhibition. *Blood* **124**, 3420–3430 (2014).

8. Inaba, H., Greaves, M. & Mullighan, C.G. Acute lymphoblastic leukaemia. *Lancet* **381**, 1943–1955 (2013).
9. Kwon, K. *et al.* Instructive role of the transcription factor E2A in early B lymphopoiesis and germinal center B cell development. *Immunity* **28**, 751–762 (2008).
10. Felice, M.S. *et al.* Prognostic impact of t(1;19)/ TCF3–PBX1 in childhood acute lymphoblastic leukemia in the context of Berlin-Frankfurt-Munster-based protocols. *Leuk. Lymphoma* **52**, 1215–1221 (2011).
11. Hunger, S.P., Ohyashiki, K., Toyama, K. & Cleary, M.L. Hlf, a novel hepatic bZIP protein, shows altered DNA-binding properties following fusion to E2A in t(17;19) acute lymphoblastic leukemia. *Genes Dev.* **6**, 1608–1620 (1992).
12. Inukai, T. *et al.* Hypercalcemia in childhood acute lymphoblastic leukemia: frequent implication of parathyroid hormone-related peptide and E2A-HLF from translocation 17;19. *Leukemia* **21**, 288–296 (2007).
13. Boller, S. & Grosschedl, R. The regulatory network of B-cell differentiation: a focused view of early B-cell factor 1 function. *Immunol. Rev.* **261**, 102–115 (2014).
14. de Boer, J. *et al.* The E2A-HLF oncogenic fusion protein acts through Lmo2 and Bcl-2 to immortalize hematopoietic progenitors. *Leukemia* **25**, 321–330 (2011).
15. Hirose, K. *et al.* Aberrant induction of LMO2 by the E2A-HLF chimeric transcription factor and its implication in leukemogenesis of B-precursor ALL with t(17;19). *Blood* **116**, 962–970 (2010).
16. Inukai, T. *et al.* SLUG, a ces-1-related zinc finger transcription factor gene with antiapoptotic activity, is a downstream target of the E2A-HLF oncoprotein. *Mol. Cell* **4**, 343–352 (1999).
17. Inoue, A. *et al.* Slug, a highly conserved zinc finger transcriptional repressor, protects hematopoietic progenitor cells from radiation-induced apoptosis in vivo. *Cancer Cell* **2**, 279–288 (2002).
18. Honda, H. *et al.* Expression of E2A-HLF chimeric protein induced T-cell apoptosis, B-cell maturation arrest, and development of acute lymphoblastic leukemia. *Blood* **93**, 2780–2790 (1999).
19. Smith, K.S., Rhee, J.W., Naumovski, L. & Cleary, M.L. Disrupted differentiation and oncogenic transformation of lymphoid progenitors in E2A-HLF transgenic mice. *Mol. Cell. Biol.* **19**, 4443–4451 (1999).
20. Hunger, S.P. Chromosomal translocations involving the E2A gene in acute lymphoblastic leukemia: clinical features and molecular pathogenesis. *Blood* **87**, 1211–1224 (1996).
21. Wiemels, J.L. *et al.* Site-specific translocation and evidence of postnatal origin of the t(1;19) E2A–PBX1 fusion in childhood acute lymphoblastic leukemia. *Proc. Natl. Acad. Sci. USA* **99**, 15101–15106 (2002).
22. Tsai, A.G. *et al.* Human chromosomal translocations at CpG sites and a theoretical basis for their lineage and stage specificity. *Cell* **135**, 1130–1142 (2008).
23. Moorman, A.V. *et al.* A novel integrated cytogenetic and genomic classification refines risk stratification in pediatric acute lymphoblastic leukemia. *Blood* **124**, 1434–1444 (2014).
24. Mangum, D.S. *et al.* VPREB1 deletions occur independent of lambda light chain rearrangement in childhood acute lymphoblastic leukemia. *Leukemia* **28**, 216–220 (2014).
25. Waanders, E. *et al.* The origin and nature of tightly clustered BTG1 deletions in precursor B-cell acute lymphoblastic leukemia support a model of multiclonal evolution. *PLoS Genet.* **8**, e1002533 (2012).
26. Tijchon, E., Havinga, J., van Leeuwen, F.N. & Scheijen, B. B-lineage transcription factors and cooperating gene lesions required for leukemia development. *Leukemia* **27**, 541–552 (2013).
27. Balbin, O.A. *et al.* Reconstructing targetable pathways in lung cancer by integrating diverse omics data. *Nat. Commun.* **4**, 2617 (2013).
28. Wright, D.D., Sefton, B.M. & Kamps, M.P. Oncogenic activation of the Lck protein accompanies translocation of the LCK gene in the human HSB2 T-cell leukemia. *Mol. Cell. Biol.* **14**, 2429–2437 (1994).
29. Schmitz, R. *et al.* Burkitt lymphoma pathogenesis and therapeutic targets from structural and functional genomics. *Nature* **490**, 116–120 (2012).
30. Ma, X. *et al.* Rise and fall of subclones from diagnosis to relapse in pediatric B-acute lymphoblastic leukaemia. *Nat. Commun.* **6**, 6604 (2015).
31. Laurenti, E. *et al.* The transcriptional architecture of early human hematopoiesis identifies multilevel control of lymphoid commitment. *Nat. Immunol.* **14**, 756–763 (2013).
32. Subramanian, A., Kuehn, H., Gould, J., Tamayo, P. & Mesirov, J.P. GSEA-P: a desktop application for Gene Set Enrichment Analysis. *Bioinformatics* **23**, 3251–3253 (2007).
33. Schepers, A.G. *et al.* Lineage tracing reveals Lgr5^{+} stem cell activity in mouse intestinal adenomas. *Science* **337**, 730–735 (2012).
34. Akahane, K. *et al.* Specific induction of CD33 expression by E2A-HLF: the first evidence for aberrant myeloid antigen expression in ALL by a fusion transcription factor. *Leukemia* **24**, 865–869 (2010).
35. Nissim, S. *et al.* Prostaglandin E2 regulates liver versus pancreas cell-fate decisions and endodermal outgrowth. *Dev. Cell* **28**, 423–437 (2014).
36. Schmitz, M. *et al.* Xenografts of highly resistant leukemia recapitulate the clonal composition of the leukemogenic compartment. *Blood* **118**, 1854–1864 (2011).
37. Bonapace, L. *et al.* Induction of autophagy-dependent necroptosis is required for childhood acute lymphoblastic leukemia cells to overcome glucocorticoid resistance. *J. Clin. Invest.* **120**, 1310–1323 (2010).
38. Stark, Z. *et al.* Two novel germline KRAS mutations: expanding the molecular and clinical phenotype. *Clin. Genet.* **81**, 590–594 (2012).
39. Boutter, J. *et al.* Image-based RNA interference screening reveals an individual dependence of acute lymphoblastic leukemia on stromal cysteine support. *Oncotarget* **5**, 11501–11512 (2014).
40. Bicocca, V.T. *et al.* Crosstalk between ROR1 and the Pre-B cell receptor promotes survival of t(1;19) acute lymphoblastic leukemia. *Cancer Cell* **22**, 656–667 (2012).
41. Heltemes-Harris, L.M. *et al.* Ebf1 or Pax5 haploinsufficiency synergizes with STAT5 activation to initiate acute lymphoblastic leukemia. *J. Exp. Med.* **208**, 1135–1149 (2011).
42. Souers, A.J. *et al.* ABT-199, a potent and selective BCL-2 inhibitor, achieves antitumor activity while sparing platelets. *Nat. Med.* **19**, 202–208 (2013).
43. Rolink, A.G., Nutt, S.L., Melchers, F. & Busslinger, M. Long-term in vivo reconstitution of T-cell development by Pax5-deficient B-cell progenitors. *Nature* **401**, 603–606 (1999).
44. Joshi, I. *et al.* Loss of Ikaros DNA-binding function confers integrin-dependent survival on pre-B cells and progression to acute lymphoblastic leukemia. *Nat. Immunol.* **15**, 294–304 (2014).
45. Clappier, E. *et al.* An intragenic ERG deletion is a marker of an oncogenic subtype of B-cell precursor acute lymphoblastic leukemia with a favorable outcome despite frequent IKZF1 deletions. *Leukemia* **28**, 70–77 (2014).
46. Grawunder, U. *et al.* Down-regulation of RAG1 and RAG2 gene expression in preB cells after functional immunoglobulin heavy chain rearrangement. *Immunity* **3**, 601–608 (1995).
47. Den Boer, M.L. *et al.* A subtype of childhood acute lymphoblastic leukaemia with poor treatment outcome: a genome-wide classification study. *Lancet Oncol.* **10**, 125–134 (2009).
48. Andersson, A.K. *et al.* The landscape of somatic mutations in infant MLL-rearranged acute lymphoblastic leukemias. *Nat. Genet.* **47**, 330–337 (2015).
49. Barker, N. *et al.* Identification of stem cells in small intestine and colon by marker gene Lgr5. *Nature* **449**, 1003–1007 (2007).
50. Liu, D. *et al.* Leucine-rich repeat-containing G-protein-coupled Receptor 5 marks short-term hematopoietic stem and progenitor cells during mouse embryonic development. *J. Biol. Chem.* **289**, 23809–23816 (2014).
51. Riddell, J. *et al.* Reprogramming committed murine blood cells to induced hematopoietic stem cells with defined factors. *Cell* **157**, 549–564 (2014).
52. Sandler, V.M. *et al.* Reprogramming human endothelial cells to haematopoietic cells requires vascular induction. *Nature* **511**, 312–318 (2014).
53. Urbánek, P., Wang, Z.Q., Fetka, I., Wagner, E.F. & Busslinger, M. Complete block of early B cell differentiation and altered patterning of the posterior midbrain in mice lacking Pax5/BSAP. *Cell* **79**, 901–912 (1994).
54. Simmons, S. *et al.* Biphenotypic B-lymphoid/myeloid cells expressing low levels of Pax5: potential targets of BAL development. *Blood* **120**, 3688–3698 (2012).
55. Papaemmanuil, E. *et al.* RAG-mediated recombination is the predominant driver of oncogenic rearrangement in ETV6-RUNX1 acute lymphoblastic leukemia. *Nat. Genet.* **46**, 116–125 (2014).
56. Peirs, S. *et al.* ABT-199 mediated inhibition of BCL-2 as a novel therapeutic strategy in T-cell acute lymphoblastic leukemia. *Blood* **124**, 3738–3747 (2014).
57. Chonghaile, T.N. *et al.* Maturation stage of T-cell acute lymphoblastic leukemia determines BCL-2 versus BCL-XL dependence and sensitivity to ABT-199. *Cancer Discov.* **4**, 1074–1087 (2014).
58. El Omari, K. *et al.* Structural basis for LMO2-driven recruitment of the SCL: E47bHLH heterodimer to hematopoietic-specific transcriptional targets. *Cell Rep.* **4**, 135–147 (2013).

Ute Fischer[1,26], Michael Forster[2,26], Anna Rinaldi[3,26], Thomas Risch[4,26], Stéphanie Sungalee[5,26], Hans-Jörg Warnatz[4,26], Beat Bornhauser[3], Michael Gombert[1], Christina Kratsch[6], Adrian M Stütz[5], Marc Sultan[4], Joelle Tchinda[3], Catherine L Worth[4], Vyacheslav Amstislavskiy[4], Nandini Badarinarayan[2], André Baruchel[7], Thies Bartram[8], Giuseppe Basso[9], Cengiz Canpolat[10], Gunnar Cario[8], Hélène Cavé[11], Dardane Dakaj[3], Mauro Delorenzi[12,13], Maria Pamela Dobay[13], Cornelia Eckert[14], Eva Ellinghaus[2], Sabrina Eugster[3], Viktoras Frismantas[3], Sebastian Ginzel[1,15], Oskar A Haas[16], Olaf Heidenreich[17], Georg Hemmrich-Stanisak[2], Kebria Hezaveh[1], Jessica I Höll[1], Sabine Hornhardt[18], Peter Husemann[1],

Priyadarshini Kachroo[2], Christian P Kratz[19], Geertruy te Kronnie[9], Blerim Marovca[3], Felix Niggli[3], Alice C McHardy[6], Anthony V Moorman[17], Renate Panzer-Grümayer[16], Britt S Petersen[2], Benjamin Raeder[5], Meryem Ralser[4], Philip Rosenstiel[2], Daniel Schäfer[1], Martin Schrappe[8], Stefan Schreiber[2], Moritz Schütte[20], Björn Stade[2], Ralf Thiele[15], Nicolas von der Weid[21], Ajay Vora[22], Marketa Zaliova[19,23], Langhui Zhang[1,24], Thomas Zichner[5], Martin Zimmermann[19], Hans Lehrach[4,20,25], Arndt Borkhardt[1,27], Jean-Pierre Bourquin[3,27], Andre Franke[2,27], Jan O Korbel[5,27], Martin Stanulla[19,27] & Marie-Laure Yaspo[4,27]

[1]Clinic for Pediatric Oncology, Hematology and Clinical Immunology, Medical Faculty, Heinrich Heine University, Düsseldorf, Germany. [2]Institute of Clinical Molecular Biology, Christian Albrechts University of Kiel, Kiel, Germany. [3]Pediatric Oncology, Children's Research Centre, University Children's Hospital Zurich, Zurich, Switzerland. [4]Department of Vertebrate Genomics, Max Planck Institute for Molecular Genetics, Berlin, Germany. [5]European Molecular Biology Laboratory (EMBL), Genome Biology Unit, Heidelberg, Germany. [6]Department of Algorithmic Bioinformatics, Heinrich Heine University, Düsseldorf, Germany. [7]Department of Pediatric Hemato-Immunology, Hôpital Robert Debré and Paris Diderot University, Paris, France. [8]Department of Pediatrics, Christian Albrechts University of Kiel and University Medical Center Schleswig-Holstein, Kiel, Germany. [9]Department of Pediatrics, Laboratory of Pediatric Hematology/Oncology, University of Padova, Padova, Italy. [10]Department of Pediatrics, Acıbadem University Medical School, Ataşehir, Istanbul, Turkey. [11]Department of Genetics, Hôpital Robert Debré and Paris Diderot University, Paris, France. [12]Ludwig Center for Cancer Research, University of Lausanne, Lausanne, Switzerland. [13]Swiss Institute for Bioinformatics (SIB), Lausanne, Switzerland. [14]Pediatric Hematology and Oncology, Charité University Hospital, Berlin, Germany. [15]Department of Computer Science, Bonn Rhine Sieg University of Applied Sciences, Sankt Augustin, Germany. [16]Children's Cancer Research Institute, Vienna, Austria. [17]Northern Institute of Cancer Research, Newcastle University, Newcastle upon Tyne, United Kingdom. [18]Federal Office for Radiation Protection, Oberschleissheim, Germany. [19]Pediatric Hematology and Oncology, Hannover Medical School, Hannover, Germany. [20]Alacris Theranostics GmbH, Berlin, Germany. [21]Universitäts-Kinderspital beider Basel (UKBB), Basel, Switzerland. [22]Sheffield Children's Hospital, Sheffield, United Kingdom. [23]Childhood Leukaemia Investigation Prague (CLIP), Department of Pediatric Hematology/Oncology, Second Faculty of Medicine, Charles University Prague, Prague, Czech Republic. [24]Department of Hematology, Union Hospital, Fujian Medical University, Fuzhou, China. [25]Dahlem Centre for Genome Research and Medical Systems Biology, Berlin, Germany. [26]These authors contributed equally to this work. [27]These authors jointly supervised this work. Correspondence should be addressed to M.S. (stanulla.martin@mh-hannover.de) or J.-P.B. (jean-pierre.bourquin@kispi.uzh.ch).

ONLINE METHODS

Study individuals and sample selection. Samples and associated clinical information from patients included in sequencing and validation analyses were collected from different countries within the International BFM Study Group (I-BFM-SG). All patients were enrolled in multicenter trials on treatment of pediatric ALL conducted by individual member groups of the I-BFM-SG: the AIEOP-BFM study group (Austria, Germany, Italy and Switzerland), the FRALLE study group (France) and the United Kingdom (UK) National Cancer Research Institute (NCRI) Childhood Cancer and Leukemia Group[59,60]. All treatment trials were approved by the respective national institutional review boards, and informed consent for the use of spare specimens for research was obtained from study individuals, parents or legal guardians. The specific research project reported here was approved by the Ethics Committee of the Medical Faculty of the Christian Albrechts University, Kiel, Germany (vote D508/13). Depending on consent and availability of samples, all enrolled patients positive for the rare *TCF3-HLF* gene fusion were included. These patients were matched with *TCF3-PBX1*–positive patients.

Cell isolation and nucleic acid purification. Mononuclear cells were isolated by Ficoll-Paque gradient centrifugation (Pharmacia) from bone marrow or peripheral blood samples followed by extraction of nucleic acids according to standardized protocols using Qiagen DNA Blood Kits (Qiagen) for DNA and Qiagen RNeasy columns (Qiagen) for RNA. The quantity of nucleic acids was determined by spectrophotometry. DNA quality was assessed visually by inspection of agarose gel electrophoresis while RNA integrity was evaluated by using the Bioanalyzer 2100 (Agilent). Nucleic acids isolated from bone marrow aspirates collected in morphological remission served as individual germ-line surrogates/references.

Sequencing. *Whole genome sequencing.* For structural variants, Illumina v2 mate-pair libraries with 5 kbp insert size and 2 × 101 bp reads were prepared from 10 µg of DNA and sequenced on the Illumina HiSeq 2000 platform (Illumina) to obtain a physical coverage of 30×. For copy number alterations, breakpoints and short variants (SNVs, short indels), Illumina TruSeq paired-end libraries with 2 × 101 bp reads were prepared from 1 µg of DNA and sequenced on HiSeq 2000/2500 instruments to a coverage of 40× for reference samples and 80× for tumor samples.

Whole exome sequencing. To increase the sensitivity of detecting short variants in coding regions, 1 µg of DNA each from the diagnostic leukemic and a corresponding remission sample of patients was used for whole exome sequencing. Whole exome capture employed a TruSeq enrichment kit (Illumina) and paired-end libraries with 2 × 101 bp reads on a HiSeq 2500 according to the manufacturer's protocol.

Whole transcriptome sequencing. Illumina TruSeq custom stranded paired-end libraries with 2 × 51 bp reads were prepared from 1 µg RNA using the Ribo-Zero Gold Kit (Epicentre) and sequenced on a HiSeq 2000 with a loading of one library per lane.

Sanger sequencing validation. Structural variant breakpoints from whole-genome sequencing approaches and SNVs from exome sequencing were validated by Sanger sequencing.

Targeted sequencing of TCF3 and RAS pathway candidate genes. TCF3 binding domain (E47 isoform, exon 18) mutations were screened for in 1,033 ALL patients using Sanger sequencing. Primer sequences are listed in **Supplementary Table 27**. Sanger sequencing was also applied for validation of relative absence of RAS pathway mutations in 24 *TCF3-PBX1*–positive ALL samples. The latter analysis included *KRAS* exon 1, *NRAS* exons 1 and 2, *FLT3* exons 14 and 20, *PTPN11* exons 3 and 13, and was conducted as described[61].

Multiplex ligation-dependent probe amplification. Detection of genomic aberrations in B cell differentiation–associated and other genes frequently deleted in ALL (*PAX5*, *IKZF1*, *ETV6*, *RB1*, *BTG1*, *EBF1*, *CDKN2A, CDKN2B* and *P2RY8-CRLF2*) were investigated by the Multiplex Ligation-dependent Probe Amplification (MLPA) assay SALSA p335 kit (MRC-Holland) using 125 ng of genomic DNA. The assays were performed according to the manufacturer's protocol as described[62]. An intensity ratio between 0.75 and 1.3 was considered to represent normal copy number, a ratio between 0.25 and 0.75 was considered a monoallelic deletion and a ratio <0.25, a biallelic deletion.

Bioinformatics analysis. *DNA data processing.* DNA reads were aligned to the human reference genome hg19 (downloaded from the UCSC Genome browser) using Elandv2 (ref. 63; mate pairs) and BWA[64] (paired ends). For xenograft samples, the human DNA reads were deconvoluted after mapping to a combined reference consisting of human hg19 and mouse mm9.

Structural variant detection. Structural variants were detected using DELLY[65] and BIC-seq[66] (DNA data) and TopHat2 (ref. 67) /deFuse[68] (RNA data).

SNV detection. Somatic protein-changing SNVs were detected using established pipelines incorporating GATK[69], MuTect[70], pibase[71], Picard, SAMtools[72] and VarScan2 (ref. 73).

Indel detection. Somatic indels in coding regions were detected using SAMtools followed by Dindel[74].

Transcriptome data analysis. RNA reads were aligned to hg19 using BWA and SAMtools and used for integrated data analysis. For xenograft samples, the human RNA reads were deconvoluted after mapping to a combined reference consisting of human hg19 and mouse mm9. Mapped reads were annotated using Ensembl v.70. Gene expression levels were quantified in reads per kilobase of exon model per million mapped reads (RPKM)[75]. RPKM calculation and differential gene expression (DGE) analysis was performed using the R package edgeR[76]. To identify DGE between ALL subtypes, and between leukemia and remission the following set-up was performed: *TCF3-PBX1* vs. *TCF3-HLF* (comparison 1), *TCF3-PBX1* vs. remission (comparison 2), *TCF3-HLF* vs. remission (comparison 3). The results were filtered by fold change (FC, $|\log_2(FC)| \geq 1$) and false discovery rate (FDR, FDR ≤ 0.001). The final list of 401 genes was created by combining the intersection between comparison 1 and comparison 2 as well as between comparison 1 and comparison 3. The functional analyses of gene lists were done using gene set enrichment analysis (GSEA)[77] and the Genomatix genome analyzer (v. 3.00801; Genomatix Software GmbH). The GeneRanker tool in Genomatix was used to test for enriched gene sets, which were based on gene-tissue annotations obtained by text mining[78]. For GSEA, protein-coding genes were filtered by a minimum expression of 1 RPKM in at least four samples among the primary pre–B cell ALLs. The remaining 11,315 genes were tested for DGE between the ALL subtypes using edgeR. The provided FDR and fold-change values were used to obtain a ranking score to measure the degree of differential expression between the ALL subtype. A pre-ranked classic GSEA was performed using the ranking score, a gene set permutation and a FDR ≤ 0.02. The analysis included gene sets for hematopoietic stages[31] and signatures from MsigDB[77] pathways (C2): KEGG, BIOCARTA, REACTOME; curated oncogenic signatures (C6); human immunologic signatures (C7).

In silico transcription factor binding site (TFBS) analysis. TFBSs in promoter regions of genes (2 kbp upstream region) corresponding to the specific transcriptome signatures of *TCF3-PBX1*- and *TCF3-HLF*–positive ALL, respectively, were analyzed using the Genomatix Genome Analyzer (v3.10124). Based on a matrix of known TFBS motifs, the software tool predicted TFBSs in the investigated promoters and compared their frequency against (i) the background of TFBSs in the promoter regions of all known protein-coding genes in the Ensembl database (v.70, 22864 genes) and (ii) the background of TFBSs in the whole genome. A *Z* score was calculated based on the TFBS frequency in the investigated promoters and the expected frequency and s.d. were estimated from the background[79]. The resulting lists were filtered by the *Z* scores based on the two backgrounds ($|\text{genomic } Z| \geq 2$, promoter $Z \geq 2$). TFBSs overrepresented in genes upregulated in both *TCF3-PBX1*- and *TCF3-HLF*–positive ALL were filtered out, to retain only TFBS specifically enriched in the respective subtypes.

Integrated data analysis. SNVs and indels were orthogonally validated by integrating genome, exome and transcriptome data of patients and xenografts, and further confirmed by Sanger sequencing. Structural variants were validated by integrating whole genome paired-end and mate-pair data and whole-transcriptome data, and finally by Sanger sequencing. Ensembl v.70 and ANNOVAR[80] were used to annotate the variants. Silent variants and known germline variants in the 1000 Genomes Project[81] population data, in 136 North German healthy controls (publicly available through GrabBlur[82]), or in the International Cancer Genome Consortium's internal healthy controls were eliminated. All final somatic non synonymous variants were inspected using IGV[83].

Preclinical characterization. *Xenograft model.* Animal experiments were approved by the veterinary office of the Canton of Zurich, Switzerland. Approval for experiments with human samples in the mouse xenograft model was obtained from the ethics commission of the Canton Zurich (approval number 2014-0383). In brief, primary ALL cells were recovered from cryopreserved samples and transplanted intrafemorally to NSG mice as previously described[36]. Mice were 5–10 weeks old; both males and females were randomly used. Leukemia progression was monitored by flow cytometry with rat anti-mouse CD45 (eFluor450, clone 30-F11, REF 48-451-82, eBioscience), mouse anti-human CD45 (Alexa Flour 647, clone HI30, REF 304018, BioLegend), and mouse anti-human CD19 (PE, clone HIB19, REF 302208, BioLegend). ALL cells recovered from spleens of NSG mice were used for molecular characterization in *in vitro* and *in vivo* experiments.

Immunophenotyping. Immunophenotyping of patient and xenograft-amplified human ALL cells after recovery from the spleen was performed as described before[84]. All included xenograft samples consisted of at least 95% human leukemic cells.

Cell culture. Human hTERT immortalized primary bone marrow mesenchymal stromal cells (MSC; provided by D. Campana, St. Jude Children's Research Hospital, Memphis, USA) were cultured in RPMI 1640 medium supplemented with 10% heat-inactivated FBS; L-glutamine (2 mM), penicillin/streptomycin (P/S; 100 IU/ml) and hydrocortisone (1 μM). Xenograft-amplified human ALL cells were co-cultured on MSC in AIM V medium (Gibco by Life Technologies) at a ratio of 10:1. All cultured cells were kept in the incubator at 37 °C, 5% CO_2. For cryopreservation, cells were frozen in heat-inactivated FBS with 10% dimethylsulfoxide and subsequently stored in liquid nitrogen.

Cell viability assay. MSCs were seeded in 24-well plates at a number of 50,000 cells per well in RPMI 1640 medium (10% heat-inactivated FBS). After 24 h primary ALL cells were thawed and seeded as suspension culture alone or in co-culture with MSCs at a number of 400,000 cells per well in AIM-V medium. Three days later, ALL cells were collected from monoculture or co-culture by scraping and stained with 7-AAD (BD Pharmingen). Cell viability (7-AAD negative population) was measured by FACS using counting beads (SPHERO Accu Count Blanc Particles, Spherotech Inc.) for cell counts normalization. Viabilities shown are average viabilities of duplicate wells (normalized to input) and s.d.

Cell cycle assay. MSCs were seeded in 96-well tissue culture plates at a concentration of 10,000 cells per well in 100 μl AIM-V medium. After 24 h ALL cells were added at a concentration of 100,000 cells per well in 90 μl AIM-V. The Click-iTEdU Alexa Fluor 488 Flow Cytometry Assay Kit (Life Technologies) in combination with propidium iodide was used to measure proliferation and to identify the different phases of the cell cycle on days 1 and 3. Co-cultured cells were incubated with EdU (10 μM) for 20 h before cell cycle read-out with flow cytometry. The cell cycle assay was performed in triplicate, and at least two independent experiments were performed for each sample. Similar variances were obtained between the groups that were statistically compared.

In vitro drug screening and automated microscopy. MSCs were seeded in 384-well plates at a concentration of 2,500 cells per well in 30 μl AIM-V medium. After 24 h, ALL cells were added at a concentration of 25,000–30,000 cells per well in 27.5 μl AIM-V. Drugs were added as single agents after an additional 24 h using the pipetting robot epMotion 5070 (Eppendorf). Drug response was normalized to ALL cells treated with the drug vehicle alone. Experiments were performed in duplicate in five different dilutions (1, 10, 100, 1,000 and 10,000 nM). For two samples comparable results were obtained in two independent drug screening experiments. After 72 h or 96 h of drug incubation, cells were stained using the CyQUANT direct cell proliferation assay (Life technologies). 20 μl staining mix (AIM V medium, CyQUANT (1:300), repressor (1:20)) was added into each well followed by an incubation time of 1 h at 37 °C, 5% CO_2. Subsequently, automated imaging was performed using the ImageXpress Micro microscope (Molecular Devices) equipped with a CoolSNAP HQ camera (Photometrics) and a 10× plan fluor objective with 0.3 NA (Nikon). Nine images were taken per well, covering 50% of each well and captured employing the MetaXpress software (Molecular Devices). Images were processed using CellProfiler software (Broad Institute). Cells were classified and counted using the Advanced Cell Classifier software. This software uses random forest classification to assign ALL cells properly.

Immunoblot. Whole cell extracts were prepared from 1×10^6 cells using radioimmunoprecipitation assay (RIPA) buffer (20 mM Tris-Cl pH 7.5, 150 mM NaCl, 1% NP-40, 1 mM EDTA pH 8.0, 0.1% SDS) supplemented with Complete mini protease inhibitor cocktail (Roche Life Science) for 20 min on ice, sonicated as necessary, and diluted with SDS loading buffer (250 mM Tris pH 6.8, 4% SDS, 0.02% bromophenol blue, 40% glycerol, 4% (vol/vol) β-mercaptoethanol). After SDS-PAGE, proteins were blotted onto nitrocellulose membranes. Membranes were blocked in 5% non-fat dry milk and incubated with primary Bcl-2 (clone 124; Dako) and tubulin antibodies diluted 1:1,000 in milk. Horseradish peroxidase–labeled anti-mouse antibodies were used for signal detection with chemiluminescence substrate and direct scanning.

In vivo experiments. ALL cells were recovered from cryopreserved xenograft samples, and per thawed sample 12 to 16 mice were transplanted with 1,000,000 cells per mouse. After three days, randomized cohorts were treated with 100 mg/kg of ABT-199 (ABBVIE) or vehicle control with 6 to 8 mice per treatment arm[85]. ABT-199 or vehicle control were administered orally daily for two weeks. Mice of the ABT-199 group transplanted with sample 7a were additionally treated with a second block (100 mg/kg of ABT-199 for 14 d) starting at day 66, when the frequency of circulating leukemia cells started to increase again. Follow-up of circulating leukemia cells was performed every 7 d by flow cytometry with rat anti-mouse CD45, mouse anti-human CD45, and mouse anti-human CD19; frequency of leukemia cells as ratio of $mCD45^-$ $hCD45^+$ $hCD19^+$ count to total lymphocytes. The investigator was blinded to the group allocation during the assessment of outcome. To evaluate the ability of ABT-199 to decrease tumor burden, four mice in the control group were treated when the frequency of leukemia cells in the peripheral blood was equal or higher than 50%. Follow-up of circulating leukemia cells was performed every 4–7 d. *In vivo* experiments were terminated when the frequency of circulating leukemia cells reached 50% or earlier if the mice showed abnormal behavior. One *in vivo* experiment was performed per each sample.

Statistical analysis. Differences in the distribution of categorical variables among patient subsets were analyzed using Fisher's exact or chi-squared test. Comparisons of continuous variables between groups were performed by *t*-test or Mann-Whitney *U* test.

Drug responses were evaluated by fitting DMSO-normalized response data with the four-parameter log-logistic function of the form:

$$f(x) = \text{base} + \frac{E_{max} - \text{base}}{1 + (x_{1/2}/x)\,\text{Coeff}}$$

as implemented in the drc package of R (version 2.3-96). Outliers were detected and removed before curve fitting using Bayesian change point analysis[25] (R package bcp, version 3.0.1). Non-convergent cases (for example, drugs with no activity) were identified based on linear fit parameters. Hierarchical clustering was performed to group patients according to their drug-response profiles (R package gplots version 2.14.2). Drugs with differential activity in patients with *TCF3-PBX1*– compared to *TCF3-HLF*–positive ALL were identified using a *t*-test ($P \leq 0.05$). In *in vivo* experiments, 25% of circulating leukemia cells or termination of the experiment if 25% of leukemia was not reached were considered as an event in the Kaplan-Meier analysis. For sample 9a, 50% was used because of the rapid engraftment. Differences in the survival of mice receiving ABT-199 or vehicle control were determined by the Mantel-Cox test and verified by the Gehan-Breslow-Wilcoxon test.

59. Conter, V. *et al.* Molecular response to treatment redefines all prognostic factors in children and adolescents with B-cell precursor acute lymphoblastic leukemia: results in 3184 patients of the AIEOP-BFM ALL 2000 study. *Blood* **115**, 3206–3214 (2010).

doi:10.1038/ng.3362

60. Harrison, C.J. *et al.* Detection of prognostically relevant genetic abnormalities in childhood B-cell precursor acute lymphoblastic leukaemia: recommendations from the Biology and Diagnosis Committee of the International Berlin-Frankfurt-Munster study group. *Br. J. Haematol.* **151**, 132–142 (2010).
61. Case, M. *et al*. Mutation of genes affecting the RAS pathway is common in childhood acute lymphoblastic leukemia. *Cancer Res.* **68**, 6803–6809 (2008).
62. Dörge, P. *et al.* IKZF1 deletion is an independent predictor of outcome in pediatric acute lymphoblastic leukemia treated according to the ALL-BFM 2000 protocol. *Haematologica* **98**, 428–432 (2013).
63. Bauer, M.J., Cox, A.J. & Evers, D.J. Fast gapped read mapping for Illumina reads. *In ISMB, ISBC* (2010).
64. Li, H. & Durbin, R. Fast and accurate short read alignment with Burrows-Wheeler transform. *Bioinformatics* **25**, 1754–1760 (2009).
65. Rausch, T. *et al.* DELLY: structural variant discovery by integrated paired-end and split-read analysis. *Bioinformatics* **28**, i333–i339 (2012).
66. Xi, R. *et al.* Copy number variation detection in whole-genome sequencing data using the Bayesian information criterion. *Proc. Natl. Acad. Sci. USA* **108**, E1128–E1136 (2011).
67. Kim, D. *et al.* TopHat2: accurate alignment of transcriptomes in the presence of insertions, deletions and gene fusions. *Genome Biol.* **14**, R36 (2013).
68. McPherson, A. *et al.* deFuse: an algorithm for gene fusion discovery in tumor RNA-Seq data. *PLOS Comput. Biol.* **7**, e1001138 (2011).
69. McKenna, A. *et al.* The Genome Analysis Toolkit: a MapReduce framework for analyzing next-generation DNA sequencing data. *Genome Res.* **20**, 1297–1303 (2010).
70. Cibulskis, K. *et al.* Sensitive detection of somatic point mutations in impure and heterogeneous cancer samples. *Nat. Biotechnol.* **31**, 213–219 (2013).
71. Forster, M. *et al*. From next-generation sequencing alignments to accurate comparison and validation of single-nucleotide variants: the pibase software. *Nucleic Acids Res.* **41**, e16 (2013).
72. Li, H. *et al.* The Sequence Alignment/Map format and SAMtools. *Bioinformatics* **25**, 2078–2079 (2009).
73. Koboldt, D.C. *et al.* VarScan 2: somatic mutation and copy number alteration discovery in cancer by exome sequencing. *Genome Res.* **22**, 568–576 (2012).
74. Albers, C.A. *et al.* Dindel: accurate indel calls from short-read data. *Genome Res.* **21**, 961–973 (2011).
75. Mortazavi, A., Williams, B.A., McCue, K., Schaeffer, L. & Wold, B. Mapping and quantifying mammalian transcriptomes by RNA-Seq. *Nat. Methods* **5**, 621–628 (2008).
76. Robinson, M.D., McCarthy, D.J. & Smyth, G.K. edgeR: a Bioconductor package for differential expression analysis of digital gene expression data. *Bioinformatics* **26**, 139–140 (2010).
77. Subramanian, A. *et al*. Gene set enrichment analysis: a knowledge-based approach for interpreting genome-wide expression profiles. *Proc. Natl. Acad. Sci. USA* **102**, 15545–15550 (2005).
78. Frisch, M., Klocke, B., Haltmeier, M. & Frech, K. LitInspector: literature and signal transduction pathway mining in PubMed abstracts. *Nucleic Acids Res.* **37**, W135–W140 (2009).
79. Ho Sui, S.J. *et al.* oPOSSUM: identification of over-represented transcription factor binding sites in co-expressed genes. *Nucleic Acids Res.* **33**, 3154–3164 (2005).
80. Wang, K., Li, M. & Hakonarson, H. ANNOVAR: functional annotation of genetic variants from high-throughput sequencing data. *Nucleic Acids Res.* **38**, e164 (2010).
81. 1000 Genomes Project Consortium. A map of human genome variation from population-scale sequencing. *Nature* **467**, 1061–1073 (2010).
82. Stade, B., Seelow, D., Thomsen, I., Krawczak, M. & Franke, A. GrabBlur–a framework to facilitate the secure exchange of whole-exome and -genome SNV data using VCF files. *BMC Genomics* **15** (suppl. 4), S8 (2014).
83. Robinson, J.T. *et al.* Integrative genomics viewer. *Nat. Biotechnol.* **29**, 24–26 (2011).
84. Ratei, R. *et al.* Lineage classification of childhood acute lymphoblastic leukemia according to the EGIL recommendations: results of the ALL-BFM 2000 trial. *Klin. Padiatr.* **225** (suppl. 1), S34–S39 (2013).
85. Festing, M.F. & Altman, D.G. Guidelines for the design and statistical analysis of experiments using laboratory animals. *ILAR J.* **43**, 244–258 (2002).

Manuscript 2

Drug response profiling to identify selective pharmacological activity in drug resistant ALL

Viktoras Frismantas[1,2,*], Maria Pamela Dobay[3*], Anna Rinaldi[1,2,*], Joachim Kunz[4], Blerim Marovca[1,2], Peter Horvath[5], Salome Higi[1,2], Sabrina Eugster[1,2], Pamela Voegeli[6], Mauro Delorenzi[3,7], Gunnar Cario[8], Martin Schrappe[8], Martin Stanulla[9], Andreas E. Kulozik[4], Martina U. Muckenthaler[4], Arend Von Stackelberg[10], Cornelia Eckert[10], Thomas Radimerski[11], Beat C. Bornhauser[1,2,*] and Jean-Pierre Bourquin[1,2,*]

1 Department of Oncology, University Children's Hospital Zurich, Zurich, Switzerland
2 Children's Research Center, University Children's Hospital Zurich, Zurich, Switzerland
3 SIB Swiss Institute of Bioinformatics, Lausanne, Switzerland
4 Department of Pediatric Oncology, Hematology and Immunology, University of Heidelberg, Heidelberg, Germany
5 Synthetic and Systems Biology Unit, Biological Research Center, Szeged, Hungary
6 Institute of Forensic Medicine, University of Zurich, Zurich, Switzerland
7 Ludwig Center for Cancer Research, University of Lausanne, Lausanne, Switzerland
8 Department of Pediatrics, University Medical Centre Schleswig-Holstein, Kiel, Germany
9 Department of Pediatric Hematology and Oncology, Hannover Medical School, Hannover, Germany
10 Department of Pediatric Oncology/Hematology, Charité Universitätsmedizin Berlin, Germany
11 Disease Area Oncology, Novartis Institutes for BioMedical Research, Basel, Switzerland

* equal contribution

Correspondence:
Jean-Pierre Bourquin,
jean-pierre.bourquin@kispi.uzh.ch

University Children's Hospital Zurich
Steinwiesstrasse 75
CH-8032 Zurich, Switzerland
Phone, +41 44 266 7304
Fax, +41 44 266 7171

Running title: Drug response profiling of ALL
Scientific category: Lymphoid neoplasia

Keywords: acute lymphoblastic leukemia, drug activity profiling, drug resistance, automated microscopy, BH3-mimetics, personalized medicine

KEY POINTS

1. Drug response profiling reveals patient subgroups, such as BCL2-dependent ALL, sensitive to new agents that may be otherwise overlooked
2. Combining venetoclax with conventional ALL chemotherapeutics as dexamethasone and vincristine is highly effective in leukemia xenografts

ABSTRACT

With the rapid development of new agents, more personalized approaches are needed to select patients with chemotherapy resistant acute lymphoblastic leukemia (ALL) that may benefit from specific therapeutic options. To complement information from existing diagnostic and genomic sources we developed a large scale drug response profiling platform that is based on an established ALL co-culture system on bone marrow stromal cells, with the advantage of standardized conditions in serum-free medium. Comparing the profiles of 61 ALL samples enriched for relapsed and refractory ALL we identified informative patterns of drug sensitivity and resistance. As a proof of concept, we focused on the striking response patterns to the BCL2-specific BH3-mimetic venetoclax (ABT-199). A relevant proportion of BCP-ALL, including *MLL-AF4* and *TCF3-HLF* positive ALL cases, and a subset of T-ALL, were revealed to be highly sensitive to BCL2 inhibition. Sensitivity to venetoclax *in vitro* correlated with anti-leukemic activity in ALL xenografts *in vivo*. Moreover combination testing on our platform indicated synergistic activity of venetoclax with conventional anti-leukemic agents such as dexamethasone and vincristine, and with the new class BRD4 inhibitors. *In vivo*, combination of venetoclax with dexamethasone and vincristine completely prevents disease progression of very aggressive *TCF3-HLF* ALL cases when full relapse occurs in the control arms, comprised of single agent venetoclax or a dexamethasone and vincristine combination treatment. Drug activity profiling should be evaluated prospectively in the clinical setting to inform more personalized strategies to treat patients with resistant disease.

INTRODUCTION

The treatment of relapsed and refractory ALL remains challenging, particularly for T-ALL, on which the most recently developed immunotherapies cannot be applied[1].,With the progress in the mapping of the genomic landscape of ALL[2], new actionable targets have emerged, including activated tyrosine kinases in different ALL subgroups[3,4,5]. Integration of genomic data and detection of intracellular signalling activity in resistant disease may yield biomarkers for targeted therapy, such as activating mutations in RAS[6,7] or IL7R[8]. Nonetheless and despite the fact that genetically defined subgroups of patients are commonly identified in existing large cooperative studies[1,9], only in a limited number of cases does molecular definition lead to clinical application of targeted therapeutics. Such high risk groups lacking druggable targets include rare subsets with genetic features such as *MLL-AF4* rearrangements, the t(17;19) translocation leading to a *TCF3-HLF* fusion[10,11], hypodiploid karyotypes[7] or cases with failure of remission-induction therapy[12]. Unfavourable risk groups are defined based on protracted response to chemotherapy, measured by persistence of minimal residual disease (MRD)[1,13], which is also a prognostic factor for the treatment of relapsed ALL[14]. MRD facilitates the identification of subgroups that might benefit from experimental intervention. For the further development of personalized medicine, more detailed genomic and biological characterization will be required to obtain more precise pre- or co-clinical rationales to guide treatment.

Given the genetic diversity and the complexity of molecular circuitries in ALL it will be challenging to define druggable targets based solely on genomic information. Indeed extensive studies using cancer cell line panels[15,16] illustrate the complexity of cancer genomics and the challenge to predict drug activity based on this information. We hypothesized that drug activity profiling of ALL may detect sensitivity that may otherwise be overlooked without *a priori* information on the genetic lesions or activated pathways. Indeed drug profiling of patient-derived acute myeloid leukemia cells detected kinase inhibitor activity that could in a few patients predict responses to these agents[17]. Leukemia cases with characteristic tyrosine kinase mutations[18], and a subset of ALL with tonic pre-BCR signalling[19] have also been identified in inhibitor screens. Here, we take advantage of an expanding repository of patient-derived xenografts (PDX) that model clinically relevant patient cohorts, including patients with relapsed and refractory disease[20-24] to develop an *in vitro* drug-testing platform. We adapted a serum free ALL co-culture system on h-TERT immortalized human bone marrow derived mesenchymal stromal cells (MSC) [25,26]. This system provides reproducible conditions to maintain leukemia cells alive for drug testing. We and others have shown that the response to conventional anti-leukemic agents *in vitro* is more restricted in samples from patients with clinically more resistant disease compared to patient with favourable response to therapy[17,18,27,21-23,28,]. Drug responses are evaluated with an automated, machine learning-based process that monitors viable ALL cells. Here we show that informative

differences in drug response profiles can be detected within ALL, pinpointing actionable targets. As a proof of concept we detect several subgroups of BCL2 dependent ALL through a remarkable sensitivity to the BH3 mimetic venotoclax (ABT-199) [29]. This confirms and expands independent observations that were achieved via molecular profiling[30,31] and illustrate how rapid drug profiling could be integrated in future clinical workflows to improve individualized therapy decisions. Finally very strong anti-leukemic activity of the combination of venetoclax and dexamethasone in ALL cases that were pre-selected based on drug profiling illustrate how this approach may contribute to the selection of patients for an experimental regimen combining venetoclax for ALL treatment.

METHODS

Human samples. Primary human ALL cells were recovered from cryopreserved bone marrow aspirates of patients enrolled in the ALL-BFM 2000, 2009 and ALL-REZ-BFM 2002 studies. Informed consent was given in accordance with the Declaration of Helsinki and the ethics commission of the Kanton Zurich (approval number 2014-0383). Samples were classified as standard risk (SR), medium risk (MR), high risk (HR), very high risk (VHR), refractory relapse (RR) or relapse samples (R) according to the clinical criteria used in ALL-BFM 2000[22].

***In vitro* drug profiling platform.** The *in vitro* drug response of ALL primary patient samples was assessed in coculture with hTERT-immortalized primary bone marrow mesenchymal stromal cells (MSC)[20] as described previously[22]. Cell culture, drug library logistics and imaging-based cell viability analysis are described in the supplementary method section.

Drug response quantification and statistical analysis. A fitting routine based on the four-parameter log-logistic function of the form:

$$f(x) = base + \frac{E_{max} - base}{1 + (\frac{x}{x_{\frac{1}{2}}})^{Coeff}}$$

as implemented in the R the drc package (version 2.3-96) was applied to data normalized against DMSO-treated samples. Outliers were detected and removed prior to curve fitting by detecting local changes in the slope with a linear fit. Non-convergent cases (e.g. drugs with no activity) were identified based on linear fit parameters. Hierarchical clustering was performed to group patients according to their drug response profile (R package gplots). Drugs that determined data variance and clustering were identified by principal component analysis. Differential responses of patient groups of interest to drugs were evaluated by using the non-parametric, one-tailed Mann-Whitney U-test.

Code availability. Fitting functions are available as R codes under https://github.com/pampernickel/Fit.funcs

RESULTS

Reproducible drug response profiles can be established from primary ALL cells using an automated microscopy based platform

To generate drug activity profiles from diagnostic patient material within one week we opted for co-cultures on hTERT-immortalized MSC derived from normal human bone marrow cells[26] combined with an imaging-based cell viability readout on a customized, high-throughput analysis platform[21] (**Figure 1**). This system provides a simple model of the tumour-microenvironment and should support B-cell precursor (BCP-) and T-ALL cell survival in a majority of cases without the need of more complicated adjustments of cell culture conditions. Contact with stroma cells may also confer more protection from the effect of therapeutic agents thus possible providing a more stringent platform for drug testing[32]. We obtained drug response profiles of patient-derived primary ALL cells from 61 cases (**Table S1**) for a selection of 60 compounds (**Table S2**) either in preclinical and clinical development, or already approved for other indications. Drug response profiles were analysed with an integrated routine, including customized scripts that handle data normalization, outlier removal, dose response

curve fitting and statistical analysis of extracted fit parameters such as the area under the curve (AUC), half-maximal inhibitory concentrations (IC50) and maximum effect (Emax) measurements. The experiments were performed starting from viably frozen aliquots of leukemia cells, which could serve as the reference database for workflows that can be applied in the setting of international multicentre clinical trials. The 61 primary samples (24 T-ALL and 37 BCP-ALL cases) (**Table S1**) showed enhanced survival in MSC co-culture compared to suspension cultures on serum-free medium, with a median cell viability of BCP-ALL and T-ALL after 96 hours on MSCs of 69% and 94% of seeded cells, compared to 1.2% and 45.5% in monoculture (**Figure 2A**). Some samples (8/24 T-ALL and 8/37 BCP-ALL cases) even exceeded the initial seeding density, indicating proliferative activity. In all cases tested, 13-70% of cells were in S-phase, with varying proportions of apoptotic cells, resulting in a balance between proliferation and survival (**Figure 2B**). These data support the amenability and robustness of this system for functional studies by systematic drug profiling on primary human ALL.

Informative differences are detected in drug response profiles from diagnostic pre-treatment ALL cases

To capture characteristic drug responses on this platform, we established dose response profiles to a selection of compounds using pre-treatment diagnostic ALL samples from the cooperative ALL-BFM-2000 study[33], enriched for high-risk cases by MRD (**Figure 3**). None of the tested compounds affected MSC viability at concentrations lethal to ALL cells, indicating that our results are not compromised by a lethal effect on the stromal component and that information on a potential therapeutic window can be captured. We detected homogeneous anti-leukemic activity for certain classes of drugs, including anthracyclines and the proteasome inhibitor bortezomib. In contrast, there were marked differences in activity for other drug classes, including infrequent but strong outlier activity for drugs that could be incorporated rapidly into salvage regimen. For example, two T-ALL cases responded well to dasatinib, while one BCP-ALL and two T-ALL cases responded to imatinib in the low nanomolar range. Interestingly, the responses do not necessarily overlap with the dasatinib response, suggesting distinct underlying molecular targets. These cases also responded to the broader spectrum tyrosine kinase inhibitor XL-228, suggesting the existence of relevant underlying molecular targets that warrant further investigation in larger cohorts of ALL samples. In contrast, the three T-ALL cases positive for NUP-ABL1 translocations did not respond to dasatinib (IC50>10 μM) and imatinib (IC50>10 μM). Similarly, strong but isolated activity was noticed for the IAP inhibitor LCL-161, and the mTOR inhibitors temsirolimus and PP242. As reported recently[19] *TCF3-PBX1* rearranged ALL forms pre-BCR+ ALL with distinctly activated signalling pathways and recognisable response to kinase inhibitors. In agreement with these published data, the six *TCF3-PBX1*-positive BCP-ALL cases in our panel showed sensitivity to dasatinib and XL-228, but resistance to imatinib. Moreover, when comparing two BH3-mimetic agents that are in clinical development, navitoclax (ABT-263), which is directed against BCL2 and BCL-XL, and venetoclax, a selective BCL2 inhibitor which was recently developed to circumvent the on-target BCL-XL specific thrombocytopenia caused by navitoclax[29]. We detected very strong activity of venetoclax in a subset of ALL that are also sensitive to navitoclax, indicating that functional BCL2 dependence could be detected by drug activity profiling in ALL.

Of note, hierarchical clustering of the drug response profiles suggest two major groups within BCP- and T-ALL, whose separation is driven by differences in response to antimetabolites (cytarabine, gemcitabine), antimitotic drugs (vincristine, docetaxel), the aurora kinase inhibitors AT9283 and barasertib, and the Polo-like kinase I inhibitor BI-2536. This indicates differences related to cell cycle regulation. Indeed, drugs targeting cycle activity (docetaxel, 6-thioguanine, gemcitabine and cytarabine, topotecan, ZM-447439 and barasertib) showed higher activity in samples with higher cycling activity as measured by fraction of cells in S-phase (**Figure S1**, p-value $\leq$ 0.05). These observations will have to be considered for data interpretation in future correlative studies. Drug response profiles were highly reproducible in biological replicates (**Table S3**). Our results further suggest that drug profiling may capture individual heterogeneity in drug responses, and could identify clinically relevant vulnerabilities in ALL on a more personalized basis.

Novel anti-leukemic activity can be identified in defined ALL subgroups with resistant disease

Given that absolute differences in dose responses between different drugs do not necessarily reflect their respective pharmacodynamics and therapeutic range *in vivo*, it is important to compare drug activity profiling data to a database built on response profiles from similar experimental conditions for a large cohort of ALL

cases over time. We tested six additional samples derived from patients with relapsed ALL that were refractory to salvage therapy (refractory relapse, RR), who did not achieve a second or third remission and qualify for inclusion in early clinical trials. RR ALL exhibited a generally more resistant response phenotype, including to chemotherapeutic agents used in ALL such as dexamethasone (5/6) cytarabine (4/6) and doxorubicin (3/6), compared to other ALL cases. Patterns of sensitivity and resistance varied from case to case (**Figure 4A**). RR ALL cases, however, appear to be more sensitive to idarubicin and mitoxantrone, which are used more frequently in the relapse setting[34,35] in relation to other ALL cases. Some of these samples were also very sensitive to new agents in clinical development, such as barasertib (3/6), dasatinib (2/6), and bortezomib (3/6), suggesting that this assay could provide additional information to select patient for candidate drugs. Of note, TCF3-PBX1 cases were recently reported to be sensitive to dasatinib[36], which again illustrates the potential of this platform to detect functional entities (Figure 4B).

MLL-AF4 positive ALL represents a genetically defined subgroup of ALL with a particularly dismal outcome[37,38]. All three *MLL-AF4* positive cases showed a strong response to a number of interesting candidate compounds, including the pan-PI3K inhibitor buparlisib, the tyrosine kinase inhibitors dovitinib and midostaurin, and AKT1/2 inhibitors (**Figure 4A**), consistent with the proposed susceptibility of *MLL*-rearranged ALL to PI3K pathway inhibition[39]. *MLL-AF4* cases were also sensitive to other agents of clinical interest including molecules targeting the P53/MDM2 axis (Nutlin) shown to be active in *MLL*-ALL xenografts[40], and to the proteasome inhibitor bortezomib, in agreement with Liu et al.[41]. We detected a strong activity of the BCL2-specific BH3 mimetic venetoclax in all *MLL-AF4* cases. Thus, as in *MLL*-rearranged acute myeloid leukemia[42], *MLL-AF4* ALL appears to be highly dependent on BCL2, providing a strong rationale to include this subgroup in a pediatric clinical trial with this new agent.

We also propose to systematically profile drug activity in relapsed T-ALL, whose treatment remains challenging[1]. 24 T-ALL cases that are included in this study provide a framework for first experiments (**Table S1**). These cases included mostly patients with high risk of relapse by MRD at first diagnosis, three T-ALL relapse cases that were refractory to relapse treatment and three matched first diagnosis and relapse cases (**Figure 4A**). We observed a broad range of drug responses across this sample set, with certain compounds as idarubicine and mitoxantrone were relatively active, even more than doxorubicine, in T-ALL relapse samples, considering the general drug activity range in T-ALL (**Figure 4A**). A subset of T-ALL relapse cases were very sensitive to drugs that could be already used clinically, including the topoisomerase I inhibitor topotecan, which is not used in standard regimens, barasertib which was also reported by others[43], and dasatinib. Three ABL1-fusion negative T-ALL cases were also highly sensitive to dasatinib, suggesting the existence of relevant albeit unidentified underlying molecular lesions. Finally, strong activity of the BRD4 inhibitor JQ1 was observed in a number of cases including relapses, again suggesting fundamental individual differences in T-ALL that will have implications for therapy.

The BCL2-specific inhibitor venetoclax is very active in several relevant ALL subsets

We detected significant venetoclax activity in a fraction of cases, which included *TCF3-HLF* and *MLL* positive BCP-ALL, as well as other BCP-ALL and several T-ALL cases, corroborating recent reports[44-46] (**Figure 5A**). We recently reported the genomic landscape of *TCF3-HLF* ALL and showed very strong venetoclax activity in six cases and in xenografts derived from residual disease after chemotherapy in matched samples[47]. These results imply differences in BCL2 and BCL-XL dependence within T-ALL. A recent study suggested a correlation between T-ALL maturation stage and sensitivity to venetoclax, with early T-cell precursor ALL (ETP-ALL) showing the highest sensitivity[48]. We detected venetoclax responsive cases also in cortical, pre- and mature T-ALL (**Figure 5B**), extending data from an independent cohort of patients[46]. Furthermore, we found no correlation between venetoclax sensitivity and mutations in *NOTCH1*, *FBXW7*, *LEF1*, *STAT5*, *IL7R* or *PTEN* (**Figure 3**, **Table S1**). The BCL2:BCL-XL ratio was suggested as a determinant of sensitivity to venetoclax[48]. While all anti-apoptotic BCL2 family proteins, BCL2, BCL-XL and MCL-1, were detected in T-ALL samples (**Figure S3**), and BCL2 levels were found to be increased in *TCF3-HLF* ALL[47], the BCL2:BCL-XL ratio did not always predict response (**Figure 5C**).

This suggests that *in vitro* drug testing results could complement suggested biomarkers of activity in patient selection for early clinical treatment protocols that will include venetoclax.

The response to venetoclax *in vitro* correlates with anti-leukemic activity in xenografts

To explore the correlation between *in vitro* and *in vivo* responses to venetoclax, we compared treatment results for three leukemia xenografts of cases that exhibited very strong, intermediate and low sensitivity to venetoclax *in vitro*. (**Figure 6A**). Xenografts treated with orally-administered 100 mg/kg venetoclax delayed leukemia progression in sensitive cases (IC50 < 100nM), but not in the non-responder (**Figure 6B**). Expectedly, the T-VHR-03 case, profiled with a low IC50 (<1nM) and low AUC on our platform, showed a more prominent response (HR=20, treated versus untreated, p<0.005) *in vivo* compared to the T-HR-11 case (HR=0.07, treated versus untreated, p<0.005), with low IC50 (<100nM) but high AUC. Moreover we also observed very strong venetoclax activity in mice with maximal leukemia burden (**Figure 6C**). The sample T-HR-10, identified by drug profiling as venetoclax-resistant, did not show any response *in vivo*. We recently reported very similar venetoclax efficacy in three *TCF3-HLF* ALL cases *in vivo*[47]

Drug-screening platform can identify novel synergistic combinations of venetoclax and other drugs

As clinical activity of new agents is more likely to be detected in combination therapy in early clinical trials, we adapted our workflow for combinatorial testing of selected compounds with venetoclax. We first evaluated six T-ALL cases, four of which were resistant to venetoclax at micromolar concentrations, and two were sensitive at concentrations below 100 nm, corresponding to large differences in AUC (**Figure S4**). We used the AUC, rather than IC50, as the AUC captures both IC50 and Emax as relevant endpoints of drug activity. Given the strong activity of venetoclax as a single agent, detection of synergy was challenging. More than additive effects were detected in combination with vincristine (6/6 cases), prednisolone and dexamethasone (5/6 cases), and topotecan (4/6 cases). Additionaly, striking synergistic activity was detected for the combination of venetoclax with the BRD4 inhibitor JQ-1 and with the PI3K-AKT inhibitor dactolosib (BEZ235) (**Figure S4**). We validated these results in co-titration matrices for optimized concentration ranges (**Figure 7A**). For clinical translation, a likely scenario would be to combine venetoclax with conventional chemotherapy for the treatment of relapse, such as the UK-ALL R3 regimen, which includes vincristine, dexamethasone, mitoxantrone and asparaginase[34]. Indeed venotoclax acts synergistically with vincristine or dexamethasone on selected venetoclax sensitive T-ALL and MLL-AF4 samples (**Figure 7B**). Similar results were obtained for TCF3-HLF ALL[47]

To model experimental therapy, we then tested the combination of venetoclax with the ALL induction drugs vincristine and dexamethasone *in vivo* in *TCF3-HLF* ALL, which is currently considered to be incurable, in the leukemia xenograft model. Both venetoclax alone or treatment with vincristine and dexamethasone delayed leukemia progression markedly, but the combination of the three drugs prevented leukemia progression completely, beyond the effects detected in the control arms (**Figure 7C**). Collectively our results indicate that drug response profiling may provide important additional information on individual pharmacological vulnerabilities in ALL and should therefore be further explored in the clinical setting.

DISCUSSION

While excellent outcomes have been achieved with current treatment protocols, resistant disease remains a major challenge in ALL[2]. Further intensification of conventional chemotherapy is unlikely to improve outcome, and results in serious toxicity. Given the genetic complexity of ALL[49], complementing genomic studies with direct functional information from *in vitro* drug profiling may provide important new insights. Promising studies have been reported recently for other hematologic malignancies[17,18]. We show that co-culture on human MSC[25,26] efficiently support a majority of primary ALL samples in serum-free conditions, providing a reasonable basis for standardization across laboratories. Taking advantage of a large repository of relevant PDX samples, we have developed an automated microscopy-based platform for monitoring effects of functional interference in a simplified model of the bone marrow niche. We provide first evidence that informative differences in drug response profiles can be detected in individual patient samples. While at first sight differences between different ALL subgroups may not appear to be extensive, comparison of individual drug response patterns to the data acquired for each small molecule tested in our large sample cohort identified recurrent patterns in

distinct ALL subsets. Importantly, reproducible responses in specific subgroups were identified for drugs that would not have been selected based on other criteria. Here we focus on the identification of ALL subgroups that are highly sensitive to the BCL2-specific inhibitor venetoclax (ABT-199), suggesting a recurrent pattern of BCL2-dependency.

The use of more selective BCL2-family inhibitors may be effective in leukemia that depend on one of these anti-apoptotic regulators. Venetoclax does not convey the clinically limiting toxicity on thrombocytes that are associated with on target BCL-XL inhibition by other BH3-mimetics[29]. However, venetoclax usage necessarily implies the accurate identification BCL2-dependent leukemias. We show that an appreciable subset of cases that respond to the BCL2 and BCL-XL inhibitor navitoclax also respond to venetoclax in the nanomolar range, including mostly BCP-ALL subtypes, but also selected T-ALL cases. We found striking activity in *TCF3-HLF* ALL and *MLL-AF4 ALL*, two genetically defined subtypes with poor outcome. We recently coordinated a large consortium to study the genomic landscape of *TCF3-HLF* ALL and have applied the platform described here to detect a reproducible profile of drug sensitivity and resistance. Testing samples from a total of 12 cases with *TCF3-HLF* ALL and a control cohort of *TCF3-PBX1* ALL, we detected very high, uniform sensitivity to venetoclax in *TCF3-HLF* ALL. This activity correlated with a delay in leukemia progression *in vivo* after single agent treatment[47]. Here we provide strong additional preclinical evidence to support the idea of a more personalized design for early clinical testing of venetoclax in ALL. We provide compelling evidence for venetoclax activity in combination with two agents from the classical ALL four-drug backbone regimen, vincristine and dexamethasone. We found a number of cases sensitive to venetoclax on our platform, including all *MLL-AF4* cases that we tested, which responded within a comparable dose response range as *TCF3-HLF* ALL. Both our data and published data[48,46] strongly support integration of selected T-ALL subsets in the clinical development of venetoclax, provided a strategy is implemented to select patients based on drug response profiles and other biomarkers. We confirm that venetoclax sensitive cases also respond to this agent *in vivo*. New agents are now being increasingly tested early drug development in combination with a conventional chemotherapy backbone, as in the successful case of bortezomib combined with a standard four drug ALL induction regimen[36,50]. Venetoclax is currently being tested in combination with different agents for chronic lymphoblastic leukemia and solid tumors[51,52]. Our data indicate that combination of venetoclax with established anti-leukemic drugs such as vincristine and dexamethasone will be of interest for a relevant subgroup with urgent medical needs.

For clinical translation, a better understanding of the mechanisms involved in selective sensitivity/resistance to BH3-mimetics will be important. The interplay between the different BCL2 family members and crosstalk with other signalling pathways will however be difficult to capture with simple laboratory assays. The BCL2:BCL-XL expression ratio has been suggested as a predictive marker for venetoclax sensitivity[48], but we have not been able to detect this correlation in our series. As an alternative, BH3 profiling using synthetic peptides has been extensively investigated[53,54].Recent access to more specific inhibitors of different BCL2-family members now provides a powerful and convenient alternative for functional profiling of cell death pathways in cancer. Such an approach identified solid tumors sensitive to BCL2 and BCL-XL inhibition by navitoclax, but remained selectively sensitive to BCL-XL inhibition by a new specific inhibitor, which in combination with docetaxel, prevents toxicities associated with the broader spectrum agent[52]. Thus integration of drug profiling should provide important support to design and test new treatments. Combinatorial drug testing *in vitro* may provide valuable additional information, but synergistic activity with small molecules that act potently as single agents at low nanomolar concentrations such as navitoclax and venetoclax are difficult to detect in these assays. Nevertheless we identified synergy between the BRD4 inhibitor JQ1 and venetoclax. JQ1, which provides an interesting rationale for further evaluation, given the fact that BRD4 inhibition was shown to modulate BCL2 and MYC activity at superenhancers in the context of resistance to gamma secretase inhibitors in T-ALL[55].

Among intriguing outlier activities, we detected several cases that were very sensitive to dasatinib in the absence of known ABL1-rearrangements in T-ALLs. Indeed, patients with mutations in activating kinases and cytokine receptor pathways (so called *BCR-ABL1*-like ALL) may benefit from combination chemotherapy with different tyrosine kinase inhibitors depending on their mutation patterns[4,56]. We have not yet identified the

underlying molecular abnormalities in these cases, but our approach enables us to define a larger cohort for molecular studies. In BCP-ALL, activity of the dual ABL1/BTK-SRC inhibitor dasatinib was detected in a Pre-B Cell Receptor signalling–dependent subset of ALL, including *TCF3-PBX1* positive ALL, showing how pathway interconnectivity can be further exploited therapeutically[57]. Accordingly, we detected dasatinib activity in *TCF3-PBX1* ALL cases on our platform (Figure 4B). Based on the experience in *BCR-ABL1* positive ALL, dasatinib can readily be incorporated in current ALL regimens[58]. Furthermore, we see differences in activity for several drugs that are immediately relevant in the context of clinical trials. These include variable responses to anthracyclines, including mitoxantrone, a major component of current reinduction schemes for high risk ALL[34] and to bortezomib, which will be investigated next in different settings for ALL[1]. It is therefore planned to evaluate drug response profiling prospectively in the context of resistant disease using a selection of therapeutic agents in order to establish cross-laboratory standards and assess the potential clinical value of this additional layer of functional information. Taken together, we provide proof of concept data that functional profiling of patient samples with selected therapeutic agents will provide valuable insights for both preclinical and clinical research. This approach is expected to contribute to the development of more precise strategies to guide leukemia treatment for patients with resistant disease.

ACKNOWLEDGMENTS

This work was supported by the Cancer League of the Canton of Zurich, the Empiris foundation, the foundation "Kinderkrebsforschung Schweiz", the Sassella foundation, the "Stiftung für Krebsbekämpfung", the Swiss National Science Foundation (310030-133108), the Fondation Panacee, the clinical research focus program "Human Hemato-Lymphatic Diseases" of the University of Zurich.

AUTHORSHIP CONTRIBUTIONS

J.-P.B., B.C.B., V.F., A.R., M.P.D., jointly designed the project. M.Sc., M.St., M.P.D., T.R., P.V., M.D., A.E.K., M.U.M., A.v.S., C.E. provided reagents, analysis tools, samples and clinical data. J.-P.B., B.C.B., V.F., A.R., designed experiments. V.F., A.R., B.M., S.H., S.E. performed experiments. M.P.D., V.F., A.R., P.H., analysed data and prepared tables and figures. J.-P.B., B.C.B. supervised research. J.-P.B., B.C.B., M.P.D., V.F. wrote the manuscript. All authors critically reviewed the manuscript for its content.

CONFLICT OF INTEREST DISCLOSURES

The authors declare that no conflict of interest exists.

The online version of the article contains a data supplement.

REFERENCES

1. Locatelli F, Schrappe M, Bernardo ME, Rutella S. How I treat relapsed childhood acute lymphoblastic leukemia. *Blood*. 2012;120(14):2807-2816.
2. Inaba H, Greaves M, Mullighan CG. Acute lymphoblastic leukaemia. *Lancet*. 2013.
3. Juric D, Lacayo NJ, Ramsey MC, et al. Differential gene expression patterns and interaction networks in BCR-ABL-positive and -negative adult acute lymphoblastic leukemias. *J Clin Oncol*. 2007;25(11):1341-1349.
4. Roberts KG, Li Y, Payne-Turner D, et al. Targetable kinase-activating lesions in Ph-like acute lymphoblastic leukemia. *N Engl J Med*. 2014;371(11):1005-1015.
5. Bercovich D, Ganmore I, Scott LM, et al. Mutations of JAK2 in acute lymphoblastic leukaemias associated with Down's syndrome. *Lancet*. 2008;372(9648):1484-1492.
6. Irving J, Matheson E, Minto L, et al. Ras pathway mutations are prevalent in relapsed childhood acute lymphoblastic leukemia and confer sensitivity to MEK inhibition. *Blood*. 2014;124(23):3420-3430.
7. Holmfeldt L, Wei L, Diaz-Flores E, et al. The genomic landscape of hypodiploid acute lymphoblastic leukemia. *Nature genetics*. 2013;45(3):242-252.
8. Shochat C, Tal N, Bandapalli OR, et al. Gain-of-function mutations in interleukin-7 receptor-alpha (IL7R) in childhood acute lymphoblastic leukemias. *J Exp Med*. 2011;208(5):901-908.
9. Pui CH, Mullighan CG, Evans WE, Relling MV. Pediatric acute lymphoblastic leukemia: where are we going and how do we get there? *Blood*. 2012;120(6):1165-1174.
10. Panagopoulos I, Micci F, Thorsen J, et al. A novel TCF3-HLF fusion transcript in acute lymphoblastic leukemia with a t(17;19)(q22;p13). *Cancer Genet*. 2012;205(12):669-672.
11. Hunger SP, Devaraj PE, Foroni L, Secker-Walker LM, Cleary ML. Two types of genomic rearrangements create alternative E2A-HLF fusion proteins in t(17;19)-ALL. *Blood*. 1994;83(10):2970-2977.
12. Schrappe M, Hunger SP, Pui CH, et al. Outcomes after induction failure in childhood acute lymphoblastic leukemia. *N Engl J Med*. 2012;366(15):1371-1381.
13. Bader P, Kreyenberg H, von Stackelberg A, et al. Monitoring of Minimal Residual Disease After Allogeneic Stem-Cell Transplantation in Relapsed Childhood Acute Lymphoblastic Leukemia Allows for the Identification of Impending Relapse: Results of the ALL-BFM-SCT 2003 Trial. *J Clin Oncol*. 2015.
14. Eckert C, Hagedorn N, Sramkova L, et al. Monitoring minimal residual disease in children with high-risk relapses of acute lymphoblastic leukemia: Prognostic relevance of early and late assessment. *Leukemia : official journal of the Leukemia Society of America, Leukemia Research Fund, UK*. 2015.
15. Garnett MJ, Edelman EJ, Heidorn SJ, et al. Systematic identification of genomic markers of drug sensitivity in cancer cells. *Nature*. 2012;483(7391):570-575.
16. Barretina J, Caponigro G, Stransky N, et al. The Cancer Cell Line Encyclopedia enables predictive modelling of anticancer drug sensitivity. *Nature*. 2012;483(7391):603-607.
17. Pemovska T, Kontro M, Yadav B, et al. Individualized systems medicine strategy to tailor treatments for patients with chemorefractory acute myeloid leukemia. *Cancer Discov*. 2013;3(12):1416-1429.
18. Tyner JW, Yang WF, Bankhead A, 3rd, et al. Kinase pathway dependence in primary human leukemias determined by rapid inhibitor screening. *Cancer Res*. 2013;73(1):285-296.
19. Geng H, Hurtz C, Lenz KB, et al. Self-Enforcing Feedback Activation between BCL6 and Pre-B Cell Receptor Signaling Defines a Distinct Subtype of Acute Lymphoblastic Leukemia. *Cancer Cell*. 2015;27(3):409-425.
20. Mihara K, Imai C, Coustan-Smith E, et al. Development and functional characterization of human bone marrow mesenchymal cells immortalized by enforced expression of telomerase. *Br J Haematol*. 2003;120(5):846-849.
21. Boutter J, Huang Y, Marovca B, et al. Image-based RNA interference screening reveals an individual dependence of acute lymphoblastic leukemia on stromal cysteine support. *Oncotarget*. 2014;5(22):11501-11512.
22. Bonapace L, Bornhauser BC, Schmitz M, et al. Induction of autophagy-dependent necroptosis is required for childhood acute lymphoblastic leukemia cells to overcome glucocorticoid resistance. *J Clin Invest*. 2010;120(4):1310-1323.
23. Schmitz M, Breithaupt P, Scheidegger N, et al. Xenografts of highly resistant leukemia recapitulate the clonal composition of the leukemogenic compartment. *Blood*. 2011;118(7):1854-1864.
24. Mirkowska P, Hofmann A, Sedek L, et al. Leukemia surfaceome analysis reveals new disease-associated features. *Blood*. 2013;121(25):e149-159.
25. Manabe A, Coustan-Smith E, Behm FG, Raimondi SC, Campana D. Bone marrow-derived stromal cells prevent apoptotic cell death in B-lineage acute lymphoblastic leukemia. *Blood*. 1992;79(9):2370-2377.
26. Iwamoto S, Mihara K, Downing JR, Pui CH, Campana D. Mesenchymal cells regulate the response of acute lymphoblastic leukemia cells to asparaginase. *J Clin Invest*. 2007;117(4):1049-1057.
27. Den Boer ML, Harms DO, Pieters R, et al. Patient stratification based on prednisolone-vincristine-asparaginase resistance profiles in children with acute lymphoblastic leukemia. *J Clin Oncol*. 2003;21(17):3262-3268.

28. Hartwell KA, Miller PG, Mukherjee S, et al. Niche-based screening identifies small-molecule inhibitors of leukemia stem cells. *Nat Chem Biol*. 2013;9(12):840-848.
29. Souers AJ, Leverson JD, Boghaert ER, et al. ABT-199, a potent and selective BCL-2 inhibitor, achieves antitumor activity while sparing platelets. *Nat Med*. 2013;19(2):202-208.
30. Van Vlierberghe P, Ambesi-Impiombato A, De Keersmaecker K, et al. Prognostic relevance of integrated genetic profiling in adult T-cell acute lymphoblastic leukemia. *Blood*. 2013;122(1):74-82.
31. Hogdal L, DeAngelo DJ, Stone RM, et al. BH3 Profiling Predicts On-Target Cell Death Due To Selective Inhibition Of BCL-2 By ABT-199 In Acute Myelogenous Leukemia. *Blood*. 2013;122(21).
32. McMillin DW, Negri JM, Mitsiades CS. The role of tumour-stromal interactions in modifying drug response: challenges and opportunities. *Nat Rev Drug Discov*. 2013;12(3):217-228.
33. Conter V, Bartram CR, Valsecchi MG, et al. Molecular response to treatment redefines all prognostic factors in children and adolescents with B-cell precursor acute lymphoblastic leukemia: results in 3184 patients of the AIEOP-BFM ALL 2000 study. *Blood*. 2010;115(16):3206-3214.
34. Parker C, Waters R, Leighton C, et al. Effect of mitoxantrone on outcome of children with first relapse of acute lymphoblastic leukaemia (ALL R3): an open-label randomised trial. *Lancet*. 2010;376(9757):2009-2017.
35. Liedtke M, Dunn T, Dinner S, et al. Salvage therapy with mitoxantrone, etoposide and cytarabine in relapsed or refractory acute lymphoblastic leukemia. *Leuk Res*. 2014;38(12):1441-1445.
36. Bicocca VT, Chang BH, Masouleh BK, et al. Crosstalk between ROR1 and the Pre-B cell receptor promotes survival of t(1;19) acute lymphoblastic leukemia. *Cancer Cell*. 2012;22(5):656-667.
37. Kowarz E, Burmeister T, Lo Nigro L, et al. Complex MLL rearrangements in t(4;11) leukemia patients with absent AF4.MLL fusion allele. *Leukemia : official journal of the Leukemia Society of America, Leukemia Research Fund, UK*. 2007;21(6):1232-1238.
38. Marschalek R. Mixed lineage leukemia: roles in human malignancies and potential therapy. *FEBS J*. 2010;277(8):1822-1831.
39. Spijkers-Hagelstein JA, Pinhancos SS, Schneider P, Pieters R, Stam RW. Chemical genomic screening identifies LY294002 as a modulator of glucocorticoid resistance in MLL-rearranged infant ALL. *Leukemia : official journal of the Leukemia Society of America, Leukemia Research Fund, UK*. 2014;28(4):761-769.
40. Richmond J, Carol H, Evans K, et al. Effective Targeting of the P53-MDM2 Axis in Preclinical Models of Infant MLL-Rearranged Acute Lymphoblastic Leukemia. *Clin Cancer Res*. 2015.
41. Liu H, Westergard TD, Cashen A, et al. Proteasome inhibitors evoke latent tumor suppression programs in pro-B MLL leukemias through MLL-AF4. *Cancer Cell*. 2014;25(4):530-542.
42. Niu X, Wang G, Wang Y, et al. Acute myeloid leukemia cells harboring MLL fusion genes or with the acute promyelocytic leukemia phenotype are sensitive to the Bcl-2-selective inhibitor ABT-199. *Leukemia : official journal of the Leukemia Society of America, Leukemia Research Fund, UK*. 2014;28(7):1557-1560.
43. Hartsink-Segers SA, Zwaan CM, Exalto C, et al. Aurora kinases in childhood acute leukemia: the promise of aurora B as therapeutic target. *Leukemia : official journal of the Leukemia Society of America, Leukemia Research Fund, UK*. 2013;27(3):560-568.
44. Alford SE, Kothari A, Loeff FC, et al. BH3 inhibitor sensitivity and Bcl-2 dependence in primary acute lymphoblastic leukemia cells. *Cancer Res*. 2015.
45. Suryani S, Carol H, Chonghaile TN, et al. Cell and Molecular Determinants of In Vivo Efficacy of the BH3 Mimetic ABT-263 against Pediatric Acute Lymphoblastic Leukemia Xenografts. *Clin Cancer Res*. 2014.
46. Peirs S, Matthijssens F, Goossens S, et al. ABT-199 mediated inhibition of BCL-2 as a novel therapeutic strategy in T-cell acute lymphoblastic leukemia. *Blood*. 2014;124(25):3738-3747.
47. Fischer U, Forster M, Rinaldi A, et al. Genomics and drug profiling of fatal TCF3-HLF-positive acute lymphoblastic leukemia identifies recurrent mutation patterns and therapeutic options. Nat Genet. 2015;advance online publication.
48. Chonghaile TN, Roderick JE, Glenfield C, et al. Maturation stage of T-cell acute lymphoblastic leukemia determines BCL-2 versus BCL-XL dependence and sensitivity to ABT-199. *Cancer Discov*. 2014;4(9):1074-1087.
49. Mullighan CG. Genomic characterization of childhood acute lymphoblastic leukemia. *Semin Hematol*. 2013;50(4):314-324.
50. Messinger YH, Gaynon PS, Sposto R, et al. Bortezomib with chemotherapy is highly active in advanced B-precursor acute lymphoblastic leukemia: Therapeutic Advances in Childhood Leukemia & Lymphoma (TACL) Study. *Blood*. 2012;120(2):285-290.
51. Woyach JA, Johnson AJ. Targeted therapies in CLL: mechanisms of resistance and strategies for management. *Blood*. 2015.
52. Leverson JD, Phillips DC, Mitten MJ, et al. Exploiting selective BCL-2 family inhibitors to dissect cell survival dependencies and define improved strategies for cancer therapy. *Sci Transl Med*. 2015;7(279):279ra240.

53. Ni Chonghaile T, Sarosiek KA, Vo TT, et al. Pretreatment mitochondrial priming correlates with clinical response to cytotoxic chemotherapy. *Science*. 2011;334(6059):1129-1133.
54. Montero J, Sarosiek KA, DeAngelo JD, et al. Drug-induced death signaling strategy rapidly predicts cancer response to chemotherapy. *Cell*. 2015;160(5):977-989.
55. Herranz D, Ambesi-Impiombato A, Palomero T, et al. A NOTCH1-driven MYC enhancer promotes T cell development, transformation and acute lymphoblastic leukemia. *Nat Med*. 2014;20(10):1130-1137.
56. Roberts KG, Mullighan CG. Genomics in acute lymphoblastic leukaemia: insights and treatment implications. *Nat Rev Clin Oncol*. 2015.
57. Muschen M. Ph+ ALL: drawing strength from a benign past. *Blood*. 2015;125(19):2879-2880.
58. Zwaan CM, Rizzari C, Mechinaud F, et al. Dasatinib in children and adolescents with relapsed or refractory leukemia: results of the CA180-018 phase I dose-escalation study of the Innovative Therapies for Children with Cancer Consortium. *J Clin Oncol*. 2013;31(19):2460-2468.

FIGURE LEGENDS

Figure 1. Workflow for co-clinical drug response profiling of leukemia cells.

For large scale drug testing, co-cultures with mesenchymal bone marrow stroma cells (MSCs) were established to maintain primary ALL cells. An automated microscopy-based image acquisition program that integrates a machine learning algorithm for quantifying both live ALL and MSC cells was used to generate dose response curves. The data was subsequently analysed with a toolkit that performs outlier removal, rapid curve fitting, and extraction of different response parameters. The same platform can be used for analyzing combinatorial drug testing results from co-titration experiments. Systematic generation of xenografts provide a model for functional validation.

Figure 2. MSCs provide adequate support for the majority of primary ALL cells.

(**A**) Cell viability analysis of T-ALL and BCP-ALL samples at day 4 normalized to seeded cell numbers shows a significantly higher number of living cells in the co-culture compared to suspension cultures using serum free medium. Note that cell counts at day 4 are significantly higher in T-ALL (n=22) than BCP-ALL (n=25) samples. *****, p<0.0001 (Paired t test)*.

(**B**) Analysis of cell cycle and apoptosis in T-ALL samples (n=18). Rates of apoptosis and distribution of cell cycle phases are displayed. Samples are ranked from highest (top) to lowest (bottom) survival. Viability was assessed after 4 days in culture.

Figure 3. Drug response profiles of BCP-ALL and T-ALL cases.

Unsupervised hierarchical clustering of diagnostic BCP-ALL (n=28) and T-ALL (n=18) samples in co-culture with MSC according to their response (log[nM] IC50) to 60 compounds after 72h. Compounds are arranged by target classes. Sample information including translocations detected by FISH and mutations detected by targeted sequencing, are summarized at the bottom.

Figure 4. Distinct drug activity patterns can be detected in specific sample groups.

(**A**) Selection of drugs with differential activity (log[nM] IC50) in refractory relapse (RR) (left panel, red, BCP-ALL n=3 and T-ALL n=3), MLL-AF4 rearranged ALL (middle panel, green, n=3) and T-ALL (right panel, diagnostic samples in blue, n=18; at relapse in orange, n=6), against a background of all other cases of the platform (grey, total n=61).

(**B**) T-ALL(blue, n=24) and *TCF1-PBX1* (yellow, n=6) differential response (log[nM] IC50) to dasatinib.

Figure 5. The BCL-2 antagonist venetoclax is highly active in, *MLL-AF4*, *TCF3-HLF* and a subset of T-ALL cases.

(**A**) *In vitro* response of T-ALL samples (i, n=23), BCP-ALL (ii, n=19), TCF1-HLF (iii, n=4) and MLL-AF4 (iv, n=3) to the BCL2 inhibitor venetoclax in co-culture on MSC. Cell viability was measured by flow cytometry using 7-AAD 72 hours after treatment. Viabilities are normalized to DMSO-treated controls.

(**B**) T-ALL samples at different maturation stages based on EGIL criteria respond to venetoclax (log[nM] IC50).

(**C**) Mean ratio (+/- SEM) of BCL2:BCL-XL protein analysed by densitometry from two independent Western blot experiments. *ns. =not significant (p.val > 0.05, two-sided t-test)*

Figure 6. *In vitro* sensitivity to venetoclax correlates with *in vivo* response in xenografts.
(**A**) Response curves of three samples used in *in vivo* validation (red curves, sensitive samples with IC50 at 0.27 and 50.1 nM; blue curve, resistant sample with IC50 at 6166 nM).
(**B**) Treatment with 100 mg/kg venetoclax administered orally delays leukemia progression in the two sensitive, but not in the resistant T-ALL samples. Kaplan-Meier survival curves (upper panel, event defined as 25% of $mCD45^{-}hCD7^{+}CD45^{+}$ leukemia cells detected by flow cytometry) and the number of leukemia cells compared to mouse lymphocytes over time (lower panel) are shown. Boxes shaded in grey indicate treatment blocks.
(**C**) Treatment of mice with overt leukemia (75% human leukemia cells in the peripheral blood) for two weeks decreased leukemia burden.

Figure 7. Synergistic activity *in vitro* and *in vivo* of venetoclax with experimental and clinically relevant drugs.
(**A**) Representative examples of co-titration assays for compounds detected to synergise with venetoclax in preselected T-ALL samples from initial combination screening. (i) topoisomerase I inhibitor topotecan, (ii) dual PI3K and mTOR inhibitor dactolosib and (iii) BRD4 inhibitor JQ1.
(**B**) Dose response curves are given for co-titration assays with increasing concentrations of venetoclax and dexamethasone or vincristine. Response curves representing the combination with three venetoclax doses (concentrations indicated in color on the x-axis) are shown. The area in which synergistic activity occurs, defined based on Loewe additivity, is shaded for reference.
(**C**) Combination treatment of two *TCF1-HLF* samples. Each treatment arm included six mice that were treated as indicated. Kaplan-Meier survival curves (upper panel, event defined as 25% of mCD45-hCD19+CD45+ leukemia cells detected by flow cytometry) and the number of leukemia cells compared to mouse lymphocytes over time (lower panel) are shown. Vincristine was given on day 1 and 8, Dexamethasone on d1-5 and 8-12, venetoclax on d1-5 and 8-12. The two weeks treatment blocks are indicated as grey shaded boxes.

Figure 1.

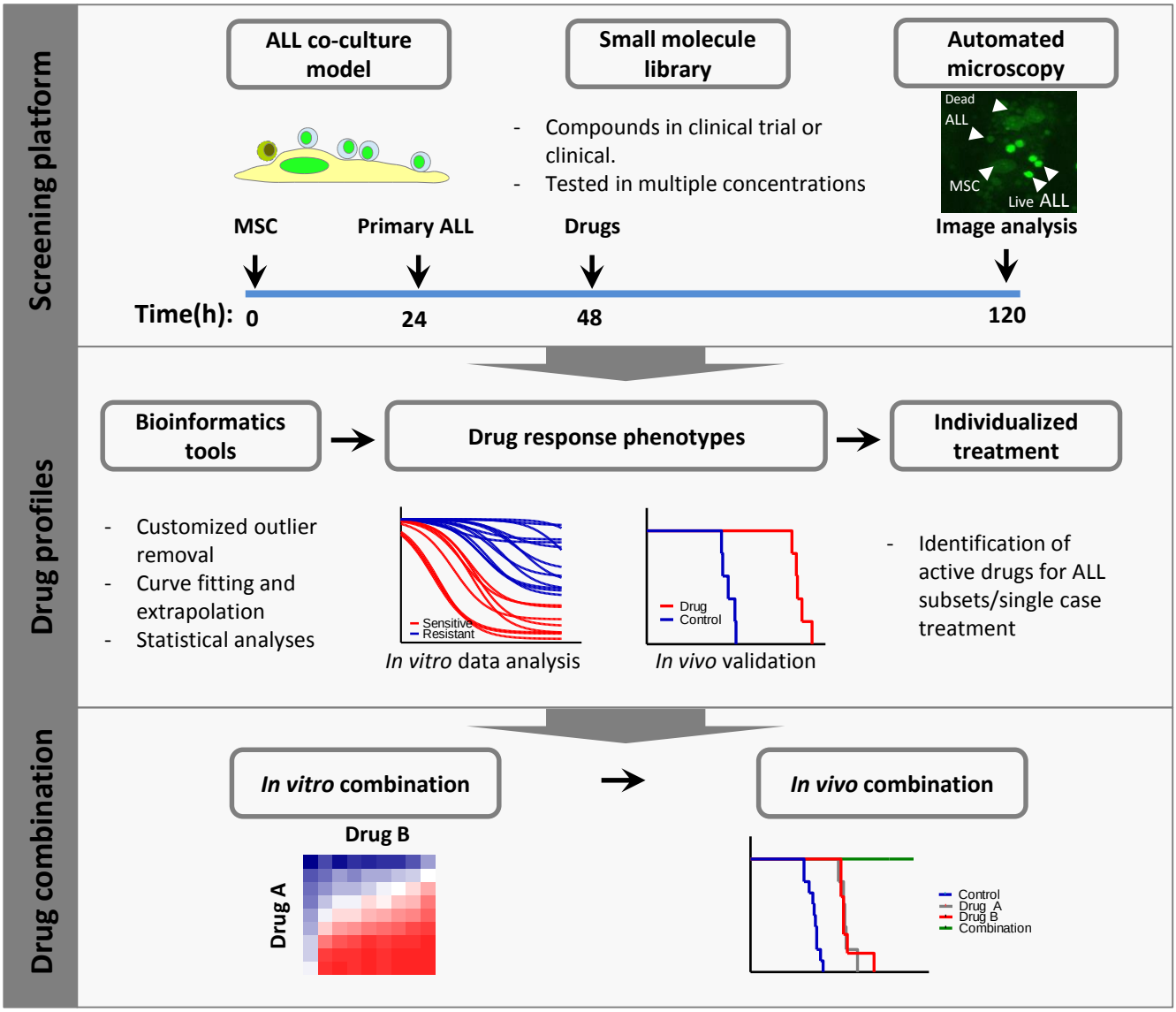
Screening platform
ALL co-culture model
Small molecule library
Automated microscopy
- Compounds in clinical trial or clinical.
- Tested in multiple concentrations
Dead
ALL
MSC
Live ALL
MSC
Primary ALL
Drugs
Image analysis
Time(h):
0
24
48
120
Drug profiles
Bioinformatics tools
Drug response phenotypes
Individualized treatment
- Customized outlier removal
- Curve fitting and extrapolation
- Statistical analyses
Sensitive
Resistant
In vitro data analysis
Drug
Control
In vivo validation
- Identification of active drugs for ALL subsets/single case treatment
Drug combination
In vitro combination
In vivo combination
Drug B
Drug A
Control
Drug A
Drug B
Combination

Figure 2.

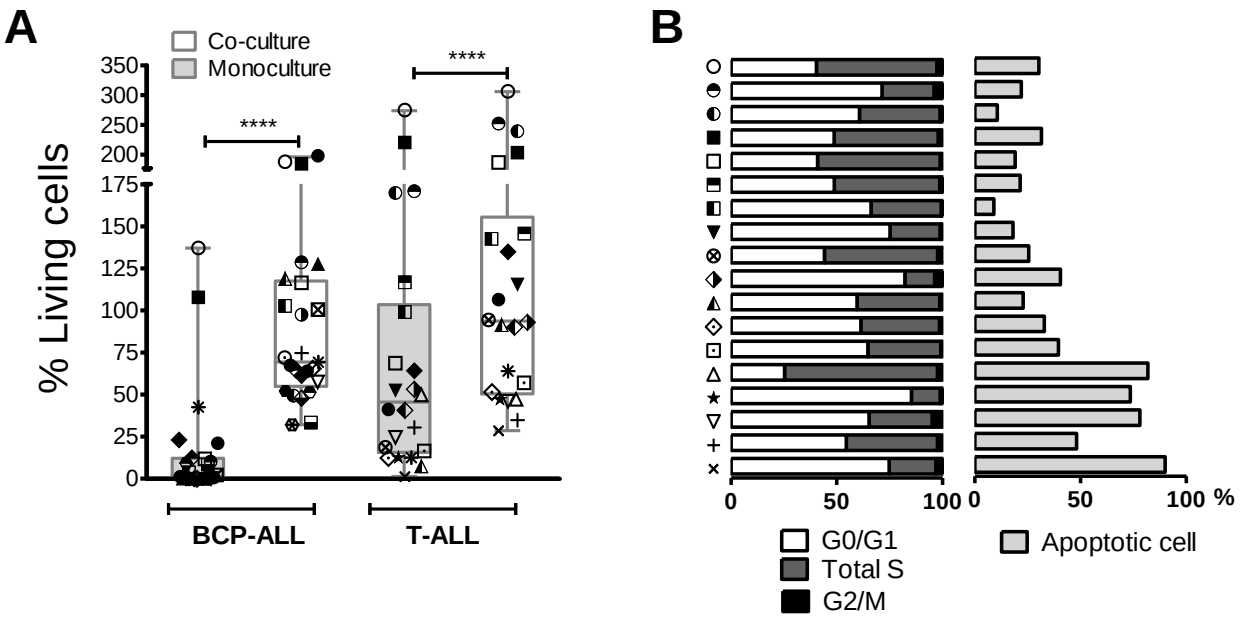
A
Co-culture
Monoculture
% Living cells
350
300
250
200
175
150
125
100
75
50
25
0
****
****
BCP-ALL
T-ALL
B
0
50
100
0
50
100 %
G0/G1
Total S
G2/M
Apoptotic cell

Figure 3.

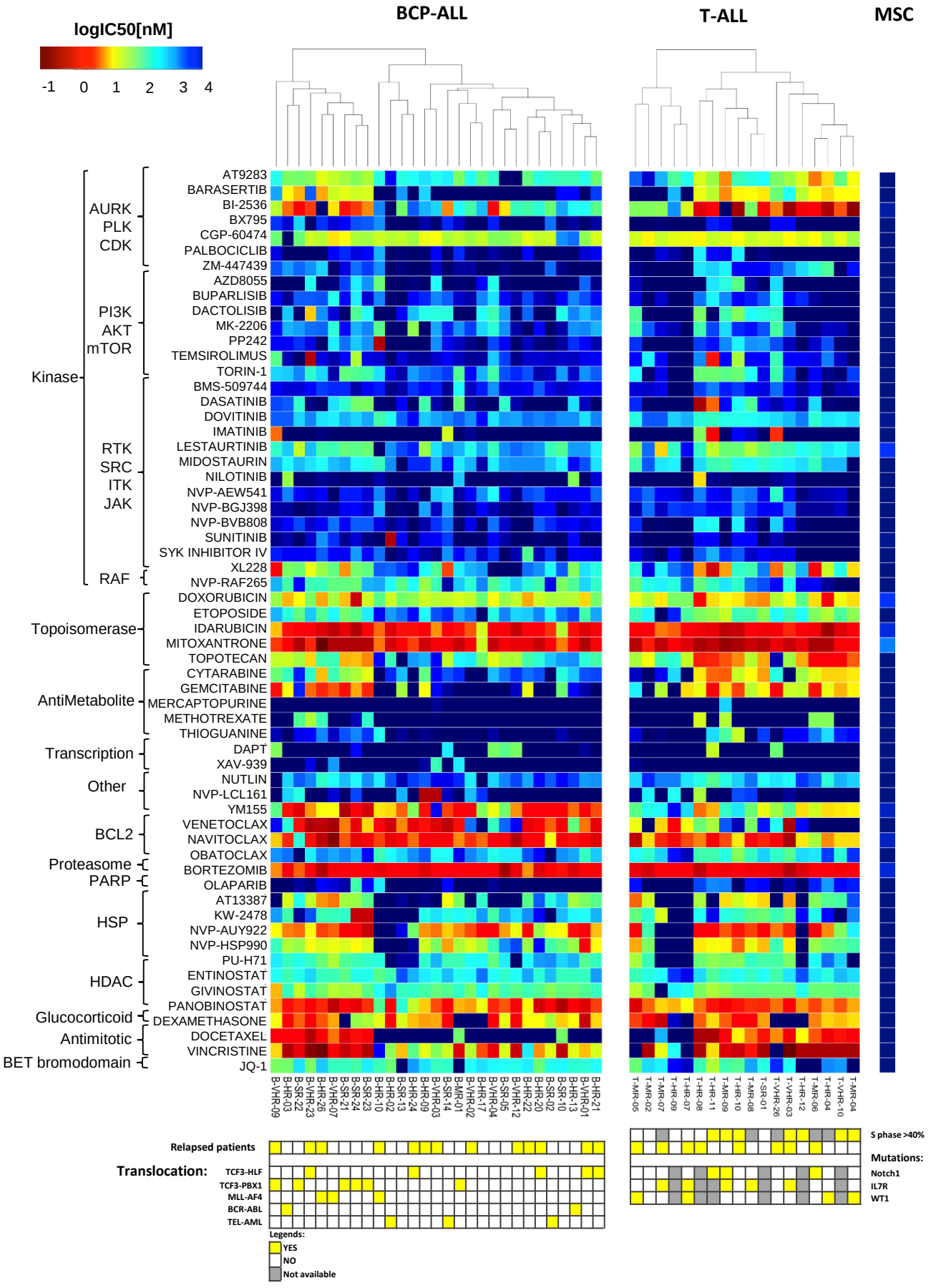
logIC50[nM]
-1 0 1 2 3 4
BCP-ALL
T-ALL
MSC
Kinase
AURK
PLK
CDK
PI3K
AKT
mTOR
RTK
SRC
ITK
JAK
RAF
Topoisomerase
AntiMetabolite
Transcription
Other
BCL2
Proteasome
PARP
HSP
HDAC
Glucocorticoid
Antimitotic
BET bromodomain
AT9283
BARASERTIB
BI-2536
BX795
CGP-60474
PALBOCICLIB
ZM-447439
AZD8055
BUPARLISIB
DACTOLISIB
MK-2206
PP242
TEMSIROLIMUS
TORIN-1
BMS-509744
DASATINIB
DOVITINIB
IMATINIB
LESTAURTINIB
MIDOSTAURIN
NILOTINIB
NVP-AEW541
NVP-BGJ398
NVP-BVB808
SUNITINIB
SYK INHIBITOR IV
XL228
NVP-RAF265
DOXORUBICIN
ETOPOSIDE
IDARUBICIN
MITOXANTRONE
TOPOTECAN
CYTARABINE
GEMCITABINE
MERCAPTOPURINE
METHOTREXATE
THIOGUANINE
DAPT
XAV-939
NUTLIN
NVP-LCL161
YM155
VENETOCLAX
NAVITOCLAX
OBATOCLAX
BORTEZOMIB
OLAPARIB
AT13387
KW-2478
NVP-AUY922
NVP-HSP990
PU-H71
ENTINOSTAT
GIVINOSTAT
PANOBINOSTAT
DEXAMETHASONE
DOCETAXEL
VINCRISTINE
JQ-1
B-VHR-09 B-HR-03 B-SR-22 B-VHR-23 B-HR-26 B-VHR-07 B-SR-21 B-SR-24 B-SR-23 B-HR-10 B-HR-02 B-SR-13 B-HR-24 B-HR-09 B-VHR-03 B-SR-14 B-MR-01 B-VHR-02 B-HR-17 B-VHR-04 B-SR-05 B-VHR-12 B-HR-20 B-SR-02 B-SR-10 B-HR-13 B-VHR-01 B-HR-21
T-MR-05 T-MR-02 T-MR-07 T-HR-09 T-HR-07 T-HR-08 T-HR-11 T-MR-09 T-HR-10 T-MR-08 T-SR-01 T-VHR-26 T-VHR-03 T-HR-12 T-MR-06 T-HR-04 T-VHR-10 T-MR-04
Relapsed patients
Translocation:
TCF3-HLF
TCF3-PBX1
MLL-AF4
BCR-ABL
TEL-AML
Legends:
YES
NO
Not available
S phase >40%
Mutations:
Notch1
IL7R
WT1

Figure 4.

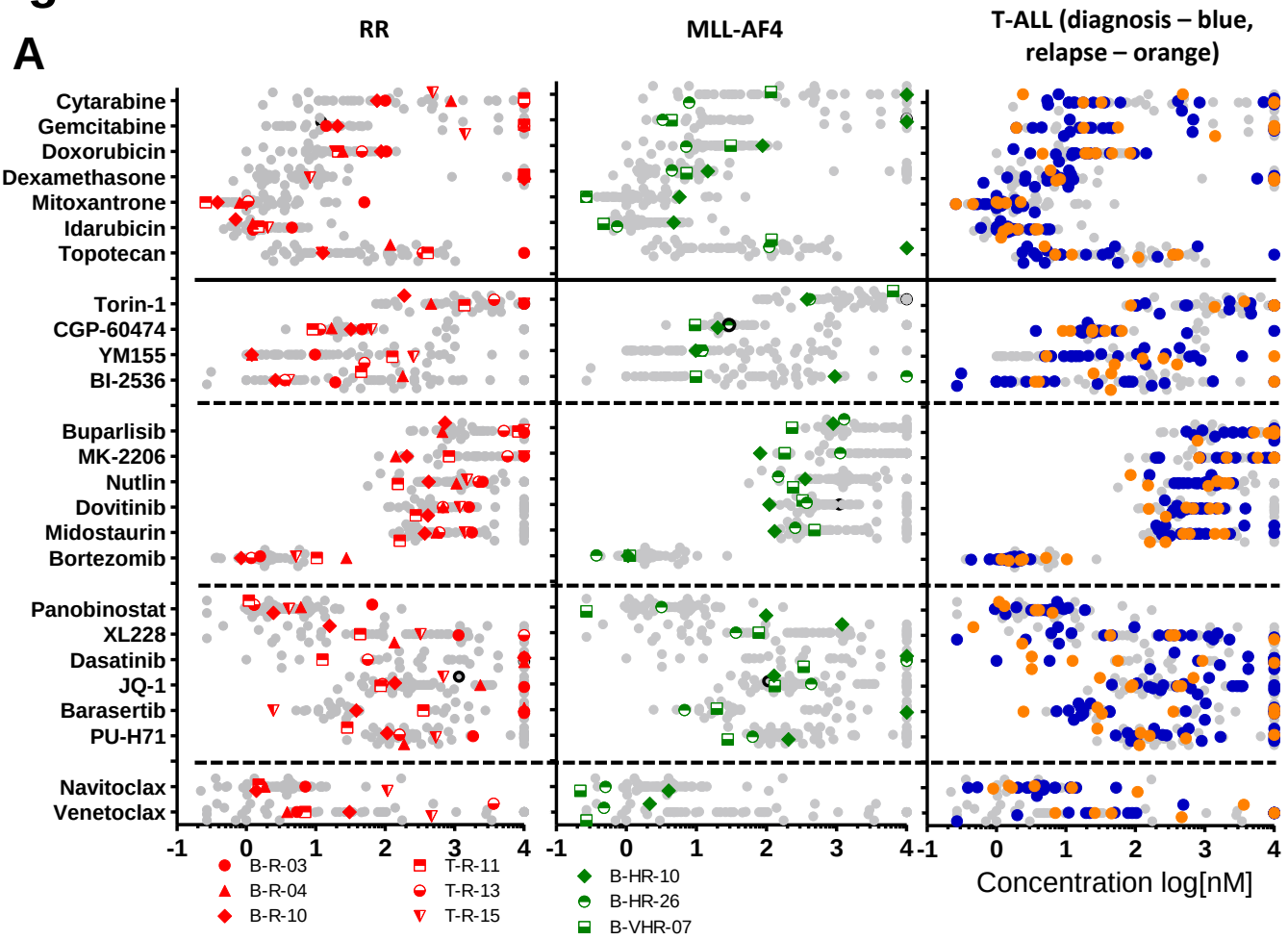
A
RR
MLL-AF4
T-ALL (diagnosis – blue, relapse – orange)
Cytarabine
Gemcitabine
Doxorubicin
Dexamethasone
Mitoxantrone
Idarubicin
Topotecan
Torin-1
CGP-60474
YM155
BI-2536
Buparlisib
MK-2206
Nutlin
Dovitinib
Midostaurin
Bortezomib
Panobinostat
XL228
Dasatinib
JQ-1
Barasertib
PU-H71
Navitoclax
Venetoclax
-1 0 1 2 3 4
B-R-03
B-R-04
B-R-10
T-R-11
T-R-13
T-R-15
B-HR-10
B-HR-26
B-VHR-07
Concentration log[nM]

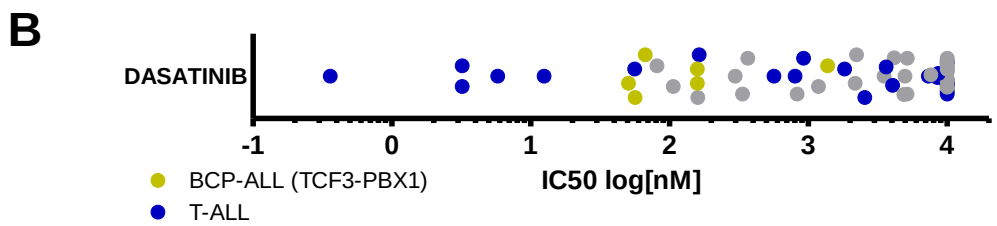
B
DASATINIB
-1 0 1 2 3 4
IC50 log[nM]
BCP-ALL (TCF3-PBX1)
T-ALL

Figure 5.

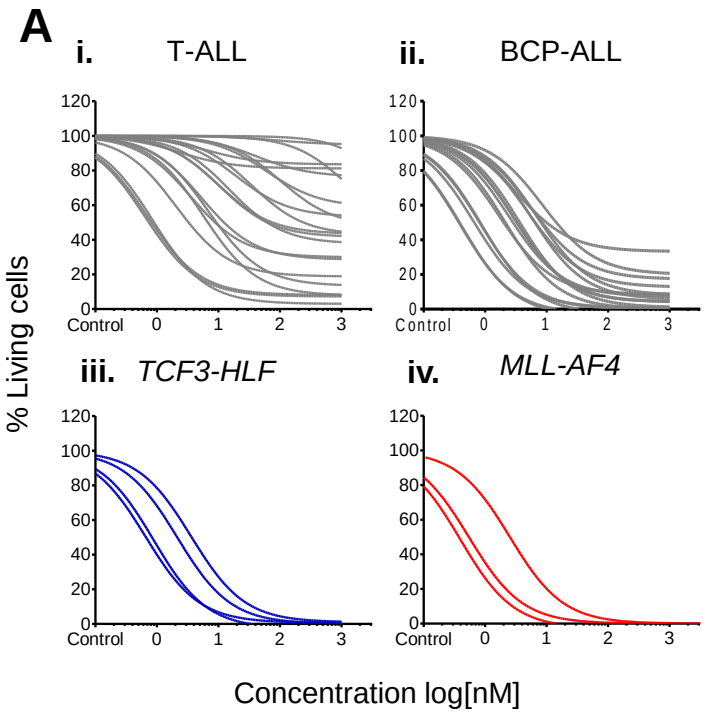
A
i.
T-ALL
ii.
BCP-ALL
iii.
TCF3-HLF
iv.
MLL-AF4
% Living cells
Control
Concentration log[nM]

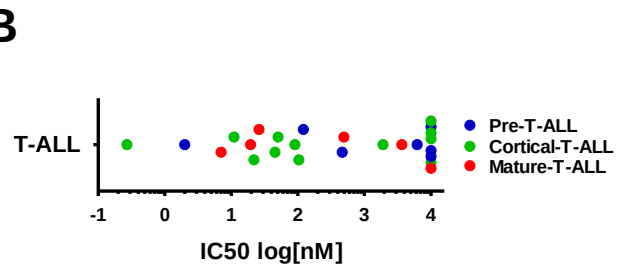
B
T-ALL
Pre-T-ALL
Cortical-T-ALL
Mature-T-ALL
IC50 log[nM]

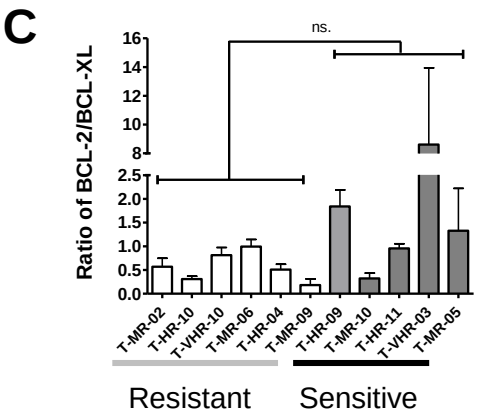
C
Ratio of BCL-2/BCL-XL
ns.
T-MR-02
T-HR-10
T-VHR-10
T-MR-06
T-HR-04
T-MR-09
T-HR-09
T-MR-10
T-HR-11
T-VHR-03
T-MR-05
Resistant
Sensitive

Figure 6.

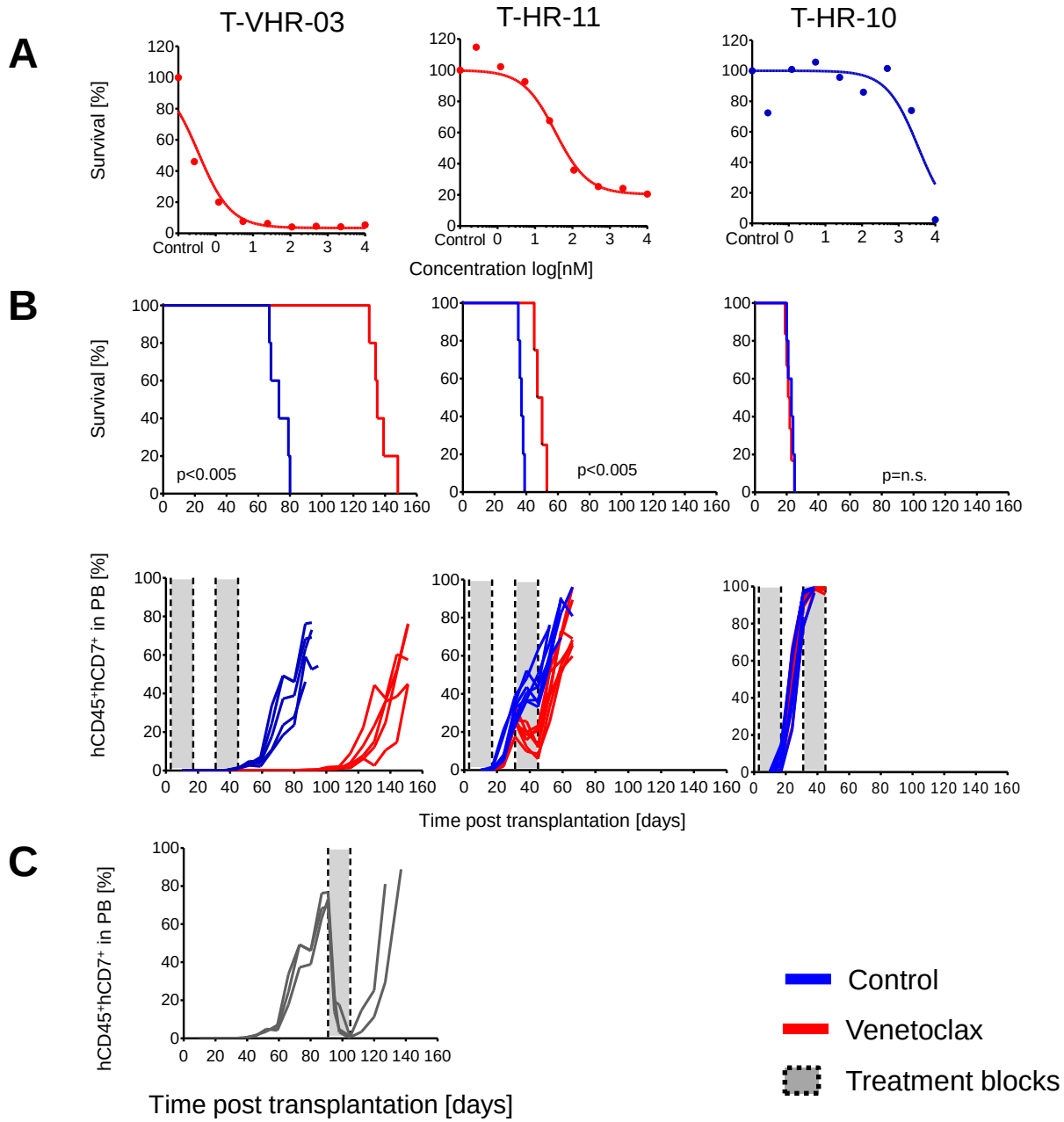
A
T-VHR-03
T-HR-11
T-HR-10
Survival [%]
Control
Concentration log[nM]
B
Survival [%]
p<0.005
p<0.005
p=n.s.
hCD45+hCD7+ in PB [%]
Time post transplantation [days]
C
hCD45+hCD7+ in PB [%]
Time post transplantation [days]
Control
Venetoclax
Treatment blocks

Figure 7.

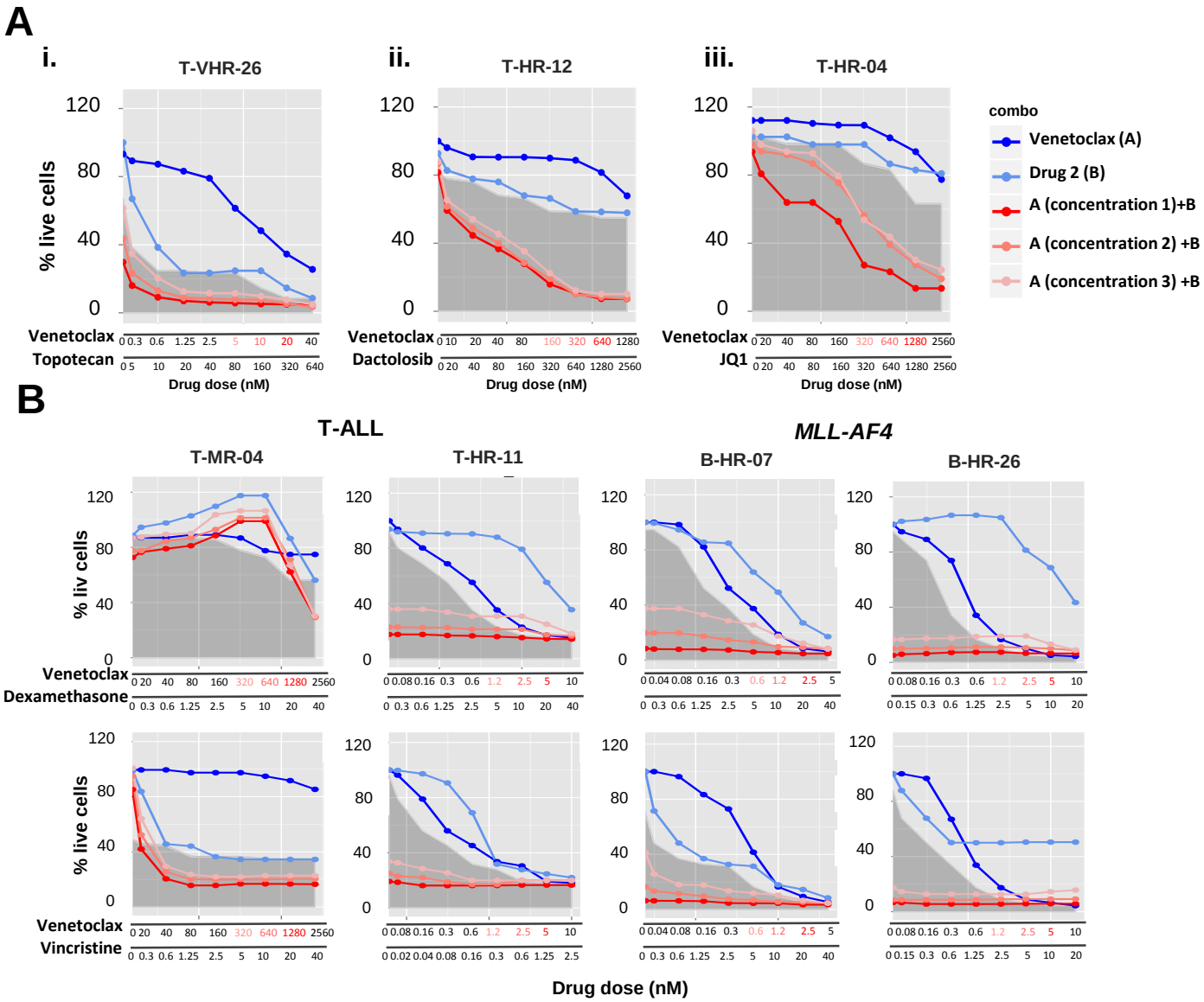
A
i.
T-VHR-26
ii.
T-HR-12
iii.
T-HR-04
% live cells
Venetoclax
Topotecan
Dactolosib
JQ1
Drug dose (nM)
combo
Venetoclax (A)
Drug 2 (B)
A (concentration 1)+B
A (concentration 2) +B
A (concentration 3) +B
B
T-ALL
MLL-AF4
T-MR-04
T-HR-11
B-HR-07
B-HR-26
% liv cells
% live cells
Venetoclax
Dexamethasone
Vincristine
Drug dose (nM)

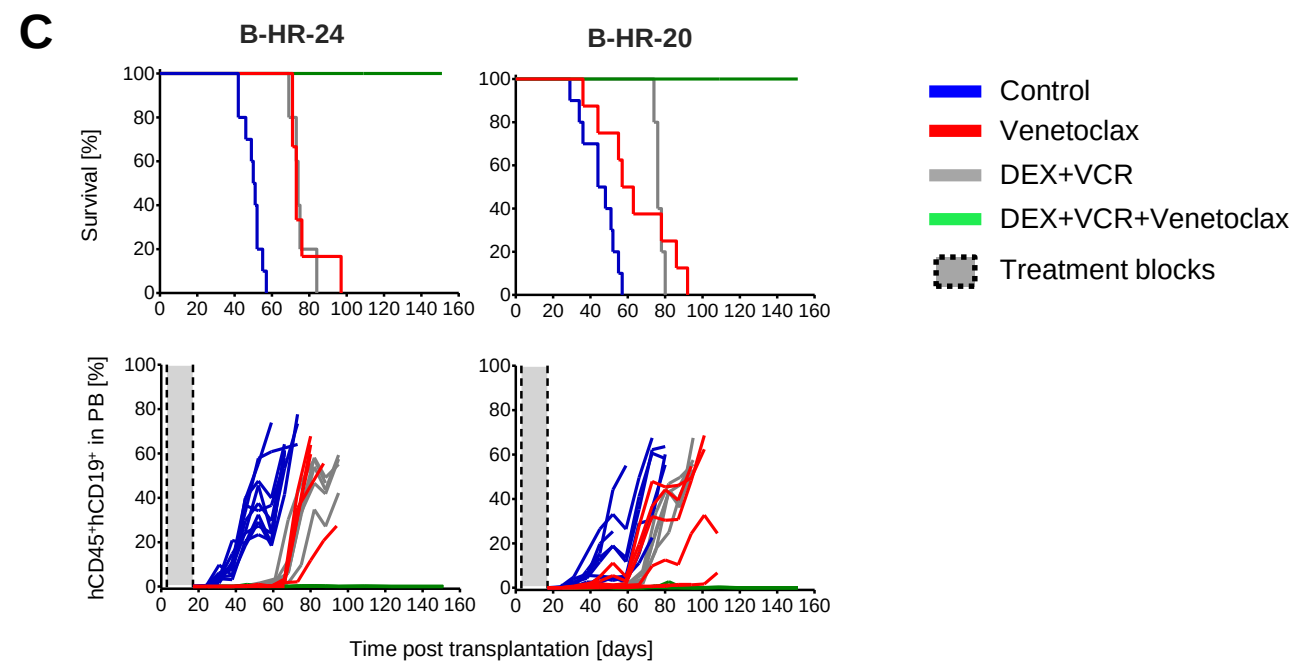
C
B-HR-24
B-HR-20
Survival [%]
hCD45+hCD19+ in PB [%]
Time post transplantation [days]
Control
Venetoclax
DEX+VCR
DEX+VCR+Venetoclax
Treatment blocks

Manuscript 3

Vanin-2 (GPI-80) identifies aggressive subtypes of childhood acute lymphoblastic leukemia

Anna Rinaldi[1], Nastassja Scheidegger[1], Gunnar Cario[2], Andreas Hofmann[3], Paulina Mirkowska[1], Elena Vendramini[4], Martina Temperli[1], Marco Giordan[4], Guimarães Andreia[1], Cornelia Eckert[5], Mecklenbräuker Astrid[6], Andishe Attabashi[6], Renate Panzer-Grümayer[6], Maria Pamela Dobay[8], Truus teKronnie[4], Giuseppe Basso[4], Martin Stanulla[7], Martin Zimmermann[7] Bernd Wollscheid[2] Beat Bornhauser[1] and Jean-Pierre Bourquin[1]

[1] Pediatric Oncology, Children's Research Centre, University Children's Hospital Zurich, 8032 Zurich, Switzerland
[2] Department of Pediatrics, University Hospital Schleswig-Holstein, 24105 Kiel, Germany
[3] Department of Biology, Institute of Molecular Systems Biology, ETH Zurich, Switzerland
[4] Department of Pediatrics, Laboratory of Pediatric Hematology/Oncology, University of Padova, 35128 Padova, Italy
[5] Pediatric Hematology and Oncology, Charité University Hospital, 13353 Berlin, Germany
[6] St. Anna Children's Hospital and Children's Cancer Research Institute, 1090 Vienna, Austria
[7] Pediatric Hematology and Oncology, Hannover Medical School, 30625 Hannover, Germany
[8] SIB Swiss Institute for Bioinformatics, 1015 Lausanne, Switzerland

ABSTRACT

The glycophosphatidylinositol anchored surface protein Vanin-2 (VNN2, GPI-80), which has been implicated in leukocyte adherence and migration, identifies human fetal liver hematopoietic stem/ progenitor cells (HSPCs) with self-renewal ability and is required for their hematopoietic function. Comparing the cell surface glycoproteome of 19 acute lymphoblastic leukemia (ALL) samples, we identified VNN2 as a unique feature in patients with a very high risk of relapse by minimal residual disease. In a retrospective analysis of 663 patients on the ALL-BFM-2000 treatment protocol high VNN2 transcript levels were associated with decreased event free survival. We show in a subset of this cohort that VNN2 detection by flow cytometry may serve as a prognostic marker instead. Furthermore all of 12 *TCF3-HLF*-positive ALL, which defines a currently incurable ALL subtype, were strongly surface VNN2, providing a simple procedure to preselect samples for specific diagnostic testing. VNN2 expression was not associated with other cytogenetic and copy number abnormality. Antibody interference with VNN2 resulted in delayed homing of ALL to the bone marrow of immunodeficient mice, suggesting a potential role of VNN2 in leukemia trafficking. Thus surface VNN2 expression identifies *TCF3-HLF*-positive ALL as well as subset of ALL with unfavorable biology that cannot be defined by other diagnostic features and warrants prospective clinical investigation.

INTRODUCTION

Therapeutic advancements combined with risk-adapted treatment strategies have significantly improved outcomes in patients with ALL. In pediatric ALL, overall cure rates are approaching 85%, but there are still subgroups for which prognosis is significantly worse and relapse ALL is still a leading cause of cancer-related deaths in the pediatric population. 26% of B-cell precursor acute lymphoblastic leukemia (BCP-ALL) is not associated with known genetic aberrations, but the remaining cases can be classified into genetically defined subtypes such as *ETV6-RUNX1*, *TCF3-PBX1* and hyperdiploidy, which correlate with a favorable outcome, whereas others, like the MLL rearrangements, *BCR-ABL1*, and hypodiploidy, are associated with a poor treatment response, and no patient survival for *TCF3-HLF*-positive cases. Although *TCF3-HLF*-translocation has been already described in the 90s (1, 2), there are no established methods that allow its discrimination in routine clinical test at diagnosis. Current treatment protocol stratifies ALL patients based on a combination of

different approaches that consider clinical factors (immunophenotyping, age and white cell count), genetic abnormalities and treatment response of the patient. So far expression patterns of markers determining lineage and developmental stage of hematopoietic differentiation has been essential for the generation of the current stratification schemes applied in the clinic at diagnosis. While *in vivo* response to treatment evaluated through the molecular quantification of minimal residual disease (MRD) during ALL induction therapy is the most powerful predictor of the risk of disease recurrence, but can be applied only after 33 days from the beginning of the treatment. In the AEIOP-BFM-ALL 2000 (3) study 15% of the patients were classified as High Risk (HR) of relapse and the remaining cases were Intermediate (IR, 42,6%) and Standard (SR, 42,6%) risk. The 5-year relapse rates of each MRD-based risk group were 2% in SR, 22% in IR and 80% in HR group. Therefore current stratification scheme and survival rates data emphasize the need of new markers for the early detection of HR cases and IR patients that relapse that constitute almost half of the BCP-ALL patients (4).
These evidences underling the need of alternative approaches for the identification of IR and HR cases that relapse, and patients with the incurable *TCF3-HLF* genetic subtype at the day of diagnosis.

Here we identify glycosylphosphatidyinositol-anchored surface protein (GPI-80 also known Vanin2 or VNN2) as a novel promising prognostic marker for the identification at diagnosis a fraction of cases with high risk of relapse and the resistant *TCF3-HLF*-positive ALL. We investigated the overall GPI-80 expression by ALL and its clinical relevance. Data suggest that the implementation of GPI-80 flow cytometry analysis in the established panel of the clinical immunophenotyping of ALL will provides new insights for the improvement of the risk stratification of IR and HR for relapse cases and importantly for the resistant *TCF3-HLF*-positive ALL subtype.

RESULTS

Detection of VNN2 (GPI-80) at the leukemia cell surface is associated with resistance to treatment

To identify cell surface markers that may be characteristic for resistant disease, we interrogated the cell surface proteomes of 19 BCP-ALL patient derived xenografts (PDX) that we had previously defined using the Cell Surface Capture (CSC) technology (5). We compared the leukemia surfaceome derived from 8 BCP-ALL cases with a very high risk of relapse based on persistence of minimal residual disease after induction chemotherapy and consolidation therapy (VHR-ALL, week 4, 9 and 22 on the ALL-BFM treatment protocol (3, 6-9) and 11 patients with an excellent clinical outcome (standard risk, SR-ALL). To enrich for cell surface glycoproteins, selective chemical tagging was performed on living cells that were then subjected to a workflow to prepare tagged peptides from membrane fractions (5). By liquid chromatography-tandem mass spectrometry, a comparable number of peptides that can be matched to proteins were identified between VHR and SR patients, on average 5481 in SR-ALL and 5714 in VHR-ALL (Figure 1A and Supplementary Table 1). Filtering this dataset for proteins that are detected preferentially in VHR-ALL resulted in the selection of 13 proteins (Figure 1A and Supplementary Table 1). Remarkably, we found several surface proteins that are normally involved in cell adhesion and migration, the glycophosphatidylinositol anchored surface proteins vanin-family proteins VNN1 and VNN2 (GPI-80), the Ig-like CEA family member CEAM1, the C-type lectin receptor CD302, the sialic acid binding Ig-like lectin CD33 and ITGAM (CD11b), which is also a subunit of the complement receptor 3 (CR3). Furthermore, the receptors for activated complement CR1 and CR2 as well as components of pro-survival signaling pathways (TNR1B, IGF1R) were detected in VHR-ALL cases. Notably, in 3 out 4 patients expressing VNN2, ITAM is co-expressed. This co-expression of VNN2 and ITGAM has recently been demonstrated in self-renewing human fetal hematopoietic stem cells, whereby RNA interference with VNN2 or ITGAM both impaired survival in vitro and engraftment/hematopoietic reconstitution ability in xenografts (10). Public available microarray data (11) show a correlation of ITGAM and VNN2 expression in ALL (Supplementary Figure 1), suggesting that these phenotypes may be functionally related.

To validate the proteomic data we correlated RNA expression by quantitative PCR and protein detection by flow cytometry for VNN2 on an extended set of 34 ALL PDXs (Figure 1B and Supplementary Table 2). As controls, we included peripheral blood cells from healthy donors that contain both positive (myeloid lineage) and negative / lower positive subpopulations (T and B lymphocytes) (Supplementary Figure 2), and a Jurkat cell

line that we lentivirally transfected to express VNN2 (Supplementary Figures 3A). We validated the monoclonal antibody 3H9 (anti-VNN2) that was generated with extracts from neutrophils (12) using these assays and established the criteria to define positive signals (Supplementary Figure 4). We obtained similar results using a second anti-VNN2 monoclonal antibody that was generated with recombinant human VNN2 (clone 04) (Supplementary Figures 3B and 5). We included patient derived Xenografts (PDXs) from diagnostic samples from patients with high risk (HR), intermediate risk (IR) and standard (low) risk (SR) of relapse based on their minimal residual disease after induction chemotherapy. As expected, we found that higher levels of VNN2 in this cohort were found preferentially in HR and MR patients. Higher levels of VNN2 transcripts correlated with detection by flow cytometry (Figure 1B, r=0.7796). Moreover, most of the MR and HR samples, 17 out of 26, and only one SR out of 12 samples were positive for VNN2 by flow cytometry. Interestingly the single SR patient that was positive for VNN2 at diagnosis experienced a relapse (Table 3). Importantly, detection of VNN2 on primary material remained stably detectable even after serial passage in NSG mice, indicating that this could be driven by a leukemia-intrinsic feature (Supplementary Figure 6)

VNN2 positive ALL is a rare subset that includes the highly aggressive *TCF3-HLF*-positive ALL subtype

In our surfaceome dataset, one case with *TCF3-HLF* positive ALL (B-ALL-09) had the most abundant spectra corresponding to VNN2. The translocation t(17;19)(q22;p13), which results in the fusion gene *TCF3-HLF*, defines a rare subtype of ALL (<1% of pediatric ALL) that is typically associated with relapse and death within two years from diagnosis (13, 14). Remarkably, the same segment of the transcription factor *TCF3* is involved in the translocation t(1;19) (15), which occurs in about 10% of precursor B cell (pre-B) ALL patients and is associated with a five-year event-free survival of 78-85% (16). We recently described the genomic landscape of *TCF3-HLF*-positive ALL as part of a research consortium and could show that *TCF3-HLF*-positive PDXs closely resemble the original patient sample (17). Here we show that in all cases of *TCF3-HLF*- positive ALL we detected VNN2 at the cell surface both in PDXs and in diagnostic samples (Figure 1B and 1C). By proteomics, besides VNN2, we detected VNN1, CR1 and CR2 strongly in the *TCF3-HLF*-positive ALL case. Interestingly, when comparing the transcriptome of *TCF3-HLF*-positive ALL and *TCF3-PBX1*-positive ALL, VNN2 expression correlates best with higher expression levels of ITGAM, confirming our initial observations in the surfaceome that VNN2 and ITGAM provide a specific pattern (Figure 1D). Co-expression of VNN2 and ITGAM could be validated in 2 *TCF3-HLF*-positive cases by flow cytometry (Supplementary Figure 7). Identification of *TCF3-HLF*-positive ALL has been a challenge in the clinic, because the translocation is not always found by conventional cytogenetics. Since in some cases, hypercalcemia occurs in this subtype, this has served as a useful indicator to perform additional FISH studies to detect *TCF3-HLF*-positive A*LL*. Thus, detection of VNN2 by flow cytometry will provide a convenient and cost effective approach to select ALL cases for specific genetic testing of the *TCF3-HLF* translocation.

Prospective pilot evaluation of VNN2 as leukemia-associated marker

To obtain a first indication of the frequency of VNN2 positivity in ALL, we included VNN2 in the diagnostic flow cytometry panel of the Swiss national reference center for the clinical study AEIOP-ALL-BFM-2009 (NCT01117441). Since April 2012 we included this marker for 158 patients and could detect 8 (5%) positive cases (Table 1). We confirmed a *TCF3-HLF* translocation in one case within less then 48 hours based on this new workflow. This has clinical implications given the importance to individualize treatment upfront for this ALL subtype at urgent need for new treatment options. For *TCF3-HLF* negative but VNN2 positive cases, no other recurrent genomic lesion could be identified. Extensive genomic studies will be required to clarify the driver mutations that cause this phenotype.

Higher VNN2 transcript levels and VNN2 detection on ALL cells are associated with a significant increased risk of relapse

Having established that transcript levels correlate with protein detection by flow cytometry, we performed a retrospective analysis on a selected cohort of 663 pediatric ALL patients that were treated on the ALL-BFM-2000 protocol (3, 9). Quantitative PCR could be performed on n=209 SR-ALL, n=345 IR-ALL and n=109 HR-ALL

cases in this retrospective cohort (Figure 2A, Supplementary Table 3). A striking observation was that very high levels of VNN2 transcripts were mostly detected in IR and HR ALL. Moreover, levels were higher on average in IR-ALL (1,076 ± 0.1522, average ± standard deviation; p-value 0.0073) and HR (2,502 + 0.6765, average ± standard deviation; p-value 0,0001) patients compared to SR-ALL (0,5409 ± 0.0444, average ± standard deviation). To explore the relevance of this observation with respect to outcome we determined a threshold to define a VNN2 high subclass using a univariate Cox model. Using a training set, a threshold value was determined for VNN2 expression corresponding to a normalized delta CT value of 1.13 (Figure 2A, dashed line), this parameter was validated in the second part of the cohort (Supplementary Figure 8). Using this threshold, 57% if HR-ALL, 27% of IR ALL and 12% of SR-ALL were defined as positive. The median event-free survival probability of VNN2-high ALL was significantly lower than the EFS of the rest of this cohort (Supplementary Figure 8), EFS n=99, 34 event vs. n=377, 60 events respectively, p= 0,0001). The strongest effect was seen in the IR-ALL subgroup (Figure 2B, p=0.0089), and in the SR group p=0.0019, (Supplementary Figure 9A). Interestingly in HR-ALL, VNN2-high cases did not experience more relapse than the remainder of the HR patients in this cohort (p=0.49, Supplementary Figure 9B). The HR-ALL group is stratified to receive more intensive post-induction chemotherapy on the ALL-BFM-2000 protocol. Based on this observation it is possible that treatment intensification will not be of benefit for this group of patients and that a better understanding of the underlying biology will be require to inform clinical strategies.

VNN2 is expressed at different levels by normal lymphocytes and myeloid cells (Supplementary Figure 2), therefore flow cytometric analysis is required to specifically assess the expression of VNN2 by blasts. In our retrospective gene expression analysis, the blast percentage in the sample was not detected as a confounder (Supplementary Table 3). We next set out to explore whether VNN2 detection by flow cytometry could provide a more stringent identification of ALL cases at risk with a retrospective pilot experiment. We retrieved frozen samples from 42 cases that were defined as positive based on RNA expression data and analyzed surface VNN2 expression by flow cytometry gating on viable cells after thaw.

To define positivity, we used the approach that was developed by an international task force for immunophenotyping of ALL at diagnosis ((18) and Supplementary Figure 4). Frequency of the VNN2 positive cells is defined respect to control, preferably Fluorecence Minus One (FMO) tube, since internal cross-lineage $CD45^{bright}CD19^{negative}$ control can express low level of VNN2. Samples with a frequency of VNN2 positive cells higher than 10% were considered positive. The workflow and proportion of samples that could be included in the analysis are summarized in the Supplementary Figure 10. From 42 samples that could be retrieved in this approach, 21 were VNN2 positive by flowcytometry. The event free survival of this group of VNN2 positive ALL was then compared to the group of patients in the same cohort that was defined as VNN2 low based on gene expression data (Figure 2C). 30% of the VNN2 positive samples relapsed. Multivariable analysis of clinical and other genetic markers confirmed that detection of VNN2 by flow cytometry was significantly associated with poor prognosis independently from other factors that are know to predict adverse outcome (Table 2). Indeed, age (p=0.038), whole blood count (p=0.00013), Central Nervous System (CNS) infiltration (p=0.0092), response to prednisolone (p=0.00019) and risk group (p=0.00009) and risk of MRD (p=0.0008) were related to the expression of VNN2. Importantly this effect was independent from the rearrangements of *CRLF2* (p=0.8), which was reported by several groups to be associated with relapse, in particular in IR-ALL. This data indicates that inclusion of VNN2 in diagnostic flow procedures should identify a relevant subgroup of patients for further biological studies and prospective validation of the prognostic significance of this marker.

VNN2 is detected more frequently in relapsed ALL

To investigate whether VNN2 protein expression or leukemic clones VNN2 positive are preserved or enriched upon disease progression, we evaluate by flow cytometry the expression of VNN2 in xenografts derived from paired samples taken at diagnosis and after treatment. Interestingly, VNN2 expression is conserved or even increased over disease progression (Figure 3).

This evidence was confirmed analyzing transcript level of ALL patients derived of an independent cohort of samples, Supplementary Figure 11. As suggested also by the xenograft model, Supplementary Figure 6, in

which VNN2 expression is conserved over serial transplantation, VNN2 is an intrinsic feature of resistant ALL, independently by the microenvironment that likely give a clonal advantage.

VNN2 contributes to leukemia trafficking

Members of the vanin family of proteins have been implicated in leukocyte trafficking and inflammation (12, 19). Furthermore, interference with VNN2 affects the function of fetal hematopoietic stem cells (10). To establish a possible role of VNN2 in the interaction of the leukemia cells with different hematopoietic compartments we investigated the effect of VNN2 blockade with a specific antibody on homing to different sites of leukemia involvement in the xenograft model. We compared the effect of a blockage using either the anti-VNN2 Ab or an anti-CD19 Ab, in order to rule out unspecific effects due to coating of the cells with immunoglobulin, such as more rapid clearance by phagocytic cells. The anti-CD19 antibody was chosen as control because of its ability to bind cells without induction of apoptosis and without impairing the homing of precursor-B cell ALL. After incubation *in vitro* with antibodies, cells were transplanted by intravenous injection and the animals were sacrificed after 4 hours for analysis of the bone marrow, spleen and peripheral blood involvement by flow cytometry (Figure 4 and Supplementary Figure 12). Comparable results were obtained when the *in vivo* homing experiment was performed at two different time points, 4 and 16 hours (data not shown), for one VNN2 positive case. Because of the smallest variation further experiment were performed at 4 hours. Repopulation of the bone marrow and the spleen was less effective for VNN2-positive ALL after incubation with anti-VNN2 antibodies specifically compared to the controls incubated with anti-CD19 treated cells (p-value <0.05). Anti-VNN2 treatment did not interfere with repopulation of bone marrow and spleen for the two VNN2-negative leukemias that we tested (Figure 6 B). Binding of VNN2 by the antibody was controlled using a secondary antibody after the in vitro incubation step and at the time of harvest (Supplementary 13). We also show that VNN2 treatment did not result in increased apoptosis in these experiments (Supplementary 14). Collectively our results indicate that VNN2 is not only a marker for more unfavorable disease but must have important functions for the disease. Follow-up experiments are warranted to clarify the underlying genomic alterations leading to this phenotype and address the function of VNN2 in leukemogenesis. The data reported here amply justify to initiate prospective follow-up clinical studies to confirm the prognostic significance of this marker and to address the underlying biology.

MATERIAL AND METHODS

Patient samples

All patients were enrolled in multicenter trials on treatment of pediatric ALL conducted by individual member groups of the International BFM-Study Group 2000 (I-BFM-SG): the AIEOP-BFM study group (Austria, Germany, Italy, Switzerland), the FRALLE study group (France), and the United Kingdom (UK) National Cancer Research Institute (NCRI) Childhood Cancer and Leukaemia Group. (3, 20) Relapse samples were included in the BFM Study Group 2002 (ALL-REZ-BFM). For all patients informed consent in accordance with the Declaration of Helsinki and ethics commission of the University of Zurich was obtained. Diagnostic samples were classified as standard risk (SR), intermediate risk (IR), high risk (HR) and very high risk (VHR) of relapse according to the clinical criteria used in ALL-BFM 2000 (7, 21). Briefly, SR patients are prednisone good responders (PGR) and have a negative Minimal Residual Disease (MRD) at time point 1 (TP1, day 33); intermediate risk are also PGR and MRD low positive (<10-3) at TP2 (week 12). Finally, the VHR patients are prednisone poor responders (PPR) and/or have MRD at TP2 of ≥10- 3 and/or presence of one of the following chromosomal rearrangements: *BCR-ABL* or *MLL-AF4*. Samples from morphological non-responder patients (MNR) were obtained at relapse on the ALL-REZ-BFM 2002 study.

Xenograft model

Primary ALL cells were recovered from cryopreserved samples and transplanted intrafemorally to NSG mice as previously described (Schmitz, 2011). Leukemia progression in the peripheral blood was monitored by flow cytometry with rat anti-mouse CD45, mouse anti-human CD45, and mouse anti-human CD19. Animal experiments were approved by the veterinary office of the Canton of Zurich, Switzerland. Approval for

experiments with human samples in the mouse xenograft model was obtained from the ethics commission of the Canton Zurich (approval number 2014- 0383).

Cell isolation and cryopreservation

Mononuclear cells (MNCs) were isolated by Ficoll-Paque gradient centrifugation (Pharmacia, Freiburg, Germany) from bone marrow of the patient and peripheral blood of healthy donors.

Xenograft material was harvested from the spleen of engrafted NSG mice and red blood cells were eliminated by lysis. For cryopreservation, cells were frozen in FBS heat inactivated with 10% dimethylsulfoxide and subsequently stored in liquid nitrogen.

Immunophenotyping

Immunophenotyping of xenograft-amplified human ALL cells after recovery from the spleen was performed with anti-human CD10 (APC, Ref 312210, BioLegend), CD19 (PeCy7, Ref 25-0198-42, eBioscience), CD20 (APCH7, Ref 641396, BD Biosciences), CD34 (PerCpCy5, Ref 347222, BD Bioscience), CD45 (Pacific Orange, Ref MHCD4530, Invitrogen), CD38 (FITC, Ref 303504, BioLegend), VNN2 (PE, Ref D087-5 MBL) and anti mouse CD45 (eFluor®450, Ref 48-0451-82, eBiosciences). In in vivo experiments CD19, CD45, CD10, VNN2 and mCD45 markers were used to identify leukemia cells. Unstained or Fluorescence Minus One samples (FMO, sample stained with all antibodies in the panel except VNN2) was included as negative control. Most of the xenograft were constitute by 95% of human leukemia cells.

For ALL cell viability analysis, 7-AAD (BD Pharmingen™, Cat No 51-68981E, BD Biosciences) and counting beads (Spherotech Inc., Cat No ACBP-70-10, SPHERO™ Accu Count Blanc Particles) were used.

Data acquisition was performed using BD FACS Canto II (BD Biosciences) and analyzed using FACSDiva version 6.1.2 (Becton Dickinson) or FlowJo version 7.1.6 (TreeStar) software. VNN2 signal was scored comparing to the FMO or unstained negative control for each sample. The frequency of VNN2 positivity was evaluated based on the standard operating procedure of AIEOP-BFM ALL Immunophenotyping Consensus Guidelines version 1.6.2 of January 16, 2013. A frequency of VNN2 positive cells higher than ≥10% respect to the control was considered as positive for VNN2. Positive samples are further classified as weak positive if the percentage of the positive population is between 10 to 50 %, and strong positive if higher than 50%.

Cell culture

Jurkat cell were cultured in RPMI 1640 medium supplemented with 10% heat-inactivated fetal bovine serum (FBS h.i.); L-glutamine (2 mM), penicillin/streptomycin (P/S; 100 IU/ml) and kept in the incubator at 37°C, 5% CO2

Transfection

Transient overexpression of VNN2 in Jurkat cells was obtained cloning VNN2 in the p-CMV-VNN2-CF plasmid (Invitrogen) with and without FLAG and transfecting Jurkat cells by electrophoresis (Neon system Invitrogen) according to the standard protocol.

RNA extraction and Reverse Transcriptase

Total RNA was isolated with Trizol reagent and subsequently with RNeasy® Mini Kit (Cat No 74106, Qiagen) according to standardized protocols. The amount and quality of the extracted RNA was measured with a Spectrophotometer (Nanodrop® ND-1000). RT-PCR was performed using 10xRTbuffer (P/N 4319981, Applied Biosystems), 25xdNTP (P/N 362271, Applied Biosystems), 10xRT Random Primer (P/N 4319979, Applied Biosystems), Multiscribe Reverse Trascriptase (P/N 4319983, Applied Biosystems), Rnase inhibitor (P/N N808-0119, Applied Biosystems) and Rnase free H20. This mix with the equal volume of RNA (1000ng of RNA for each PCR reaction) was process according tot he following protocol: Preheating: 25°C/10min, Synthesis cDNA: 37°C/120min, RT inactivation: 85°C/5s.

Quantitative PCR

TaqMan Gene Expression Assays were used to measure mRNA abundance of VNN2, with SDHA as control gene. The TaqMan® Gene Expression Master Mix (P/N 4369016, Applied Biosystems, Foster City, USA), the assay on demand (TaqMan® Gene Expression Assays, Hs01546812_m1 VNN1, Hs00190581_m1 VNN2, Hs00417200_m1 SDHA, Applied Biosystems) and water were mixed (5:3:2) are mixed and cDNA (1:3 dilution) added. The same was done with a Sybrgreen assay for VNN2 and SDHA as housekeeping gene (QuantiTect SYBR® Green PCR Kit, Power SYBR®Green PCR Master Mix, P/N 4367659, Applied Biosystems, Quantitect® Primer Assay, Hs_VNN2_1_SG, Cat No QT00034902 and Hs_SDHA_1_SG, Cat No QT00059486, Qiagen).

For both methods, iScience, 7900HT, Fast Real-Time PCR-System, from Applied Biosystems was used. Program: 2min 50°C, 10min 95°C, 50x(10sec 95°C/1min 60°C) Analysis was performed with SDS 2.2 software, calculating the $\mathbf{2}^{-\Delta CT}$ value. nature protocol thomas D schmittgen livak

***In vivo* experiment**

ALL cells were recovered from cryopreserved xenograft samples and incubated at 37°C for 20min Survival rate after thawing was ≥60%. Cells were blocked for 1hour at 37°C with 1mg/mL of either anti-VNN2 antibody (VNN2, Ref D087-3, MBL) or anti-CD19 antibody (LEAF™Purified anti-human CD19, clone HIB19, BioLegend). Blocked cells were transplanted in 6 mice each group. 10,000,000 cells per mouse were injected in the tail vein of 12 NSG mice with similar weight and age. 4h after transplantation, bone marrow, spleen and the peripheral blood were examined for the presence of leukaemia cells using flow cytometry. A secondary antibody (Goat F(ab') 2 Anti-Mouse Ig-FITC, Human, Cat No 2012-02, Southern Biotech) was incubated for 10min at 4°C, after washing 1ug/ml IgG of mouse was added, left for 5 min and the samples stained with CD19, CD45, CD10, mCD45, VNN2 and 7-AAD. The number of human $hCD45^{+}hCD19^{+}hCD10^{+}mCD45^{-}$ leukemia cell was normalized for the total number of lymphocytes acquired.

Statistics

VNN2 threshold based on Sybrgreen PCR values was defined dividing the 663 ALL patients included in the I-BFM –SG in Germany, in a training set (1/3 of the patients) and a test set (2/3). Definition of the VNN2 threshold associated with higher risk of relapse was identified based on the lowest p-value in a univariate Cox model in the training set. This threshold was used for dichotomizing the patients in the test set. For the definition of VNN2 high and low cases in the Swiss and Austrian cohort (n=113) screened by TaqMan, average + standard deviation of the values of the $\mathbf{2}^{-\Delta CT}$ of the SR cases was used. $\Delta Ct=Ct_{VNN2}-Ct_{SDHA.}$

Samples included in the I-BFM –SG with $\mathbf{2}^{-\Delta\Delta CT}> 1.13$ (cut off VNN2 transcript level predictive of relapse) and in the Swiss –Austrian –SG with $\mathbf{2}^{-\Delta CT}>$ X (Average + SD of $\mathbf{2}^{-\Delta CT}$ values of SR cases) were Tested by flow cytometry based on sample availability.

All statistical tests were performed using Graph Pad Prism version 5.0 (Graph Pad Software).

DISCUSSION

To improve therapeutic options for patients with resistant disease additional biomarkers are required to precise leukemia classification already at diagnosis. Here we report converging evidence that supports an association of the glycosylphosphatidyinositol-anchored surface protein VNN2/GPI80 with ALL subtypes that are more resistant to current chemotherapy. We identified VNN2 to be preferentially detected in the cell surface proteome of leukemia that were highly resistant to induction chemotherapy based on the persistence of high levels of minimal residual disease. In a retrospective analysis of selected cohorts of ALL patients with high risk, intermediate risk and low risk of relapse per current clinical stratification methods, we detected a significant correlation of VNN2 expression levels or detection by flow cytometry with relapse. Importantly, VNN2 expression identified patients at risk of relapse in the intermediate risk group, which still constitutes the group with the largest number of relapses in ALL but for which currently no alternative markers have been defined. We also found VNN2 to be detected more frequently at relapse, which indicates that VNN2 expression is associated with more aggressive disease features. Interestingly, VNN2 expression was associated with other standard clinical features of high risk ALL, including high white blood cell count (p=0.00013), CNS infiltration

(p=0.0092), poor response to prednisolone (p=0.00019), and detection of MRD (p=0.0008). Thus, this marker may reflect a more general mechanism of resistant disease.
Indeed, VNN2 was recently identified as a marker of human fetal hematopotietic stem cells based on transcriptome analysis of sorted human fetal hematopoietic cells (10). VNN2 detection by flow cytometry identifies a stem cell population in different stages of fetal hematopoiesis (placenta, fetal liver, fetal bone marrow). Sorting this subset of stem cells enriches for hematopoietic repopulation capacity in xenograft experiments. RNA interference with VNN2 affected proliferation of this stem cell fraction in co-cultures in vitro as well as engraftment in vivo, indicating that VNN2 has important functional roles at these early hematopoietic stages. VNN2 has been implicated in leukocyte adhesion and migration (12, 22) possibly by interaction with other cell surface receptors including ITGAM1. Association with ITGAM was also detected in fetal hematopoiesis and in our proteomic dataset in ALL. ITGAM (CD11b) has been described as a leukemia associated marker on MRD cells (23). However we did not detect universal co-expression of VNN2 and ITGAM by flow cytometry in VNN2 positive ALL (data not shown), suggesting that underlying mechanism may be more complex. VNN2 expression was maintained in serial passages in xenograft experiments, indicating that this expression pattern is a stable feature, driven by mechanisms that are intact in the xenograft setting. Anti-VNN2 antibodies interfere with homing to ALL cells to the spleen and to the bone marrow in a VNN2 specific manner. Thus, VNN2 could play an important functional role in ALL as well, possibly by affecting tissue invasion or trafficking properties. We also detected the vanin-family member VNN1 in the surfeasome of VHR-ALL more frequently. Experiments with Vanin1 deficient mice show that this protein is involved in inflammatory reaction and stress response pathways (24). Thus display of vanin family members in more resistant ALL cases could reflect the activation of cellular programs that are also required in early stages of hematopoiesis.

Based on current evidence, VNN2 may serve as an indicator of more aggressive disease. A preliminary analysis of systematic prospective detection by flow cytometry in ALL indicates that VNN2 is detected in about 10 percent of all cases. In a smaller subset of these patients, VNN2 is detected strongly but the value of this observation remains to be evaluated prospectively. These included one case with *TCF3-HLF*-positive ALL, a rare but mostly fatal subtype of ALL (our nature genetics, references), which fits to an expected frequency of this subtype between 0.5-1 % of childhood ALL. The translocation t(17;19) can be cryptic and difficult to detect by routine cytogenetics. Our studies show consistently very high VNN2 expression in *TCF3-HLF*-positive ALL. The detection of VNN2 by flow cytometry, helps preselect samples for specific diagnostic testing for this rare and highly aggressive disease.
Given that we detected VNN2 uniformly in a larger series of *TCF3-HLF*-positive ALL cases, flow cytometry for VNN2 provides a simple and economical way to preselect leukemia for further genetic assays. The correct diagnosis of this subtype is very relevant for clinical management, because these patients are likely to not benefit from current conventional chemotherapy (17) and should be offered alternative treatment options to bridge them towards stem cell transplantation, including immunotherapy. We recently obtained full molecular remission using blinatumomab in a patient who was refractory to the first induction chemotherapy (unpublished observation). As such inclusion of VNN2 in diagnostic FACS panel appears justified.

Our retrospective analysis indicates that the more frequent non-*TCF3-HLF* translocated VNN2 positive cases also have a significant risk of relapse. A systematic prospective study has been initiated including VNN2 as a marker in diagnostic immunophenotyping of patients that are enrolled on the AEIOP-BFM-ALL-2009 protocol, first in the Swiss national reference laboratory and more recently internationally. Because VNN2 is implicated at different stages in hematopoiesis, both in stem cells and fully differentiated myeloid cells (10, 22), the best approach will be to detect VNN2 at a single cell level by flow cytometry. We validated two independent monoclonal antibody clones and established criteria for gating according to standards of our international working group ((25) and manuscript in preparation). To establish the threshold for positivity in this prospective study we will compare to controls with the same backbone of antibodies but omitting the VNN2 antibody. It will be important to carefully analyze the overlap of VNN2 surface expression with other biomarkers. Based on current data, we did not see an association with cytogenetic risk factors that are routinely detected at diagnosis, including MLL rearrangement, nor did we detect an overlap with the so-called 'switch'-ALL

phenotype that has been reported most recently and describes a subset in ALL with lineage switch to myelomonocytic features and typical expression of surface CD2 (26). The current size of our prospective data is too limited to study association with more complex patterns copy number alterations, including deletions of *IKAROS*, that have been demonstrated to be associated with an increased risk of relapse (27-29). It will also be important to evaluate an association with activation mutations in tyrosine kinases that are enriched in patients with high risk ALL (30) for which retrospective data are currently not available.

Taken together, we show here that VNN2, a marker of the fetal hematopoietic 'stemness', can be used to detect ALL subtypes with an unfavorable biology and worse outcome on current therapeutic modalities, including the deadly subtype of *TCF3-HLF*-positive ALL. Our experiments show that VNN2 plays a role in leukemia propagation by contributing to leukemia homing to different sites of involvement. Our data provide a basis for prospective clinical studies as well as for the interrogation of underlying drivers of VNN2 and its functional role in leukemia.

FIGURE LEGENDS

Figure 1. Transcript levels of VNN2 correlate with higher risk of relapse in B-cell precursor ALL

A) Comparison of cell surface proteomes of 8 very high-risk (VHR) and 11 standard-risk (SR) BCP-ALL. The surfaceome dataset was filtered in two steps, first for peptides that match to proteins that were detected in at least 50% of VHR-ALL cases and in less than 25% of SR-ALL cases, second by selecting peptides more stringently that were present in at least 75% of VHR-ALL and in less than 25% SR-ALL or in 60% VHR-ALL and less than 18% SR-ALL. Proteins are displayed based on functional annotation. **B)** Correlation of transcript and protein level in patients derived xenografts (PDXs) from patients that were risk stratified according to the criteria used in the ALL-BFM 2000 protocol. Standard risk (SR) are indicated in green (n=12), intermediate risk (IR) in orange (n=10), and high risk (HR/VHR) in turquoise (n=16). Four of the HR/VHR cases were *TCF3-HLF*-positive and are depicted by a square. The percentage of VNN2 positive cells by flow cytometry is plotted on the Y-axis against the mRNA levels by Q-PCR as logarithmic value of $2^{-\Delta Ct}$ ($\Delta Ct=Ct_{VNN2}-Ct_{SDHA}$) on the X-axis. **C)** Strong detection of VNN2 on 10 samples from *TCF3-HLF*-positive patients (7 PDXs in the upper panel, 3 primary diagnostic samples in the lower panel). The fluorescence minus one control is shown as grey histogram. **D)** transcriptome data corresponding to the genes identified in A. RPKM values are displayed as a heatmap.

Figure 2. Surface VNN2 detection is associated with resistant disease in ALL

A) VNN2 mRNA expression of 663 ALL patients, SR (n=209), IR (n=345), HR (n=109). VNN2 mRNA is presented as logarithmic value of $2^{-\Delta\Delta Ct}$ ($\Delta Ct=Ct_{VNN2}-Ct_{SDHA}$) normalized for a reference sample with lowest VNN2 expression. **B)** Event Free Survival (EFS) analysis of a retrospective cohort of samples from patients with intermediate risk (IR) ALL. A threshold was defined with a test set on the entire cohort of 663 patients. The probability of EFS is displayed for 195 patients with VNN2 expression less than 1.13 and 52 patients more than 1.13 normalized deltaCT value. Log Rank p 0.0089. See also Supplementary Figure 9 for the analysis of the entire cohort and other risk groups. **C)** Pilot evaluation of VNN2 detection by flow cytometry based selection of cryopreserved samples from a retrospective cohort including the 663 cases above and 113 additional cases from Switzerland and Austria. The strategy for sample selection is outlined in Supplementary Figure 4. From 12 samples that were confirmed to be VNN2 positive by flow cytometry 6 patients had an event. The probability of EFS is compared to samples with VNN2 transcript levels lower than 1.13 deltaCT values. Log Rank p 0.0029.

Figure 3. VNN2 positive clones are preserved or enriched during disease progression

A) VNN2 expression flow cytometry analysis of pair diagnostic and relapse samples (n=7). MFI are plotted. **B)** Representative expression of VNN2 at diagnosis (Dx) and relapse (R).

Figure 4. VNN2 blockade reduces homing ability to bone marrow and spleen of VNN2 positive leukemia

A) Homing assay was performed with patient derived xenograft cells recovered after thawing. Subsequent blocking with anti-VNN2 and anti-CD19 antibody was performed for 1 hr at 37°C 5% CO_2. 10.000.000 of cells were intravenously injected in 6 NSG mice per condition. Leukemia cell number in bone marrow, spleen and blood was measured after 4 hrs from the injection by flow cytometry. Dot plots represent the number of leukemia cells defined as $hCD45^{+}hCD19^{+}mCD45^{-}$ and normalized for the total number of lymphocytes, distinct based on FCS ad SSC. VNN2 positive leukemia samples **(B)** and leukemia samples with undetectable level of VNN2 protein based on flow cytometry data **(C)** were tested. Error bars represent mean ± SEM. Significant difference between anti-VNN2 and CD19 blocking, p-value<0.05, in VNN2 positive samples.

REFERENCES

1. Hunger SP, Brown R, Cleary ML. DNA-binding and transcriptional regulatory properties of hepatic leukemia factor (HLF) and the t(17;19) acute lymphoblastic leukemia chimera E2A-HLF. Molecular and cellular biology. 1994;14(9):5986-96.
2. Panagopoulos I, Micci F, Thorsen J, Haugom L, Tierens A, Ulvmoen A, et al. A novel TCF3-HLF fusion transcript in acute lymphoblastic leukemia with a t(17;19)(q22;p13). Cancer genetics. 2012;205(12):669-72.
3. Conter V, Bartram CR, Valsecchi MG, Schrauder A, Panzer-Grumayer R, Moricke A, et al. Molecular response to treatment redefines all prognostic factors in children and adolescents with B-cell precursor acute lymphoblastic leukemia: results in 3184 patients of the AIEOP-BFM ALL 2000 study. Blood. 2010;115(16):3206-14.
4. Flohr T, Schrauder A, Cazzaniga G, Panzer-Grumayer R, van der Velden V, Fischer S, et al. Minimal residual disease-directed risk stratification using real-time quantitative PCR analysis of immunoglobulin and T-cell receptor gene rearrangements in the international multicenter trial AIEOP-BFM ALL 2000 for childhood acute lymphoblastic leukemia. Leukemia. 2008;22(4):771-82.
5. Mirkowska P, Hofmann A, Sedek L, Slamova L, Mejstrikova E, Szczepanski T, et al. Leukemia surfaceome analysis reveals new disease-associated features. Blood. 2013;121(25):e149-59.
6. Schrappe M. Minimal residual disease: optimal methods, timing, and clinical relevance for an individual patient. Hematology / the Education Program of the American Society of Hematology American Society of Hematology Education Program. 2012;2012:137-42.
7. Schrappe M, Hunger SP, Pui CH, Saha V, Gaynon PS, Baruchel A, et al. Outcomes after induction failure in childhood acute lymphoblastic leukemia. The New England journal of medicine. 2012;366(15):1371-81.
8. Eckert C, von Stackelberg A, Seeger K, Groeneveld TW, Peters C, Klingebiel T, et al. Minimal residual disease after induction is the strongest predictor of prognosis in intermediate risk relapsed acute lymphoblastic leukaemia - long-term results of trial ALL-REZ BFM P95/96. European journal of cancer. 2013;49(6):1346-55.
9. Schrappe M, Valsecchi MG, Bartram CR, Schrauder A, Panzer-Grumayer R, Moricke A, et al. Late MRD response determines relapse risk overall and in subsets of childhood T-cell ALL: results of the AIEOP-BFM-ALL 2000 study. Blood. 2011;118(8):2077-84.
10. Prashad SL, Calvanese V, Yao CY, Kaiser J, Wang Y, Sasidharan R, et al. GPI-80 defines self-renewal ability in hematopoietic stem cells during human development. Cell stem cell. 2015;16(1):80-7.
11. MILE. Gene Expression Omnibus Accession No GSE132042004.
12. Suzuki K, Watanabe T, Sakurai S, Ohtake K, Kinoshita T, Araki A, et al. A novel glycosylphosphatidyl inositol-anchored protein on human leukocytes: a possible role for regulation of neutrophil adherence and migration. Journal of immunology. 1999;162(7):4277-84.
13. Hunger SP, Ohyashiki K, Toyama K, Cleary ML. Hlf, a novel hepatic bZIP protein, shows altered DNA-binding properties following fusion to E2A in t(17;19) acute lymphoblastic leukemia. Genes & development. 1992;6(9):1608-20.
14. Inukai T, Hirose K, Inaba T, Kurosawa H, Hama A, Inada H, et al. Hypercalcemia in childhood acute lymphoblastic leukemia: frequent implication of parathyroid hormone-related peptide and E2A-HLF from translocation 17;19. Leukemia. 2007;21(2):288-96.
15. Kwon K, Hutter C, Sun Q, Bilic I, Cobaleda C, Malin S, et al. Instructive role of the transcription factor E2A in early B lymphopoiesis and germinal center B cell development. Immunity. 2008;28(6):751-62.
16. Felice MS, Gallego MS, Alonso CN, Alfaro EM, Guitter MR, Bernasconi AR, et al. Prognostic impact of t(1;19)/ TCF3-PBX1 in childhood acute lymphoblastic leukemia in the context of Berlin-Frankfurt-Munster-based protocols. Leukemia & lymphoma. 2011;52(7):1215-21.
17. Fischer. Genomics and drug profiling of fatal TCF3-HLF-positive pediatric acute lymphoblastic leukemia identifies recurrent mutation patterns and novel therapeutic options. Nature genetics2015.
18. Dworzak. manuscript in preparation.

19. Aurrand-Lions M, Galland F, Bazin H, Zakharyev VM, Imhof BA, Naquet P. Vanin-1, a novel GPI-linked perivascular molecule involved in thymus homing. Immunity. 1996;5(5):391-405.
20. Harrison CJ, Haas O, Harbott J, Biondi A, Stanulla M, Trka J, et al. Detection of prognostically relevant genetic abnormalities in childhood B-cell precursor acute lymphoblastic leukaemia: recommendations from the Biology and Diagnosis Committee of the International Berlin-Frankfurt-Munster study group. British journal of haematology. 2010;151(2):132-42.
21. Attarbaschi A, Mann G, Panzer-Grumayer R, Rottgers S, Steiner M, Konig M, et al. Minimal residual disease values discriminate between low and high relapse risk in children with B-cell precursor acute lymphoblastic leukemia and an intrachromosomal amplification of chromosome 21: the Austrian and German acute lymphoblastic leukemia Berlin-Frankfurt-Munster (ALL-BFM) trials. Journal of clinical oncology : official journal of the American Society of Clinical Oncology. 2008;26(18):3046-50.
22. Huang JB, Takeda Y, Araki Y, Sendo F, Petty HR. Molecular proximity of complement receptor type 3 (CR3) and the glycosylphosphatidylinositol-linked protein GPI-80 on neutrophils: effects of cell adherence, exogenous saccharides, and lipid raft disrupting agents. Molecular immunology. 2004;40(17):1249-56.
23. Rhein P, Mitlohner R, Basso G, Gaipa G, Dworzak MN, Kirschner-Schwabe R, et al. CD11b is a therapy resistance- and minimal residual disease-specific marker in precursor B-cell acute lymphoblastic leukemia. Blood. 2010;115(18):3763-71.
24. Berruyer C, Pouyet L, Millet V, Martin FM, LeGoffic A, Canonici A, et al. Vanin-1 licenses inflammatory mediator production by gut epithelial cells and controls colitis by antagonizing peroxisome proliferator-activated receptor gamma activity. The Journal of experimental medicine. 2006;203(13):2817-27.
25. Hrusak O, Basso G, Ratei R, Gaipa G, Luria D, Mejstrikova E, et al. Flow diagnostics essential code: a simple and brief format for the summary of leukemia phenotyping. Cytometry Part B, Clinical cytometry. 2014;86(4):288-91.
26. Slamova L, Starkova J, Fronkova E, Zaliova M, Reznickova L, van Delft FW, et al. CD2-positive B-cell precursor acute lymphoblastic leukemia with an early switch to the monocytic lineage. Leukemia. 2014;28(3):609-20.
27. Moorman AV, Enshaei A, Schwab C, Wade R, Chilton L, Elliott A, et al. A novel integrated cytogenetic and genomic classification refines risk stratification in pediatric acute lymphoblastic leukemia. Blood. 2014;124(9):1434-44.
28. Bourquin JP. The clinical path to integrated genomics in ALL. Blood. 2014;124(9):1380-1.
29. Dagdan E. The Strong Prognostic Effect of Concurrent Deletions of IKZF1 and PAX5, CDKN2A, CDKN2B or PAR1 in the Absence of ERG Deletions (IKZF1plus) in Pediatric Acute Lymphoblastic Leukemia Strongly Depends on Minimal Residual Disease Burden after Induction Treatment ASH 2014.
30. Roberts KG, Mullighan CG. Genomics in acute lymphoblastic leukaemia: insights and treatment implications. Nature reviews Clinical oncology. 2015.

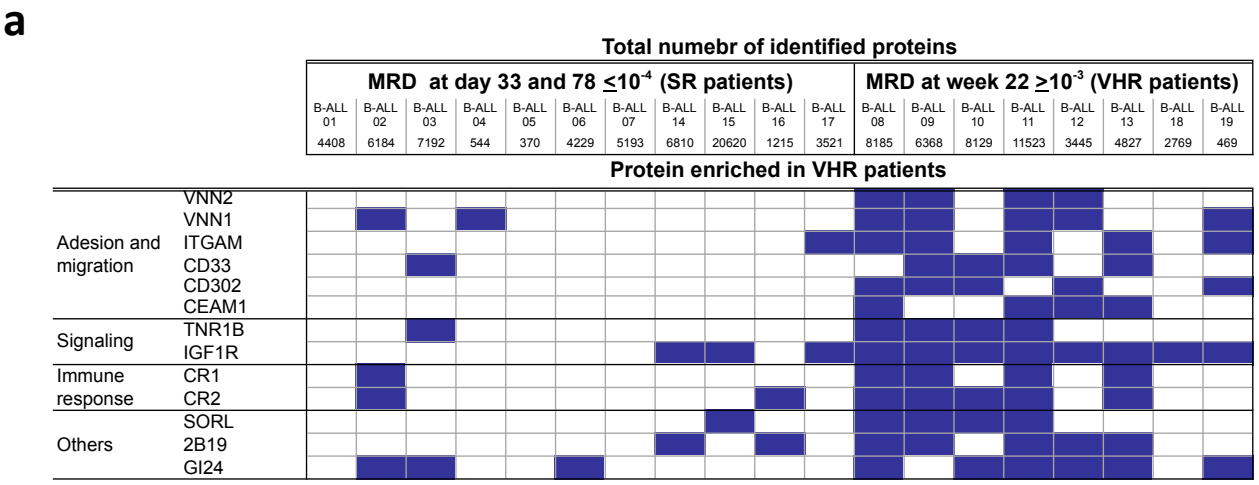
a
Total numebr of identified proteins
MRD at day 33 and 78 ≤10-4 (SR patients)
MRD at week 22 ≥10-3 (VHR patients)
B-ALL 01 4408
B-ALL 02 6184
B-ALL 03 7192
B-ALL 04 544
B-ALL 05 370
B-ALL 06 4229
B-ALL 07 5193
B-ALL 14 6810
B-ALL 15 20620
B-ALL 16 1215
B-ALL 17 3521
B-ALL 08 8185
B-ALL 09 6368
B-ALL 10 8129
B-ALL 11 11523
B-ALL 12 3445
B-ALL 13 4827
B-ALL 18 2769
B-ALL 19 469
Protein enriched in VHR patients
Adesion and migration
VNN2
VNN1
ITGAM
CD33
CD302
CEAM1
Signaling
TNR1B
IGF1R
Immune response
CR1
CR2
Others
SORL
2B19
GI24

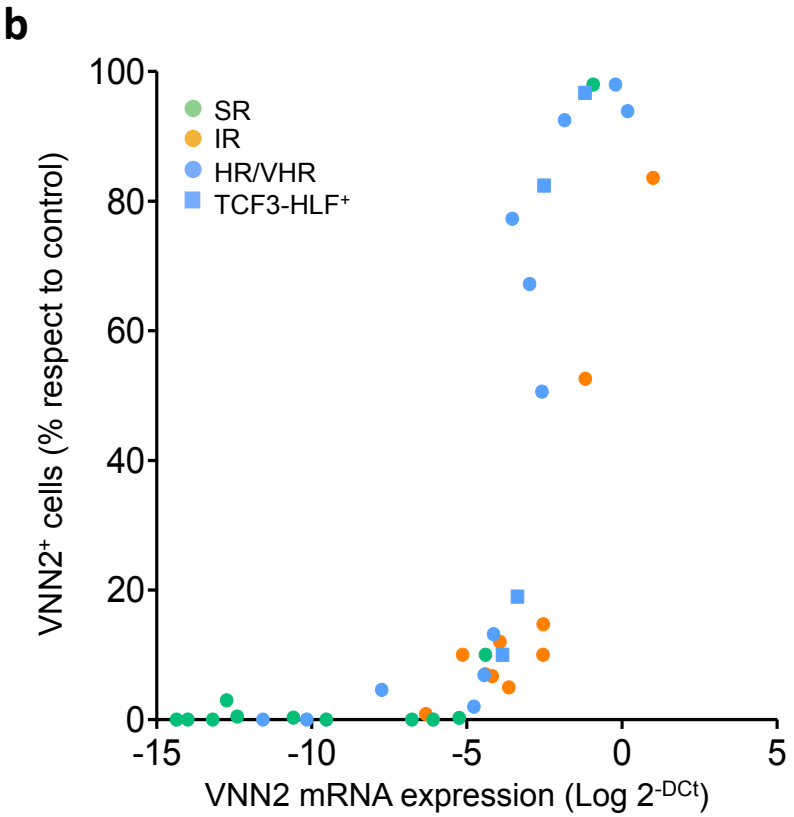
b
SR
IR
HR/VHR
TCF3-HLF+
VNN2+ cells (% respect to control)
VNN2 mRNA expression (Log 2-DCt)

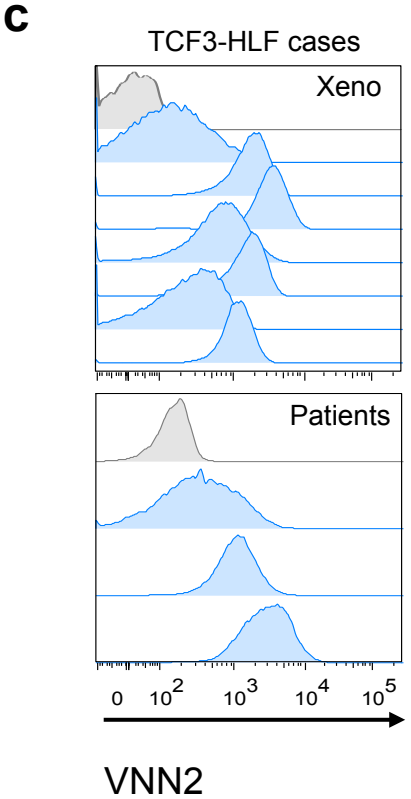
c
TCF3-HLF cases
Xeno
Patients
VNN2

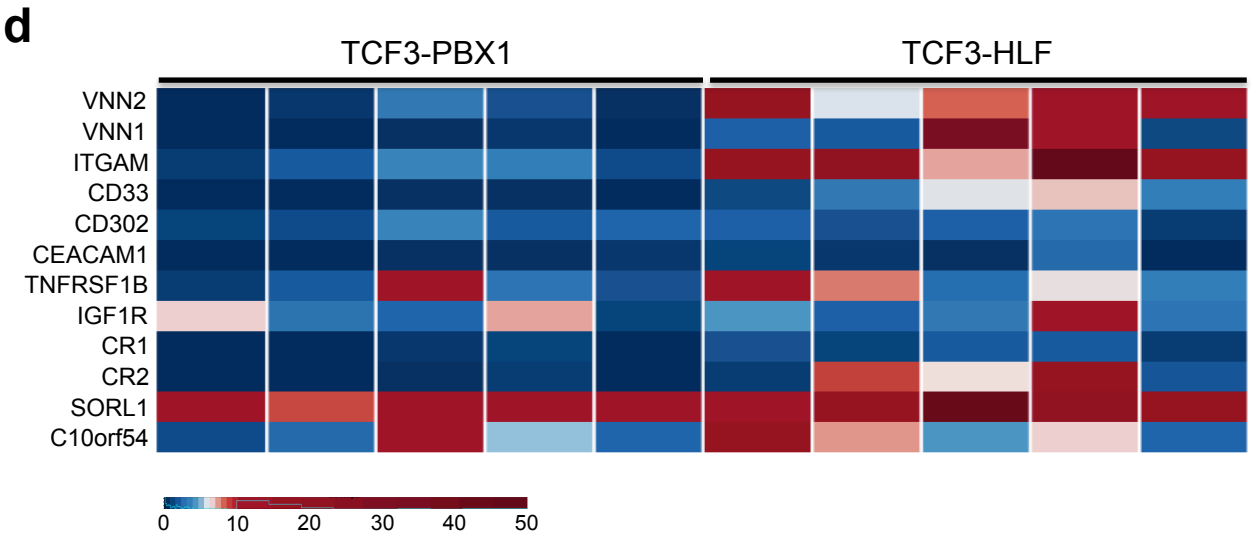
d
TCF3-PBX1
TCF3-HLF
VNN2
VNN1
ITGAM
CD33
CD302
CEACAM1
TNFRSF1B
IGF1R
CR1
CR2
SORL1
C10orf54

Figure 1

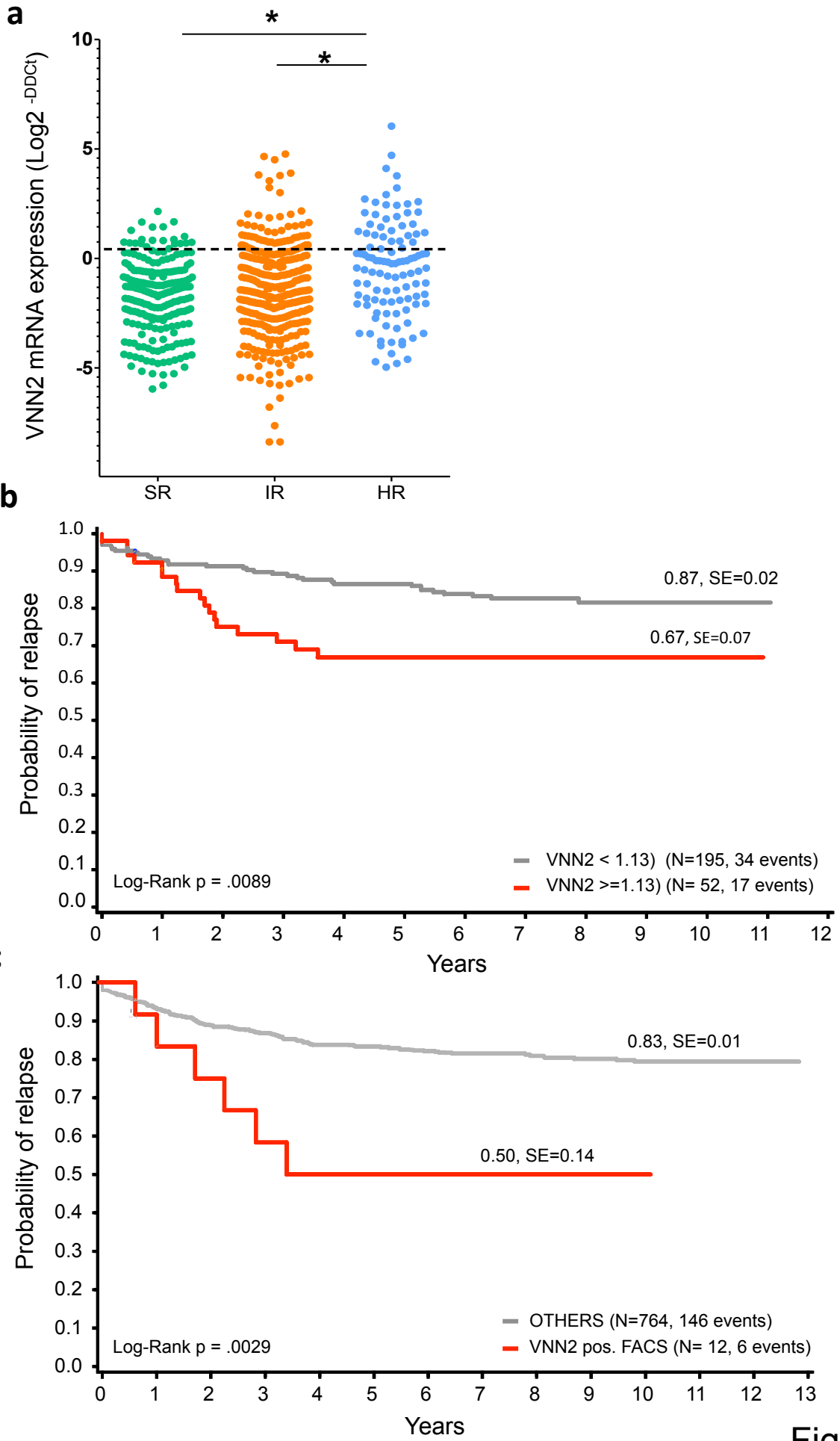
a
*
*
10
5
0
-5
VNN2 mRNA expression (Log2 -DDCt)
SR
IR
HR
b
1.0
0.9
0.8
0.7
0.6
0.5
0.4
0.3
0.2
0.1
0.0
Probability of relapse
0.87, SE=0.02
0.67, SE=0.07
Log-Rank p = .0089
VNN2 < 1.13) (N=195, 34 events)
VNN2 >=1.13) (N= 52, 17 events)
0 1 2 3 4 5 6 7 8 9 10 11 12
Years
c
1.0
0.9
0.8
0.7
0.6
0.5
0.4
0.3
0.2
0.1
0.0
Probability of relapse
0.83, SE=0.01
0.50, SE=0.14
Log-Rank p = .0029
OTHERS (N=764, 146 events)
VNN2 pos. FACS (N= 12, 6 events)
0 1 2 3 4 5 6 7 8 9 10 11 12 13
Years

Figure 2

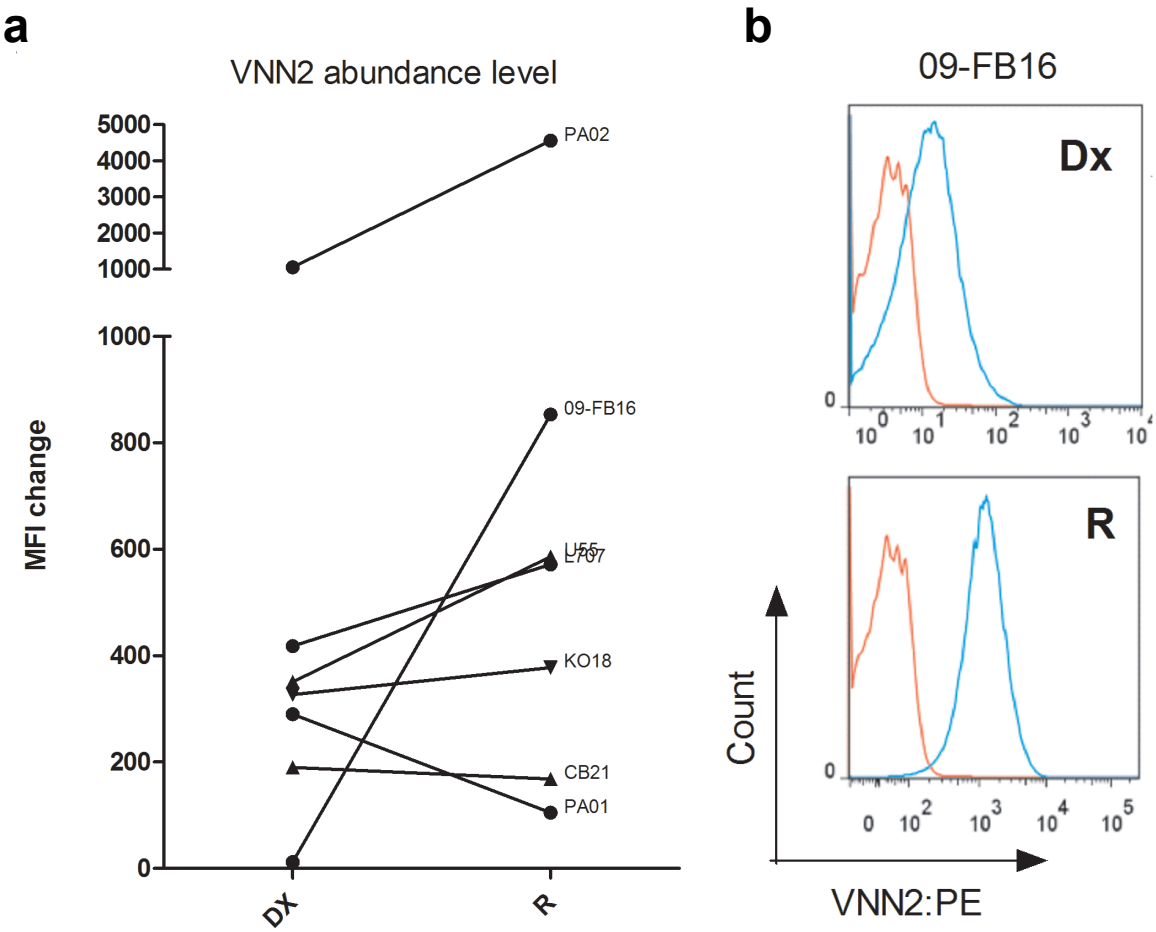
a
VNN2 abundance level
MFI change
5000
4000
3000
2000
1000
1000
800
600
400
200
0
PA02
09-FB16
U55
L707
KO18
CB21
PA01
DX
R
b
09-FB16
Dx
R
Count
VNN2:PE

Figure 3

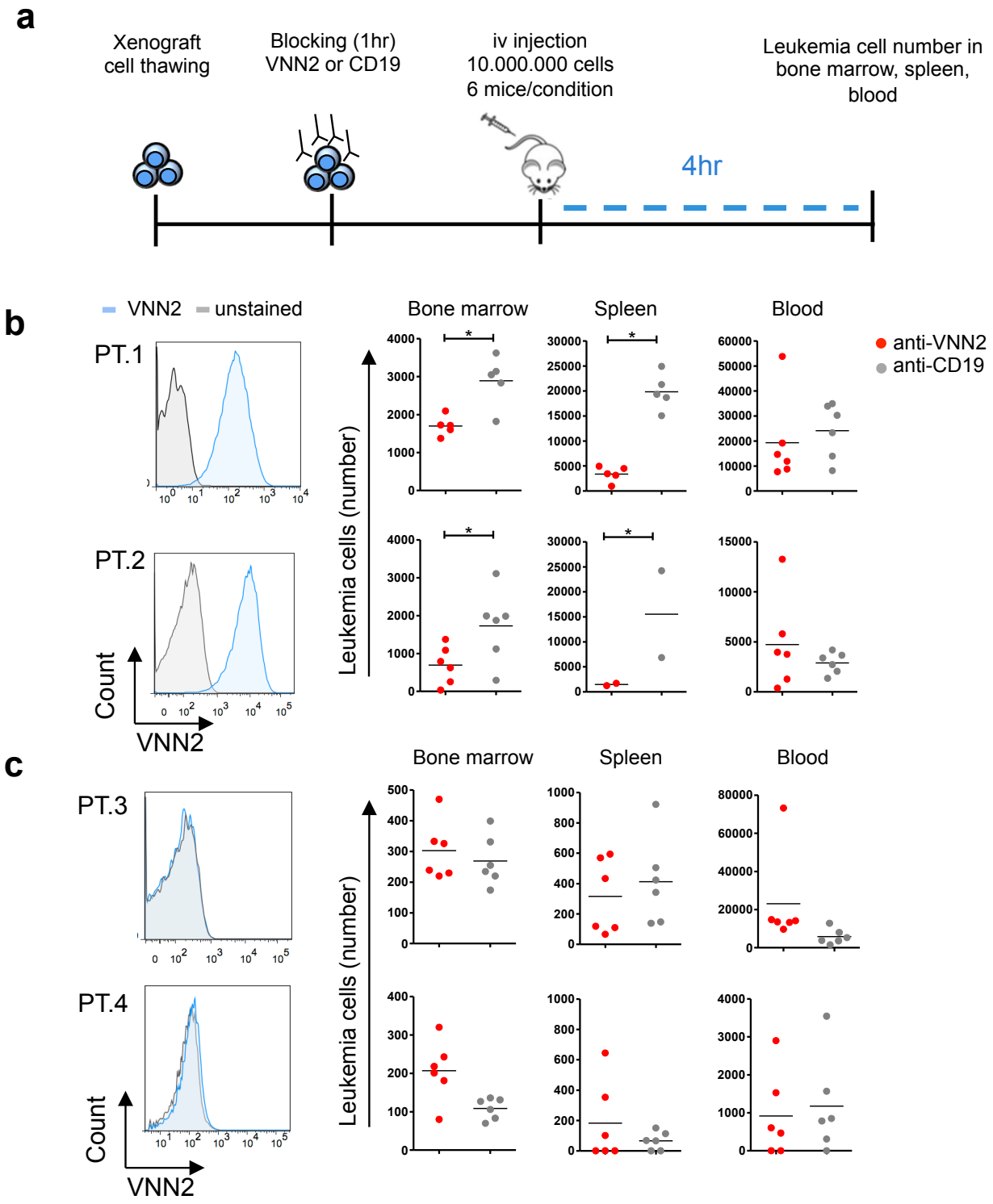
a
Xenograft cell thawing
Blocking (1hr) VNN2 or CD19
iv injection 10.000.000 cells 6 mice/condition
Leukemia cell number in bone marrow, spleen, blood
4hr
b
VNN2
unstained
PT.1
PT.2
Count
VNN2
Bone marrow
Spleen
Blood
Leukemia cells (number)
anti-VNN2
anti-CD19
c
PT.3
PT.4
Count
VNN2
Bone marrow
Spleen
Blood
Leukemia cells (number)

Figure 4

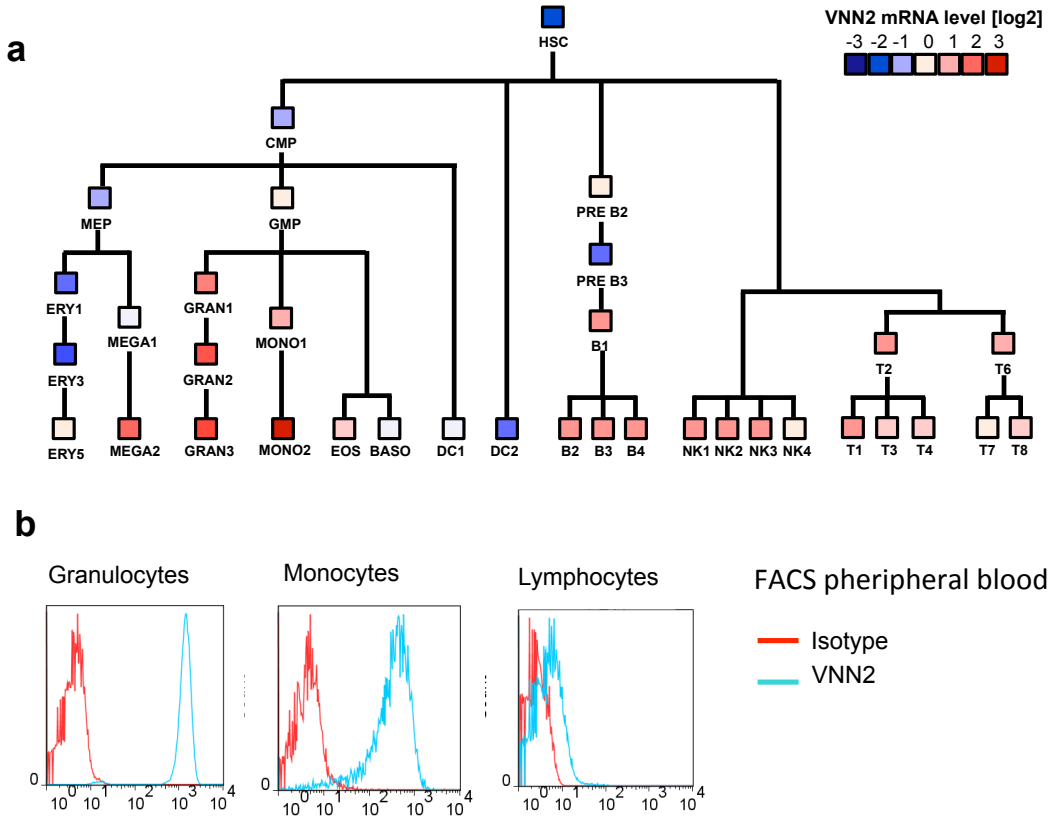

Supplementary Figure 2. VNN2 expression in normal hematopoetic system. a) VNN2 transcript level in different progenitors, DMAP (Novershtern et al, Cell 2011). b) VNN2 protein expression by cells of peripheral blood of healthy donor.

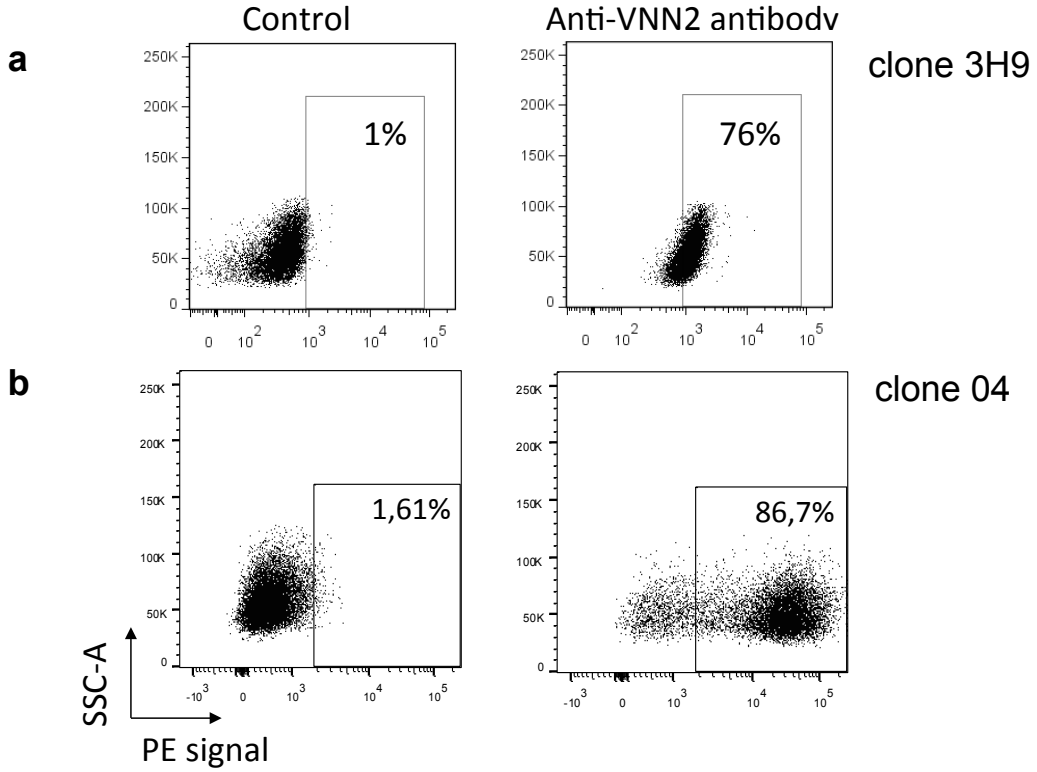

Supplementary Figure 3. Exogenous overexpression of VNN2 in cell line. (A) cDNA of VNN2 human proteins was cloned in the commercial plasmid pCMV with C –terminal flag. Representative FACS of VNN2 expression after 1 week from transfection and 3 days of G418 selection. (B) cDNA of VNN2 human protein was cloned in the commercial pInducer21, an inducible lentiviral plasmid. After transduction, the cells were sorted through the GFP marker and treated with 1000ng/mL of doxycycline (dox). Representative FACS of VNN2 expression after 4 days of dox treatment.

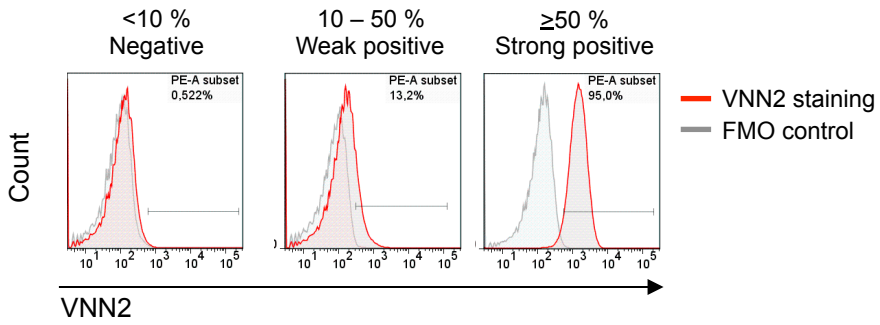

Supplementary Figure 4. Representative FACS analysis of VNN2 signal on leukemia cells according to the criteria define by the AIEOP-BFM Flow Network . Samples with frequency of VNN2 positive cells lower than 10% respect to the control are considered negative of negative for the antigen. Weak positive and strong positive is frequency of VNN2 positive cells is between 10-50% and higher than 50% respectively.

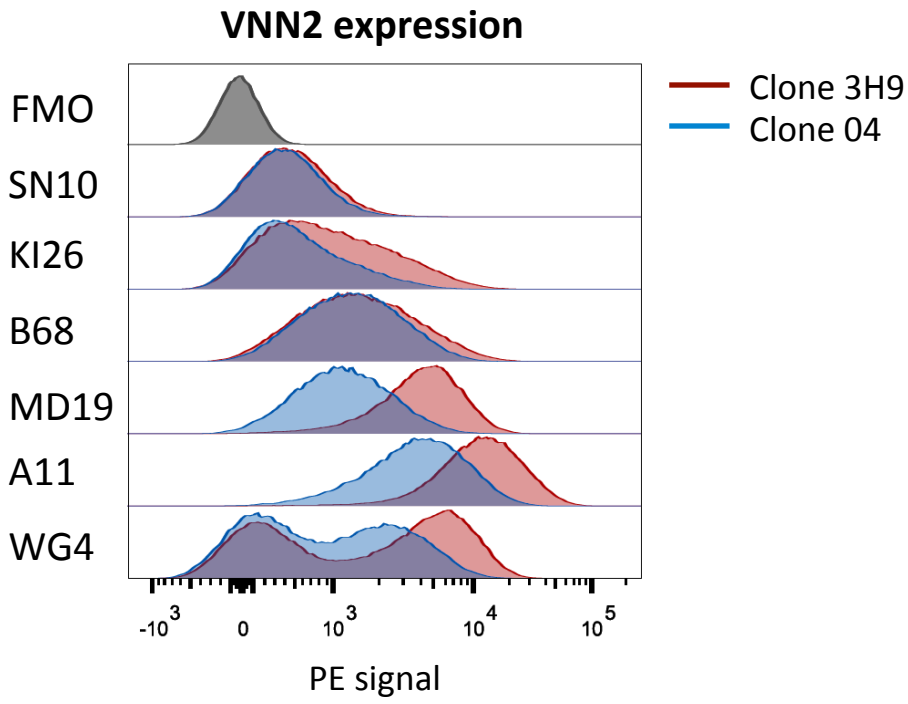

Supplementary Figure 5. VNN2 expression in 6 TCF3-HLF positive ALL patients. VNN2 expression was validated with two anti-VNN2 antibodies (clone 3H9 and 04).

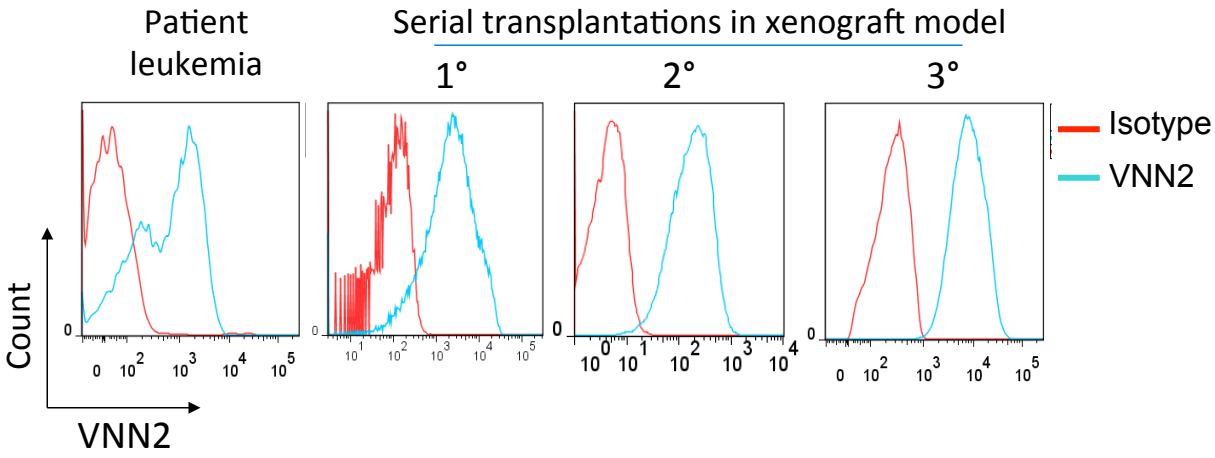

Supplementary Figure 6. VNN2 phenotype is maintained after xenotransplantation and remains stable over several serial transplantations in the xenograft model . This indicates that the underlying mechanism is intrinsic to the leukemia. Representative of X samples tested.

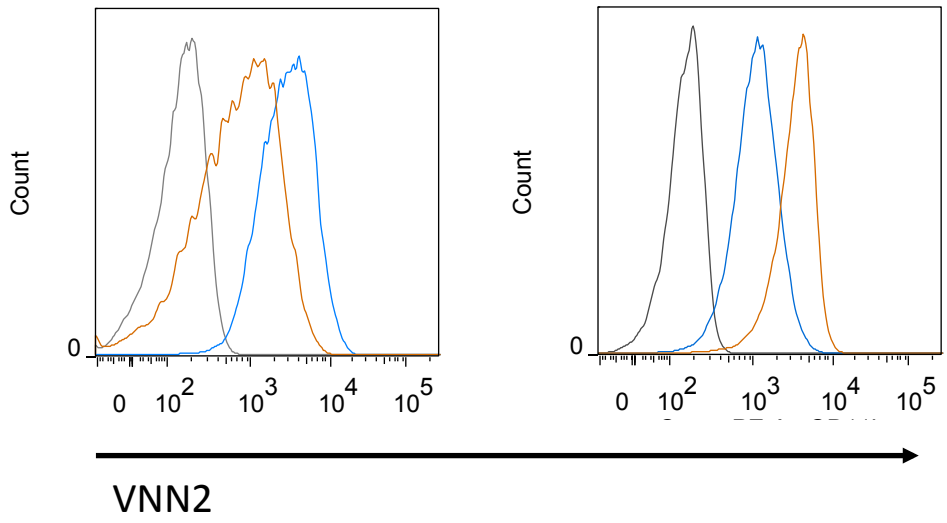

Supplementary Figure 7. Co-expression of VNN2 and ITGAM by 2 TCF3-HLF positive ALL.
Bone marrow cells were analyzed by flow cytomery for the expression of VNN2 (turquoise) and ITGAM (orange) respect to the FMO (fluorescence minus one control)

Scheme: VNN2 identification and clinical relevance validation

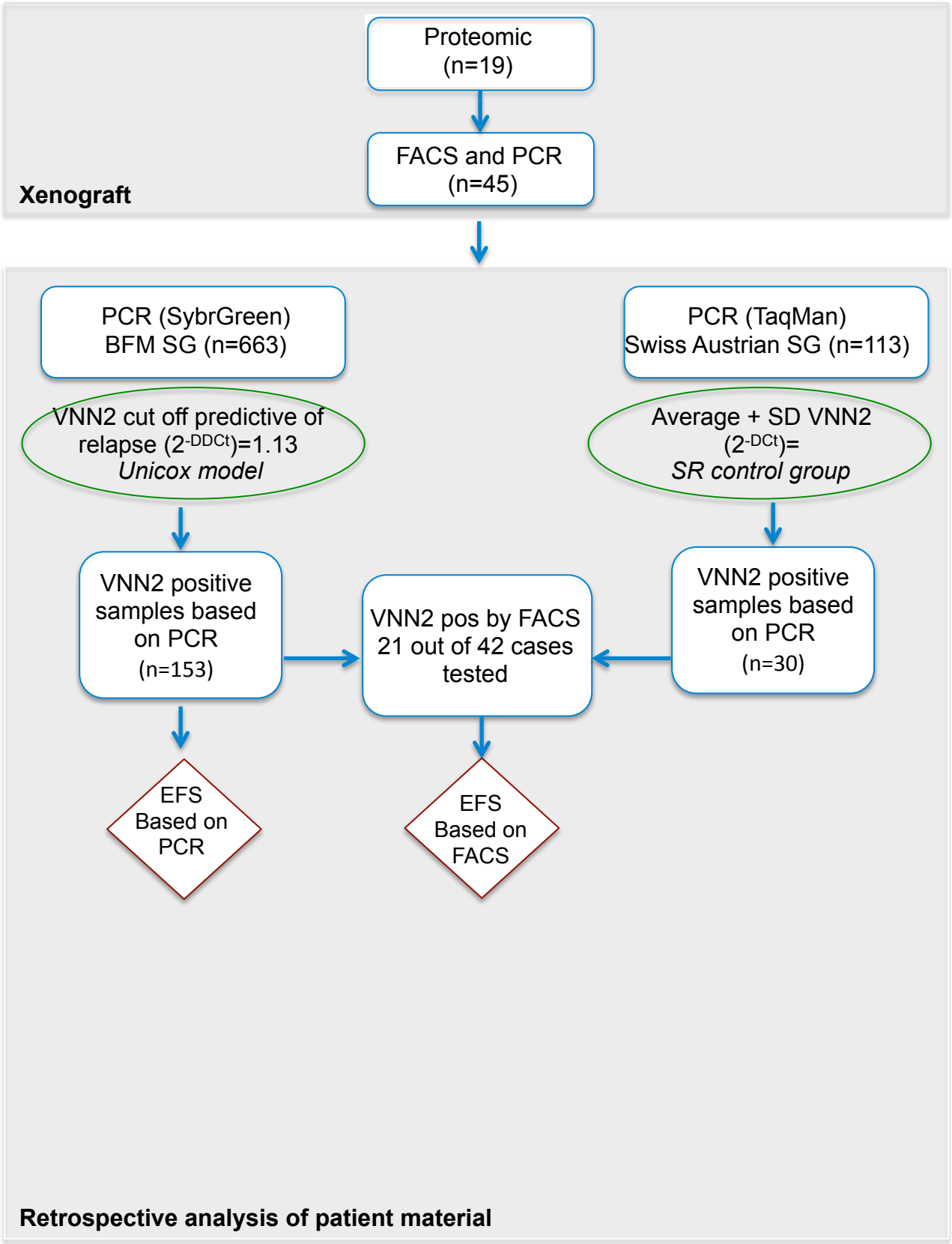

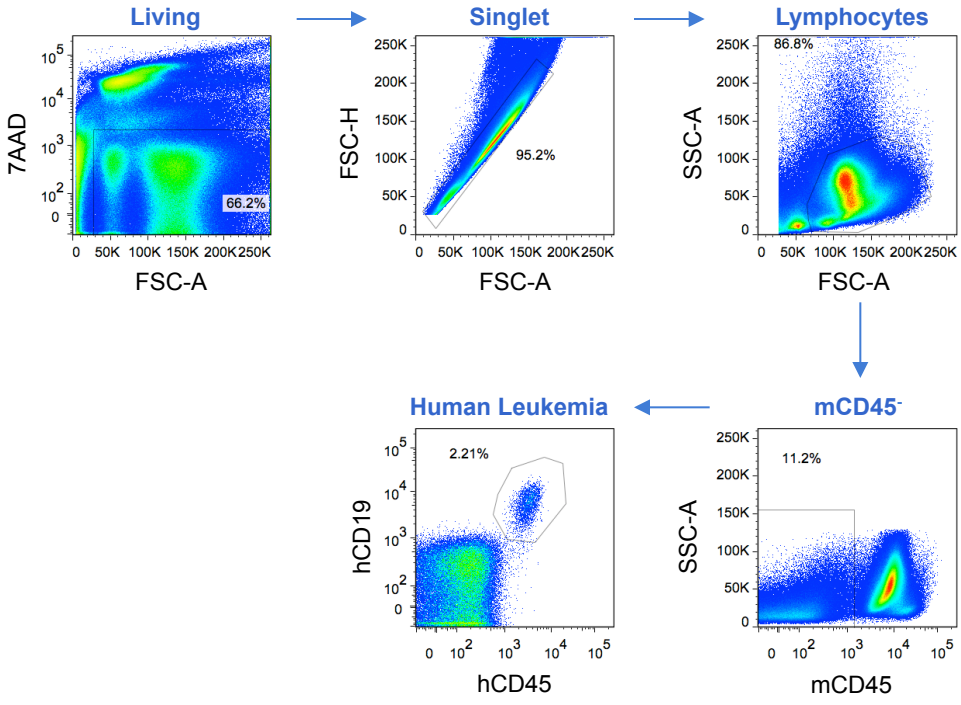

Supplementary 12. FACS gating strategy to identify leukemia cells in in vivo homing assay.
7AAD staining is used to exclude dead cells and singlets by FCS-A and FSC-H. Lymphocytes are defined based on physical parameters and enrichment for human cells is obtained excluding murine CD45 positive cells. Leukemia cells are discriminated as CD45 and CD19 positive. At least of 1.000.000 of total events per specimen was acquired.

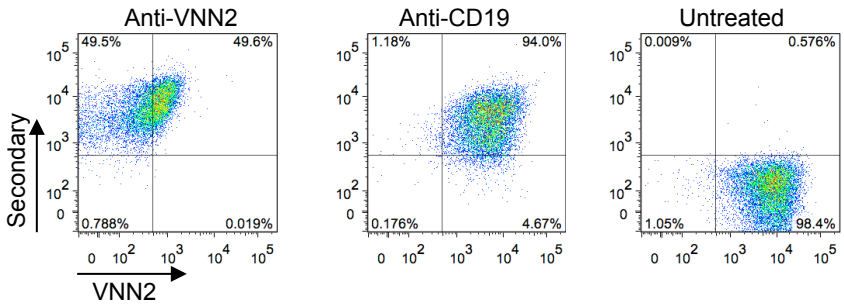

Supplementary 13. Validation of antibodies binding.
Secondary anti-mouse FITC antibody was used following in vitro blocking and in vivo homing assay. Positive signal for secondary antibody confirms the binding of the blocking antibody to the cells. Representative FACS of a VNN2 positive cases in the 3 different condition

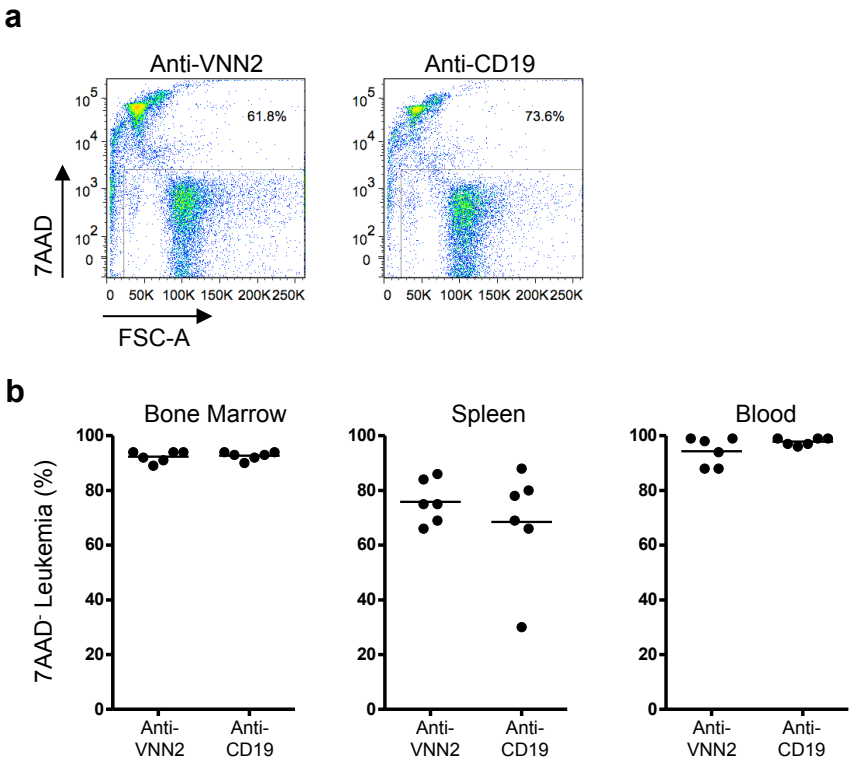

Supplementary 14. Blockade with anti-VNN2 and CD19 antibodies does not effect the survival rates. Frequency of living cells was assessed excluding 7AAD positive dead cells after in vitro blocking and after homing assay, untreated condition was included as control. A) Representative FACS analysis after blocking. B) Representative analysis of the frequency of living (7AAD negative) cells in BM, spleen and blood for all the mice.

PROPOSAL FOR PROSPECTIVE EVALUATION OF VNN2 AS PROGNOSTIC MARKER BY FACS FOR BCP-ALL (18-11-2014)

Rationale

We identified VNN-2 by CSC glycoproteomics as one of the cell surface proteins that was almost uniquely found in high risk ALL compared to SR ALL. Vanin-2 (VNN2) is a GPI anchored cell surface protein with potential function in cell trafficking and inflammation and most recently functionally shown to be required for fetal HSC. VNN2 is expressed at different levels by normal hematopoietic cells, importantly by lymphocytes and myeloid cells (Figure 1, DMAP data based on RNA from sorted human populations). Given the correlation for VNN2 expression at RNA and protein level (Figure 2), we assessed a cohort of 663 BFM patients retrospectively.

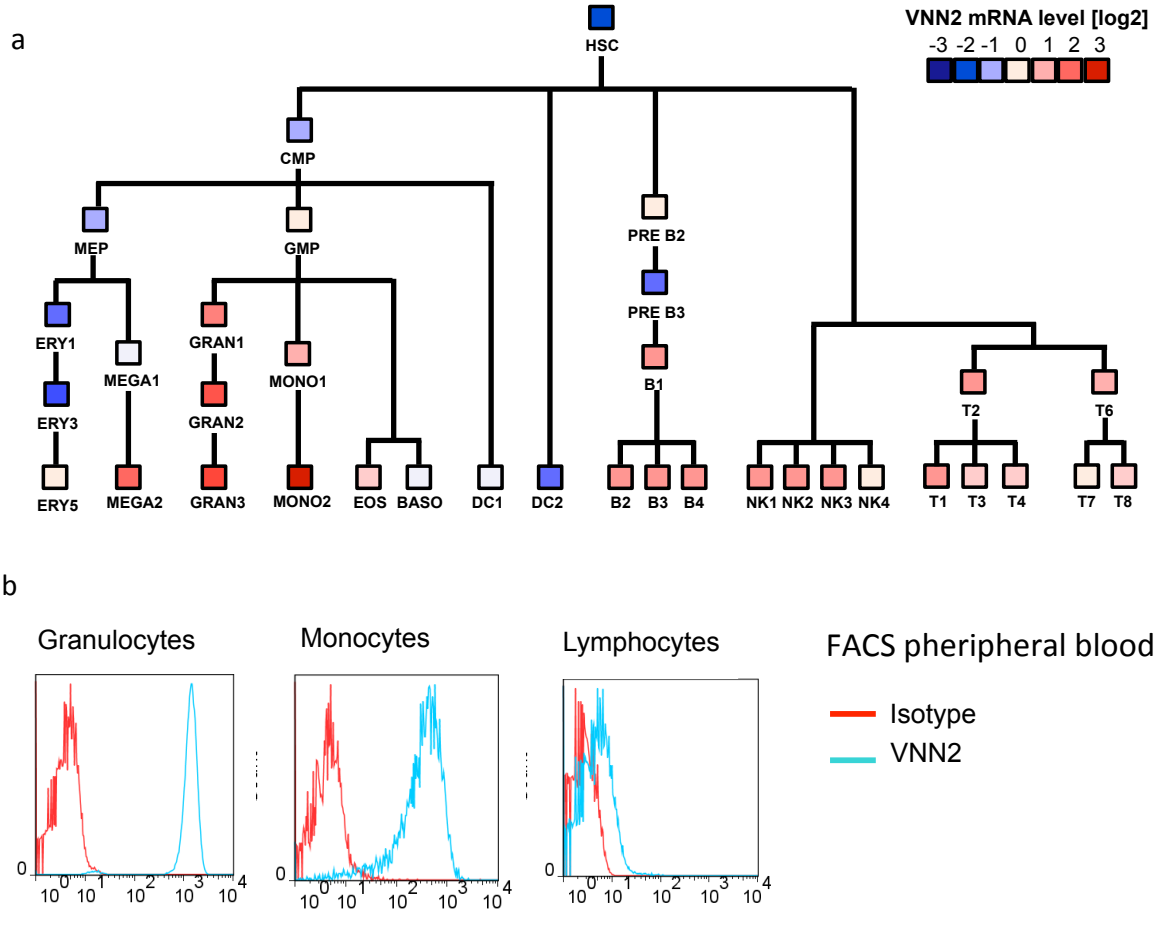

Figure 1. VNN2 expression in normal hematopoetic system. a) VNN2 transcript level in different progenitors, DIMAP, Novershtern, Cell 2011. b) VNN2 protein expression by cells of peripheral blood of healthy donor.

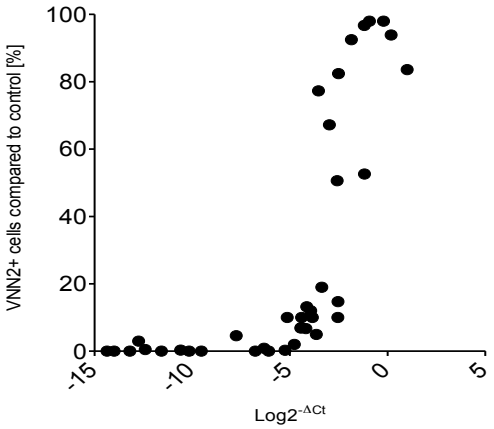

Figure 2. Correlation between protein and transcript level of VNN2. Y axis shows the percentage of VNN2 positive cells compare to the staining control tube (Fluorescence Minus One); X axis shows the Real Time PCR data as delta Ct between VNN2 and SDHA house keeping gene.

Retrospective analysis of VNN2 expression

Very high levels of VNN2 were detected by RQ-PCR only in HR and SR ALL patients from selected cohorts of the ALL-BFM-2000-Study. Moreover, VNN2 expression was found to be increased in paired relapse samples (collaboration with Truus teKronnie, AIEOP). Martin Zimmerman could show that a cut off can be defined for high levels of VNN2 expression which is significantly associated with relapse (not shown). We next decided to evaluate the potential for FACS based on this retrospective cohort. We could retrieve 14 cryopreserved samples from 153 BFM samples that were above cut of by QPCR for VNN2 high. By FACS 7 samples were clearly VNN2 positive, two were borderline. Survival analysis of this small subgroup is shown in Figure 3.

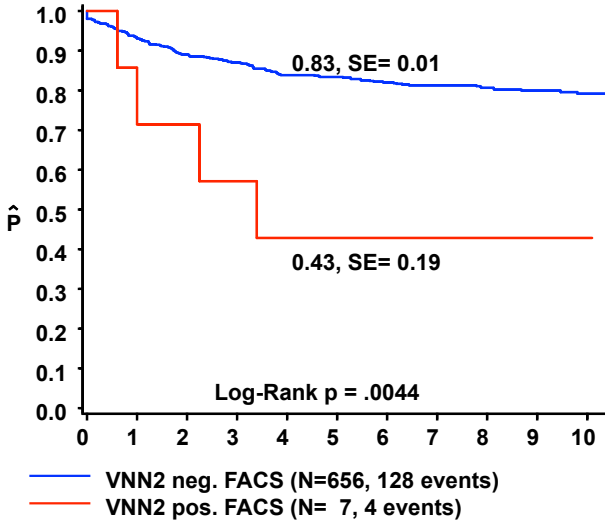

Figure 3. EFS based on flow cytometry. 663 ALL cases of the German ALL-BFM-2000 clinical study are screened by RT-PCR for VNN2 expression. 7 out of 14 patients for which cells were available were positive for VNN2 by FACS and are included in the EFS analysis.

In this analysis samples with a frequency of $VNN2^{pos}$ cells higher than 10% compared to the Fluorescence Minus One (FMO) tube are considered positive. The FMO-tube includes all the antibodies used in the VNN2-tube for the staining of the sample except VNN2 antibody.

A similar distribution was found in an independent retrospective cohort from BFM-CH and BFM-A (not shown). In addition 4/8 cases in the Swiss-Austrian cohort relapsed. Finally, VNN2 is also strongly positive in TCF3-HLF ALL. This is added value for the VNN2 tube, as we will probably detect more cases with t(17;19) positive ALL.

Prospective analysis on VNN2 expression

We have included VNN2 in PE in the diagnostic panels of BFM-CH (Zurich) for paitents enfroled on ALL-BFM-2009 since April 2012. In total 160 patients have been screened by flow cytometry. This provides a basis for this proposal. This series included always a negative control tube according to the AEIOP-BFM FCM task force. We scored the VNN2 signal comparing to the intra sample control population $CD45^{pos}CD19^{neg}$ (normal NK and T lymphoid cells). 11 patients resulted VNN2 positive with a frequency of VNN2 positive cells higher than 10% respect to the control (Table1). 3 out 11 have a percentage of $VNN2^{pos}$ cells very close to the threshold (10-15%), 5 of them are weak positive (15-50%) and 3 of them are strong positive (50-10%). Thus the frequency of VNN2 positivity in this cohort is in the range of 5 % (8/160).

SAMPLE ID	% VNN2 positive cells	Classification (% of blasts $VNN2^{pos}$)
CHZ 19	99.00	Strong positive (50-100%)
CHBL 24	67.00	
CHBE 19	57.00	
CHSG 13	35.20	Weak Positive (15-50%)
CHZ 3	30.00	
CHZ 30	28.60	
CHAR 10	24.60	
CHZ 33	18.00	
CHSG17	14.30	Borderline (10-15%)
CHZ 38	14.10	
CHZ 44	12.60	

Table 1. Results of the Swiss prospective analysis (FACS).

We next looked at the distribution of the Mean Fluorescence Intensity (MFI) of patient samples that we scored as VNN2 negative compared to the negative controle tube (CD45 stain only) and the intra sample negative control $CD45^{pos}CD19^{neg}$ population. Please note that we noticed a sample to sample variability of VNN2 positivity in both normal T cells and B cells, which is in line with DMAP RNA data reported by the Broad Institute. We therefore detected a systematic difference between our suspected negative samples and the $CD45^{pos}CD19^{neg}$ population for VNN2. Thus, comparision with this intra lineage control may limit our resolution in the very low positive range. But we hypothesize that the most relevant information will be associated with strong VNN2 positivity. It would be useful to obtain a larger series of prospective data including a negative tube (CD45 only), an FMO tube (BCP backbone excluding VNN2 in PE), and the VNN2 tube.

.

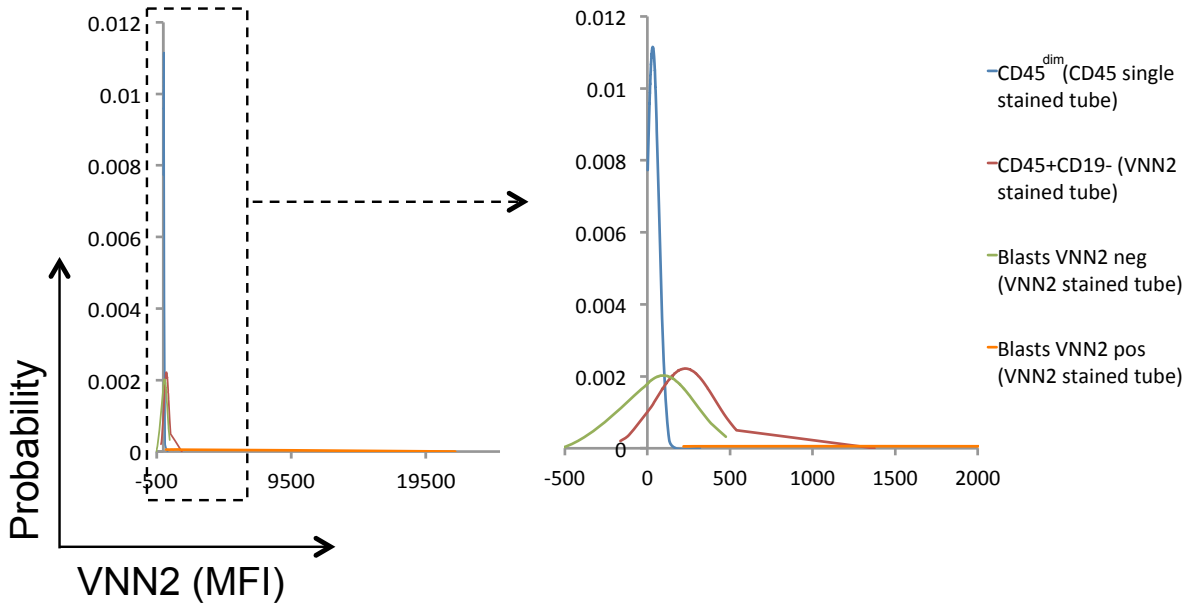

Figure 4. Normal distribution of the MFIs for Swiss ALL cases included in the prospective analysis. In blue are depicted the MFIs derived from the blasts of the CD45 single stained tube, in red the MFIs of $CD45^{pos}CD19^{neg}$ population in the tube stained with VNN2, green and orange represent the MFIs of the blasts of the VNN2 negative and VNN2 positive samples, respectively. Patient number included in the graph: N=80.

Proposal

As discussed at the BFM Meeting in Zurich, we would like to ask each reference center to include an experimental VNN2 tube to the diagnostic panel for ALL. We propose to perform a first series including the CD45 single stained control tube, FMO-control tube. Results can then be analysed against the FMO and cross lineage $CD45^{pos}CD19^{neg}$ population as negative controls to make sure that we do not loose important information.

SOP FOR PROSPECTIVE EXPERIMENTAL ANALYIS OF VNN2 SURFACE MARKER ON BCP-ALL

Process the leukemia samples according to the current standard operating procedure: FLOW-Immunophenotyping at diagnosis AIEOP – BFM-A/G/S – CPH – INS – NSW version "International" 1.6.2 of January 16, 2013

VNN2 antibody reference:

Anti-human GPI-80/VNN2 mAb-PE, clone 3H9, D087-5, MBL International.

250-270 euro per antibody aliquot (50 test)

Procedure to obtain the antibody:

- we propose that you order the antibody directly. We do not think that we can get a better deal with a collective order and shipment via our center. We will reimburse your costs if you send us an invoice from your department with both your address and our address along the account detail for reimbursement:

Billing address for invoice:

Universitäts-Kinderspital Zurich

Kreditor/Buchhaltung

Steinwiesstrasse 75

8032 Zurich

But please send the bill to

Dr. Beat Bornhauser
Division of Oncology
Research Laboratory
Universitäts-Kinderspital Zurich
August Forel Strasse 1
CH 8008 Zürich
Swizerland

Titer: the company recommends 10-20 uL per reaction. Anna used down to 5 uL for 500000 cells. As positive control you can titer on myeloid cells. We expect 10 uL to be correct concentration.

Staining condition:

Resuspend 500.000 - 1.000.000 of cells in 100-200uL of staining volume and add 10-20uL of the PE labelled anti-human VNN2 monoclonal antibody. Stain at RT for at least 15 minutes protect from light.

Antibody panel to include in the VNN2-tube

Minimum markers: CD45, CD19, CD34, CD10 to identify blasts as $CD45^{dim}CD19^{pos}CD34^{pos}CD10^{pos}$ and negative control population as $CD45^{bright}CD19^{neg}$.

Antibody to include in the CD45 single stained tube:

CD45

Antibody panel to include in the FMO-tube

All the antibodies included in the VNN2-tube except VNN2

NEGATIVE controls:

A negative region is defined by

1) **Blasts in the CD45 single stained sample** ($CD45^{dim}$) (Figure 5)
2) **Cross-lineage population control** ($CD45^{bright}CD19^{neg}$) **in the VNN2 tube** (Figure 6)
3) **Blasts** ($CD45^{dim}CD19^{pos}$) **in the FMO tube** (Figure7)

POSITIVE control

Strong expression of VNN2 on granulocyte or monocyte (Figure 8).

Definition of antigen expression levels

A degree of overlap of the blast population with the negative control population is rated as either **negative** (positivity in <10% of blasts), **weak positive** (positivity in ≥10% to <50% of blasts), Figure 9, or **strong positive** (positivity in ≥50% of blasts), Figure 10.

Percentage of blasts VNN2 positive cells respect the three controls and MFI of the three negative controls and of the blasts in the FMO-tube and VNN2-tube should be exported and collected in an excel file as represented in table 2.

Sample ID	VNN2 positive cells respect blast in CD45 single stained tube	VNN2 positive cells respect cross lineage CD45+CD19-	VNN2 positive cells respect blast in FMO tube	Blast CD45 single stained tube	Cross lineage CD45+CD19-	Blast in FMO tube	Blasts in VNN2 tube
	(%)	VNN2 positive cells (%)	VNN2 positive cells (%)	MFI VNN2 -PE (mean)	MFI VNN2 -PE (mean)	MFI VNN2 -PE (mean)	MFI VNN2 -PE (mean)

Table 2. Representative scheme for data collection.

Contacts:

Jean-Pierre Bourquin

Jean-pierre.bourquin@kispi.uzh.ch

+41 44 266 7304 (mobile hospital)

+41 79 365 0837 (mobile)

Beat Bornhauser

beat.bornhauser@kispi.uzh.ch

+41 44 634 8817

Anna Rinaldi

anna.rinaldi@kispi.uzh.ch

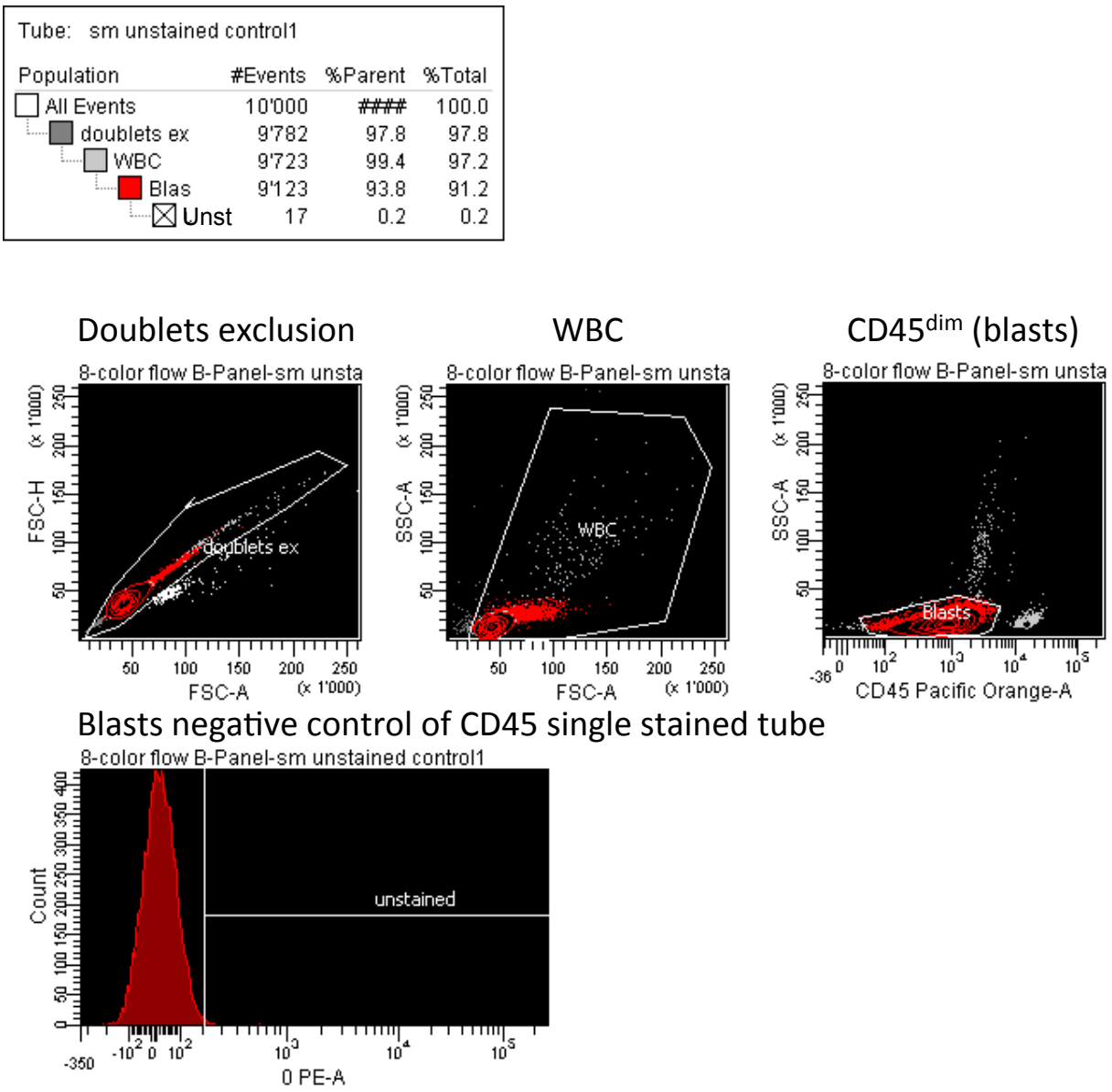

Figure 5. Gating strategy to define the blasts (CD45^{dim}) as NEGATIVE control population in the CD45 single stained tube.

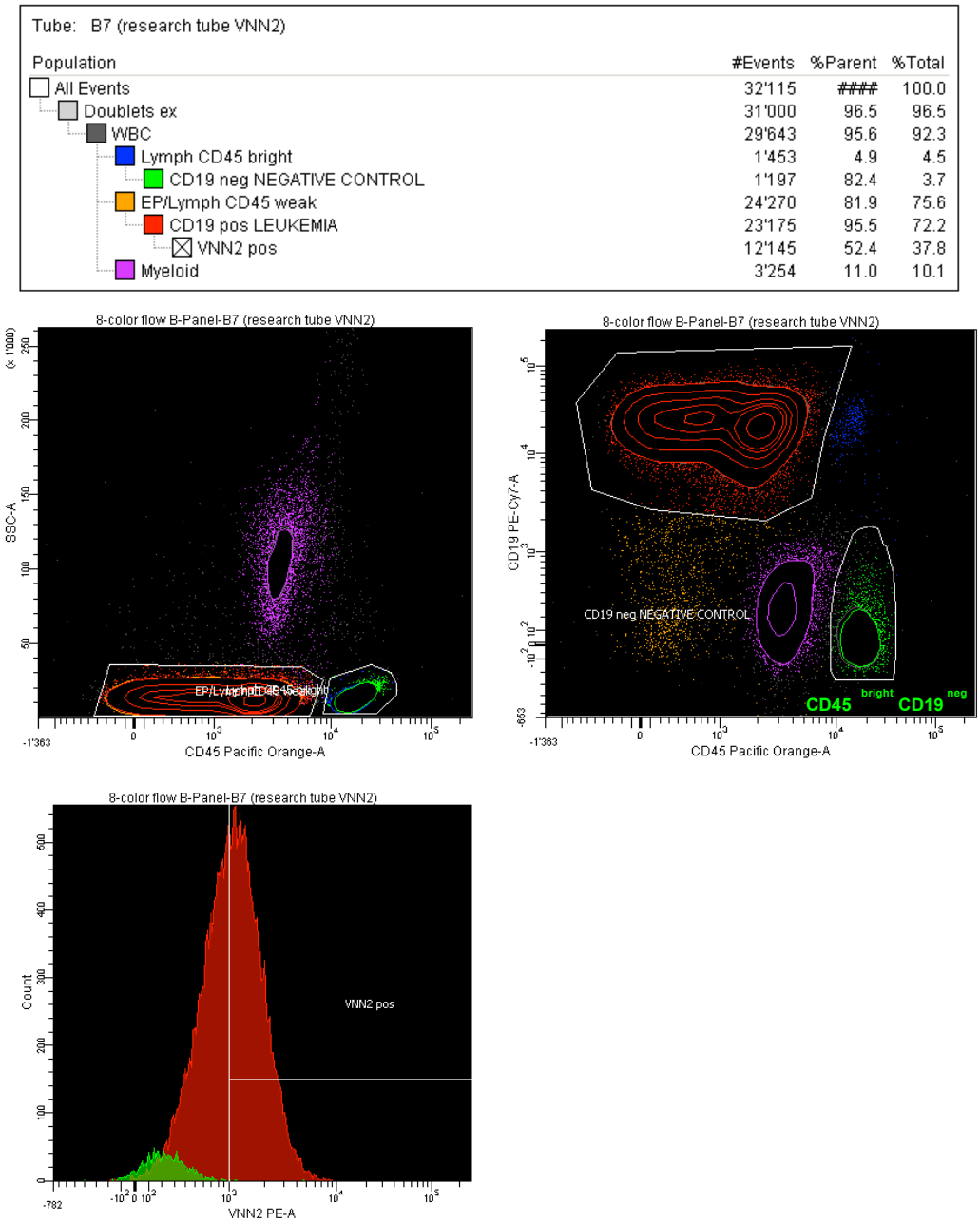

Figure 6. Gating strategy to identify the in-sample cross-lineage ($CD45^{bright}$ $CD19^{neg}$) NEGATIVE control population. Negative population is defined as mature lymphocytes $CD45^{bright}$ $CD19^{neg}$ in green.

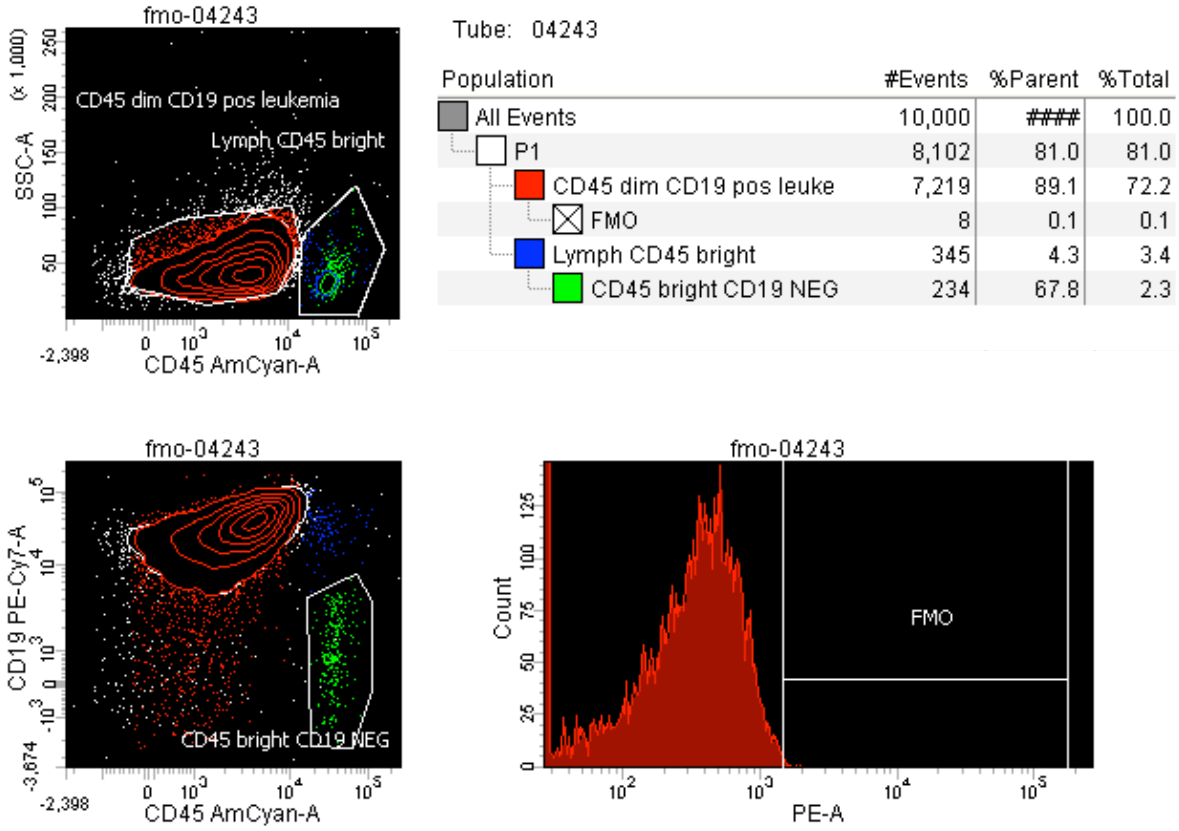

Figure 7. Gating strategy to identify the blasts ($CD45^{dim}CD19^{pos}$) in the FMO tube as NEGATIVE control population.

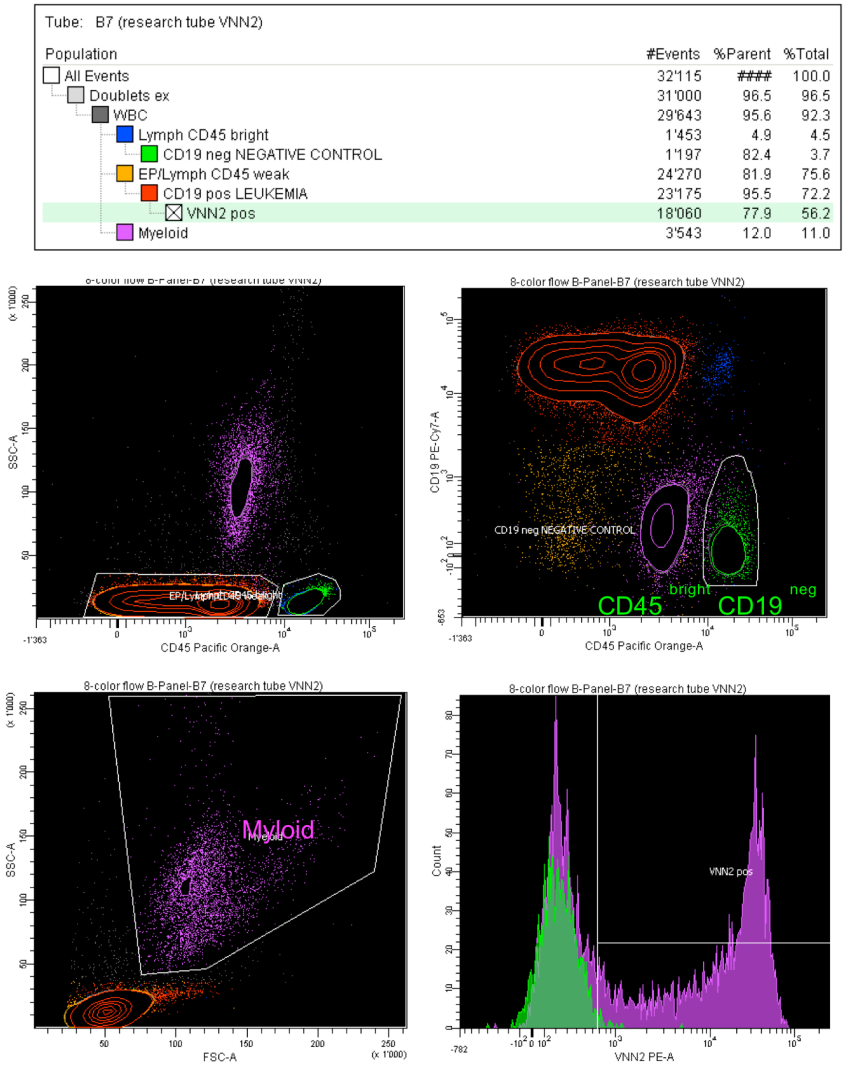

Figure 8. Cross-lineage POSITIVE-control myeloid population

Myeloid population, depicted in purple, is identified based on SSC and FSC. Negative population is defined as $CD45^{bright}CD19^{neg}$, in green.

Tube: B7 (research tube VNN2)

Population	#Events	%Parent	%Total
All Events	32'115	####	100.0
Doublets ex	31'000	96.5	96.5
WBC	29'643	95.6	92.3
Lymph CD45 bright	1'453	4.9	4.5
CD19 neg NEGATIVE CONTROL	1'197	82.4	3.7
EP/Lymph CD45 weak	24'270	81.9	75.6
CD19 pos LEUKEMIA	23'175	95.5	72.2
VNN2 pos	18'060	77.9	56.2

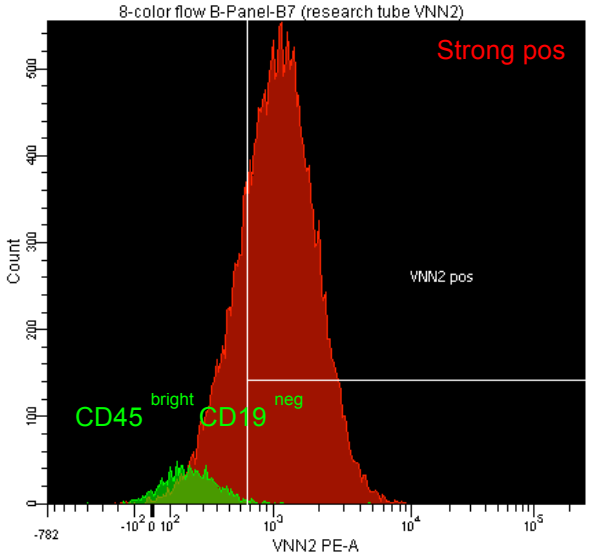

Figure 9. Example of sample considered STRONG POSITIVE for VNN2 expression. In red, leukemia sample ($CD45^{dim}$ $CD19^{pos}$) and in green, in-sample cross-lineage negative control ($CD45^{bright}CD19^{neg}$).

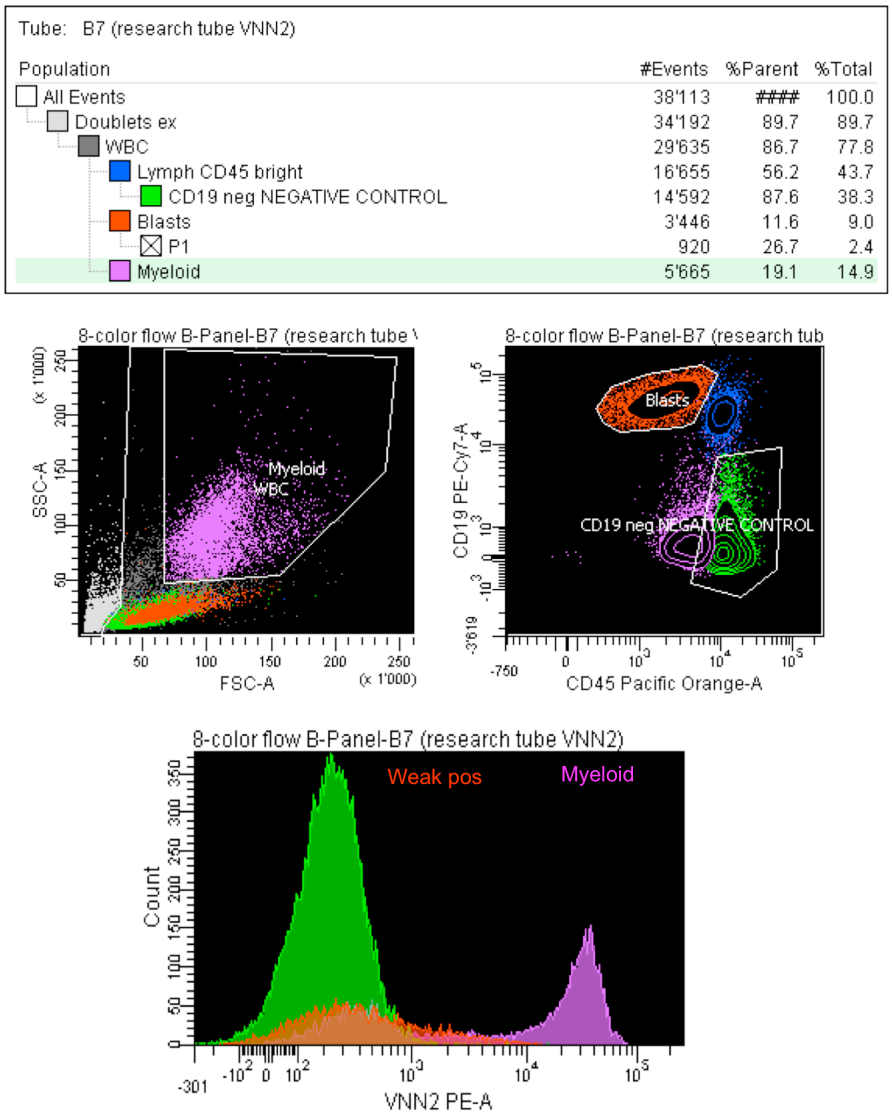

Figure 10. Example of sample considered WEAK POSITIVE for VNN2 expression. In red, leukemia population ($CD45^{dim}$ $CD19^{pos}$), in green, in-sample cross-lineage negative control ($CD45^{bright}CD19^{neg}$), in purple, in-sample cross-lineage positive control (Myeloid).